

**FACTS BASED STABILIZERS FOR DYNAMIC STABILITY
ENHANCEMENT OF WEAKLY INTERCONNECTED
POWER SYSTEMS**

BY

MALIK MOHAMMED ASHTAR AL-HAJJI

A Thesis Presented to the
DEANSHIP OF GRADUATE STUDIES

KING FAHD UNIVERSITY OF PETROLEUM & MINERALS

DHAHRAN, SAUDI ARABIA

In Partial Fulfillment of the
Requirements for the Degree of

MASTER OF SCIENCE

In

ELECTRICAL ENGINEERING

JANUARY 2015

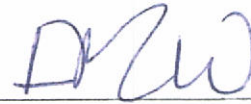
KING FAHD UNIVERSITY OF PETROLEUM & MINERALS
DHAHRAN-31261. SAUDI ARABIA
DEANSHIP OF GRADUATE STUDIES

This thesis, written by MALIK AL HAJJI under the direction of his thesis advisor and approved by his thesis committee, has been presented and accepted by the Dean of Graduate Studies, in partial fulfillment of the requirements for the degree of **MASTER OF SCIENCE IN ELECTRICAL ENGINEERING.**

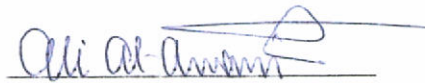
Thesis Committee



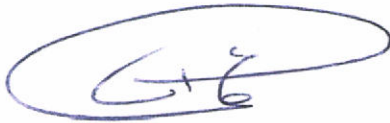
Dr. Mohammed A. Abido
(Advisor)



Dr. Ibrahim M. El-Amin
(Member)



Dr. Ali T. Al-Awami
(Member)



Dr. Ali A. Al Shaikhi
Department Chairman



Dr. Salam A. Zummo
Dean of Graduate Studies

Date

6/1/15



Dedicated to

My Family

My Beloved Parent

Sincere Wife

Son Ibrahim

&

Daughter Zahra

ACKNOWLEDGMENTS

In the name of Allah the Greatest, the most merciful and the lord of everything. All praise and thanks are due to him. Peace be upon the Prophet Mohammad and his family.

It is a great pleasure to thank everyone who helped me successfully accomplished my master degree. Thus, I would like to thank King Fahd University of Petroleum & Minerals and the Electrical Engineering Department for the support given to this research through their facilities. I am really thankful to Saudi Electricity Company which without its facilities this dissertation would not be possible.

Special thanks and deep appreciation to my thesis advisor Professor Mohammed Ali Abido who provided an excessive and endless support besides his continues encouragement toward achieving this work. Similarly, I highly appreciate the constructive comments, suggestions, recommendations and valuable contributions of the thesis committee members Professor Ibrahim El Amin and doctor Ali Al Awami. I am obliged to my colleague Engineer Mohammed Mahdi Al Hulail who supported me throughout this work.

Special thanks is due to my wife who was very patient and supportive throughout my study and research. I am truly indebted and thankful to my parents, brothers, sisters and all family members for their continuous encouragement.

TABLE OF CONTENTS

ACKNOWLEDGMENTS	IV
TABLE OF CONTENTS	V
LIST OF TABLES	XII
LIST OF FIGURES	XIV
LIST OF ABBREVIATIONS	XIX
THESIS ABSTRACT (ENGLISH)	XXII
THESIS ABSTRACT (ARABIC)	XXIII
CHAPTER ONE	1
1. INTRODUCTION	1
1.1 Introduction	1
1.2 Thesis Motivations	2
1.3 Thesis Objectives	3
1.4 Thesis Contribution	4
1.5 Thesis Organization	5
CHAPTER TWO	6
2. LITERATURE REVIEW	6
2.1 Overview	6
2.2 Fundamentals of Power System Dynamic Stability	6

2.3 Power System Control Equipment	11
2.4 Synchronous Generator Modeling	11
2.5 Power System Reduction	12
2.6 Power System Stabilizer (PSS)	15
2.6.1 General Concept of Power System Stabilizer	15
2.6.2 Optimal Location of Power System Stabilizer	16
2.6.3 Power System Stabilizer Parameters Optimization	17
2.7 Flexible AC Transmission System (FACTS).....	18
2.7.1 General Concept about FACTS	18
2.7.2 Coordination of PSSs and FACTS	19
2.7.3 Thyristor Controlled Series Capacitor (TCSC)	20
2.8 Modal Analysis.....	25
CHAPTER THREE	27
3. SYSTEM MODELING	27
3.1 Overview	27
3.2 Bus Modeling.....	27
3.3 Transmission Line Modeling.....	28
3.4 Load Modeling	29
3.5 Synchronous Generator Modeling	30
3.5.1 Load Flow Representation	30
3.5.2 Dynamic Representation	31
3.6 Generator's Control Devices	33
3.6.1 Governor Models	33
3.6.2 Excitation System Models	33
3.6.3 PSSs Models	34

3.7 TCSC Model	35
3.7.1 Description of the TCSC Power Oscillation Damper (POD)	36
3.7.2 TCSC Input Signals.....	38
3.8 Utilized Software	39
3.8.1 Power System Simulator for Engineers (PSS/E)	39
3.8.2 Python Program	40
CHAPTER FOUR.....	41
4. PROPOSED CONTROLLER DESIGN APPROACH.....	41
4.1 Overview	41
4.2 Base Case Preparation.....	43
4.3 Power System Reduction	46
4.4 Load Flow Solution Method.....	47
4.5 Dynamic Simulation	47
4.6 Modified Particle Swarm Optimization Technique (MPSO)	48
4.6.1 Modified PSO Algorithm	48
4.6.2 The Objective Function (Fitness Function)	51
4.6.3 MPSO Steps.....	52
4.6.4 MPSO Flowchart.....	54
4.7 Modal Analysis.....	55
4.7.1 Basic Principles of Modal Analysis.....	55
4.7.2 Modal Analysis Methodologies	58
4.7.3 Modal Analysis Flowchart.....	59
CHAPTER FIVE.....	60
5. POWER SYSTEM REDUCTION.....	60

5.1 Overview	60
5.2 The Static Reduction	61
5.3 The Dynamic Reduction	62
5.3.1 Generator Model Reduction	63
5.3.2 Control Devices Reduction	66
5.4 Application of Power System Reduction Technique.....	67
5.4.1 Description of the Considered Power System.....	67
5.4.2 Considered Assumptions.....	68
5.4.3 Power System Reduction's Steps.....	69
5.4.4 Power System Reduction's Results.....	69
5.5 Summary of the Power System Reduction.....	81
CHAPTER SIX.....	82
6. COORDINATION OF POWER SYSTEM STABILIZERS	82
6.1 Overview	82
6.2 Modal Analysis Results of the Existing Power System	83
6.3 Optimal Location of PSS	86
6.4 Coordinated Design of PSSs.....	89
6.5 Modal Analysis Results of the Proposed Power System	91
6.5.1 Eigenvalue Results Concomitant with Rotor Speed Deviations.....	91
6.5.2 Eigenvalue Results Concomitant with Active Power Flow.....	92
6.6 Nonlinear Time-domain Simulation Results.....	94
6.6.1 Rotor Angles' Responses	94
6.6.2 Machines' Electrical Power Responses.....	96
6.6.3 Rotor Speed Deviations' Responses	98
6.6.4 Voltages' Responses	100

6.6.5 Active Power Flow Responses	102
6.7 Robustness of the Proposed Coordination of the PSSs.....	104
6.7.1 Existing Maximum Power Transfer Limit.....	106
6.7.2 Maximum Power Transfer Limit with the Proposed PSSs.....	107
6.7.3 Sensitivity Analyses	108
6.8 Summary of the Coordinated Design of PSSs.....	110
CHAPTER SEVEN	111
7. INDIVIDUAL DESIGN OF TCSC.....	111
7.1 Overview	111
7.2 Placement and Design of TCSC Controller.....	112
7.2.1 Site Selection.....	112
7.2.2 Design of TCSC Controller.....	113
7.2.3 Comparison of Alternative Input Signals	114
7.3 Modal Analysis Results with the Proposed TCSC.....	118
7.3.1 Eigenvalue Results Concomitant with Rotor Speed Deviations.....	119
7.3.2 Eigenvalue Results Concomitant with Active Power Flow.....	119
7.4 Nonlinear Time-domain Simulation Results.....	121
7.4.1 Rotor Angles' Responses	121
7.4.2 Machines' Electrical Power Responses.....	123
7.4.3 Rotor Speed Deviations' Responses	125
7.4.4 Voltages' Responses	128
7.4.5 Active Power Flow Responses	131
7.5 Robustness of the Proposed TCSC	133
7.5.1 Existing Maximum Power Transfer Limit.....	134
7.5.2 Maximum Power Transfer with the Proposed TCSC.....	134

7.5.3 Sensitivity Analyses	136
7.6 Summary of the Individual Design of TCSC	137
CHAPTER EIGHT	138
8. COORDINATION OF PSSs AND TCSC	138
8.1 Overview	138
8.2 Coordinated Design of PSSs and TCSC	138
8.3 Modal Analysis Results	140
8.3.1 Eigenvalue Results Concomitant with Rotor Speed Deviations	141
8.3.2 Eigenvalue Results Concomitant with Active Power Flow	143
8.4 Nonlinear Time-domain Simulation Results	144
8.4.1 Rotor Angles' Responses	144
8.4.2 Machines' Electrical Power Responses	148
8.4.3 Rotor Speed Deviations' Responses	151
8.4.4 Voltages' Responses	154
8.4.5 Active Power Flow Responses	156
8.5 Robustness of the Proposed Coordinated Design of the TCSC and PSSs	158
8.5.1 Existing Maximum Power Transfer Limit	158
8.5.2 Maximum Power Transfer Limit with the Proposed PSSs and TCSC	159
8.5.3 Sensitivity Analyses	160
8.6 Summary of the Coordinated Design of the TCSC and PSSs	162
CHAPTER NINE	163
9. CONCLUSION AND RECOMMENDATIONS	163
9.1 Conclusion	163
9.2 Recommendations	166

9.3 Future Work	166
REFERENCES.....	168
APPENDICES	180
APPENDIX A GENERATOR MODEL.....	180
APPENDIX B TURBINE GOVERNOR MODELS.....	181
APPENDIX C EXCITATION SYSTEMS MODELS.....	183
APPENDIX D POWER SYSTEM STABILIZER MODELS	187
VITA	189

LIST OF TABLES

Table 3-1 Bus Types and PSS/E codes	28
Table 3-2 Transmission Line Parameters	28
Table 3-3 Load Modeling	30
Table 3-4 Generator Input Data in Load Flow.....	31
Table 3-5 Transformer Input Data	31
Table 3-6 Turbine Governors Models.....	33
Table 3-7 Excitation System Models	34
Table 3-8 Power System Stabilizer Models.....	35
Table 3-9 TCSC Parameter Typical Values.....	37
Table 5-1 Summary of the Full Power System.....	67
Table 5-2 Summary of the Full & Reduced Power Systems	70
Table 5-3 Steady State Comparison, Full vs Red. Power Systems, Voltage Results	71
Table 5-4 Steady State Comparison, Full vs Red. Power Systems, Angle Results	71
Table 5-5 Steady State Comparison, Full vs Red. Power Systems, Active Power Flow..	72
Table 6-1 Modal Decomposition of Rotor Speed Deviations of Machine 28	84
Table 6-2 Existing Modal Analysis for the Inter Area 0.5 Hz – Mode	85
Table 6-3 Normalized Eigenvectors Based on Machine 28.....	88
Table 6-4 Optimized PSSs Parameters Based on the Coordinated Design of PSSs.....	90
Table 6-5 Modal Analysis for the Inter Area 0.5 Hz – Mode, Cord. PSSs.....	92

Table 6-6 Modal Decomposition of Active Power Flow of Line 44 – 63	93
Table 6-7 Comparison of Modal Analysis Results for the Existing and Proposed PSSs .	93
Table 7-1 Optimized TCSC Parameters, Individual Design of TCSC	114
Table 7-2 Modal Analysis for the Inter Area 0.5 Hz – Mode, Prop. TCSC	120
Table 7-3 Active Power Modal Analysis, 0.5 Hz – Mode, Prop. TCSC	120
Table 8-1 Optimized PSSs Parameters, Cord. PSSs&TCSC	140
Table 8-2 Optimized TCSC Parameters, Cord. PSSs&TCSC	140
Table 8-3 Modal Analysis for the Inter Area 0.1-0.7 Hz – Modes, Cord. PSSs&TCSC	141
Table 8-4 Machine 28 Rotor Speed Deviation Modal Analysis, Cord. PSSs&TCSC....	142
Table 8-5 Machine 24 Rotor Speed Deviation Modal Analysis, Cord. PSSs&TCSC....	142
Table 8-6 Machine 9 Rotor Speed Deviation Modal Analysis, Cord. PSSs&TCSC.....	143
Table 8-7 Active Power Modal Analysis for Inter Area Modes, Cord. PSSs&TCSC....	144

LIST OF FIGURES

Fig. 2.1 Types of Power System Stability.....	8
Fig. 3.1 Transmission Line Modeling in PSS/E	28
Fig. 3.2 Generator Modeling in Load Flow	30
Fig. 3.3 Generator Modeling for Dynamic Simulation (Norton Equivalent)	32
Fig. 3.4 TCSC Power Oscillations Damper (POD)	37
Fig. 4.1 Proposed Controller Design Approach Flowchart.....	45
Fig. 4.2 Integration of MPSO with Nonlinear Time-domain Simulation in PSS/E.....	53
Fig. 4.3 Modified PSO Flowchart.....	54
Fig. 4.4 Modal Analysis Flowchart	59
Fig. 5.1 Aggregation of Power Plants in the Load Flow	65
Fig. 5.2 The Main Interconnected Areas of the Considered Power System.....	68
Fig. 5.3 Power System Reduction Flowchart.....	70
Fig. 5.4 Comparison of Rotor Speed Deviations of Machine # 2 in Area 3	73
Fig. 5.5 Comparison of Rotor Speed Deviations of Machine # 16 in Area 1	74
Fig. 5.6 Comparison of Rotor Speed Deviations of Machine # 28 in Area 2.....	74
Fig. 5.7 Comparison of Rotor Angle of Machine # 2 in Area 3	75
Fig. 5.8 Comparison of Rotor Angle of Machine # 17 in Area 1	76
Fig. 5.9 Comparison of Rotor Angle of Machine # 28 in Area 2	76
Fig. 5.10 Comparison of Bus Voltage of Bus # 110 in Area 3	77

Fig. 5.11 Comparison of Bus Voltage of Bus # 30 in Area 1	78
Fig. 5.12 Comparison of Bus Voltage of Bus # 44 in Area 1	78
Fig. 5.13 Comparison of Bus Voltage of Bus # 63 in Area 2	79
Fig. 5.14 Comparison of Active Power Flow of Line 115 – 38.....	80
Fig. 5.15 Comparison of Active Power Flow of Line 112 – 32.....	80
Fig. 5.16 Comparison of Active Power Flow of Line 44 – 63.....	81
Fig. 6.1 Inter-Area Oscillations Between Areas 1 and 3 Against Area 2	86
Fig. 6.2 Enlarge View of the Inter-Area Oscillations	87
Fig. 6.3 MPSO Convergence Curve for Coordinated Design of PSSs	90
Fig. 6.4 Rotor Angle, Unit 3-Area 3, 3-Ph. Fault for 0.1s, Cord. PSSs.....	95
Fig. 6.5 Rotor Angle, Unit 28-Area 2, 3-Ph. Fault for 0.1s, Cord. PSSs.....	95
Fig. 6.6 Rotor Angle, Unit 16-Area 1, 3-Ph. Fault for 0.1s, Cord. PSSs.....	96
Fig. 6.7 Electrical Power, Unit 28-Area 2, 3-Ph. Fault for 0.1s, Cord. PSSs	97
Fig. 6.8 Electrical Power, Unit 16-Area 1, 3-Ph. Fault for 0.1s, Cord. PSSs	97
Fig. 6.9 Electrical Power, Unit 2-Area 3, 3-Ph. Fault for 0.1s, Cord. PSSs	98
Fig. 6.10 Speed Deviations, Unit 2-Area 3, 3-Ph. Fault for 0.1s, Cord. PSSs.....	99
Fig. 6.11 Speed Deviations, Unit 16-Area 1, 3-Ph. Fault for 0.1s, Cord. PSSs.....	99
Fig. 6.12 Speed Deviations, Unit 28-Area 2, 3-Ph. Fault for 0.1s, Cord. PSSs.....	100
Fig. 6.13 Voltage, Bus 118-Area 3, 3-Ph. Fault for 0.1s, Cord. PSSs	101
Fig. 6.14 Voltage, Bus 63-Area 2, 3-Ph. Fault for 0.1s, Cord. PSSs	101
Fig. 6.15 Voltage, Bus 44-Area 1, 3-Ph. Fault for 0.1s, Cord. PSSs	102
Fig. 6.16 Active Power, Line 115 to 38, 3-Ph. Fault for 0.1s, Cord. PSSs.....	103
Fig. 6.17 Active Power, Line 112 to 32, 3-Ph. Fault for 0.1s, Cord. PSSs.....	103

Fig. 6.18 Active Power, Line 44 to 63, 3-Ph. Fault for 0.1s, Cord. PSSs.....	104
Fig. 6.19 Identification of the Critical Incident, 420 MW Power Transfer	106
Fig. 6.20 Ex. Max. Power Transfer, Line 44 to 63, 3-Ph. Fault for 0.1s, Cord. PSSs	107
Fig. 6.21 New Max. Power Transfer, Line 44 to 63, 3-Ph. Fault for 0.1s, Cord. PSSs..	108
Fig. 6.22 New Max. Power Transfer, Line 44 to 63, Sensitivity 1, Cord. PSSs.....	109
Fig. 6.23 New Max. Power Transfer, Line 44 to 63, Sensitivity 2, Cord. PSSs.....	110
Fig. 7.1 Interconnected Areas with TCSC Installed Between Area 1 and 2.....	113
Fig. 7.2 MPSO Convergence Curve for Individual Design of TCSC.....	114
Fig. 7.3 Active Power, Line 44 to 63, Prop. TCSC-Volt. Input Signal	115
Fig. 7.4 Active Power, Line 44 to 63, Prop. TCSC-Freq. Input Signal	116
Fig. 7.5 Active Power, Line 44 to 63, Prop. TCSC-Active Power Input Signal	117
Fig. 7.6 Active Power, Line 44 to 63, Prop. TCSC-Best Input Signals.....	118
Fig. 7.7 Rotor Angle, Unit 28-Area 2, 3-Ph. Fault for 0.1s, Prop. TCSC	121
Fig. 7.8 Rotor Angle, Unit 17-Area 1, 3-Ph. Fault for 0.1s, Prop. TCSC	122
Fig. 7.9 Rotor Angle, Unit 3-Area 3, 3-Ph. Fault for 0.1s, Prop. TCSC.....	122
Fig. 7.10 Electrical Power, Unit 28-Area 2, 3-Ph. Fault for 0.1s, Prop. TCSC	123
Fig. 7.11 Electrical Power, Unit 18-Area 1, 3-Ph. Fault for 0.1s, Prop. TCSC.....	124
Fig. 7.12 Electrical Power, Unit 11-Area 3, 3-Ph. Fault for 0.1s, Prop. TCSC.....	124
Fig. 7.13 Speed Deviations, Unit 28-Area 2, 3-Ph. Fault for 0.1s, Prop. TCSC	125
Fig. 7.14 Speed Deviations, Unit 24-Area 2, 3-Ph. Fault for 0.1s, Prop. TCSC	126
Fig. 7.15 Speed Deviations, Unit 18-Area 1, 3-Ph. Fault for 0.1s, Prop. TCSC	126
Fig. 7.16 Speed Deviations, Unit 16-Area 1, 3-Ph. Fault for 0.1s, Prop. TCSC	127
Fig. 7.17 Speed Deviations, Unit 7-Area 3, 3-Ph. Fault for 0.1s, Prop. TCSC	127

Fig. 7.18 Speed Deviations, Unit 3-Area 3, 3-Ph. Fault for 0.1s, Prop. TCSC	128
Fig. 7.19 Voltage, Bus 63-Area 2, 3-Ph. Fault for 0.1s, Prop. TCSC.....	129
Fig. 7.20 Voltage, Bus 44-Area 1, 3-Ph. Fault for 0.1s, Prop. TCSC.....	129
Fig. 7.21 Voltage, Bus 115-Area 3, 3-Ph. Fault for 0.1s, Prop. TCSC.....	130
Fig. 7.22 Voltage, Bus 38-Area 1, 3-Ph. Fault for 0.1s, Prop. TCSC.....	130
Fig. 7.23 Active Power, Line 112 to 32, 3-Ph. Fault for 0.1s, Prop. TCSC	131
Fig. 7.24 Active Power, Line 118 to 41, 3-Ph. Fault for 0.1s, Prop. TCSC	132
Fig. 7.25 Active Power, Line 115 to 38, 3-Ph. Fault for 0.1s, Prop. TCSC	132
Fig. 7.26 Active Power, Line 44 to 63, 3-Ph. Fault for 0.1s, Prop. TCSC	133
Fig. 7.27 Ex. Max. Power Transfer, Line 44 to 63, 3-Ph. Fault for 0.1s, Prop. TCSC...	135
Fig. 7.28 New Max. Power Transfer, Line 44 to 63, 3-Ph. Fault for 0.1s, Prop. TCSC.	135
Fig. 7.29 New Max. Power Transfer, Line 44 to 63, Sensitivity 1, Prop. TCSC	136
Fig. 7.30 New Max. Power Transfer, Line 44 to 63, Sensitivity 2, Prop. TCSC	137
Fig. 8.1 MPSO Convergence Curve for the Coordinated Design of PSSs&TCSC	139
Fig. 8.2 Rotor Angle, Unit 28-Area 2, 3-Ph. Fault for 0.1s, Cord. PSSs&TCSC.....	145
Fig. 8.3 Rotor Angle, Unit 27-Area 2, 3-Ph. Fault for 0.1s, Cord. PSSs&TCSC.....	145
Fig. 8.4 Rotor Angle, Unit 25-Area 2, 3-Ph. Fault for 0.1s, Cord. PSSs&TCSC.....	146
Fig. 8.5 Rotor Angle, Unit 24-Area 2, 3-Ph. Fault for 0.1s, Cord. PSSs&TCSC.....	146
Fig. 8.6 Rotor Angle, Unit 23-Area 2, 3-Ph. Fault for 0.1s, Cord. PSSs&TCSC.....	147
Fig. 8.7 Rotor Angle, Unit 17-Area 1, 3-Ph. Fault for 0.1s, Cord. PSSs&TCSC.....	147
Fig. 8.8 Rotor Angle, Unit 3-Area 3, 3-Ph. Fault for 0.1s, Cord. PSSs&TCSC.....	148
Fig. 8.9 Electrical Power, Unit 28-Area 2, 3-Ph. Fault for 0.1s, Cord. PSSs&TCSC	149
Fig. 8.10 Electrical Power, Unit 25-Area 2, 3-Ph. Fault for 0.1s, Cord. PSSs&TCSC ..	149

Fig. 8.11 Electrical Power, Unit 20-Area 2, 3-Ph. Fault for 0.1s, Cord. PSSs&TCSC ..	150
Fig. 8.12 Electrical Power, Unit 16-Area 1, 3-Ph. Fault for 0.1s, Cord. PSSs&TCSC ..	150
Fig. 8.13 Electrical Power, Unit 3-Area 3, 3-Ph. Fault for 0.1s, Cord. PSSs&TCSC	151
Fig. 8.14 Speed Deviations, Unit 28-Area 2, 3-Ph. Fault for 0.1s, Cord. PSSs&TCSC.	152
Fig. 8.15 Speed Deviations, Unit 19-Area 2, 3-Ph. Fault for 0.1s, Cord. PSSs&TCSC.	152
Fig. 8.16 Speed Deviations, Unit 16-Area 1, 3-Ph. Fault for 0.1s, Cord. PSSs&TCSC.	153
Fig. 8.17 Speed Deviations, Unit 3-Area 3, 3-Ph. Fault for 0.1s, Cord. PSSs&TCSC...	153
Fig. 8.18 Voltage, Bus 63-Area 2, 3-Ph. Fault for 0.1s, Cord. PSSs&TCSC.....	154
Fig. 8.19 Voltage, Bus 44-Area 1, 3-Ph. Fault for 0.1s, Cord. PSSs&TCSC.....	155
Fig. 8.20 Voltage, Bus 115-Area 3, 3-Ph. Fault for 0.1s, Cord. PSSs&TCSC.....	155
Fig. 8.21 Active Power, Line 63 to 44, 3-Ph. Fault for 0.1s, Cord. PSSs&TCSC	156
Fig. 8.22 Active Power, Line 115 to 38, 3-Ph. Fault for 0.1s, Cord. PSSs&TCSC	157
Fig. 8.23 Active Power, Line 118 to 41, 3-Ph. Fault for 0.1s, Cord. PSSs&TCSC	157
Fig. 8.24 Ex. Max. Power Transfer, 3-Ph. Fault for 0.1s, Cord. PSSs&TCSC	159
Fig. 8.25 New Max. Power Transfer, 3-Ph. Fault for 0.1s, Cord. PSSs&TCSC	160
Fig. 8.26 New Max. Power Transfer, Line 44 to 63, Sensitivity 1, Cord. PSSs&TCSC	161
Fig. 8.27 New Max. Power Transfer, Line 44 to 63, Sensitivity 2, Cord. PSSs&TCSC	161

LIST OF ABBREVIATIONS

ANN	:	Artificial Neural Network
APBIL	:	Adaptive Population Based Incremental Learning algorithm
AVR	:	Automatic voltage regulator
CIGRE	:	Council for Large Electric Systems
Cord.	:	Coordinated
D	:	Machine damping coefficient
DE	:	Differential Evolution
DYNRED	:	Dynamic Reduction Program
EP	:	Evolutionary Population Algorithm
EPRI	:	Electric Power Research Institute
Eq'	:	Generator q-axis internal voltage
ESST4B	:	Proportional/Integral Excitation System
Ex.	:	Existing
EXAC1	:	IEEE Type AC1 Excitation System
EXAC2	:	IEEE Type AC2 Excitation System
EXPIC1	:	Proportional/Integral Excitation System
EXST1	:	IEEE Type ST1 Excitation System
EXST2	:	IEEE Type ST2 Excitation System
FACTS	:	Flexible AC Transmission Systems
FSC	:	Fixed Series Compensation
FVSI	:	Voltage Stability Index
Fig.	:	Figure
GA	:	Genetic Algorithm
GAST	:	Gas turbine-governor model
GENROU	:	Round Rotor Generator Model (Quadratic Saturation)
HVDC	:	High Voltage Direct Current
id, iq	:	d and q axis armature current
IEE2ST	:	Dual-input signal power system stabilizer model
IEEE	:	Institute of Electrical and Electronics Engineers
IEEG1	:	IEEE type 1 turbine-governor model
IEEEST	:	IEEE power system stabilizer model
IEEET1	:	IEEE type 1 excitation system model
I_{source}	:	Generator current
K_s, T₁- T₄, T_w	:	Gain and time constant of power system stabilizers
K_{TCSC}, T_{1TCSC}- T_{4TCSC}, T_{wTCSC}	:	Gain and time constant of Thyristor Controlled Series Capacitors
M, H	:	Machine inertia coefficient and inertia constant
NSGAI	:	Non-dominated Sorting Genetic Algorithm

NYPS	: New York City power System
PBIL	: Population Based Incremental Learning
PF	: Participation Factor
P_{gen}	: Dispatched power – Specified output power
PID	: Proportional-Integral-Derivative Control
P_m , P_e	: Generator mechanical and electrical power
P_{max}	: Generator maximum active power
P_{min}	: Generator minimum active power
POD	: Power Oscillation Damping
Prop.	: Proposed
PSO	: Particle Swarm Optimizer
PSS	: Power System Stabilizer
PSS/E	: Power System Simulator for Engineers
PSS2A	: IEEE Dual-Input Stabilizer Model
PSSPLT	: Power System Simulator plotting program
Pu	: Per Unit
Q	: Reactive Power
Q_{max}	: Generator maximum reactive power
Q_{min}	: Generator minimum reactive power
Red.	: Reduced
R_{machine}	: Machines Resistance
ROW	: Right of Way
S	: Apparent Power
SCRX	: Bus or solid fed SCR bridge excitation system model
SMIB	: Single-Machine Infinite Bus
SOPF	: Sequential Optimal Power Flow
SQP	: Sequential Quadratic Programming
STATCOM	: Shunt Synchronous Static Compensator
SVC	: Static Var Compensator
t	: Time in second
TCSC	: Thyristor-Controlled Series Compensator
Tdo'	: Open circuit field time constants in d-axis
tg	: Transformer tap ration
TGOV1	: Steam turbine-governor model
TGOV3	: Modified IEEE type 1 turbine-governor model with fast valving
Tqo'	: Open circuit field time constants in q-axis
UPFC	: Unified Power Flow controller
V₁, V₂	: Voltage magnitudes of buses 1 and 2
vd, vq	: d and q axis terminal voltage
Volt.	: Voltage
X_C	: Controlled TCSC reactance combined with fixed-series capacitor

\mathbf{X}_L	:	Line-inductive reactance
$\mathbf{X}_{\text{machine}}$:	Machines Reactance
\mathbf{X}_{max}	:	Maximum TCSC reactance compensation
\mathbf{X}_{min}	:	Minimum TCSC reactance compensation
\mathbf{X}_{ref}	:	Steady-state reactance-reference signal
$\mathbf{x}_q, \mathbf{x}_q'$:	q-axis reactance and q-axis transient reactance
\mathbf{X}_{TCSC}	:	TCSC equivalent reactance
\mathbf{Y}	:	Network Admittance Matrix
$\mathbf{Z}_{\text{negative}}$:	Generator sub-transient saturated negative sequence impedance
$\mathbf{ZTR}_{\text{negative}}$:	Transformer negative sequence impedance
$\mathbf{Z}_{\text{positive}}$:	Generator sub-transient saturated positive sequence impedance
$\mathbf{ZTR}_{\text{positive}}$:	Transformer positive sequence impedance
$\mathbf{Z}_{\text{source}}$:	Generator sub-transient unsaturated positive sequence impedance
\mathbf{Z}_{zero}	:	Generator sub-transient saturated zero sequence impedance
\mathbf{Z}_t	:	Step up transformer impedance
$\mathbf{ZTR}_{\text{zero}}$:	Transformer zero sequence impedance
δ	:	Phase angle of the Norton equivalent current
$\Delta\omega$:	Generators speed deviation
$\ddot{\Psi}_d', \ddot{\Psi}_q'$:	Generator d and q axis flux linkage
ω_0, ω	:	Synchronous speed and rotor speed, respectively

THESIS ABSTRACT

Full Name : Malik Mohammed Ashtar Al Hajji
Thesis Title : FACTS Based Stabilizers for Dynamic Stability Enhancement
of Weakly Interconnected Power Systems
Major Field : Electrical Engineering
Date of Degree : January 2015

Low frequency oscillations phenomenon in power system could cause system instability after a severe disturbance and it could limit power system operation and control. Therefore, attenuating these oscillations has to be accomplished effectively, so the system remains stable and reliable. Thus, the objectives of this research are to investigate the existence of such phenomenon in a real large-scale power system and then scrutinize the impact of three controller design approaches on enhancing its overall dynamic stability. It is worth to mention that instead of using the complete model of the power system to perform the analyses, a reduced version is utilized. The latter is constructed via developing a systematic approach for building static and dynamic equivalent of such huge power system. The first controller design approach inspects a coordinated design between a proposed and existing Power System Stabilizers (PSSs). The second approach studies an individual design of a proposed Thyristor Controlled Series Capacitor (TCSC) based stabilizer. The last approach tests a simultaneous design of the aforementioned PSSs and TCSC. In each case, the design problem is manipulated and solved by a novel technique integrating a Modified Particle Swarm Optimization technique (MPSO) with nonlinear time-domain simulations. The objective function of the MPSO is based on nonlinear fitness function for minimizing Integral Time Weighted Absolute Error (ITAE). In all cases, the expected enhancement on the overall dynamic stability is assessed by modal analyses as well as nonlinear time-domain simulations. To examine the robustness of the proposed controllers, their optimized parameters are incorporated into the full power system and then several severe incidents are tested considering different operating conditions. The results show that each method can successfully damp the low frequency oscillations and increase power transfer capability among the weakly interconnected areas with superiority of the third design approach. In addition, this research demonstrates the accuracy of the developed systematic approach for reducing large-scale power system, so the reduced model can be utilized for controller design.

MASTER OF SCIENCE DEGREE

KING FAHD UNIVERSITY OF PETROLEUM & MINERALS, DHAHRAN

JANUARY 2015

ملخص الرسالة

الاسم الكامل: مالك بن محمد بن أشتر الحاجي

عنوان الرسالة: تحسين الاستقرار الديناميكي للنظم الطاقة الكهربائية باستخدام مضبطات نظم الطاقة و المضبطات المستندة على الأنظمة المرنة لنقل التيار المتردد

التخصص: ماجستير علوم هندسة كهربائية

تاريخ الدرجة العلمية: يناير 2015

قد تؤدي ظاهرة الاهتزازات ذات الترددات الضئيلة في نظم الطاقة الكهربائية إلى تضييق استقرار النظام الكهربائي أو إلى عدم استقراره بعد حدوث قصر كهربائي شديد. لذلك أولى كثير من الباحثين اهتماما كبيرا للحد من هذه الظاهرة عبر تقديم بعض الحلول الفنية كاستخدام أجهزة مضبطات نظم الطاقة و المضبطات المستندة على الأنظمة المرنة لنقل التيار المتردد. حيث اثبتت كثير من البحوث العلمية و العملية كفاءة هذه الأجهزة في تهيبط الترددات الضئيلة إلى الحدود المسموحة فنية أو إخمادها كليا. كذلك تبين كثير من البحوث العلمية أفضلية تصميم مكونات هذه الأجهزة باستخدام إحدى طرق التصميم المثلى بدلا من استخدام الطرق التقليدية. كما اثبت العديد من الباحثين أن التنسيق بين نظم التحكم المختلفة في المنطقة الواحدة او المناطق المترابطة يسهم في الاستفادة القصوى منها. لذلك يتضمن هذا البحث دراسة مستقبضة لإحدى نظم الطاقة الكهربائية المحلية للكشف عن وجود هذه الظاهرة بين المناطق المترابطة. لكن قبل البدء في التحاليل الديناميكية، يتطلب البحث اختزال النظام الكهربائي لتقليص حجمه دون فقد خواصه الديناميكية لتسهيل عملية تحليله و تصميم مكونات أجهزة التحكم. بعد ذلك يتم تحليل النظام الكهربائي المختزل للكشف عن وجود ترددات ضئيلة عن طريق التحاليل الشكلية و المحاكاة الزمنية الغير خطية لإشارات الشبكة. يهدف هذا البحث إلى دراسة ثلاث طرق لتصميم مكونات أجهزة التحكم لتحسين الاستقرار الديناميكي و لتقليل الترددات الضئيلة أو إخمادها كليا. الطريقة الأولى تعتمد على تركيب أجهزة مضبطات نظم الطاقة و تصميم مكوناتها بشكل متزامن مع بقية الأجهزة المماثلة القائمة. الطريقة الثانية تدرس خيار تركيب أحد أجهزة المضبطات المستندة على الأنظمة المرنة لنقل التيار المتردد و تصميم مكوناته بشكل منفرد. الطريقة الثالثة تدمج الطريقتين السابقتين، حيث يتم تصميم أجهزة مضبطات نظم الطاقة و الأجهزة المستندة على الأنظمة المرنة لنقل التيار المتردد بشكل متزامن. تم استخدام عدة برامج أهمها برنامجي محلل نظم الطاقة الكهربائية (PSS/E) لتحليل و اختزال النظام الكهربائي و برنامج الأفعى (Python) لبرمجة تقنية التصميم المثلى التي يطلق عليها اسم طريقة الحل المثلى سرب الجسيمات المعدلة. يتم تصميم مكونات المضبطات باعتبار نقطة تشغيل واحدة و من ثم يتم اختبار التصاميم المقترحة على النظام الغير مختزل باعتبار نقاط تشغيلية أخرى لتأكد من قوة ثبات نظم التحكم المقترحة. تثبت نتائج الدراسة بأن الطرق المقترحة لتصميم أجهزة التحكم فعالة و تسهم في تحسين الاستقرار الديناميكي للنظام و زيادة كفاءته و بالتالي زيادة قدرات النقل بين المناطق المترابطة. كذلك تبين الدراسة أن أفضل طريقة لتصميم نظم التحكم هي الطريقة الأخيرة من حيث أداء النظام الكهربائي. بالإضافة إلى ذلك تبين الدراسة ان الطريقة المتبعة لاختزال النظام الكهربائي دقيقة و يمكن استخدامها لتقليص حجم نظم الطاقة الكهربائية الكبيرة لاستخدامها في تصميم نظم التحكم.

درجة الماجستير في العلوم
جامعة الملك فهد للبترول و المعادن
يناير 2015

CHAPTER 1

INTRODUCTION

1.1 Introduction

In the past, present and it might continue in the future, power system utilities interconnect different areas to build the needed level of redundancy, improve system reliability, meet the rapid load growth continuously and dispatch generated power economically. However, they usually encounter many environmental and energy source constraints which prevent them from constructing new transmission lines or power generation plants. An example of such constraints is Right-of-Ways (ROWs) acquisition. These are required to construct overhead or underground transmission, however, they are very expensive and difficult to be obtained. Another example is the limitation or restriction of energy sources such that power plants cannot be built wherever required. These constraints force power utilities to stress their available power facilities to operate close to their thermal and/or dynamic stability limits. Thus, while transmitting bulk power between weakly interconnected areas through very long and heavily loaded transmission lines, low frequency oscillations (0.1-3 Hz) might occur. Another reason for such phenomenon could be the continuous changes on load demand. These oscillations might impose undesired limitations on power systems' operation and control. In case of a severe disturbance, continuous growing of these signals brings about the separation of weakly interconnected power systems [1].

Fortunately, there is a number of techniques which have been proposed to mitigate low frequency oscillations such as wide spread installations of Power System Stabilizers (PSSs) which are very effective devices in damping such oscillations. PSS is typically used to suppress machine electromechanical modes and improve overall power systems' stability. However, they may negatively affect the voltage profile and may lead to a leading power factor, when they are not designed properly. Also, the use of PSSs alone may not be, in some cases, sufficient to damp inter-Area oscillations.

Therefore, Flexible Alternating Current Transmission Systems (FACTS) have been suggested to lighten in such conditions. FACTS have a very essential effect to control power flow along transmission lines as well as to enhance dynamic stability. In spite of that, uncoordinated design of FACTS and PSSs may excite unwanted relations that lead to system deterioration. Therefore, power system utilities should carefully design the PSSs and FACTS in order to improve the overall dynamic stability of power systems.

1.2 Thesis Motivations

The main motivations of this research are summarized below:

- 1) Coordinated design of multiple PSSs for real power systems have not been implemented practically and have not been well addressed in literature.

- 2) Similarly, coordinated design of multiple PSSs and FACTS for practical power systems have not been investigated thoroughly in literature and have not been applied in real power systems.
- 3) Optimization techniques have not been practically employed for designing PSSs or FACTS.
- 4) Interest of developing an easy, accurate and systematic approach for building dynamic equivalent.

1.3 Thesis Objectives

The following points describe the main objectives of this thesis:

- 1) Investigate the practicality of deploying optimization techniques on a real power system for designing the following controllers:
 - a. Coordinated design of multiple PSSs.
 - b. Individual design of Thyristor Controlled Series Capacitor (TCSC).
 - c. Coordinated design of multiple PSSs and TCSC.
- 2) Study the effectiveness of the above controllers in damping inter-Area oscillations and increasing power transfer capability among weakly interconnected areas.
- 3) Examine the feasibility of employing a systematic approach for reducing large power systems to design the aforementioned controllers.

1.4 Thesis Contribution

The Following are the main contributions of this work:

- 1) Development of a novel method for integrating Power System Simulator for Engineers (PSS/E) and Modified Particle Swarm Optimization technique (MPSO) within PSS/E environment to formulate the design problem to an optimization problem.
- 2) Deployment of the MPSO to design three types of controllers.
- 3) Development of a systematic approach for reducing large power systems utilizing the built in tools within PSS/E and using python program to automate the process.
- 4) Investigation of best input signals to the TCSC Power Oscillator Damper controller (TCSC-POD) via nonlinear time-domain simulations.
- 5) Utilization of Residue Method to find the optimal location for installing PSSs.

The success of this work will enrich the dynamic stability enhancement methods. Moreover, it will provide systematic procedures to coordinate the design of PSSs and FACTS based stabilizers aspiring for eco-technical solutions to improve the dynamic stability and increase power transfer capability among interconnected areas.

1.5 Thesis Organization

The thesis is organized as follow:

Chapter 2 presents the literature review which discusses related subjects such as power system modeling, power system reduction, PSS tuning methods, FACTS tuning methods and location optimization, optimization techniques, modal analysis, etc. Chapter 3 describes the considered power system models, such as types of synchronous machine, turbine governors, excitation systems, PSSs, TCSC, etc. Also, it gives brief introduction about the used programs for executing the required analyses. The controller design approaches is illustrated in chapter 4. Chapter 5 introduces power system reduction's theory, describes the considered power system, illustrates the deployed reduction methodology as well as demonstrates the accuracy of the implemented technique via applying it to the considered system. The coordinated design of multiple PSSs, optimal location and parameter settings are discussed in chapter 6. The individual design of TCSC is presented in chapter 7. In this chapter the best input signal to the TCSC-POD is investigated. In chapter 8, the simultaneous design of PSSs and TCSC is presented. Finally, the conclusion, recommendations and future work are stated in chapter 9.

CHAPTER 2

LITERATURE REVIEW

2.1 Overview

The following sections summarize the literature survey. The second and third sections cover the fundamental concepts of power system stability and control equipment, respectively. The fourth section discusses synchronous generators modeling. Then, the available methods used to reduce large power system is presented in the fifth section. The sixth section covers PSS's main concepts and tuning techniques. FACTS devices' concepts, optimal location and optimal parameter setting are presented in the seventh section. In the same section, the methodologies of coordinating the design of the PSS and FACTS devices are discussed. Also in the same section, TCSC's general concept, optimal location, optimal parameters setting and coordination are presented. Finally, the modal analysis technique is presented in the last section of this chapter.

2.2 Fundamentals of Power System Dynamic Stability

Large power systems contain many rotating equipment and control devices. Therefore, mixture of dynamic interactions could occur. There are many reasons causing power system dynamic stability to occur such as, change in power demand, single or three phase faults, loss of large generator, etc. These incidents create changes in network topology

and structure. Consequently, they could lead to either stable state or unstable one. The former happens when the power system returns to the same steady state point or reaches a new stable equilibrium point. While the latter occurs if the rotor angles of some of synchronous generators accelerate or decelerate up to a point which can cause full loss of synchronism with other generators [2].

Definition of power system stability: recently, IEEE and CIGRE proposed a definition to the power system stability which links initial operating conditions and nature and duration of certain disturbance with the power system stability. It states that power system stability is: “the ability of an electric power system, for a given initial operating condition, to regain a state of operating equilibrium after being subjected to a physical disturbance, with system variables bounded so that practically the entire system remains intact” [3].

There are three main types of power system stability which are classified according to the following:

- The physical nature of the resulting mode of instability as indicated by the main system variable in which instability can be observed.
- Considering the size (magnitude and duration) of the disturbance which influences the method of calculation and prediction of stability.
- The devices, processes, and the time span that must be taken into consideration in order to assess stability.

The three types are shown in the below Fig. 2.1:

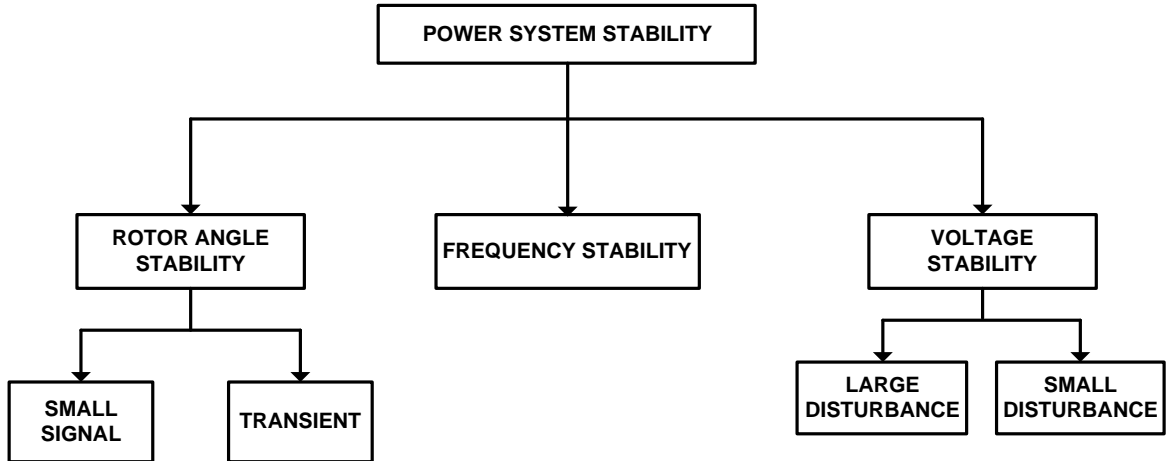


Fig. 2.1 Types of Power System Stability

Rotor Angle Stability is the ability of a power system to maintain synchronism during severe or small disturbances. It can be divided to transient stability and small signal stability. These two types are briefly described below:

Transient Stability is mainly caused by sever disturbances such as, three phase faults, loss of large generating unit, sudden loss of large loads, etc. The main reason of the instability, caused by this type of stability, is insufficient synchronizing torque to maintain synchronism. The behavior of power system is highly nonlinear in transient stability analysis, therefore, the nonlinear differential equations are used to describe and simulate the power system. The simulation period covering the transient stability

phenomena is from 1 up to 20 seconds, however, its effects appears within the first few cycles following the disturbances [2].

Small Signal Stability mainly happens due to small disturbances. The latter could be due to a continuous change in load demand, changes in scheduled voltages at generation plants, etc. This phenomenon occurs due to a lack of adequate damping of a natural resonance frequency in the electric system. The interactions, which cause small signal instability, are basically linear in nature. Thus, small signal stability analysis is normally calculated using linearized power system equations by applying linear algebra techniques such as, eigenvalues and eigenvectors. In addition to that, small signal stability could be analyzed by combining both linear and dynamic analysis to investigate the existence of this phenomenon. Thus, the simulation period of this type of simulation could reach up to 30 seconds, so the system regains its linearity. This phenomenon consists of many oscillation modes such as local, inter-area, control and torsional modes. The following paragraph explains main causes and frequency ranges of these modes of oscillations [2].

Local Modes are usually associated with units at an individual power plant or a group of plants, sited at nearby power stations, oscillating with respect to the remainder of the system. Their frequency range is between 1 up to 2 Hz. **Inter-Area modes** occur when two power systems oscillate against each other. Their frequency range lays between 0.1 up to 1 Hz. The **Control Modes** are usually associated with control systems such as excitation systems, FACTS devices, etc. Their frequency range is almost similar to the

previous modes 0.2 up to 2 Hz. **Torsional Modes** are associated with shaft trains of turbine systems. Their frequency range for steam turbines, which is usually the machines of greatest concern due to shaft length, stiffness, damping and torsional modes, is usually between 10 to 50 Hz for 60 Hz machines [2].

Frequency stability can be defined as the ability of a power system to maintain constant frequency within a normal range of the operating frequency following a severe system disturbance resulting in a significant imbalance between generations and loads. Frequency stability depends on the ability to maintain or restore equilibrium between system generation and load, with minimum unintentional loss of load [2].

Voltage Stability can be defined as the ability of a power system to maintain acceptable voltages at all buses in a power system under normal operating conditions and contingency or disturbance conditions. A system could be vulnerable to voltage instability situation when there is an increase in demand while the system is not able to meet the demand for reactive power. Thus, any disturbances or any change in system conditions results in progressive uncontrollable decline in voltage. On the other hand, a system is voltage stable when, for all buses in the system, the voltage increase as the reactive power injection is increased [2].

2.3 Power System Control Equipment

Power systems have to be highly reliable and secured to avail continuous power to end users. Moreover, they should meet instantaneous changes in load demand. Also, they should keep the frequency almost constant all the time. Similarly, they should be planned to maintain constant level of voltage.

Therefore, various components of power systems have to be carefully coordinated and controlled. These components are mainly controlled by the following devices [2]:

- Generators Controllers, such as turbine governors, excitation systems and PSSs.
- Transmission lines Control like FACTS devices, High Voltage Direct Current transmission lines HVDC, synchronous condensers, static reactive power devices, tap-changing transformers, etc.
- System Control such as monitors system voltage and frequency, monitors tie-line flows, monitors stability margin, performs control operation, Phasor Measurement Units, etc.

2.4 Synchronous Generator Modeling

Generator modeling is the most important factor in power system analysis. Once it is modeled correctly, more accurate results are expected. Therefore, during 1920s and 1930s, many researches had intensively concentrated in working out this important

problem [2]. In general, there are many models which have been introduced in the literature, such as the classical model, third order model, fourth order model, sixth order model, etc. The degree of accuracy and complexity increases as the order increases. Patel et al adopted a second order simplified representation of a generator model. The latter was represented by a constant voltage source behind a direct axis transient reactance [4]. However, this model neglects many important characteristics of the machine's dynamics such as saliency, variation in flux linkages, governor control and load dynamics. On the other hand, more detailed approaches of synchronous generator modeling have been illustrated in [5-7]. These references considered most of the neglected dynamic behavior of the synchronous machine. As such, generators could be represented by any of the aforementioned models, however, this depends on the type of required studies. Indeed to gain a full representation of actual systems, detailed representation of synchronous machines is highly recommended.

2.5 Power System Reduction

Due to the huge size of most of power systems, simulations and control design are very complex and time consuming. Therefore, many techniques have been proposed to reduce large power systems. The reduction methods can be divided into two types: 1) Static Reduction and 2) Dynamic Reduction. The former is useful for load flow analysis, while, the latter is used for dynamic simulations and control design. The dynamic reduction entails three steps as follows: 1) identification of coherent machines, 2) aggregation of coherent units and 3) static reduction of the network.

The dynamic reduction methods have been discussed thoroughly in literature [8-41]. However, the most famous methods are coherency based method [8-18], modal analysis equivalent method [19], time-domain aggregation method using structure preservation [20-25] and slow coherency base method [17,26].

One of the coherency based method utilized Least Square Fit method to build the dynamic equivalent for a group of coherent units. These units were equivalent via aggregating their turbine governor, exciter and PSSs. The advantage of this method is that it keeps the physical meaning of the aggregated units such that after reduction the reduced system can be modeled in most of conventional utility programs [18]. However, this method requires a lot of matrix manipulations and optimization techniques for reducing the error between the full and reduced power system. Unlike this method, modal analysis was utilized to recognize and eliminate unexcited modes of oscillations occurred due to certain disturbances in certain areas [19]. However, this method was not used extensively due to the difficulties of determining the unexcited modes. Also, it was not widely employed due to the need of modifying stability simulation programs to use a state matrix form of the equations of the equivalent system. These disadvantages could be avoided by utilizing the time-domain aggregation method using structure preservation. The control devices of the machines can be dynamically aggregated using time-domain aggregation using structure preservation. Thus, the equivalent models can maintain the same dynamic characteristics of the complete power system [20-25].

To automate the above methods, many computer programs have been developed [28-40]. As an example, in the late 1960s, EPRI developed a powerful program called DYNRED for building the dynamic equivalent of power systems. This program was tested and extensively discussed in reference [28 - 30]. Also, Power System Simulator for Engineers PSS/E was utilized to perform time-domain simulation and identify coherent generators to construct the required equivalent dynamic model [31,32].

Besides the conventional computer programs, intelligent techniques, such as Artificial Neural Network (ANN), have been also used to get the equivalent model of external power system and it revealed promising results [33,34]. In 2012, a hybrid dynamic equivalent, consisting of both coherency-based conventional equivalent and artificial neural network (ANN)-based equivalent, was studied [35]. While in 2013, a measurement-based method replaces an external system with a simple equivalent and estimates its parameters through optimization method [36]. An interesting reduction method is presented in [37], where the algorithm runs PSS/E within MATLAB environment such that the dynamic data for a set of equivalent machines are tuned to minimize the difference between the transient responses obtained from both full and reduced models.

2.6 Power System Stabilizer (PSS)

Excitation systems with high transient gain and small time constants tend to reduce the damping of generator rotor angles' oscillations. This negative damping effect can be counteracted by making the excitation system respond to rotor angle motion as well as deviations of terminal voltage under transient conditions, while being sensitive only to terminal voltage in the steady state. This could be done by applying a supplementary stabilizing signal derived from the deviation of rotor speed, generator frequency, accelerating power, or dual signal combining any two of them. In the following paragraphs a comprehensive discussion and latest update associated with PSSs are presented.

2.6.1 General Concept of Power System Stabilizer

In early 1950s, many researches were carried out for investigating the effects of excitation control on damping low frequency oscillations which characterize the phenomena of stability. Specifically, it was found useful and practical to incorporate transient stabilizing signals derived from speed, terminal frequency, power, or dual signal superposed on the normal voltage error signal of voltage regulators to provide additional damping to these oscillations.

The basic concepts of adding supplementary stabilizing signal via PSSs were discussed in [42-48]. Demello and Concordia investigated stability of single machine infinite bus model of synchronous machine. They provided valuable explanation of excitation system effect. Also, they established a clear understanding of the stabilizing requirement [42]. Larsen and Swann extended the fundamental concepts of Demello and Concordia. They published three papers which discuss in details the main concepts, design and application of PSSs, respectively [43-45]. In addition to those papers, extensive explanations and analysis were demonstrated in [2] related to PSSs. In chapter 12, Kundur illustrated the basic function and fundamentals of PSSs. He discussed systematic procedures for designing PSSs parameters in order to add a supplementary signal to the exciters to compensate for the rotor speed deviation.

2.6.2 Optimal Location of Power System Stabilizer

A lot of work has been done to select the optimal location of PSSs to damp local mode as well as inter area modes of oscillations. There are many methods developed to select the best location of PSSs, however, the widely used are Participation Factor (PF), Eigenvalue Sensitivity Analysis and Residue (Prony) techniques [49-51]. The disadvantage of PF is that when the system has very closed eigenvalues, the eigenvectors could lose their physical meaning. Thus, one cannot conclude the best location of PSS easily. On the other hand, Prony analyses are rooted on time-domain simulations. So, in case of very close eigenvalues, the dominate eigenvector can be determined by the higher magnitude of oscillations [50].

2.6.3 Power System Stabilizer Parameters Optimization

In addition to the importance of selecting the optimal PSS's location, PSS's parameters shall be carefully designed, so the PSSs could provide enough damping to the local modes as well as inter area modes of oscillations. Many methods have been presented in the literature for tuning PSSs parameters such as self-tuning adaptive, Fuzzy logic integrated with Artificial Neural Network, weighting functions and H_{∞} methods [52-55].

Also, many optimization techniques have been utilized to design the PSS's parameters such as, Evolution Algorithm (EA), Gradient based, Genetic Algorithm (GA), Artificial Neural Network (ANN), Intelligence Swarm, Population Based Incremental Learning (PBIL), Adaptive Population Based Incremental Learning (APBIL) algorithm, Evolutionary Population (EP) algorithm, Fuzzy System and so on [56-64]. One of the most promising techniques for designing PSS's parameter is Particle Swarm Optimization (PSO) technique. It is a population based optimization technique created by Dr. James Kennedy and Dr. Russell Eberhart in 1995. PSO is a robust stochastic optimization technique inspired by the intelligent movement and social behavior of bird flocking or fish schooling. Moreover, it applies the concept of social interaction to problem solving. PSO has shown its rapid allocation of optimal solutions in many unimodal and multimodal search problems. It has been proven that the system performance after implementing this method is much better than that of gradient based and GA, since the oscillations are damped out much faster [60].

2.7 Flexible AC Transmission System (FACTS)

2.7.1 General Concept about FACTS

The primary function of FACTS is enhancing voltage stability. However, FACTS are also equipped with Power Oscillation Damping controllers (POD). Thus, FACTS controllers have been used to attenuate power system oscillations. The effectiveness of these controllers depends on their optimal location and parameters setting.

The optimal location, size and control parameters settings of FACTS are, in some cases, selected to achieve different objective functions like increasing power transfer capability, maximizing benefit to cost ration, relieving congestion in transmission lines, minimizing active power losses and so on. Thus, many techniques have been proposed to achieve the aforementioned objective functions. For instance, PSO, Differential Evolution (DE), GA, Heuristic, Practical rules, EP, eigenvalue analysis of network Jacobin matrix and Simulated Annealing are different methods which have been utilized to achieve the objective functions of interest [65 - 75].

Most of the above objective functions are mainly improving the steady state operation conditions. However, there are several publications which investigated the effect of the FACTS in enhancing the dynamic stability. Some of them used linear control approaches [76,77] while others applied nonlinear control approaches [78]. In addition to that, PSO

technique was employed in several research papers [79,80] to get the optimal setting of FACTS controllers.

2.7.2 Coordination of PSSs and FACTS

As mentioned in the introduction, PSSs are effective devices for damping generators local modes. However, they may not effectively damp inter-Area modes. Therefore, coordination between PSSs and FACTS better serve in damping inter-Area oscillations. Thus, several techniques have been presented in the literature discussing the coordinated design between PSSs and FACTS. Some of them employed optimal control and others used adaptive control strategies [81 - 99]. An interesting paper used ANN to coordinately design and optimize the parameters of PSSs and FACTS. The ANN was trained offline for wide range of operating conditions and credible contingencies. The considered objective function was based on maximizing the damping ratio of the electromechanical modes. The effectiveness of the proposed method was tested by time-domain simulations using a reduced power system [87]. Another author developed eigenvalue-eigenvector equalities constraints to simultaneously optimize the parameters of FACTS and PSSs. The author claimed that this method can avoid the iteration process required to calculate eigenvalues associated with new control parameters. Also, it does not require any special eigenvalue calculation software. The utilized objective function was based on minimizing the real part of any selected number of eigenvalue. The simulation results showed the usefulness of the above method in enhancing the dynamic stability of the considered power system [88].

Simultaneous design of dual-channel PSS, AVR and Thyristor Controlled Series Capacitor (TCSC) was researched for the first time in reference [98]. The Authors utilized PSO technique with multi-objective function for improving the damping ratio and damping factor. In the same year, other authors used different technique to design PSS and FACTS. They used conic programming to shift under-damped or unstable modes into a region of sufficient damping in the complex plane. This method involved two stages, the first stage was a phase compensation design that accounts for multiple operating conditions with FACTS and PSS while the second stage was gain tuning [99].

2.7.3 Thyristor Controlled Series Capacitor (TCSC)

2.7.3.1 General Concepts of TCSC

TCSC is a FACTS device that can provide fast and continuous changes of transmission line reactance. It is used to regulate power flow of transmission lines as well as to effectively damp inter-Area oscillations [100 - 113]. Basically, the series compensation is implemented to reduce the effects of series inductance of certain lines. Therefore, it mainly improves the maximum power transfer capacity of transmission lines. However, compensation of transmission lines by Fixed Series Capacitors (FSC) is most likely causing the below issues:

- Increases the loadability of the series compensated transmission lines.
- Adds losses in the compensated lines due to the enhanced power flow.

- Excites responsiveness of power flow in the series compensated line caused by outage of correlated transmission line in the system.
- Could cause new need for adding series compensation on parallel lines.

Fortunately, the above undesirable effects of series compensation can be resolved by controlling the level of series compensation instead of fixing it to certain value. This could be achieved by deploying the TCSC rather than FSC. The former can be partially applied to the total required level of compensation or for the whole series compensation. Some of the possible advantages of the TCSC are listed below [1]:

- Control the level of series compensation rapidly and continuously.
- Enable optimal power flow conditions and reduce the loop flow of power due to its dynamic controllability.
- Enhance the level of protection for series compensation via the thyristor. Since, the later rapidly bypass the series capacitors once it senses development of over-voltages across the capacitors after faults.
- Insert the series capacitors rapidly after the faults cleared to increase the level of dynamic stability.
- Reduce short circuit current level. Since during high short circuit current event the TCSC can switch from controllable-capacitive mode to inductive mode. Consequently, it restricts the short circuit current level.

2.7.3.2 Optimal Location of TCSC

Many researches have been done to identify the optimal location of TCSC, most of them are based on steady state analysis [100 - 106]. In 2011, an eco-technical evolution of TCSC placement with the emphasis on generation cost was performed. GA was used to find the best location of the TCSC based on minimizing the TCSC's investment cost, cost of installation and annual maintenance, and cost of generated active and reactive power [100]. In 2013, the same authors proposed an optimization approach to determine the best place for installing the TCSC in deregulated power systems. The proposed approach is based on investment recovery of FACTS devices with step by step variation in control parameters of the device. In this research Sequential Optimal Power Flow (SOPF) was used to find the maximum recovery cost [101]. Almost the same objective function was used in [102]. However, the second version of Non-Dominated Sorting Genetic Algorithm (NSGAI) was deployed to locate the best site of TCSC. The authors applied an objective function which considers real power flow performance index sensitivity and reduction of total system reactive power losses. The objective function was based on minimizing generation rescheduling cost. In 2013, the same authors used the same optimization technique to find the optimal location, number and steady state parameters setting of multiple TCSCs. However, the considered objective function is based on reducing the TCSCs' installation cost and the active power losses [103].

Also, PSO algorithm was used in [104] to select the optimal location of single TCSC device based on maximizing system loadability within system security and stability

margins. The authors considered different stability indices to assure security and stability margins, such as eigenvalues analysis, Fast Voltage Stability Index (FVSI) as well as line stability index. The authors claimed that by optimal allocation of TCSC, system loadability can be maximized and simultaneously the installation cost and active power loss of the controller can be reduced [104]. Unlike the latter reference, in [105] DE technique was applied to find the best location and settings of the TCSC based on minimizing transmission lines active power losses. According to the authors, DE produced better results than GA. All of the above publications [100 - 105] are simple and efficient, however, a major function of TCSC, which is damping power system oscillations, was not considered in these papers.

On the other hand, the dynamic aspects of the TCSC was investigated in a comprehensive study done for studying the application of TCSC on the New York State power system [106]. In this report, a controllability index was used to determine the best candidate transmission line for installing the TCSC. The controllability analysis was carried out by applying a small and temporary change in line reactance of several candidate lines, one at a time, and then assessing the magnitudes of the resulting network oscillations. The advantage of such approach is its simplicity and efficiency.

2.7.3.3 Optimal Parameters Setting of the TCSC

In contrast to the steady state methods used for calculating the TCSC location, many researches have been conducted to determine its optimal parameters based on dynamic stability. Some investigators utilized objective functions which are based on nonlinear time-domain simulations while others employed linear system analysis. In [107], PSO was deployed to design the TCSC and to find the best site for its installation. The objective function was based on maximizing the damping ratio of the eigenvalues concomitant with rotor speed deviations. The authors utilized three machines nine buses system to test the practicality of this technique. The same optimization technique was also used in [108]. However, the considered objective function was based on nonlinear dynamic simulation. It targets to minimize the overall rotor speed deviations. Other authors utilized Multi-Start Clustering Global Optimization technique to design two different types of TCSC structures namely a lead-lag and PID. The objective function was based on minimizing the performance index Integrated Absolute Error (IAE). The authors tested the effectiveness of the proposed controller approach by using SMIB [109].

2.7.3.4 Coordination of PSSs and TCSC

Besides the individual design of TCSC, a considerable number of publications has investigated the impact of the coordinated design between PSSs and TCSC for damping power system oscillations. For example, in reference [110] , a comprehensive research

studied the effects of the individual as well as the coordinated design of PSSs and TCSC on enhancing the power system stability. The tested power system was multi-machine power systems and the optimization technique was PSO. The eigenvalue analysis and nonlinear simulation results were carried out to demonstrate the effectiveness of the proposed stabilizers in enhancing system stability. Similarly, PSO was used in [111] for coordinating the PSS and TCSC. However, the objective function was different than that used in [110]. It was based on rotor speed deviations ($\Delta\omega$) minimization. Another optimization based tuning algorithm was proposed in [112] to coordinate the design of PSSs and TCSC simultaneously. The utilized algorithm was Sequential Quadratic Programming method (SQP) and the objective function was a multi-objective function for maximizing system damping ratios and minimizing real parts of poorly damped eigenvalues. In [113], the authors coordinated the design of PSSs and TCSC by transforming the design problem into a constrained optimization problem to search for the optimal settings. They implemented an objective function based on minimizing the real parts of any number of eigenvalues.

2.8 Modal Analysis

The modal analysis serves as an aid for interpreting dynamic simulation results; particularly analysis of cases with poor damping. In general, dynamic simulations run for an extended period of time to allow well-damped modes to attenuate and the system to regain linearity. Thus, the remaining lightly damped modes are characterized in terms of frequency and damping ratio. Then, oscillation nodes and antinodes are determined by

comparing the relative oscillation amplitudes and phases of representative units in the system [115].

However, application of this technique entails thorough understanding of important concepts such as eigenvectors, participation factors and residues. Eigenvalues and eigenvectors are valuable information in assessing both the severity of the damping problems and the best approach to their solutions. The latter include application of PSSs, FACTS devices, or network reinforcements. Moreover, comparison of damping performances before and after application of a particular remedial action, or between alternative mitigation actions (e.g., PSSs at alternative locations) guides the engineer towards the most cost-effective solution [50].

CHAPTER 3

SYSTEM MODELING

3.1 Overview

This chapter presents the models and programs used in this research. The following three sections cover load flow data modeling. Then, the fifth section discusses the utilized synchronous generator models. The sixth, seventh and eighth sections present governors, excitation systems and PSS models, respectively. In the ninth section, the deployed TCSC model is briefly described. Last but not least, a brief introduction about the utilized programs is presented in the last section of this chapter.

3.2 Bus Modeling

In PSS/E, there are many types of buses which can be modeled. However, in this work mainly three types are used as described in Table 3-1 below.

Table 3-1 Bus Types and PSS/E codes

Bus Type	Description	PSS/E Code
Constant P & Q	This is used mainly for load and non-generator buses. Where, P represents the constant active power of the load and Q indicates the constant reactive part	1
Constant P & V	This is used for generator or voltage controlled buses. Where, P represents the output active power of the unit and V indicates the scheduled voltage	2
Constant V & δ	This is specified for the swing bus. Where, V is fixed in magnitude and phase	3

3.3 Transmission Line Modeling

The transmission line model is represented in PSS/E by the general equivalent Pi model shown in Fig. 3.1 below. The description of the line parameters is listed in the below Table 3-2.

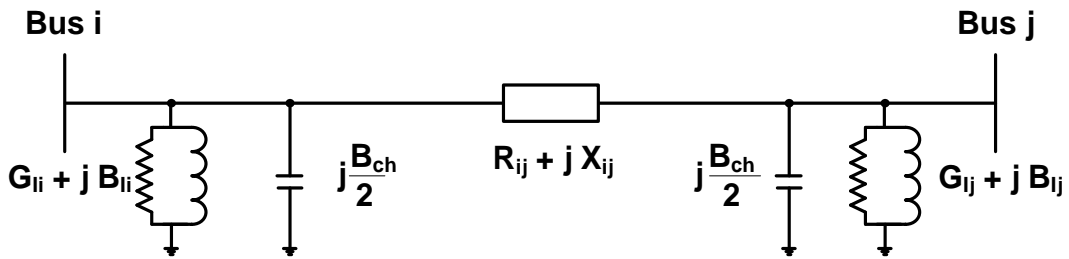


Fig. 3.1 Transmission Line Modeling in PSS/E

Table 3-2 Transmission Line Parameters

Parameter	Description
$R_{ij} + jX_{ij}$	Branch impedance in p.u.
$G_{1i} + jB_{1i}$	Sending end bus admittance in p.u.
$G_{1j} + jB_{1j}$	Receiving end bus admittance in p.u.
B_{ch}	Line charging in p.u.

3.4 Load Modeling

The utilized load model is a static load model. In the load flow simulation, it is represented as constant MVA consisting of real power component P in MW and reactive power component Q in MVAR. In the load flow, the load can be described by the following equation (3.1):

$$S = P + j Q \quad (3.1)$$

For dynamic simulation, the load is expressed as constant impedance model which represents the behavior of the load at any instant of time as algebraic functions of the bus voltage magnitude. The active power P and reactive power Q are considered separately as described in the following equations (3.2) and (3.3):

$$P(V, t) = P_0 \left(\frac{V(t)}{V_0} \right)^a \quad (3.2)$$

$$Q(V, t) = Q_0 \left(\frac{V(t)}{V_0} \right)^b \quad (3.3)$$

Where, $P(V, t)$ and $Q(V, t)$ are the real and reactive power as functions of voltage and time. While, P_0 and Q_0 are the initial values of the real and reactive power which are calculated from load flow solution. $V(t)$ is the voltage which is calculated for each time step, whereas, V_0 is the initial value of the voltage from load flow calculation. The exponential parameters a and b are the main identifiers of the relationship between the load and the voltage. The below Table 3-3 explains this relation:

Table 3-3 Load Modeling

Load Type	Value of a and b
Constant Power	$a = b = 0$
Constant Current	$a = b = 1$
Constant Impedance	$a = b = 2$

3.5 Synchronous Generator Modeling

3.5.1 Load Flow Representation

The standard generator structure used throughout the load flow analysis is shown in Fig. 3.2. It consists of voltage source behind a step up transformer. The former requires many input data as listed in Table 3-4 below, whereas, the latter needs the input data shown in Table 3-5.

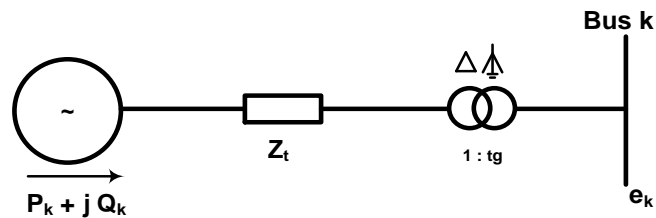


Fig. 3.2 Generator Modeling in Load Flow

Table 3-4 Generator Input Data in Load Flow

Input Data	Description
P_{gen}	Dispatched power / specified output power in MW
P_{max}	Maximum active power in MW
P_{min}	Minimum active power in MW
Q_{max}	Maximum reactive power in MVAR
Q_{min}	Minimum reactive power in MVAR
MVA base	Complex power – machine MVA
Z_{source}	Generator sub-transient unsaturated positive sequence impedance
$Z_{positive}$	Generator sub-transient saturated positive sequence impedance p.u.
$Z_{negative}$	Generator sub-transient saturated negative sequence impedance p.u.
Z_{zero}	Generator sub-transient saturated zero sequence impedance p.u.

Table 3-5 Transformer Input Data

Input Data	Description
$ZTR_{positive}$	Transformer positive sequence impedance in p.u. based on 100 MVA
$ZTR_{negative}$	Transformer negative sequence impedance in p.u. based on 100 MVA
ZTR_{zero}	Transformer zero sequence impedance in p.u. based on 100 MVA
Tap ratio	Transformer tap position
Connection Code	Transformer connection code (Y-Y, Y-delta,...etc.)

With the exception of real and reactive power and real and reactive power limits, all generator parameters are specified in per unit with respect to generator MVA base.

3.5.2 Dynamic Representation

In order to conduct dynamic simulation, the generator has to be converted to Norton equivalent circuit as shown in Fig. 3.3. The amplitude and phase of the Norton equivalent current are calculated using the below equation (3.4), while, the equivalent admittance is obtained using equation (3.5).

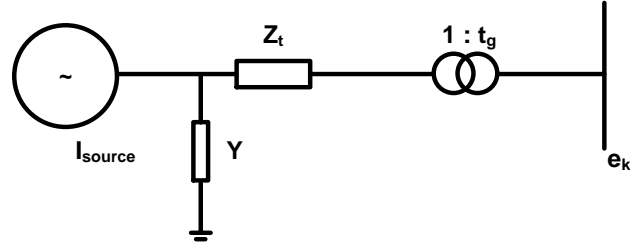


Fig. 3.3 Generator Modeling for Dynamic Simulation (Norton Equivalent)

$$I_{source} = (i_q - j i_d)(\cos \delta + j \sin \delta) = \frac{(\ddot{\psi}_d'' + j \ddot{\psi}_q'') \frac{\omega}{\omega_0}}{Z_{source}} (\cos \delta + j \sin \delta) \quad (3.4)$$

$$Y = \frac{1}{Z_{source}} \quad (3.5)$$

Where, I_{source} is the Norton equivalent current, Y is the Norton equivalent admittance, Z_{source} is the unsaturated sub-transient reactance, and δ is the phase angle of the Norton equivalent current. Z_t is the step up transformer impedance and t_g is its tap ratio. ω_0 and ω are the synchronous speed and rotor speed, respectively.

The utilized dynamic model of all generators is the electromagnetic solid round rotor model which is called (*GENROU*) in the PSS/E library. The block diagram of *GENROU* model is shown in appendix A [116,117].

3.6 Generator’s Control Devices

3.6.1 Governor Models

The considered turbine governor models are practical international standard turbine governors. Table 3-6 below summarizes the types and briefly describes each turbine governor [116,117].

Table 3-6 Turbine Governors Models

Governor Model	Description
IEEEG1	<i>“is the IEEE recommended general model for steam turbine speed governing systems.”</i>
TGOV3	<i>“is a modification of the IEEEG1 model, is now PTI’s recommended model for fast valving studies.”</i>
GAST	<i>“represents the principal dynamic characteristics of industrial gas turbines driving generators connected to electric power systems.”</i>
TGOV1	<i>“is a simple model representing governor action and the reheated time constant effect for a steam turbine.”</i>

The block diagrams for these four turbine governor types are shown in appendix B.

3.6.2 Excitation System Models

In this thesis, the used excitation systems are also practical international standard. They are summarized in Table 3-7 below [116,117].

Table 3-7 Excitation System Models

Exciter Model	Description
ESST4B	<i>“is used to represent static systems with both potential and compound source rectifier excitation.”</i>
EXPIC1	<i>“is recommended to be used for excitation systems where voltage regulator control element is a proportional plus integral type (PI).”</i>
EXST2	<i>“utilize both current and voltage sources derived from the generator terminal quantities as components of the power source. These compound source rectifier excitation systems are modeled by these ST2 models.”</i>
EXST1	<i>“is intended to represent systems in which excitation power is supplied through a transformer from the generator terminals (or the unit’s auxiliary bus) and is regulated by a controlled rectifier.”</i>
EXAC2	<i>“emulate a high initial response field controlled alternator-rectifier excitation system in which the alternator main exciter is used with non-controlled rectifier.”</i>
EXAC1	<i>“emulate a field-controlled alternator rectifier excitation system consisting of an alternator main exciter with non-controlled rectifiers.”</i>
SCRX	<i>“is a general model, not tailored to the representation of any specific excitation system.”</i>
IEEET1	<i>“is used to represent systems with shunt dc exciters as well as systems with alternator exciters and uncontrolled shaft-mounted rectifier bridges.”</i>

The block diagrams for these eight exciter types are shown in appendix C.

3.6.3 PSSs Models

Regarding the PSSs, three types are utilized in this study. Table 3-8 below shows these types and describes each one of them [116,117].

Table 3-8 Power System Stabilizer Models

PSS Model	Description
IEEEEST	<i>“implements the general-purpose supplementary stabilizer representation given in the 1979 IEEE modeling recommendations.”</i>
IEE2ST	<i>“is a derivative of IEEEEST, it allows two input signals to be summed to create the signal for processing by the phase-lead blocks.”</i>
PSS2A	<i>“Like IEEEEST, is a dual-input stabilizer. This model can represent a variety of stabilizers with inputs of power, speed, or frequency.”</i>

The block diagrams for these three types are shown in appendix D.

3.7 TCSC Model

The rapid adjustment of the series compensation, which is provided by the TCSC, maintains desirable magnitudes of power flow along transmission lines of interest. The following equation (3.6) illustrates the relationship between the power flow and the series compensation capacitance:

$$P_{12} = \frac{V_1 V_2}{(X_L - X_C)} \sin \delta \quad (3.6)$$

Where,

P_{12} : the power flow from bus 1 to bus 2

V_1, V_2 : the voltage magnitudes of buses 1 and 2, respectively

X_L : the line inductive reactance

X_C : the controlled TCSC reactance combined with fixed series capacitor

δ : the difference in the voltage angles of buses 1 and 2

From the above equation, it is quite evident that the power flow P_{12} of line 1 to 2 increases as the level of compensation increases in the same line. In other word, as X_C increases the dominator decreases and consequently the resultant value of P_{12} increases. In addition to that, the fast dynamic response of the TCSC provides fast changes on the compensation level, which in terms greatly enhances the system damping.

3.7.1 Description of the TCSC Power Oscillation Damper (POD)

PSS/E offers a TCSC model called "CRANI/TRANI" model. This model can be applied to any branch in the network except for transformers and zero impedance lines. The below Fig. 3.4 shows CRANI/TRANI controller which comprises of four blocks. The first block is a measurement block with time constant T_1 . The second block is a washout stage with time constant T_w for eliminating the average component of the measured input signal. The third blocks is a lead-lag filter with time constants T_2 and T_3 which provides the required phase compensation. Then, these are followed by a gain K_{TCSC} which determines the damping level of power oscillation. X_{ref} is a steady state reactance reference signal which is added to an output signal emanating from the POD controller. Then two limits, X_{max} and X_{min} , are imposed in the limitation block on the TCSC reactance output X_{TCSC} .

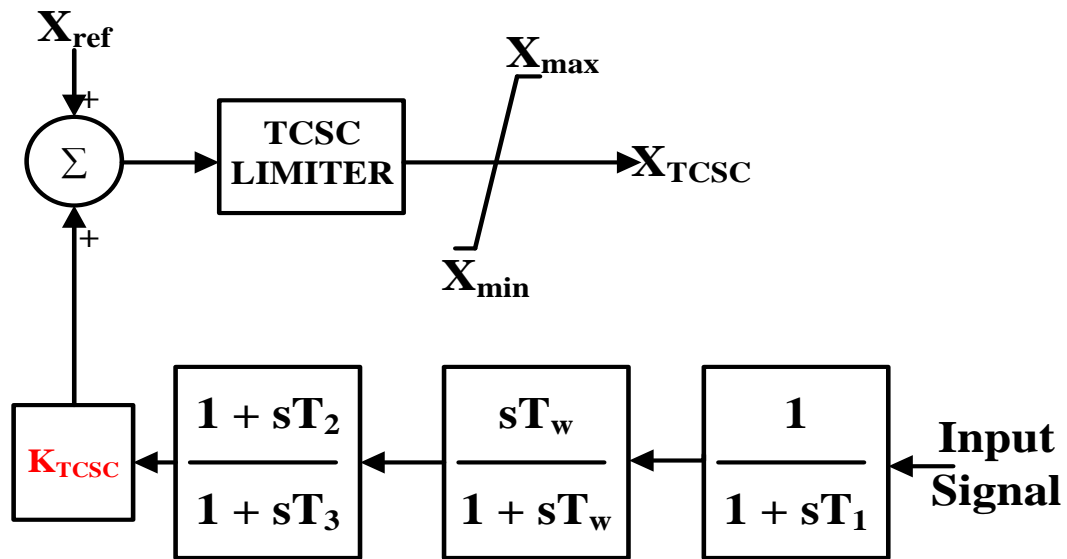


Fig. 3.4 TCSC Power Oscillations Damper (POD)

CRANI/TRANI model requires several input data as listed in Table 3-9 below. This table shows typical values of the controller's parameters [116,117].

Table 3-9 TCSC Parameter Typical Values

Parameter	Range Values
T_{1TCSC}	0 to 5
T_{wTCSC}	0 to 2
T_{2TCSC}	0 to 5
T_{3TCSC}	1 to 20
K_{TCSC}	$\leq (1/3 \text{ the gain of the instability of the TCSC})$
X_{max}	$X_{max} = 1.50 \times X_{ref}$
X_{min}	$X_{min} = 0.25 \times X_{ref}$

3.7.2 TCSC Input Signals

Any damping device must have controllability, observability and must define a stable control loop. Controllability means that the device must be able to impact a critical lightly damped oscillation. Observability means that the input signal to the controller of the damping device must be responsive to the aforementioned oscillation modes. Since there are various input signals which can be fed to the TCSC, observability index has to be used to determine the most effective one. The following are possible input signals which can be used for the TCSC [1,106]:

- Line current
- Active power of the compensated line
- Bus voltage
- Bus frequency
- Rotor angle/speed deviation of a remote generator
- Rotor angle/ speed (frequency) differences across the system
- Active Power on adjacent line

In chapter 7, nonlinear time-domain simulation is utilized to identify the best observable input signal that leads to the best damping effects on the power oscillations of the compensated line.

3.8 Utilized Software

3.8.1 Power System Simulator for Engineers (PSS/E)

Power System Simulator for Engineers (PSS/E) is a comprehensive power system analysis program which is widely used by power system utilities in many countries. It was created in 1976 by Power Technology Institute (PTI) which is currently owned by Siemens.

PSS/E has many powerful tools for conducting various kinds of power system analysis. The below functions are examples of the PSS/E's built-in tools:

- Load Flow Simulation
- Balanced and unbalanced short Circuit Calculation
- Network Equivalent
- Optimal Power Flow
- Modal Analysis
- Dynamic Simulation

In this thesis the load flow, network equivalent, modal analysis and dynamic simulations are executed using PSS/E.

3.8.2 Python Program

The Python program is an open source programming language. It was created by Guido Van Rossum in 1991. Python is an interactive, interpreted, object-oriented, high level programming language. It has many significant features, where, the most important one is its capability to interact with various windows programs. Microsoft Excel, Microsoft word, MATLAB and PSS/E are some examples of these accessible programs which can be integrated using Python language.

In this thesis, Python is used to automate the network reduction, dynamic simulation and to develop and integrate MPSO with PSS/E to design PSSs and TCSC within PSS/E environment. Moreover, it is used to integrate PSS/E with Excel, notepad and MATLAB for plotting purpose.

CHAPTER 4

PROPOSED CONTROLLER DESIGN APPROACH

4.1 Overview

Power System stability can be analyzed thoroughly using modal analysis , linear analysis or nonlinear time-domain simulations. Moreover, it can be significantly enhanced via deploying well-designed control devices, such as PSS and TCSC. In this thesis, three controller design approaches will be employed to improve the dynamic stability and increase power transfer capability between weakly interconnected areas. The first one will be achieved by implementing coordinated design technique to tune multiple PSSs. The second technique will be accomplished by installing a new TCSC in series with a selected transmission line and individually tuning its POD controller's parameters. Lastly, multiple PSSs and the TCSC will be simultaneously designed. It is worth mentioning that, all of the aforementioned design problems will be formulated as optimization problems in which MPSO will be used to perform the optimization task. Also before and after deploying the optimized controllers, modal analysis and nonlinear time-domain simulations will be used to assess the dynamic stability of the considered power system.

The proposed controller design is performed by implementing a simple but effective approach as described below:

- 1) The first step is preparing a base case representing the full version of the considered power system.
- 2) The second step is carrying out load flow and contingency analysis to solve the base case and assure its convergence for all single and double circuit contingencies.
- 3) The third step is reducing the full version of the considered power system to a lower order via static and dynamic reduction.
- 4) The fourth step is executing dynamic simulation via applying a severe three phase fault for 0.1 second and then clearing it by tripping a double circuit line. The considered simulation period is 20 seconds.
- 5) In case of multiple PSSs coordination, residue method will be deployed to locate the optimal place for installing new PSSs.
- 6) In case of individual design of TCSC, nonlinear time-domain simulation will be employed to assess the best input signal to the TCSC.
- 7) The MPSO integrated with the nonlinear time-domain simulation, which is executed by PSS/E, will be utilized to optimize the controller parameters.
- 8) Nonlinear time-domain simulation and modal analysis will be carried out to investigate the existence of small signal oscillations, identify dominant Electromechanical Modes (EM) and to evaluate the power system's performance.

- 9) To validate the effectiveness and robustness of the proposed controllers, they will be incorporated into the full version of the considered power system and then the following additional cases will be executed:
 - a) Determination of the maximum power transfer of the existing power system, without and with the proposed controller.
 - b) Calculation of the new maximum power transfer capabilities.
 - c) Application of several faults in different locations considering the new maximum transfer base cases and monitoring several electrical and electromechanical quantities..

Fig. 4.1 illustrates the flowchart of the above steps while the next subsections describe them in details.

4.2 Base Case Preparation

The following points briefly describe the main steps required to develop the study case:

- 1) Preparation of a converged load flow base case: this includes modeling of different types of buses, transmission line branches, two and three winding transformers, power plants, loads, reactive power resources, TCSC, etc.

- 2) Adjustment of generation dispatch and loads: this involves balancing the generation with load demand. Also, enough generation reserve has to be maintained.
- 3) Limit checking: bus voltages and transmission line facilities overloading limits have to be monitored and then adjusted as possible.
- 4) Preparation of dynamic models file: this includes modeling of all rotating equipment and control devices, such as synchronous generators, governors, exciters, PSSs, and TCSC-POD.
- 5) Conversion of loads and generators: before starting the dynamic simulation, loads and generators have to be converted in the load flow base case as explained here after:
 - The load conversion process changes the constant power loads (constant MVA) to 100 % constant current for real power components and 100 % constant admittance for reactive power part. This is what so called constant impedance load . Activity convert load (CONL) in PSS/E is used to perform this task.
 - Also, the generators have to be converted using activity convert generators (CONG) , such that voltage sources in series with their sub-transient impedances are changed to Norton equivalent current sources in parallel with their sub-transient shunt admittances.
- 6) The change of generators modeling to their dynamic forms removes all swing buses (bus code 3) from the system. This necessitates re-ordering and factorizing the resultant Y network matrix to form the optimal ordering of the Y matrix.

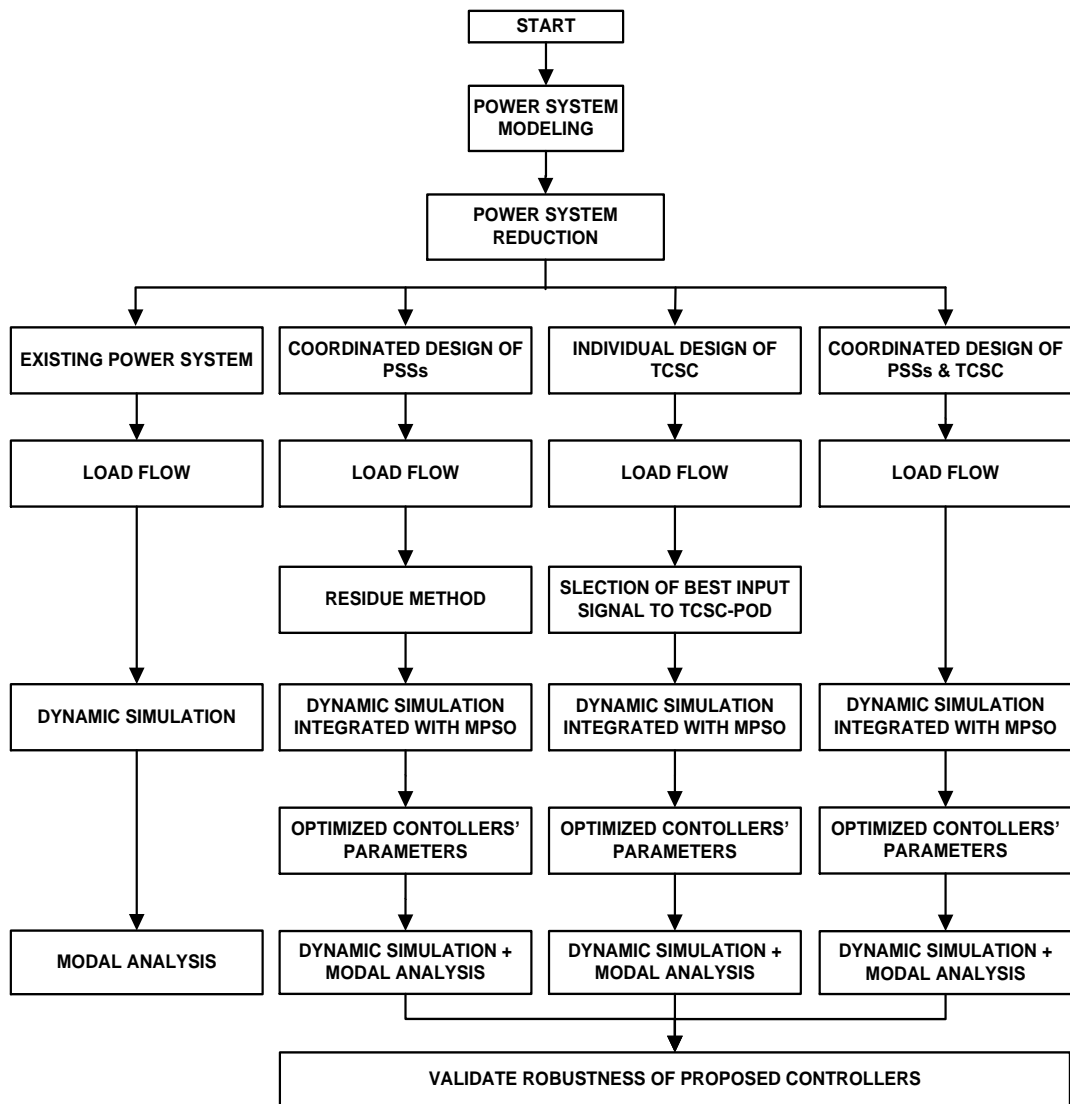


Fig. 4.1 Proposed Controller Design Approach Flowchart

7) Before reading the dynamic models, the base case has to be solved using the Triangularized Y matrix network solution (TYSL). This step as well as factorization step gives a refinement of the power flow solution to obtain the smallest possible mismatch at all buses.

- 8) Finally, the dynamic models have to be read to build communication environment between the converted base case along with the calculated initial conditions and the dynamic models along with their state variables.

4.3 Power System Reduction

This work presents a systematic approach to develop dynamic equivalents of large-scale power systems using PSS/E. The proposed approach entails three main steps:

- 1) Identification of small power plants, which are connected to high voltage network (< 380 kV level), and netting them with loads.
- 2) Aggregation of coherent generators using static and dynamic reduction equations which will be described in chapter 5.
- 3) Static reduction of high, medium and low voltage buses using PSS/E built in functions while retaining the extra high voltage network.

In order to demonstrate the accuracy of the reduced power system, a severe three phase fault, cleared by tripping a double circuit line, will be applied on both the reduced as well as the full versions of the considered power system and then compare their dynamic responses.

4.4 Load Flow Solution Method

PSS/E offers five power flow solution algorithms as listed below:

- 1) Fully coupled Newton-Raphson iteration.
- 2) Decoupled Newton-Raphson iteration.
- 3) Fixed slope Decoupled Newton-Raphson iteration.
- 4) Gauss-Seidel iteration
- 5) Modified Gauss-Seidel iteration

In this work, the first method will be utilized due to its rapid convergence and low buses mismatches

4.5 Dynamic Simulation

The dynamic simulation will be conducted to monitor the performance of several electrical and electromechanical quantities such as rotor angles, rotor speed deviations, bus voltages, active power flows of intertie lines, etc. Also, it will be used to analyze the dynamic stability performance before and after implementing the proposed controllers.

The dynamic simulation will be executed as follows:

- 1) A pre fault simulation will be run for 1 second.
- 2) Then, a sever three phase fault will be applied for 0.1 second.
- 3) After that, the fault will be cleared by tripping a double circuit line.

- 4) Finally, the post fault simulation will be run up to 20 seconds.

4.6 Modified Particle Swarm Optimization Technique (MPSO)

MPSO has many advantages over other optimization techniques. The following are some of these advantages:

- It solves linear as well as non-linear problems in robust manner.
- It improves the speed of convergence and find the global optimum value of fitness functions.
- It solves the same problem as other optimization techniques, such as GA, without facing difficulties.
- It is easy to implement and has few parameters to adjust.
- It has a more effective memory capability than the GA.

4.6.1 Modified PSO Algorithm

It starts with a population of feasible random solution called “particles”. The i^{th} particle is represented by $X_i = (x_{i1}, x_{i2}, \dots, x_{iN})$, where x_{i1}, x_{i2}, x_{iN} are the elements of the i^{th} particle to be optimized. These particles fly through a search space by learning from the previous solutions. A potential solution is represented by equations (4.1) and (4.2) below. The position of each particle is updated in each iteration by adding the velocity vector to the position vector.

$$x_{id}^{(t+1)} = x_{id}^{(t)} + v_{id}^{(t+1)} \quad (4.1)$$

Where,

$$v_{id}^{(t+1)} = wv_{id}^{(t)} + c_1r_1(pbest_{id}^{(t)} - x_{id}^{(t)}) + c_2r_2(gbest_{id}^{(t)} - x_{id}^{(t)}) \quad (4.2)$$

Where, t is the time index, i is the particle index and d is the dimension index. $pbest$ is the individual best position. $gbest$ is the global best position. w is the inertia weight calculated as in the below equation (4.3). c_1 and c_2 are the acceleration rates of the cognitive and social parts, respectively. r_1 and r_2 are random values different for each particle i as well as for each dimension d .

$$w_i = w_{max} - \left(\frac{(w_{max} - w_{min})(i + 1)}{\text{number of generation}} \right) \quad (4.3)$$

Basically, each particle keeps track of its coordinates in the solution space, d , which are associated with the fittest solution it has achieved. The value of the fitness for particle i $pbest$ is also stored as $pbest_i = (pbest_1, pbest_2, \dots, pbest_i)$. In addition to that, the global best of the MPSO keeps track of the fittest value $gbest$, and its corresponding location, which is recently calculated.

Referring to equation (4.2), the second term, $pbest_{id}^{(t)} - x_{id}^{(t)}$, is called the cognitive part while the last term, $gbest_{id}^{(t)} - x_{id}^{(t)}$, is called social part. In the PSO, particles are

attracted to their corresponding previous best particles and the global best particle according to these parts. With the movement of particles, they get close to $pbest_i$ and $gbest$, and then the cognitive term and social term becomes smaller and smaller. According to the updating equation of velocity, the velocity of each particle becomes small till reach to zero. Once the $pbest_i$ or $gbest$ drop into local optima, all the particles will quickly converge to the positions of them.

Therefore, the cognitive and social terms has to be modified to escape from stagnating in local optima. This could be done by creating two new indicators. One is counting the number of repeated $pbest$, $pbest_monitor > T_{1th}$, while the other one is counting the repeated $gbest$, $gbest_monitor > T_{2th}$. Once these indicators exceed certain number of a pre-specified iteration, the cognitive and social terms are calculated as per the following equations (4.4) and (4.5):

$$pbest_{id}^{(t)} - d_1 x_{id}^{(t)} \quad (4.4)$$

$$gbest_{id}^{(t)} - d_2 x_{id}^{(t)} \quad (4.5)$$

Where, T_{1th} and T_{2th} are the pre-specified thresholds associated with the cognitive and social terms, respectively. While d_1 and d_2 are random numbers within specified range from 0 to 1. Accordingly, the velocity update equation (4.2) is modified as per the following equation (4.6) [114]:

$$v_{id}^{(t+1)} = wv_{id}^{(t)} + c_1 r_1 (pbest_{id}^{(t)} - d_1 x_{id}^{(t)}) + c_2 r_2 (gbest_{id}^{(t)} - d_2 x_{id}^{(t)}) \quad (4.6)$$

4.6.2 The Objective Function (Fitness Function)

To select the best controllers' parameters that enhance the power system dynamic performance the most, an Integral of Time weighted Absolute Error (*ITAE*) based objective function is considered as given in equation (4.7). It is worth mentioning that, this fitness function is selected to minimize the settling time and reduce the overshoots of all machines' rotor speed deviations.

$$J = \int_{t=t_0}^{t=t_{simulation}} t \times |\Delta\omega| dt \quad (4.7)$$

Where, t_0 is the initial time, $t_{simulation}$ is the total simulation time and $\Delta\omega$ is the generator speed deviation.

The optimized parameters for PSSs are T_1, T_2, T_3, T_4 as well as K_{PSS} . Whereas the optimized parameters of the TCSC are T_{TCSC1}, T_{TCSC2} and K_{TCSC} . Thus, the design problem is formulated to minimize J which is subjected to the following PSSs' and TCSC's constrains:

$$T_{1i}^{max} \geq T_{1i} \geq T_{1i}^{min}$$

$$T_{2i}^{max} \geq T_{2i} \geq T_{2i}^{min}$$

$$T_{3i}^{max} \geq T_{3i} \geq T_{3i}^{min}$$

$$T_{4i}^{max} \geq T_{4i} \geq T_{4i}^{min}$$

$$K_{PSSi}^{max} \geq K_{PSSi} \geq K_{PSSi}^{min}$$

$$T_{TCSC1}^{max} \geq T_{TCSC1} \geq T_{TCSC1}^{min}$$

$$T_{TCSC2}^{max} \geq T_{TCSC2} \geq T_{TCSC2}^{min}$$

$$K_{TCSC}^{max} \geq K_{TCSC} \geq K_{TCSC}^{min}$$

4.6.3 MPSO Steps

The following points summarize the steps of the MPSO:

Step 1: Specify parameters to be optimized along with their constrains.

Step 2: Initialize first population as well as initial velocities.

Step 3: Check if the parameters and the velocities are inside the problem space or not. If

not, adjust their positions to the nearest specified limits.

Step 4: Evaluate the fitness of each particle.

Step 5: For each individual particle, compare the new fitness value with the previous best

value. If the new fitness value is better, assign the new particles' values to local

best particles. Also, assign the new fitness function to the local best fitness.

Step 6: Determine the new global best among the new local best particles.

Step 7: If the new global best is better than the previous one, assign its fitness function

value as well as particle parameters' values to the global best values.

Step 8: Check $pbest_monitor > T_{1th}$ and $gbest_monitor > T_{2th}$. If any one of these

conditions satisfied, change the velocities according to the modified equation (4.6). If these conditions are not satisfied, change the velocities according to original equation (4.2).

Step 9: Move each particle to the new position according to equation (4.1) and return to Step 3.

Step 10: Loop around Step3-Step9 until the stopping criteria is satisfied.

It is worth mentioning that, MPSO is integrated with PSS/E environment such that it is executed during nonlinear time-domain simulation to optimize the controllers' parameters. The following Fig. 4.2 shows the interaction process between MPSO and the dynamic simulations.

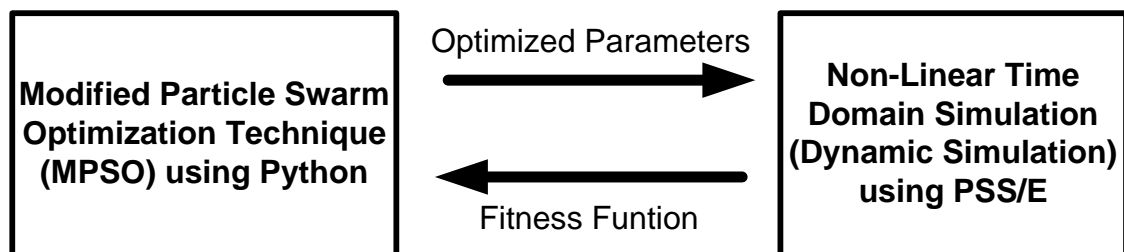


Fig. 4.2 Integration of MPSO with Nonlinear Time-domain Simulation in PSS/E

4.6.4 MPSO Flowchart

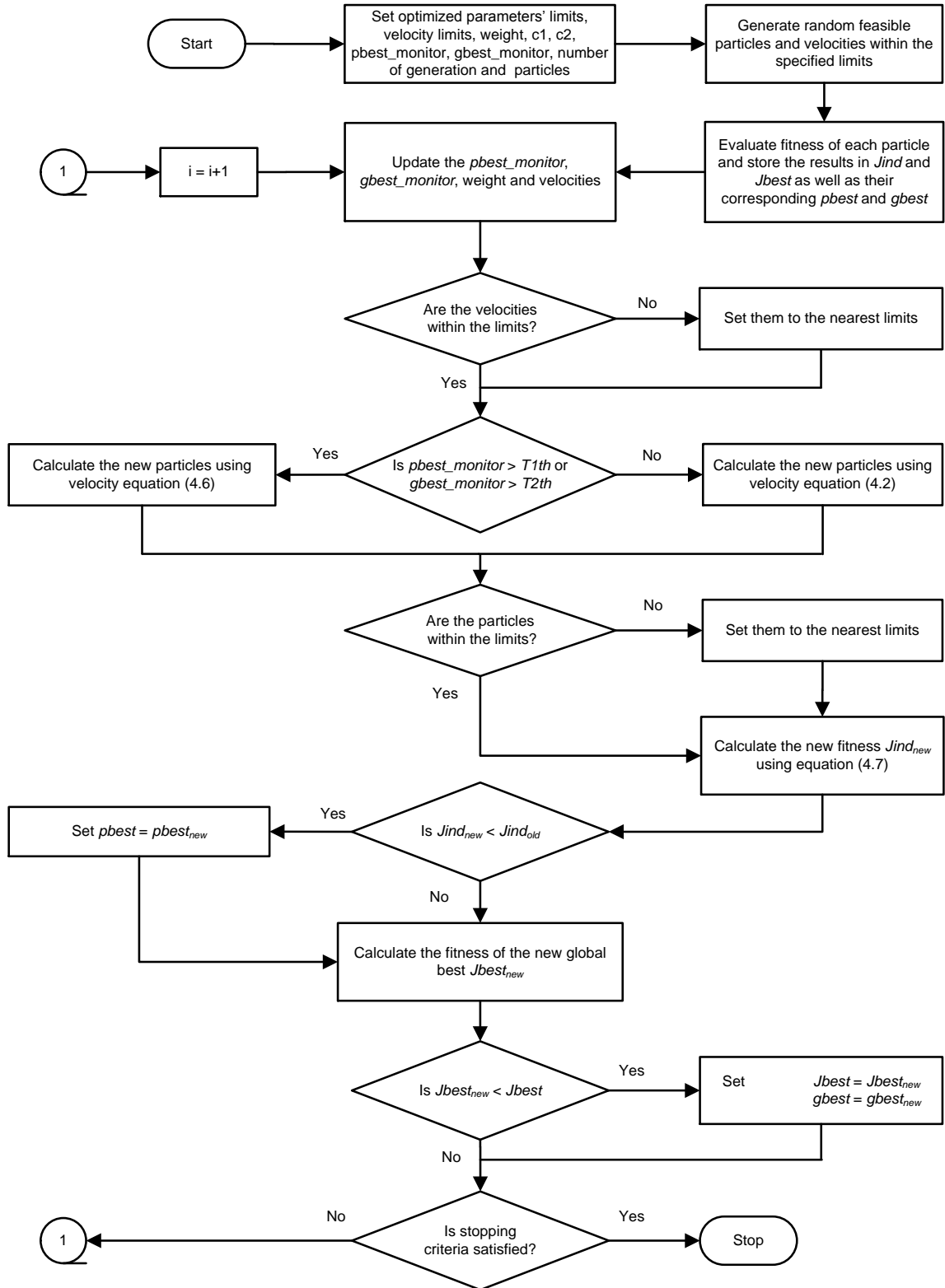


Fig. 4.3 Modified PSO Flowchart

4.7 Modal Analysis

Post fault simulation is extended to 20 seconds, so the modal analysis can investigate the existence of low frequency oscillations phenomenon. The extended time simulation is required to allow well damped modes to attenuate and the system to regain linearity. Thus, the remaining lightly damped modes are then characterized in terms of frequency and damping ratio. After That, oscillation nodes and antinodes are determined by comparing the relative oscillation amplitudes and phases of representative units in the system. In this work, modal analysis is used to investigate and determine the following:

- Low frequency oscillations.
- Optimal location of PSS.
- Assess the dynamic stability enhancement.

4.7.1 Basic Principles of Modal Analysis

Basically, eigenvalue analysis assumes that the study system is linear around certain equilibrium point X_0 and that no additional inputs affect the system. Therefore:

$$\dot{X} = A X + B U \quad (4.8)$$

Where, X is the vector of the state variables, U is the vector of input variables, while, A is the open loop matrix and B is the control matrix. Therefore, the natural response of the study system can be rendered via solving the above set of differential equations (4.8)

considering that $U=0$. The solution to the above differential equations can be done by applying Laplace Transformation method as follow:

$$[s X] = [A][X] + X_0 \quad (4.9)$$

Assuming that a modal matrix M is determined such that:

$$[\lambda] = [M]^{-1}[A][M] \quad (4.10)$$

By changing the coordinates of equation (4.10) to a new coordinates as follow:

$$[Y] = [M]^{-1}[X] \text{ and } [Y_0] = [M]^{-1}[X_0] \quad (4.11)$$

Then, equation (4.11) can be rewritten as:

$$[s Y] = [\lambda][Y] + Y_0 \quad (4.12)$$

Where, $[Y]$ and $[Y_0]$ are vectors while $[\lambda]$ is a diagonal matrix. The last equation consists of "n" number of equations of type:

$$s Y_i = \lambda Y_i + Y_{0_i} \quad (4.13)$$

Where $i=1,2,3,\dots,n$.

Solving equation (4.13) for Y_i gives:

$$Y_i = \frac{Y_{0_i}}{s - \lambda_i} \quad (4.14)$$

Inverting the above equation (4.14) using inverse Laplace Transformation method yields the following time-domain exponential equation:

$$Y_i(t) = Y_{0_i} e^{-\lambda_i t} \quad (4.15)$$

Then, the above equation can be inverted to the original system coordinates as below:

$$[X(t)] = [M][Y(t)] \quad (4.16)$$

The last two equations illustrate that the natural behavior of the system depends on the values of λ . For example, if λ_i is real number then the system response will be a linear combination of exponentials. On the other hand, if λ_i and λ_{i+1} are complex conjugate then the system response will be damped or oscillatory sinusoidal. Consequently, it can be concluded that modal analysis can decompose any linear system response into a summation of terms like the following:

$$x_i(t) = \sum_{real} A_i e^{\sigma_i t} + \sum_{complex} B_j e^{\sigma_j t} \cos(\omega_j t \phi_j) \quad (4.17)$$

In the above equation (4.17), A_i and B_j are the magnitudes of the modal components, σ_i are the real eigenvalues, σ_j and ω_j are the real and the imaginary parts of complex eigenvalues. Therefore, participation and phase of each term are dictated by its respective A_i , B_j and ϕ_j coefficients. The larger a particular A_i or B_j coefficient is relative to those of other modes; the more dominant is the particular mode. The less negative (or more positive) the associated σ_i or σ_j exponent is, the longer the mode will "linger" relative to other better damped modes [50,115].

4.7.2 Modal Analysis Methodologies

Theoretically, large power systems have as many roots or eigenvalues as their state variables in the dynamic model. Therefore, the study system has thousands of terms in equation (4.17). However, due to pole – zero cancellations, a few number of these modes are excited by a certain incidence. Moreover, a fewer number are observable on any particular output signal. On the other words, the majority of modes have A_i or B_j either zero or extremely small. In addition to that, most of the remaining modes are well damped. Therefore, only few modes characterized by either a single lightly damped oscillations, two or more oscillatory modes continue to exist. Basically, modal analysis techniques intend to capture those few remaining modes. Then, it produces A_i and σ_i or B_j , σ_j , ω_j and ϕ_j factors.

In PSS/E, there are two modal decomposition methods which can be used to analyze the study system

- The first one makes use of Prony's method and is best suited for cases where linearity has been restored.
- The other method is based on recursive least-square approximations and is better suited for evaluation of nonlinear simulation results.

In this thesis, the second method is used to cover both the linear and nonlinear parts of the dynamic simulation.

4.7.3 Modal Analysis Flowchart

Fig. 4.4 illustrates the process used to run modal analysis within PSS/E. All of these steps are done using PSSPLT tool.

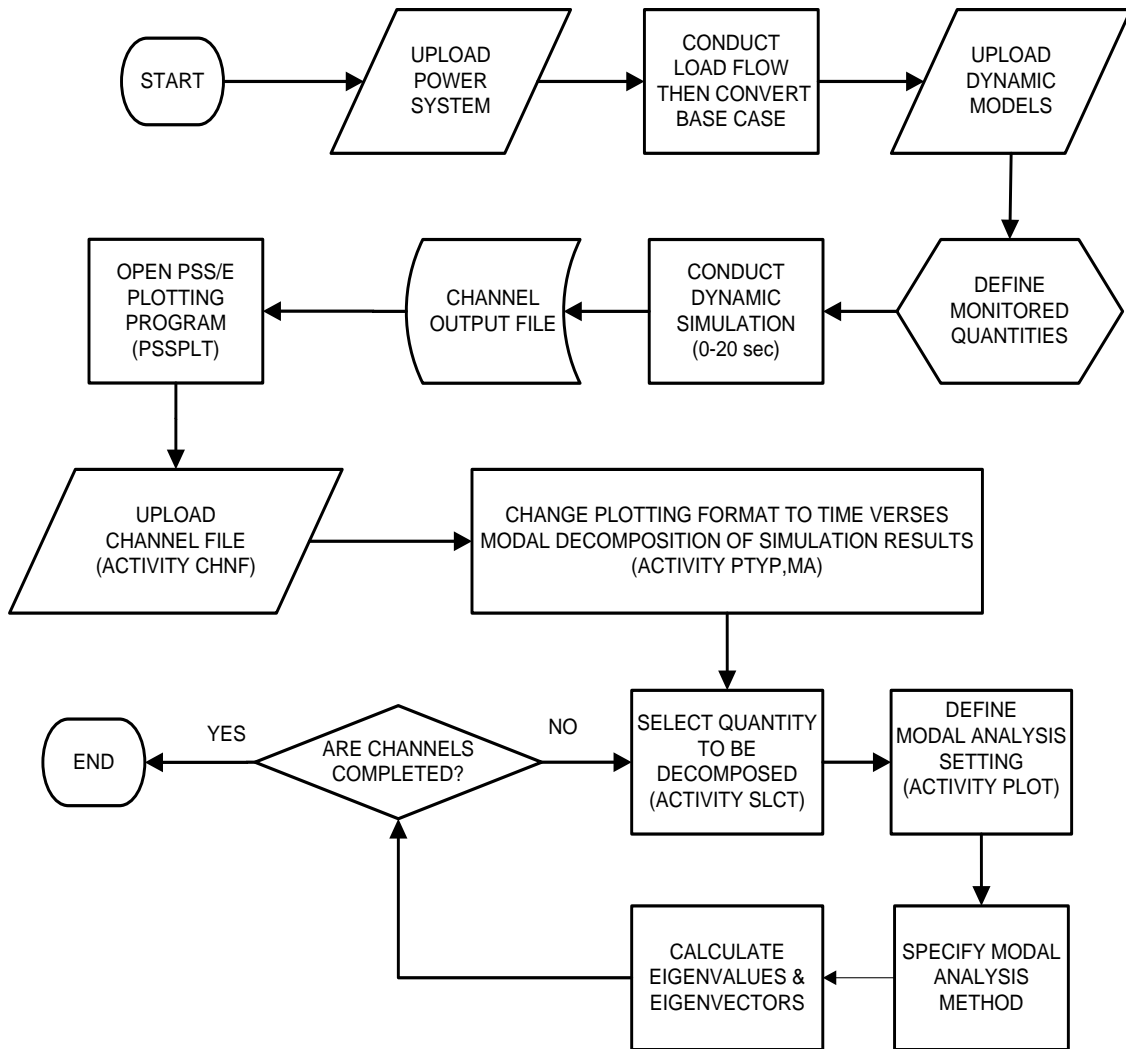


Fig. 4.4 Modal Analysis Flowchart

CHAPTER 5

POWER SYSTEM REDUCTION

5.1 Overview

Since most interconnected power systems are very large, power system modeling becomes very complex. Therefore, power system analysis programs usually do not model the complete system in details. This issue of modeling a large scale power system is stemmed from several reasons such as:

- The excessive computing time required by large power systems, particularly when executing dynamic simulations.
- Parts of power systems are located far away from a disturbance and have little effects on the dynamic characteristics of the considered power system. Therefore, they are usually modeled using simple representation.
- In some countries, network data is considered confidential information. So, many power utilities are reluctant to reveal detailed information about their network to others.
- Maintaining the relevant databases would be very difficult and expensive.
- High order power systems are usually difficult to be used for controller design.

To overcome the above problems, only part of the power system is modeled in details, while, the rest is represented by an equivalent model. The former part is called the internal power system, whereas, the latter is called equivalent system or external power system.

In fact, there are two major steps required to produce the electric equivalent of the external power system namely static and then dynamic reduction steps. The following two sections illustrate the theoretical background of these steps.

5.2 The Static Reduction

The static reduction is achieved by transforming the large power system into a smaller one. This can be done by running a reduction operation on the admittance matrix of the external power system. The admittance matrix equation of the external power system can be expressed as per the below equation (5.1):

$$\begin{bmatrix} I_1 \\ I_2 \end{bmatrix} = \begin{bmatrix} Y_1 & Y_2 \\ Y_3 & Y_4 \end{bmatrix} \begin{bmatrix} V_1 \\ V_2 \end{bmatrix} \quad (5.1)$$

Where, I_1 and V_1 are vectors of bus currents and voltages at the internal system and I_2 and V_2 are those of the external system. The electrical equivalent can be attained by manipulating the above equation such that it will be explicitly expressed in terms of I_1 and V_1 and implicitly expressed by I_2 and V_2 . The latter quantities are assumed to be linearly dependent on I_1 and V_1 .

Then, the electrical equivalent can be determined by reordering the second row of equation (5.1) as shown in equation (5.2) and substituting it into the first row of equation (5.1) to obtain equation (5.3):

$$V_2 = Y_4^{-1}(I_2 - Y_3 V_1) \quad (5.2)$$

$$I_1 = (Y_1 - Y_2 Y_4^{-1} Y_3) V_1 + Y_2 Y_4^{-1} I_2 \quad (5.3)$$

The last equation contains a set of equivalent branches and static shunt elements connecting the retained buses. Also, it specifies a set of currents that must be imposed on the retained buses to reproduce the effect of load currents at the eliminated buses.

It is worth mentioning that, in this work the static reduction is done using the available tool within PSS/E. This facility executes all the mathematical operations needed to produce the equivalent admittance matrix of the external power system [116,117].

5.3 The Dynamic Reduction

Basically, the main power system facilities which could be dynamically aggregated are synchronous generators along with their control devices. Coherent generators can be dynamically reduced using two methods. The first method is called the classical aggregation method, where a group of coherent generators is simply represented by a classical equivalent machine. However, the disadvantage of such modeling is the basic

representation of the machine which only includes machine's inertia and transient reactance. The second method is called the detailed model aggregation. In this method, a group of coherent generators is represented as a single equivalent unit along with detailed modeling of its control devices. In this thesis, the latter technique is deployed to perform the dynamic reduction process [22-25]. The below subsections show the mathematical equations used to determine an equivalent machine and describe the basic principle of control models aggregation.

5.3.1 Generator Model Reduction

To obtain the equivalent generator of a group of coherent machines, they have to be statically and dynamically reduced as explained below.

5.3.1.1 Generator Static Reduction

Generators within the same power plant and having the same voltage, angle and machine MVA base, are aggregated in PSS/E load flow base case as expressed in the following equations (5.4)-(5.13):

$$P_{gen_{eqv}} = \sum_{i=1}^n P_{gen_i} \quad (5.4)$$

$$P_{max_{eqv}} = \sum_{i=1}^n P_{max_i} \quad (5.5)$$

$$P_{min_{eqv}} = \sum_{i=1}^n P_{min_i} \quad (5.6)$$

The above equations are the generated, maximum and minimum real power of the equivalent units, respectively.

$$Q_{max_{eqv}} = \sum_{i=1}^n Q_{max_i} \quad (5.7)$$

$$Q_{min_{eqv}} = \sum_{i=1}^n Q_{min_i} \quad (5.8)$$

The above equations (5.7) and (5.8) are the maximum and minimum reactive power of the aggregated power plants, respectively.

Also, the equivalent machines' MVA bases have to be calculated as per the below expression (5.9):

$$S_{machine_{eqv}} = \sum_{i=1}^n S_{machine_i} \quad (5.9)$$

In addition to that, positive, negative and zero sequence impedances of the aggregated machines and the associated step-up transformers must be calculated as described below:

$$X_{machine_{eqv}} = \frac{1}{\sum_{i=1}^n 1/X_{machine_i}} \times \frac{S_{machine_{eqv}}}{S_{machine_i}} \quad (5.10)$$

$$R_{machine_{eqv}} = \frac{1}{\sum_{i=1}^n 1/R_{machine_i}} \times \frac{S_{machine_{eqv}}}{S_{machine_i}} \quad (5.11)$$

$$X_{ST_{eqv}} = \frac{1}{\sum_{i=1}^n 1/X_{ST_i}} \quad (5.12)$$

$$R_{ST_{eqv}} = \frac{1}{\sum_{i=1}^n 1/R_{ST_i}} \quad (5.13)$$

Where, $X_{machine_i}$ and $R_{machine_i}$ are the reactance and resistance of a single machine i and n is the number of machines. $X_{machine_{eqv}}$ and $R_{machine_{eqv}}$ are the equivalent reactance and resistance of the equivalent machine. $X_{ST_{eqv}}$ and $R_{ST_{eqv}}$ are the equivalent reactance and resistance of the equivalent step-up transformer. X_{ST_i} and R_{ST_i} are the reactance and resistance of a single step-up transformer. Fig. 5.1 illustrates the lumped generator model for multiple identical generators connected to the same bus:

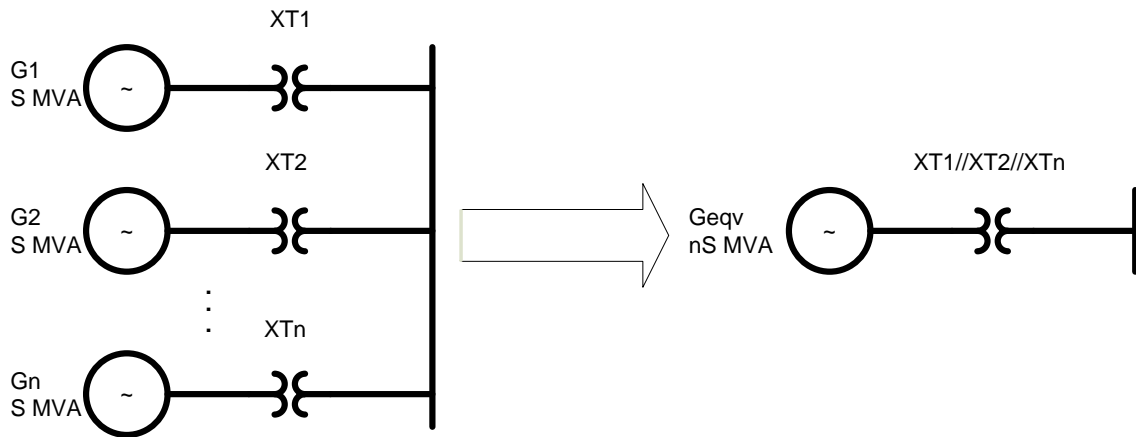


Fig. 5.1 Aggregation of Power Plants in the Load Flow

5.3.1.2 Generator Dynamic Reduction

The proposed aggregation method uses a non-iterative procedure to estimate the parameters of the equivalent generating unit. The mechanical equation of the coherent machines is:

$$\left(\sum_{i=1}^n M_i \right) \times \dot{\omega} = \sum_{i=1}^n P_{mi} - \sum_{i=1}^n P_{ei} - \left(\sum_{i=1}^n D_i \right) \times \omega \quad (5.14)$$

where ω , P_{mi} , P_{ei} , M , and D_i are respectively the angular speed, mechanical power, electrical power, inertia and damping constants of generator i . Therefore, the equivalent machine's inertia and damping constant are calculated as per the below equations:

$$H_{eqv} = \frac{\sum_{i=1}^n H_i}{n} \quad (5.15)$$

$$D_{eqv} = \frac{\sum_{i=1}^n D_i}{n} \quad (5.16)$$

5.3.2 Control Devices Reduction

The control devices of the generator are mainly governor, exciter, and PSSs models. The main parameters of these controllers are gains and time constants. In this work, only the identical units within the same power plant are dynamically reduced using the detailed models aggregation [22 - 25]. Since all machines to be dynamically reduced are sited within the same power plant, having the same voltage, angle, MVA base and control devices, their parameters (i.e. time constants and gains) are considered the same as those of the individual machine's parameters.

5.4 Application of Power System Reduction Technique

5.4.1 Description of the Considered Power System

The considered power system consists of variety of voltage levels starting from 380 kV down to 10 kV. Also, it consists of four geographically widely separated areas. These areas are electrically interconnected via the 380 kV network with numerous of tie lines as shown in Fig. 5.2.

It is worth noting that, a light load base case is utilized in this work. Since, it is expected that such a base case could have low inertia which could bring about low frequency oscillations phenomenon. Table 5-1 below presents the main components of this base case.

Table 5-1 Summary of the Full Power System

Component	Full System
Number of Buses	2785
Number of Branches	4413
Number of Generators	116

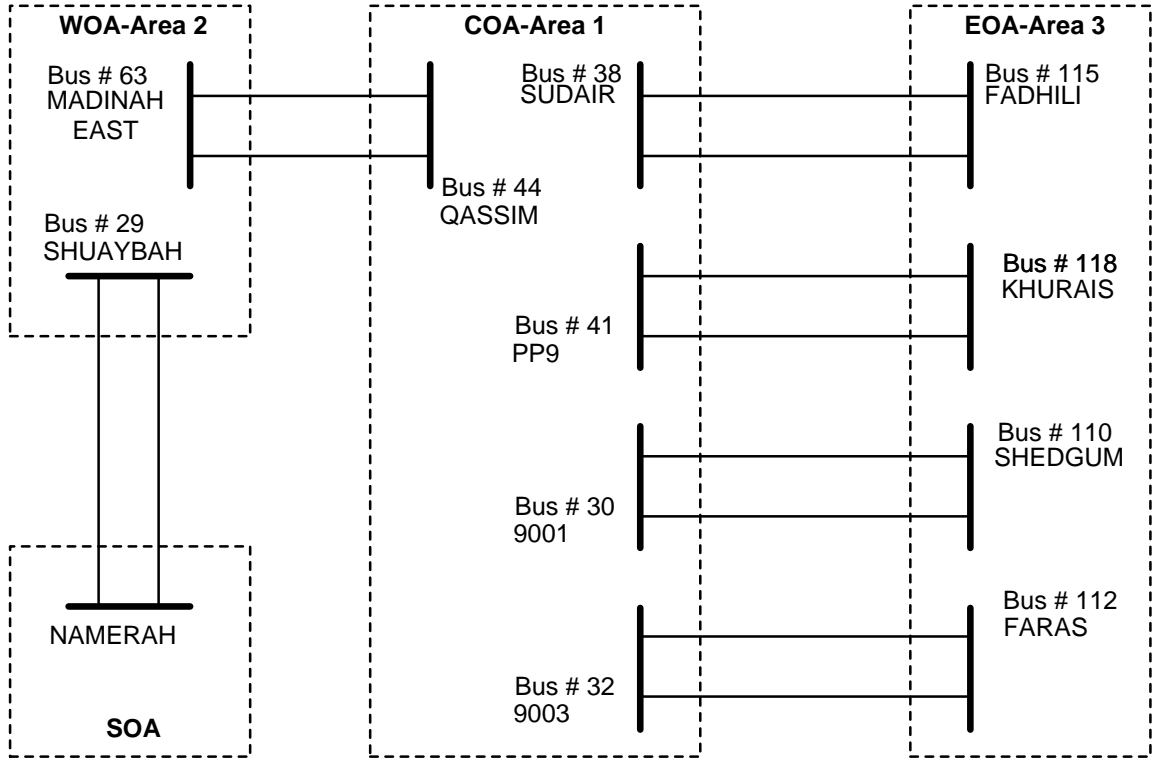


Fig. 5.2 The Main Interconnected Areas of the Considered Power System

5.4.2 Considered Assumptions

Before starting the reduction steps, the considered power system is divided into internal and external systems. The internal power system consists of the extra high voltage buses (buses with voltage ≥ 230 kV) along with the generators dispatched through the 380 kV network. While, the external part includes all high and medium voltage levels (buses having voltage < 230 kV) along with the small generators connected to these buses.

5.4.3 Power System Reduction's Steps

The below steps summarize a simple systematic approach for reducing large scale power systems and Fig. 5.3 below depicts its conceptual flowchart.

- 1) Identification of small power plants, which are connected to high voltage network (< 380 kV level), and netting them with loads.
- 2) Detailed aggregation of coherent units, located within the same power plants and having the same machine MVA base, voltage level, angle and control devices.
- 3) Static reduction of high, medium and low voltage buses using PSS/E built in functions while retaining the extra high voltage network.

5.4.4 Power System Reduction's Results

Table 5-2 lists the total components of the full model verses the reduced one. It can be observed that the component of the considered power system is significantly reduced. For example, the number of buses is reduced from 2785 to 127 buses while the number of generators is considerably decreased from 116 to 29 generators. Also, the number of branches is substantially reduced from 4413 down to 222 branches.

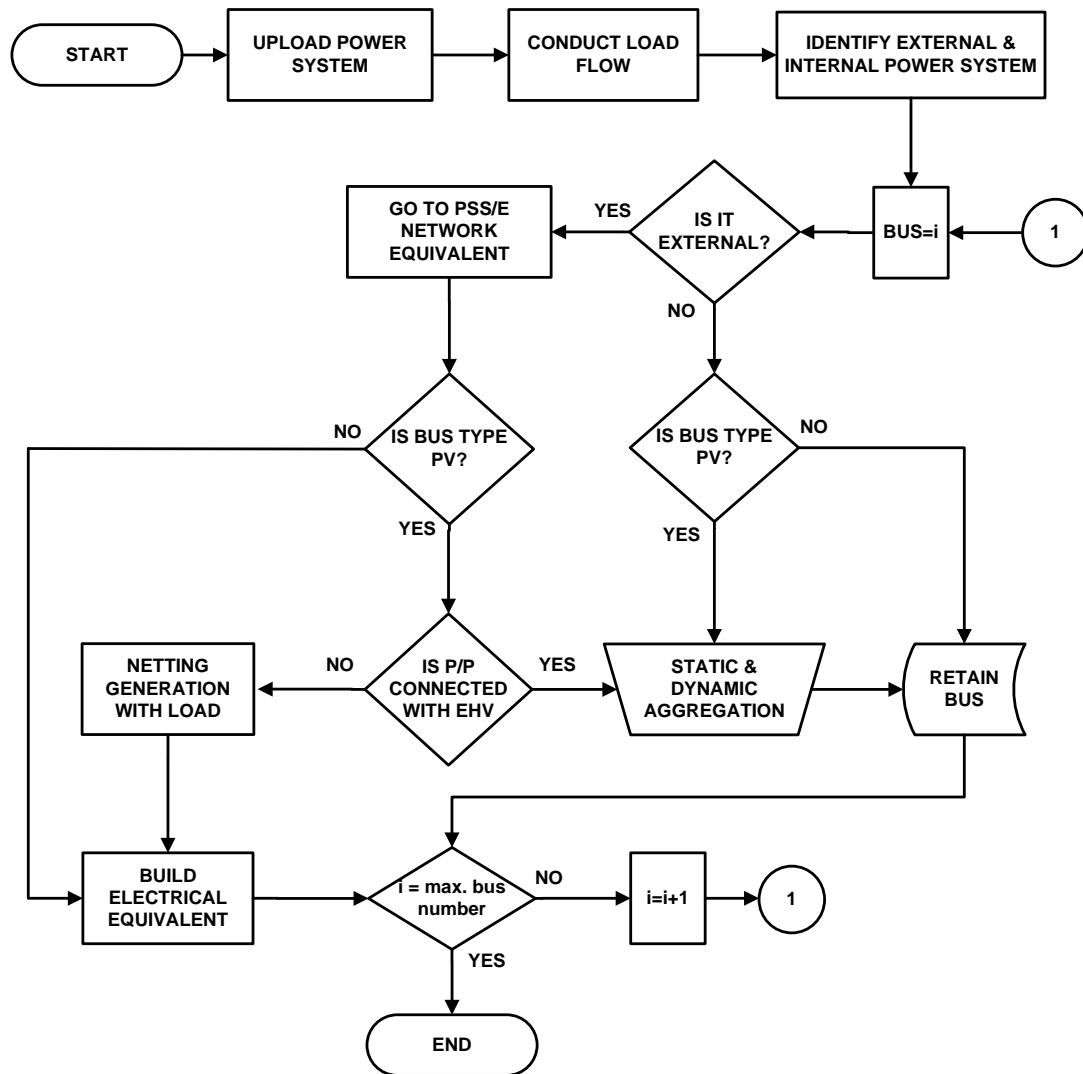


Fig. 5.3 Power System Reduction Flowchart

Table 5-2 Summary of the Full & Reduced Power Systems

Totals	Full System	Reduced System
Number of Buses	2785	127
Number of Branches	4413	222
Number of Generators	116	29

In order to validate the accuracy of the reduced power system, different electrical and electromechanical quantities, such as bus voltages, machine angles, active power flow of transmission lines, rotor speed deviations, rotor angles, electrical output power of the machines, etc. are commonly compared. Thus, subsections 5.4.4.1 and 5.4.4.2 demonstrate the comparisons of both the steady state and dynamic simulations of both the full versus the reduced power systems.

5.4.4.1 The Steady State Comparison

Table 5-3 to Table 5-5 present the largest mismatches between the full and the reduced power systems in bus voltages, bus angles and active power flow of intertie lines:

Table 5-3 Steady State Comparison, Full vs Red. Power Systems, Voltage Results

Quantity	Bus	Voltage (kV)	Full System	Reduced System	Voltage Deviation
Voltage (p.u.)	37	380	0.99986	0.99977	-0.00009
	45	380	1.02215	1.02206	-0.00009
	44	380	0.99441	0.99434	-0.00007
	34	380	1.02609	1.02604	-0.00005
	38	380	1.01571	1.01566	-0.00005
	31	380	1.02348	1.02345	-0.00003

Table 5-4 Steady State Comparison, Full vs Red. Power Systems, Angle Results

Quantity	Bus	Voltage (kV)	Full System	Reduced System	Angle Deviation
Angle (degree)	20	380	-42.68	-42.67	0.01
	21	380	-40.16	-40.15	0.01
	26	380	-41.95	-41.94	0.01
	52	380	-41.73	-41.72	0.01
	53	380	-38.43	-38.42	0.01
	57	380	-42.02	-42.01	0.01

Table 5-5 Steady State Comparison, Full vs Red. Power Systems, Active Power Flow

Quantity	Sending Bus	Receiving Bus	Full System	Reduced	Active Power Deviation
Active Power Flow (MW)	44	63	421.8	422	-0.2
	110	30	735.2	735	0.2

It can be seen that the highest voltage differences between the two models are extremely negligible. Moreover, it can be observed that the highest error in the bus angles is very small. Last but not least by comparing the full and the reduced power systems, it can be observed that the highest deviations in the active power flow of the intertie lines are insignificant. Therefore, the reduced power system is very accurate and can be used for steady state analyses.

5.4.4.2 The Dynamic Simulation Comparison

In addition to the validation of the steady state results, the dynamic responses of both systems have to be examined. To demonstrate the precision of the reduced power system, a sever three phase fault is applied on bus 110 after 1 second of steady state simulation and for a period of 0.1 second and then it is cleared by tripping the line connecting buses 110 and 30. The simulation time is extended up to 20 seconds to monitor the dynamic behavior for extended time. The following subsections validate the dynamic simulation results of the electrical and electromechanical quantities.

5.4.4.2.1 Rotor Speed Deviations' Responses

Fig. 5.4 to Fig. 5.6 show the rotor speed deviations for three machines in different areas which are machine 2, 16 and 28. It is quite clear that both the full and the reduced models are closely matching. The overshoot, settling time and oscillations trends are almost identical.

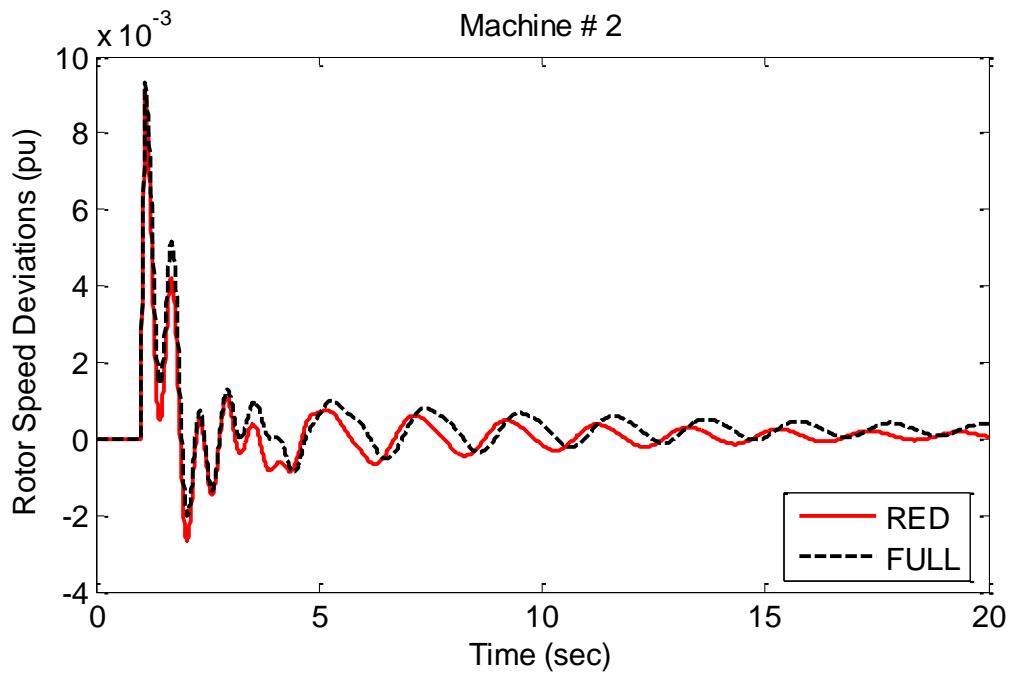


Fig. 5.4 Comparison of Rotor Speed Deviations of Machine # 2 in Area 3

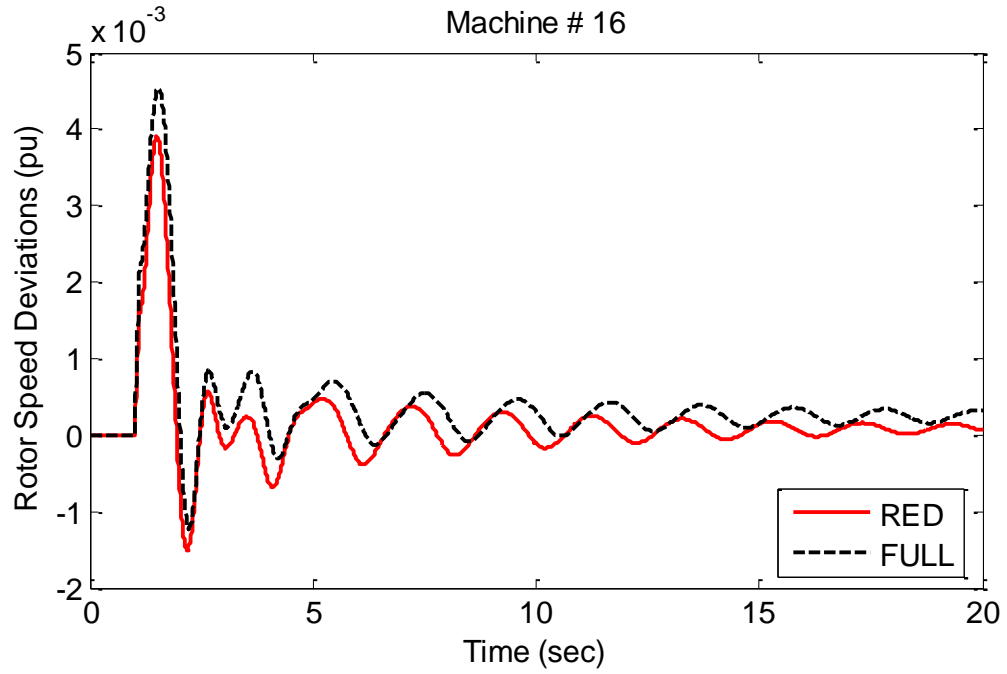


Fig. 5.5 Comparison of Rotor Speed Deviations of Machine # 16 in Area 1

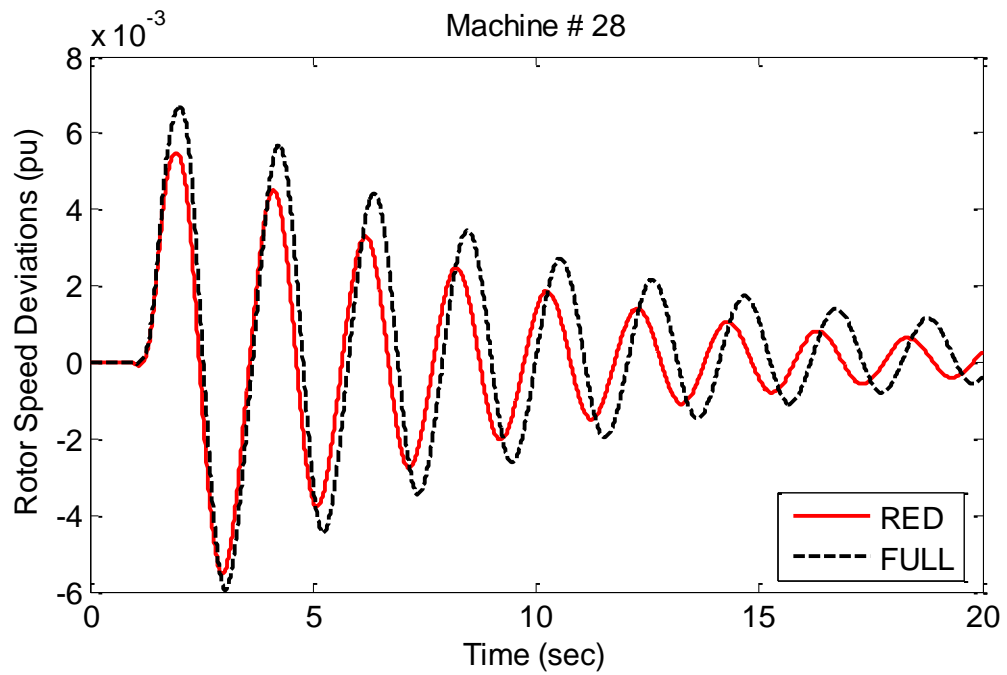


Fig. 5.6 Comparison of Rotor Speed Deviations of Machine # 28 in Area 2

5.4.4.2.2 Rotor Angles' Responses

Similarly, Fig. 5.7 to Fig. 5.9 below show the rotor angles' responses for machines 2, 17 and 28. The oscillations of the rotor angles of these machines clearly demonstrate the same phase relations. Also, it can be observed that the angles are heading to the same steady state values.

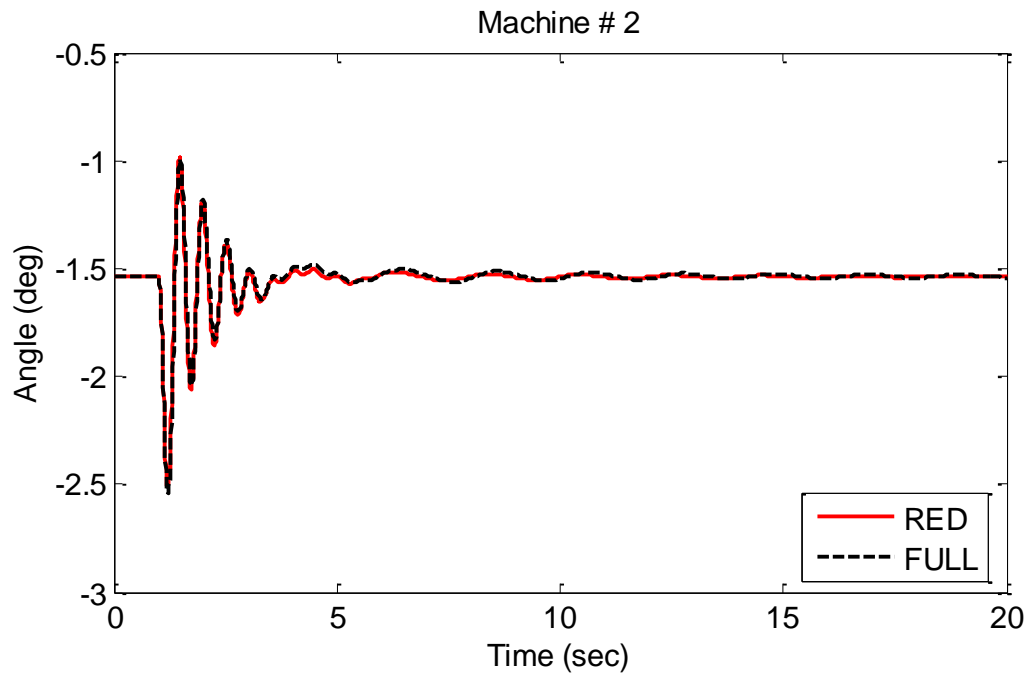


Fig. 5.7 Comparison of Rotor Angle of Machine # 2 in Area 3

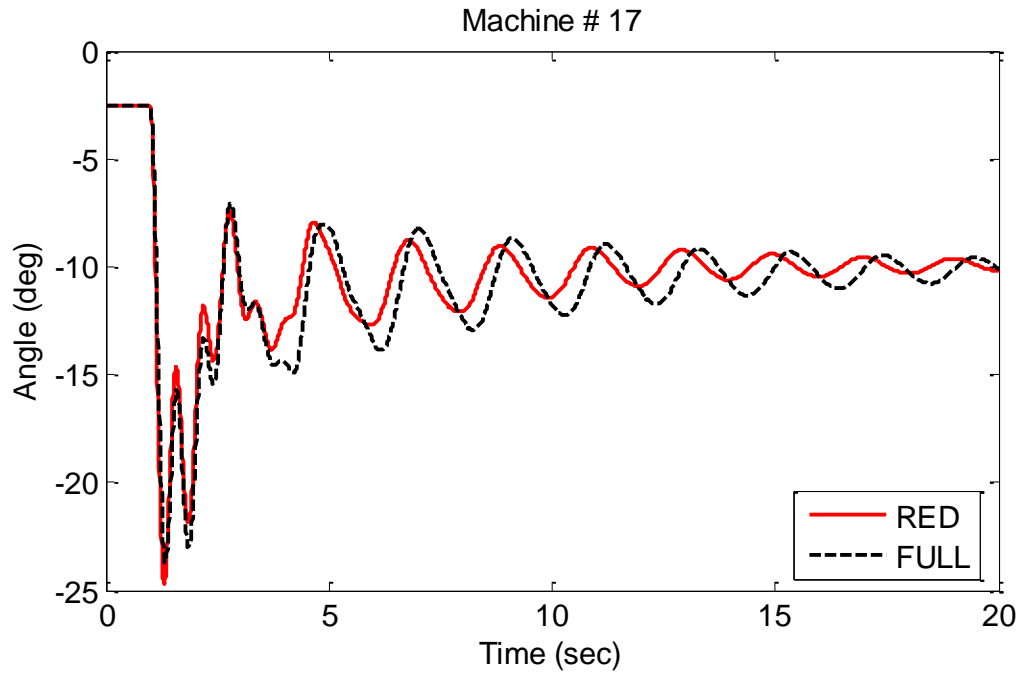


Fig. 5.8 Comparison of Rotor Angle of Machine # 17 in Area 1

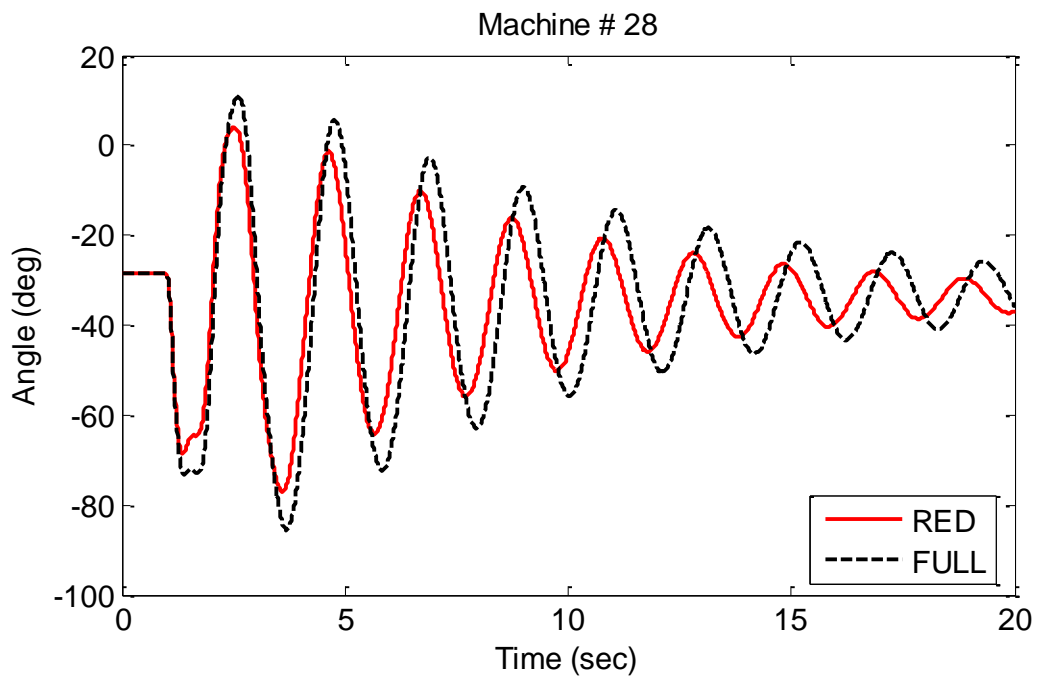


Fig. 5.9 Comparison of Rotor Angle of Machine # 28 in Area 2

5.4.4.2.3 Voltage Responses

Fig. 5.10 to Fig. 5.13 present the voltage responses of randomly selected boundary buses. Notwithstanding the minute deviations in voltage magnitudes and phase angles during the post fault period, it is quite evident that the overall voltage responses have more or less similar behavior.

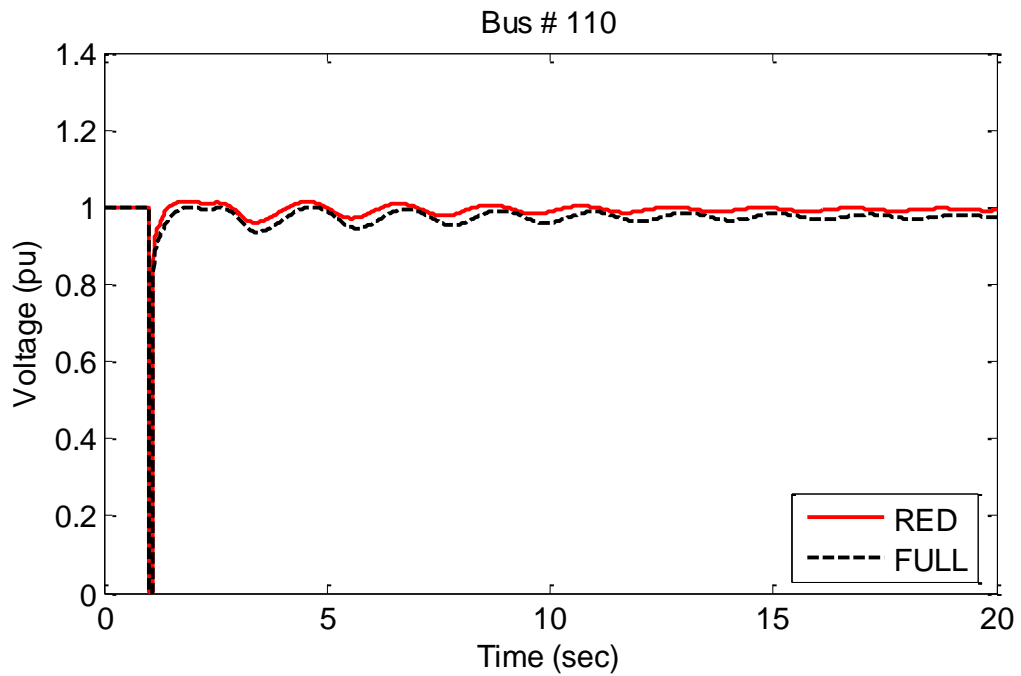


Fig. 5.10 Comparison of Bus Voltage of Bus # 110 in Area 3

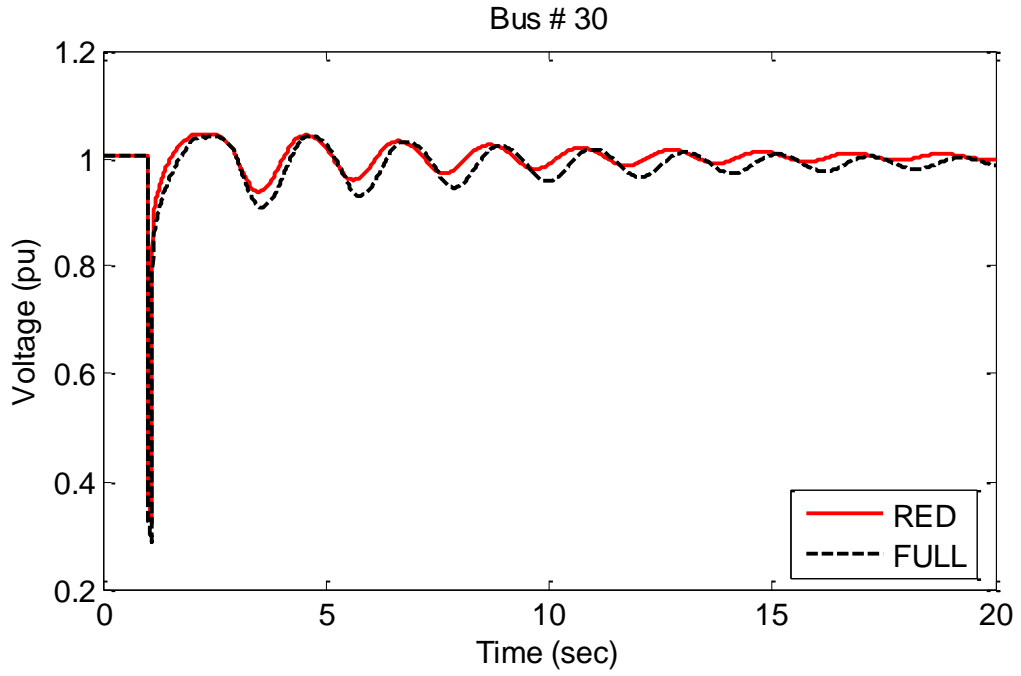


Fig. 5.11 Comparison of Bus Voltage of Bus # 30 in Area 1

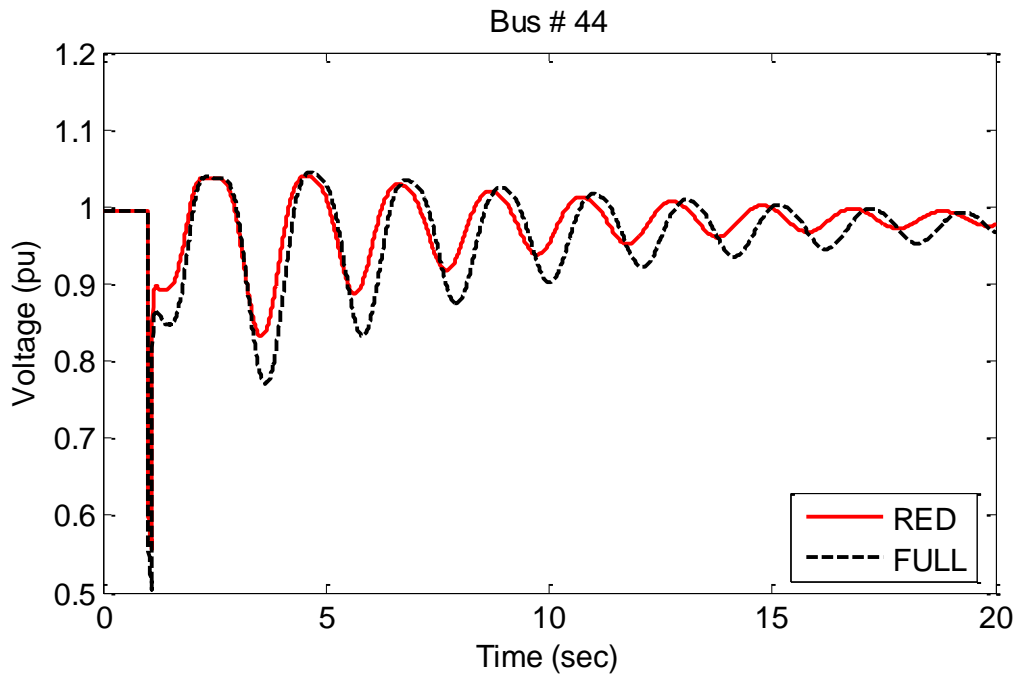


Fig. 5.12 Comparison of Bus Voltage of Bus # 44 in Area 1

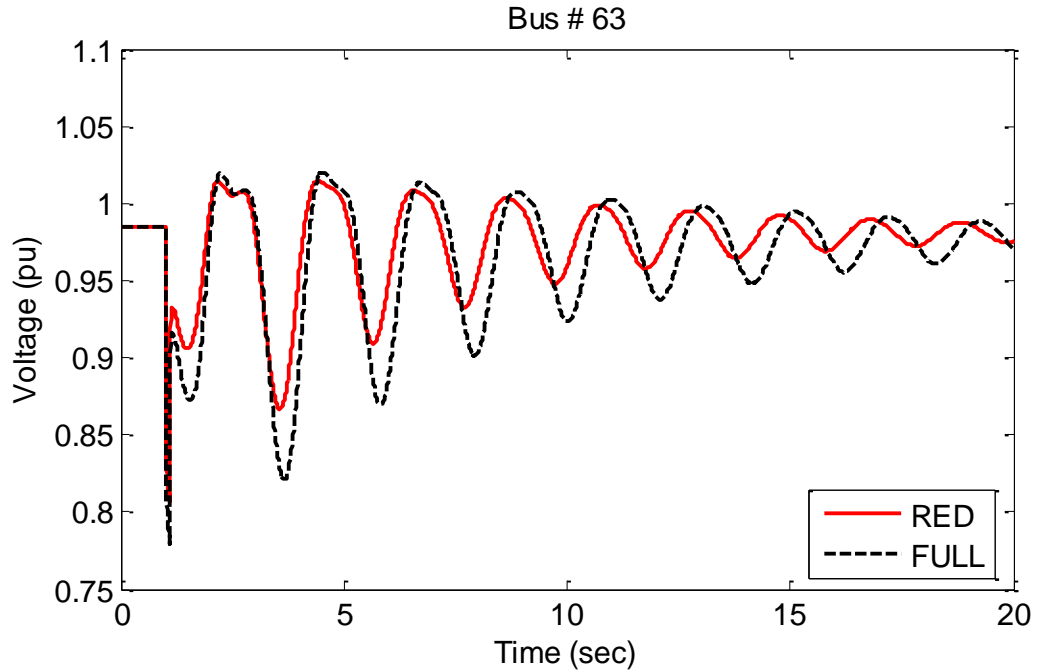


Fig. 5.13 Comparison of Bus Voltage of Bus # 63 in Area 2

5.4.4.2.4 Active Power Flow Responses

Beside the rotor speed deviations, rotor angles and bus voltages, it is essential to monitor the dynamic responses of the active power flow of the intertie lines. Fig. 5.14 to Fig. 5.16 depict the active power flow of the intertie lines connecting area-1, area-2 and area-3. Obviously, the dynamic responses for both systems are more or less the same. They have exactly the same steady state values and they are heading to the same post fault values. Also, they have nearly the same overshoot and settling time with little deviation in the magnitudes and the phase shifts.

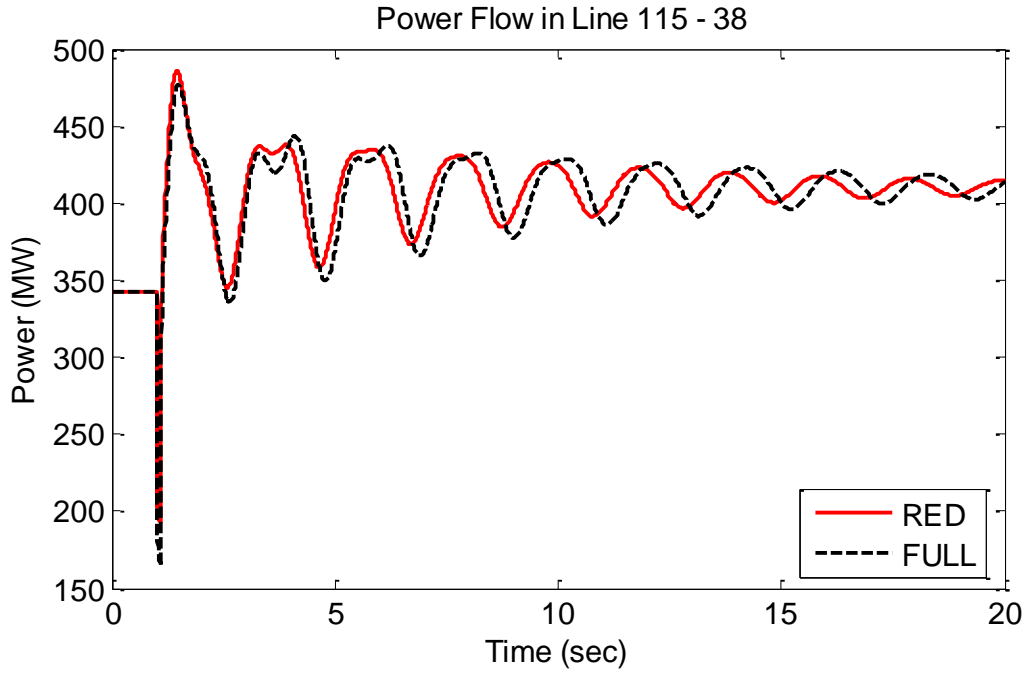


Fig. 5.14 Comparison of Active Power Flow of Line 115 – 38

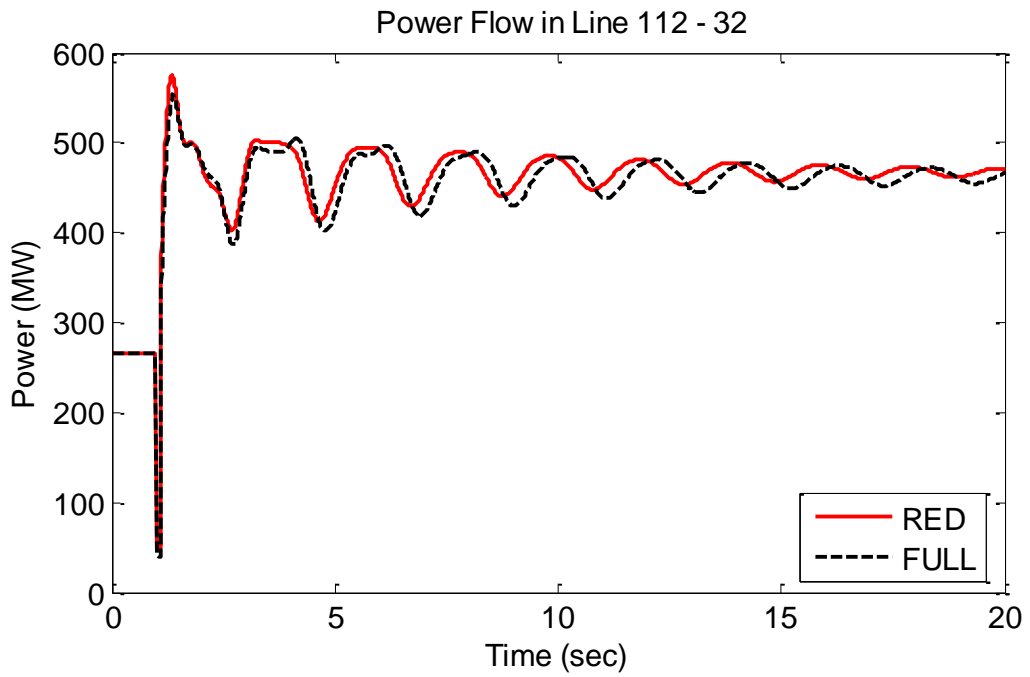


Fig. 5.15 Comparison of Active Power Flow of Line 112 – 32

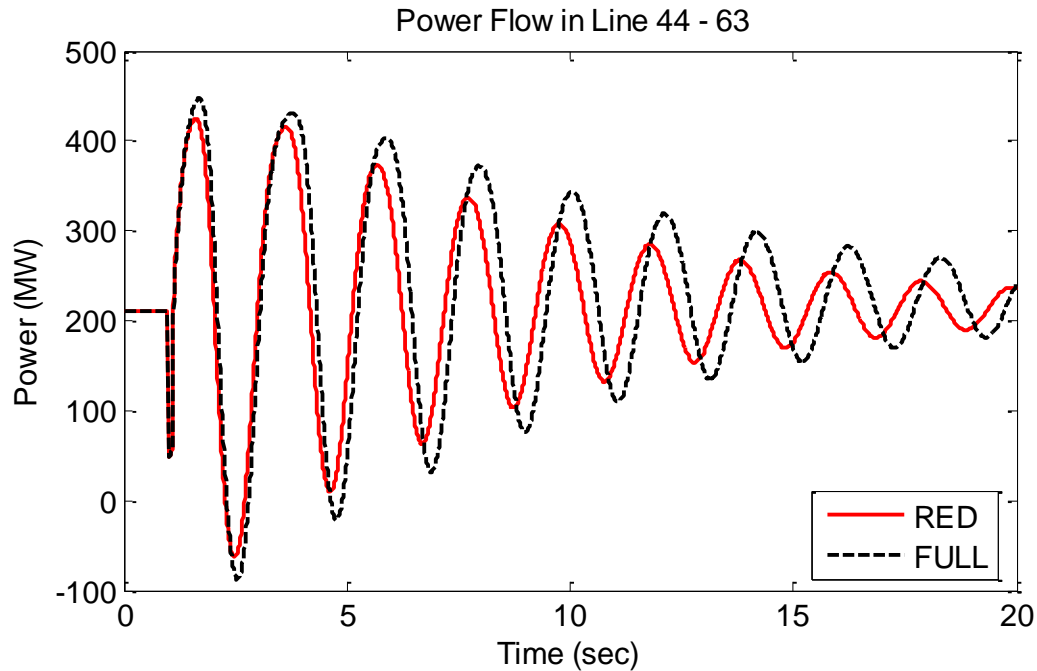


Fig. 5.16 Comparison of Active Power Flow of Line 44 – 63

5.5 Summary of the Power System Reduction

This chapter discusses the proposed systematic approach for constructing the dynamic equivalent of a large-scale power system using PSS/E. The proposed reduction steps have been applied on a real power system. Then, steady state and nonlinear time-domain simulation have been conducted and their results have been compared. The steady state and the dynamic simulation results prove excellent agreements among the variations. Therefore, the reduced power system can be utilized to perform the intended power system analyses and controller design.

CHAPTER 6

COORDINATION OF POWER SYSTEM STABILIZERS

6.1 Overview

Power system stability can be analyzed using different analytical methods, such as modal analysis, linear analysis, nonlinear time-domain simulations, etc. Moreover, it can be significantly enhanced via deploying well-designed control devices. In this work, modal analysis and nonlinear time-domain simulations are used to assess the dynamic stability of the considered power system. Also, they are utilized to identify the best location for PSSs installation or tuning. More specifically, the location of such PSSs is determined using residue method while their parameters are designed simultaneously using MPSO.

The second section of this chapter discusses the optimal location for deploying a new PSS. Then, in the third section, MPSO is used to coordinate and optimize the parameters of the proposed PSS and the existing PSSs. After determining the best location and parameters, modal analysis is carried out to validate the effectiveness of the proposed PSSs on improving the overall dynamic stability. The eigenvalue and eigenvectors' results with and without the proposed PSSs are presented in section 6.5. After that, nonlinear time-domain simulations are executed to evaluate the power system dynamic stability with and without the proposed controllers. Next, to confirm the effectiveness of

the proposed design, the parameters of the optimized PSSs are modeled in the full version of the considered power system and then a new maximum power transfer between area 1 and 2 is determined. Lastly, several sensitivity analyses are carried out to test the robustness of the proposed simultaneous design of the PSSs.

6.2 Modal Analysis Results of the Existing Power System

In order to perform modal analysis, nonlinear time-domain simulation has to be executed. Therefore, a sever three phase fault is applied after 1 second of steady state simulation. The fault period is 0.1 second and it is cleared by tripping one of the intertie lines connecting area 3 and 1 namely line 110 – 30 circuits 1 and 2. The simulation period is extended up to 20 seconds. Then, modal analysis is carried out for the period between 14 to 20 seconds. The resultant model decomposition of all machines' rotor speed deviations are recorded for analysis purpose. For instance, the below Table 6-1 shows the modal decomposition of machine 28. These results show that machine 28 has an oscillatory mode of approximately 0.5 Hz and damping ratio of 0.08. The damping ratio is calculated as follows:

$$\zeta = \frac{-\sigma}{\sqrt{\sigma^2 + \omega^2}} = \frac{-(-0.2533)}{\sqrt{(-0.2533)^2 + (3.1504)^2}} = 0.08$$

Table 6-1 Modal Decomposition of Rotor Speed Deviations of Machine 28

No.	Eigenvector		Eigen Vector		Freq. (Hz)
	Real (σ)	Imaginary (ω)	Magnitude (pu)	Angle (deg.)	
1	-0.2533	3.1504	0.000260	163.9	0.501
2	0.0424	--	0.000053	--	
3	-4.7830	38.2851	0.000006	-29.0	6.093
4	-4.2144	33.553	0.000006	-123.1	5.34
5	-15.9450	87.9297	0.000005	9.8	13.994
6	-4.1983	24.0154	0.000005	-138.4	3.822
7	-0.9758	5.91927	0.000004	-104.9	0.942
8	-1.5340	15.4936	0.000002	-147.1	2.466
9	-2.8330	47.7897	0.000001	-17.3	7.606
10	-2.9062	57.3684	0.000001	-25.2	9.13
11	-2.3286	90.0585	0.000001	-158.6	14.333
12	-1.8486	66.6694	0.000000	-30.6	10.611
13	-1.5228	79.6683	0.000000	-106.8	12.68

Table 6-2 below lists the eigenvalue and eigenvectors of all machines having the inter area oscillatory modes of 0.5 Hz. By analyzing these results, it can be seen that the machines sited in area 2 have large magnitude of oscillations. More specifically, the largest magnitude of oscillations is concomitant with machine 28. Also, it can be observed that the damping ratio for all machines are ranged between 0.071 to 0.08. The highest damping ratio is associated with machine 28 in area 2 and the lowest is concomitant with machine 9 in area 3.

Table 6-2 Existing Modal Analysis for the Inter Area 0.5 Hz – Mode

M/C	Eigenvalue		Eigenvector		Freq. (Hz)	ζ
	Real (σ)	Imaginary (ω)	Magnitude (pu)	Angle (deg.)		
1	-0.248932	3.15998	0.000057	-22.6	0.503	0.078533
2	-0.237364	3.15314	0.000056	-21.1	0.502	0.075066
3	-0.235124	3.14929	0.000059	-25.6	0.501	0.074452
4	-0.239138	3.16009	0.000061	-22.2	0.503	0.075459
5	-0.238292	3.16186	0.000052	-17.4	0.503	0.075151
6	-0.234580	3.15578	0.000050	-19.7	0.502	0.074129
7	-0.237569	3.15324	0.000058	-27.6	0.502	0.075128
8	-0.234382	3.15665	0.000059	-33.8	0.502	0.074046
9	-0.226894	3.16663	0.000024	-37.9	0.504	0.071468
10	-0.235121	3.15648	0.000060	-31.5	0.502	0.074283
11	-0.242429	3.14718	0.000060	-35.7	0.501	0.076803
12	-0.232918	3.14983	0.000061	-36.3	0.501	0.073745
13	-0.238432	3.15027	0.000060	-33.3	0.501	0.075470
14	-0.242838	3.15167	0.000059	-36.3	0.502	0.076823
15	-0.236881	3.14958	0.000056	-24.8	0.501	0.074999
16	-0.252447	3.14339	0.000034	-20.1	0.500	0.080053
17	-0.248304	3.13771	0.000033	-12.9	0.499	0.078889
18	-0.249688	3.14200	0.000055	-18.8	0.500	0.079218
19	-0.245024	3.14939	0.000251	169.1	0.501	0.077566
20	-0.240876	3.14951	0.000253	168.6	0.501	0.076258
21	-0.242529	3.15137	0.000228	169.4	0.502	0.076733
22	-0.241265	3.14681	0.000254	169.0	0.501	0.076445
23	-0.251090	3.15058	0.000201	170.2	0.501	0.079445
24	-0.242818	3.15403	0.000216	168.8	0.502	0.076759
25	-0.240052	3.15172	0.000233	168.7	0.502	0.075945
26	-0.243505	3.14771	0.000243	169.8	0.501	0.077129
27	-0.243938	3.14860	0.000244	169.9	0.501	0.077244
28	-0.253335	3.15040	0.000260	163.9	0.501	0.080155
29	-0.249398	3.15388	0.000246	169.6	0.502	0.078830

6.3 Optimal Location of PSS

Fig. 6.1 shows the rotor speed deviations for three generators located in different areas. It can be seen that generator 28, which is located in area 2, is oscillating against units 17 and 2, located in area 1 and 3, respectively. Fig. 6.2 shows enlarge view for the same figure for the period between 14 and 20 seconds. It can be observed that generator 28 is the most dominate unit for the inter area mode of oscillations. Since, it has the highest magnitude of oscillation.

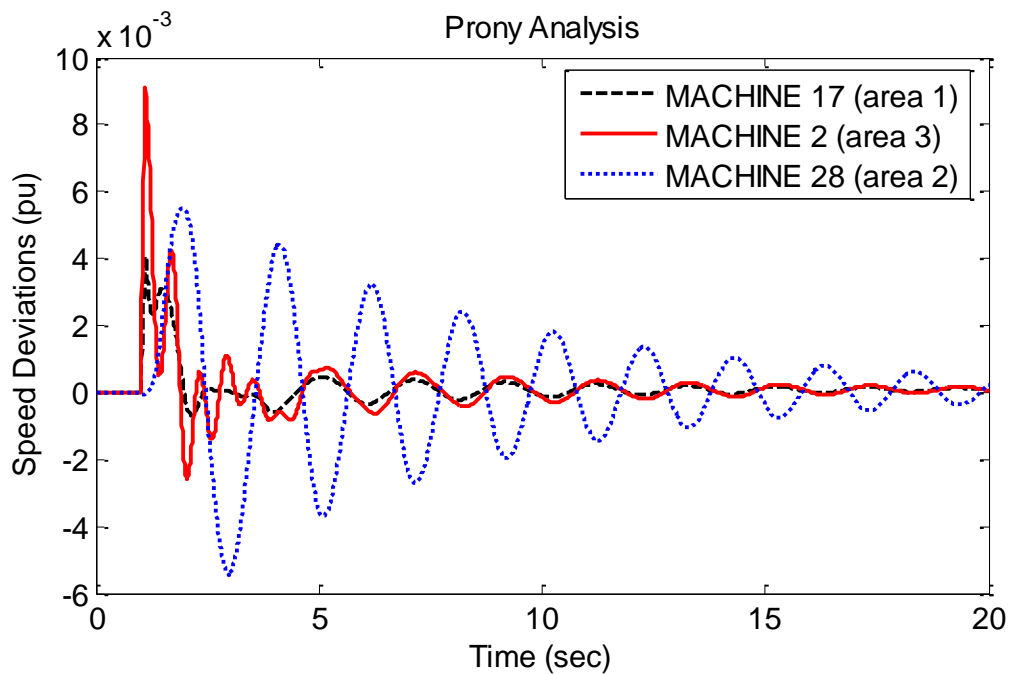


Fig. 6.1 Inter-Area Oscillations Between Areas 1 and 3 Against Area 2

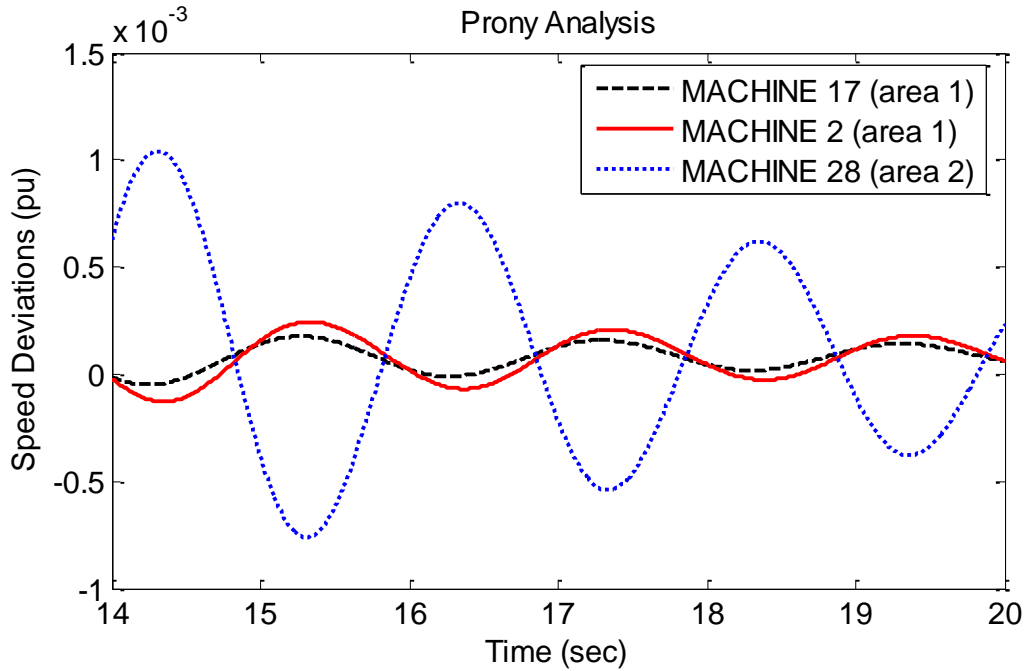


Fig. 6.2 Enlarge View of the Inter-Area Oscillations

In addition to the nonlinear time-domain simulation, residue method is used to identify the best location for installing the new PSS. Therefore, all eigenvectors' components for the 0.5 Hz mode are normalized based on machine 28, so the eigenvector is reconstructed as shown in Table 6-3 below.

By analyzing the normalized eigenvector, it can be noticed that the inter area oscillations exist between the machines which are located in area 2 against those located in area 1 and 3. For example, machine number 28 in area 2 and machine 17 in area 1 are completely out of phase, since the angular displacement between them is about 183 degree. The latter totally agrees with the nonlinear time-domain simulation shown above.

Table 6-3 Normalized Eigenvectors Based on Machine 28

Machine	Magnitude (pu)	Angle (deg)
28	1.00	0.00
22	0.98	5.09
20	0.97	4.72
19	0.96	5.22
29	0.95	5.69
27	0.94	5.99
26	0.93	5.85
25	0.89	4.81
21	0.88	5.45
24	0.83	4.92
23	0.77	6.30
4	0.23	173.92
12	0.23	159.79
11	0.23	160.36
13	0.23	162.81
10	0.23	164.62
14	0.23	159.83
3	0.23	170.49
8	0.23	162.32
7	0.22	168.46
1	0.22	173.45
2	0.22	174.97
15	0.21	171.25
18	0.21	177.26
5	0.20	178.68
6	0.19	176.43
16	0.13	175.99
17	0.13	183.17
9	0.09	158.21

In addition to that, it is worth to mention important criteria for selecting the best location for tuning or installing PSSs [115]:

- Selected units should be large units.

- PSSs should be installed in units that oscillate most (i.e. units which have large eigenvector magnitudes or large participation factor).
- PSSs should be installed in units with medium to fast excitation systems.

By applying the aforementioned criteria for selecting the optimal location for installing new PSS, it is quite clear that machine 28 is the best candidate for deploying a new PSS. Since, it has the highest magnitude of oscillation and a fast excitation system. Besides that, it is a large power plant.

6.4 Coordinated Design of PSSs

The optimization approach described in chapter 4 is applied to coordinate the design of the proposed and the existing PSSs. The optimization problem is based on a nonlinear objective function aims to minimize the Integral of Time Weighted Absolute Error (ITAE) described in chapter 4 equation (4.7). The convergence curve of the objective function is shown in Fig. 6.3 while the existing and optimized parameters of the coordinated PSSs are presented in Table 6-4.

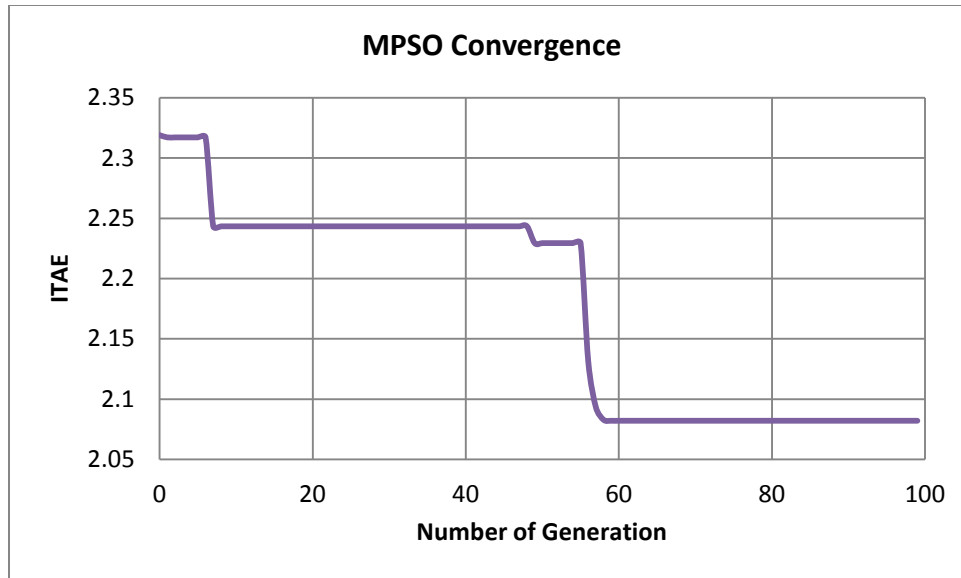


Fig. 6.3 MPSO Convergence Curve for Coordinated Design of PSSs

Table 6-4 Optimized PSSs Parameters Based on the Coordinated Design of PSSs

Machine	K_{s1}^*		T_1^*		T_2^*		T_3^*		T_4^*	
	Ex.	Prop.	Ex.	Prop.	Ex.	Prop.	Ex.	Prop.	Ex.	Prop.
1	-0.367	-1.28	0.2	0.2	0.05	0.0099	0.2	0.2	0.05	0.0099
2	-0.367	-1.28	0.2	0.2	0.05	0.0099	0.2	0.2	0.05	0.0099
3	-1	-0.5	0.15	0.5	0.016	0.05	0.15	0.5	0.033	0.05
10	50	50	2.5	2.5	1.57	1.57	0.202	0.2	0.05	0.05
11	5	5	0.4	0.4	0.02	0.02	0.06	0.4	0.01	0.02
12	15	15	0.3	0.3	0.04	0.04	0.1	0.3	0.01	0.04
13	15	15	0.3	0.3	0.04	0.04	0.1	0.3	0.01	0.04
14	10	10	0.3	0.3	0.02	0.02	0.06	0.3	0.01	0.02
16	15	15	0.3	0.3	0.04	0.04	0.1	0.3	0.01	0.04
17	15	10	0.15	0.75	0.02	0.202	0.15	0.75	0.03	0.202
28	15	18	0.15	0.15	0.025	0.02	0.12	0.15	0.03	0.02

* The optimized time constants for PSS type IEE2ST are T_5, T_6, T_7, T_8 instead of $T_1 - T_4$ and K_1 instead of K_{s1}

6.5 Modal Analysis Results with the Proposed Power System

In order to compare the performance of the considered power system before and after the deployment of the proposed PSSs, the same fault described in section 6.2 is simulated. The below two subsections summarize the modal analysis results for rotor speed deviations and active power flow of line 44 – 63, respectively.

6.5.1 Eigenvalue Results Concomitant with Rotor Speed Deviations

The results in Table 6-5 show that most of the inter-Area oscillations within areas 1 and 3 are eliminated. Moreover, the damping factors and damping ratios for most of the remaining inter-Area modes are noticeably improved. Also, the magnitude of oscillations are markedly reduced. For instance, it can be seen that the smallest damping ratio of the inter-Area mode of oscillation after implementing the optimized PSSs is 0.081 concomitant with machine 29 in area 2, compared to the previous smallest damping ratio of 0.071 associated with machine 9 in area 3. On the other hand, the new highest damping ratio is 0.75 for machine 11 compared to the previous highest damping ratio of 0.08 for machine 28. This is a clear evident that the overall power system performance is significantly enhanced after implementing the proposed coordinated PSSs.

Table 6-5 Modal Analysis for the Inter Area 0.5 Hz – Mode, Cord. PSSs

M/C	Eigenvalue		Eigen Vector		Freq. (Hz)	ζ
	Real (σ)	Imaginary (ω)	Magnitude (pu)	Angle (deg.)		
9	-0.319430	0.93601	0.00000330	-46.2	0.149	0.322979
11	-1.690790	1.49757	0.00000327	51.7	0.238	0.748585
19	-0.803702	4.34957	0.00000143	-97.9	0.692	0.181701
20	-0.727758	4.10317	0.00000171	-79.3	0.653	0.174639
21	-1.254350	4.30118	0.00000181	-79.0	0.685	0.279967
22	-0.727645	3.84275	0.00000146	-48.7	0.612	0.186049
23	-0.562742	4.33978	0.00000115	-89.6	0.691	0.128594
24	-0.700889	4.20346	0.00000100	-80.4	0.669	0.164470
25	-0.832976	4.20675	0.00000065	-114.9	0.670	0.194238
26	-1.219140	3.77314	0.00000320	-73.6	0.601	0.307459
27	-0.672590	3.49796	0.00000191	-25.5	0.557	0.188822
28	-0.623019	3.57495	0.00000043	-66.6	0.569	0.171686
29	-0.309061	3.79958	0.00000063	-43.3	0.605	0.081073

6.5.2 Eigenvalue Results Concomitant with Active Power Flow

In addition to the eigenvalues of rotor speed deviations, Table 6-6 below shows the modal components of the oscillatory power flow of the transmission line connecting areas 1 and 2 for the existing power system. Similar to the previous modal analysis of the existing system, the period from 14 to 20 seconds is selected. As stated before, the selected range of time is basically chosen to ignore the first two peaks of Fig. 6.1, so that angular related phenomena are excluded.

Table 6-6 Modal Decomposition of Active Power Flow of Line 44 – 63

Component No.	Eigenvalue		Eigen Vector		Freq. (Hz)	ζ
	σ	ω	Mag. (MW)	Ang. (deg.)		
1	0.000366	--	214.67	--		
2	-0.243306	3.14817	17.426	71.87	0.501	0.077055
3	-0.323858	--	0.65535	--	3.088	
4	-0.493318	6.28895	0.1309	-26.63	1.001	0.078202
5	-0.358357	7.79232	0.004073	-39.47	1.24	0.04594
6	-0.329588	10.3028	0.000312	-138.93	1.64	0.031974

The modal decomposition of the power flow can be explained as follow; the first component is the constant power flow of about 214.67 MW. Whereas, the second component is the dominate EM which is slowly damped with damping ratio of 0.077 and a sinusoidal wave form with magnitude of 17.43 MW and a frequency of 0.501 Hz. The third, fourth, fifth and sixth components are also slowly damped but they have very low magnitudes.

Similar analysis is repeated with the proposed coordinated design, the below Table 6-7 compares the existing and the proposed cases results.

Table 6-7 Comparison of Modal Analysis Results for the Existing and Proposed PSSs

Case	Eigenvalue		Eigen Vector		Freq. (Hz)	ζ
	σ	ω	Mag. (MW)	Ang. (deg.)		
Existing PSSs	-0.24332	3.14816	17.426	71.87	0.501	0.077
Proposed PSSs	-0.59105	4.23575	0.063	111.27	0.674	0.138

It can be observed that the damping factor of the EM after deploying the optimized PSSs (-0.59) is much better than the existing one (-0.243). Moreover, it can be seen that the damping ratio of the proposed system is much better than the existing case. It is increased

from 0.077 to 0.138. In addition to that, the magnitude of oscillations after deploying the optimized PSSs is substantially decreased from 17.4 MW to 0.063 MW.

6.6 Nonlinear Time-domain Simulation Results

6.6.1 Rotor Angles' Responses

Fig. 6.4 to Fig. 6.6 show the rotor angles for three machines in different areas. These figures compare the dynamic stability of the power system before and after deploying the coordinated design of the PSSs. By analyzing these figures, it is quite clear that the dynamic performances of the system with the proposed controller is considerably improved. For example, the overshoot and settling time of machine 28 in area 2 are noticeably decreased. The overshoot is considerably reduced to one third of its previous value, while, the settling time is decreased from about 20 to 6 seconds.

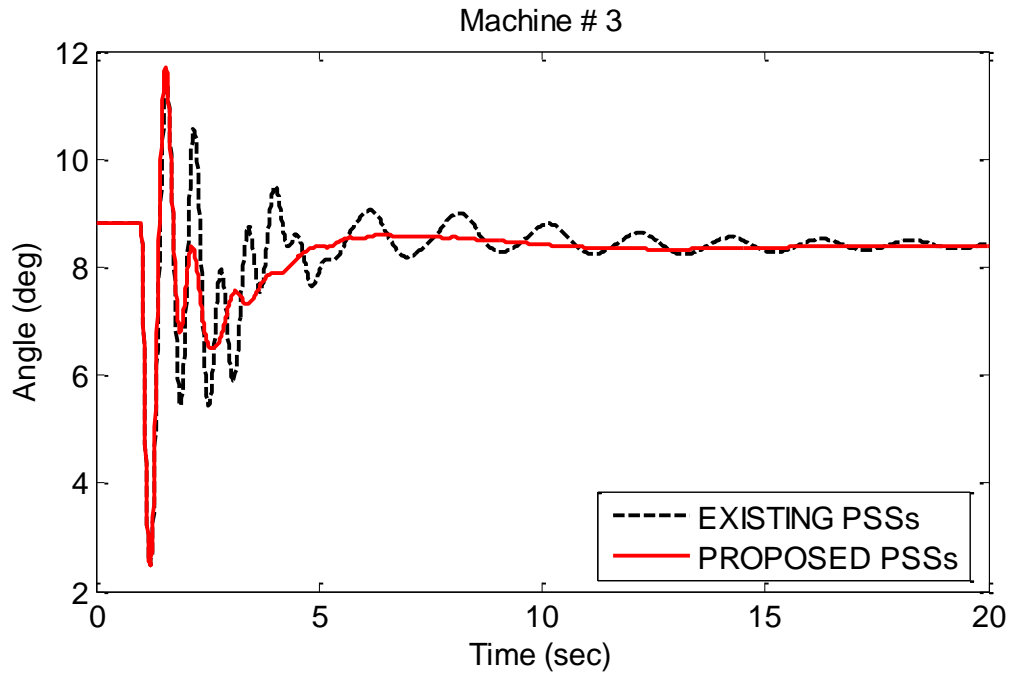


Fig. 6.4 Rotor Angle, Unit 3-Area 3, 3-Ph. Fault for 0.1s, Cord. PSSs

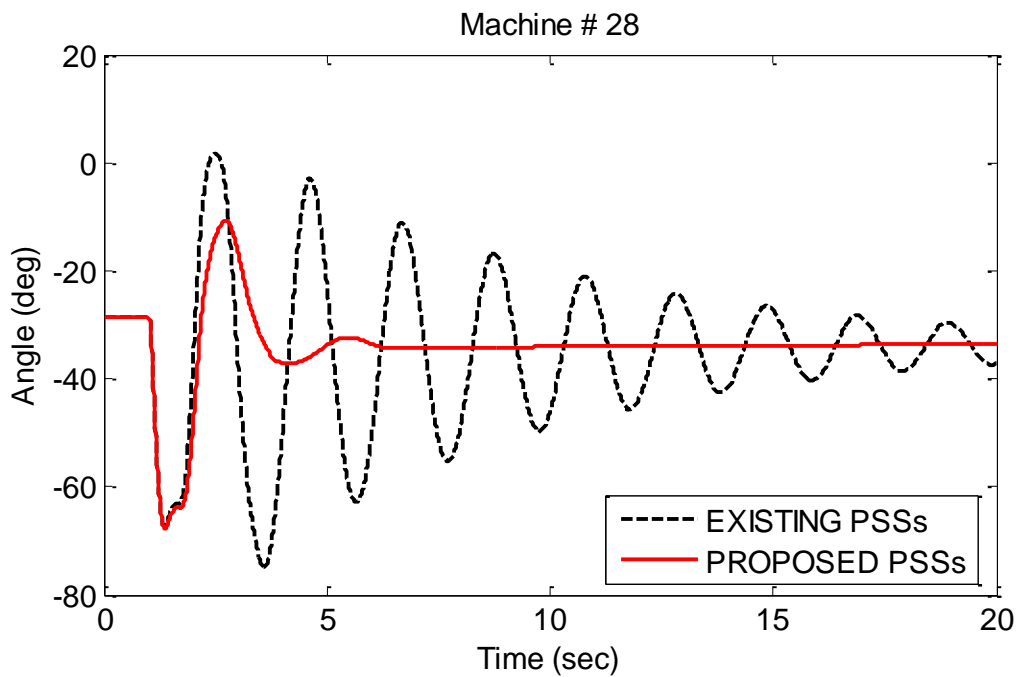


Fig. 6.5 Rotor Angle, Unit 28-Area 2, 3-Ph. Fault for 0.1s, Cord. PSSs

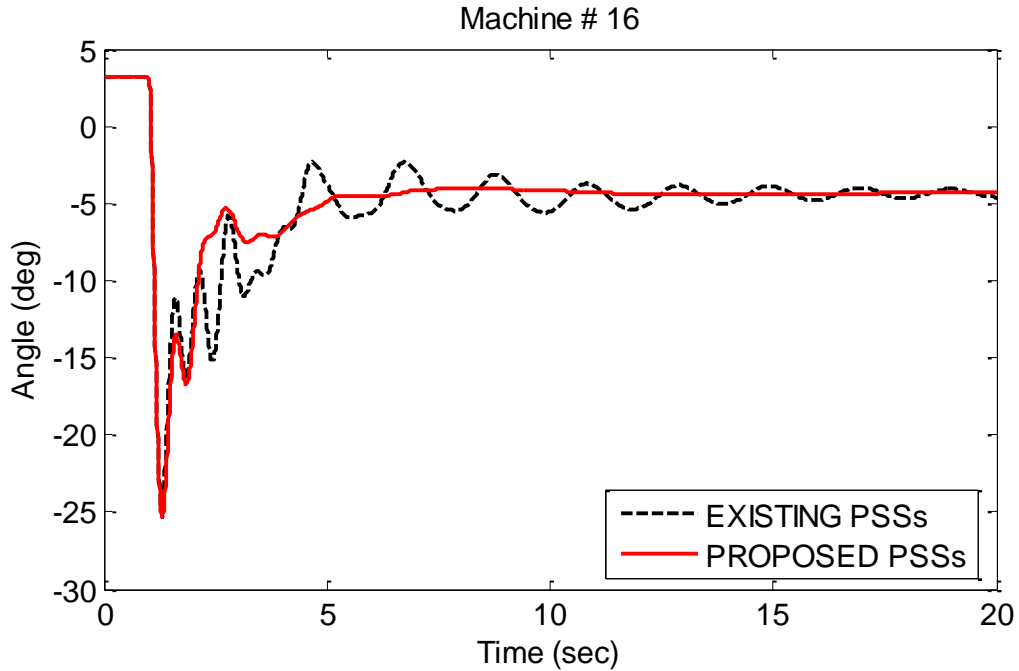


Fig. 6.6 Rotor Angle, Unit 16-Area 1, 3-Ph. Fault for 0.1s, Cord. PSSs

6.6.2 Machines' Electrical Power Responses

Fig. 6.7 to Fig. 6.9 display the electrical power for three machines in different regions. Similar to the previous figures, these figures show the dynamic stability of the power system before and after deploying the coordinated design of the PSSs. As can be observed, the machines' electrical power oscillations rapidly attenuate after implementing the coordinated design. For instance, it can be seen that machine 28 has overshoot and settling time much less than the existing system.

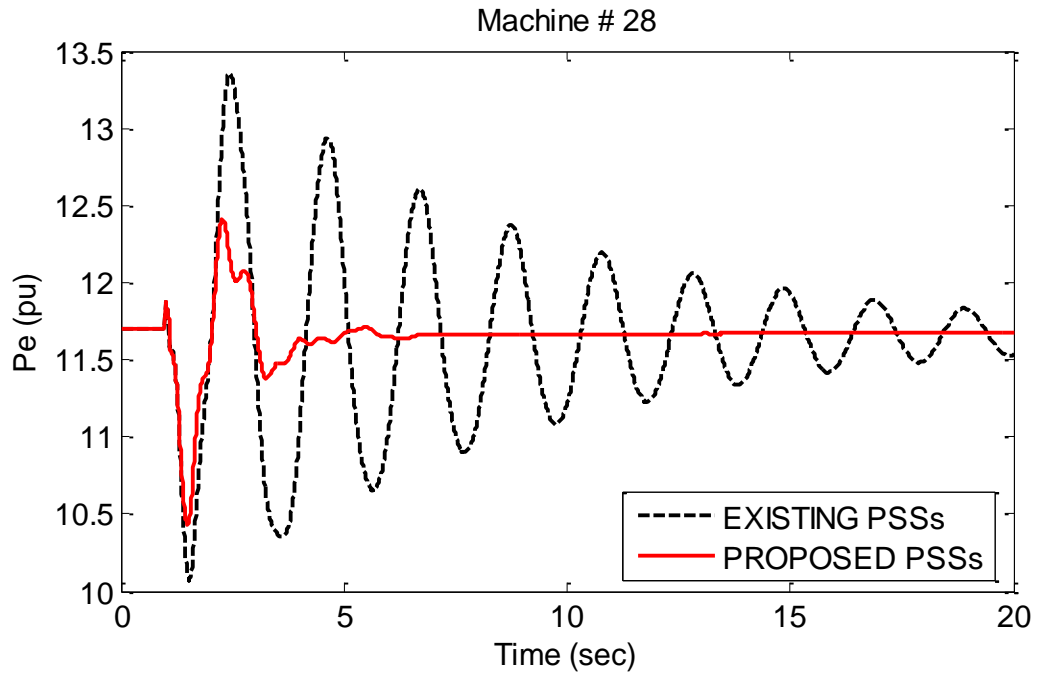


Fig. 6.7 Electrical Power, Unit 28-Area 2, 3-Ph. Fault for 0.1s, Cord. PSSs

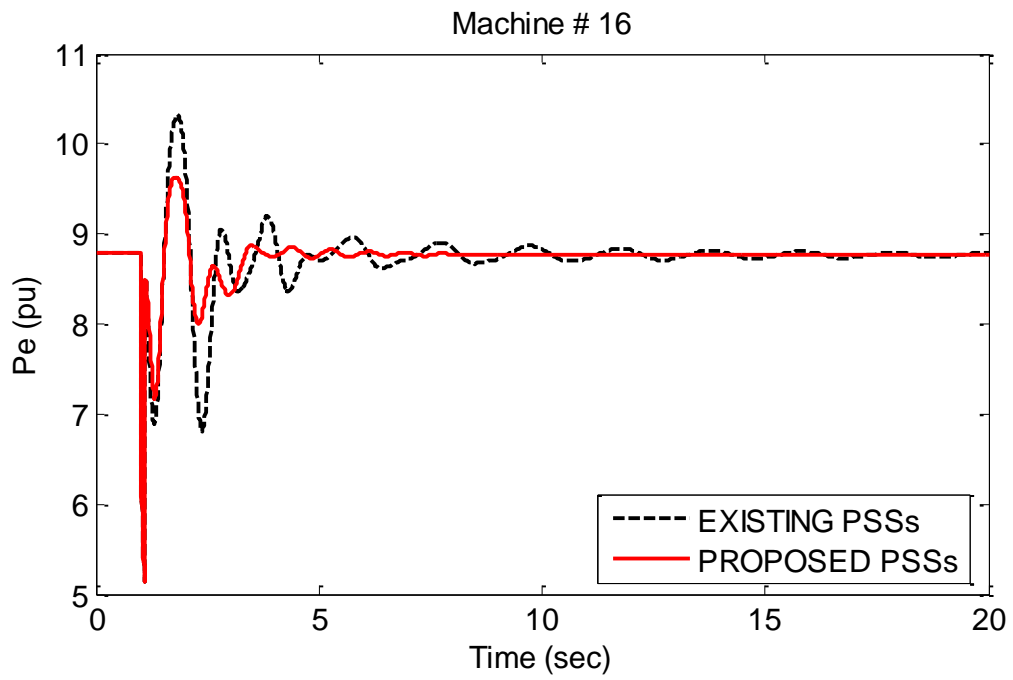


Fig. 6.8 Electrical Power, Unit 16-Area 1, 3-Ph. Fault for 0.1s, Cord. PSSs

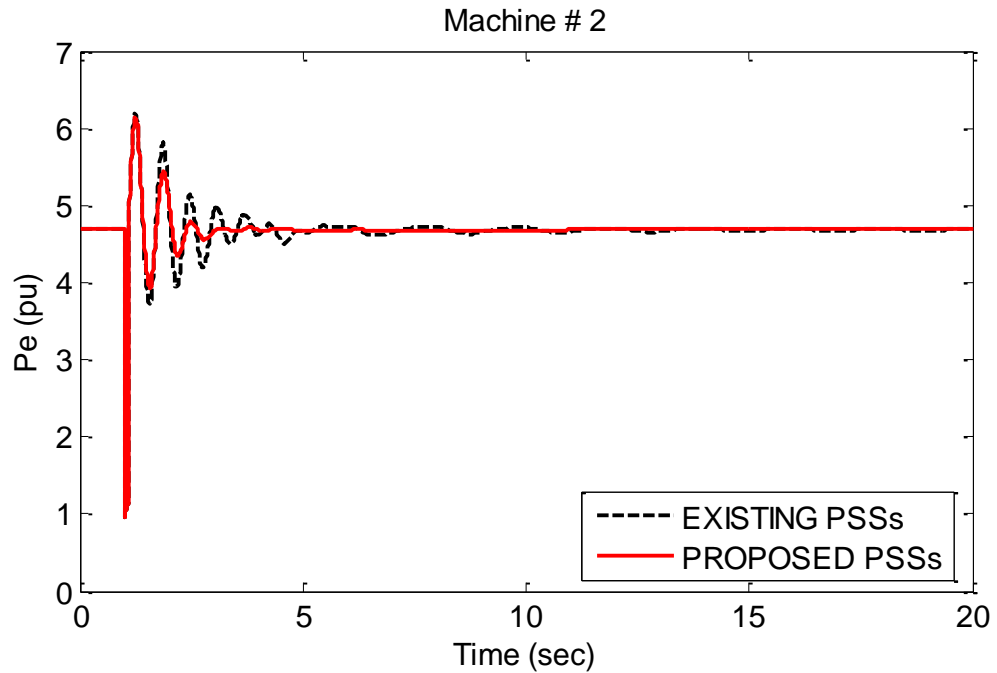


Fig. 6.9 Electrical Power, Unit 2-Area 3, 3-Ph. Fault for 0.1s, Cord. PSSs

6.6.3 Rotor Speed Deviations' Responses

Fig. 6.10 to Fig. 6.12 show the rotor speed deviations for different machines. As can be seen, the dynamic response of the rotor speed deviations with the proposed design is much better than the existing situation. To illustrate, it can be observed that machines 28, 16 and 2 have fewer oscillations, less overshoot and settling time than the existing system.

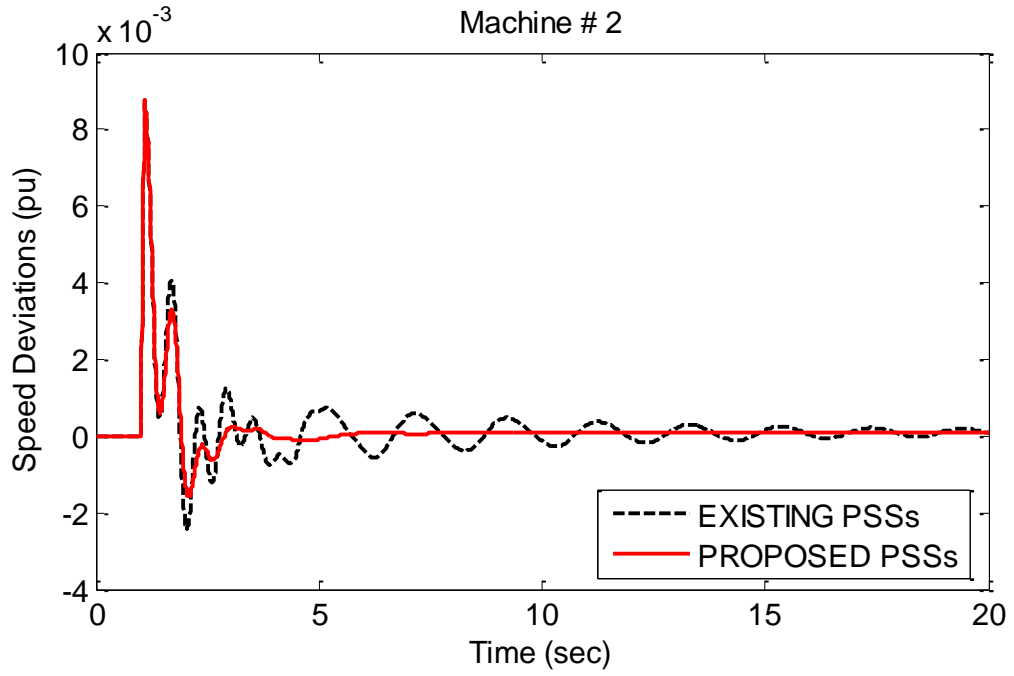


Fig. 6.10 Speed Deviations, Unit 2-Area 3, 3-Ph. Fault for 0.1s, Cord. PSSs

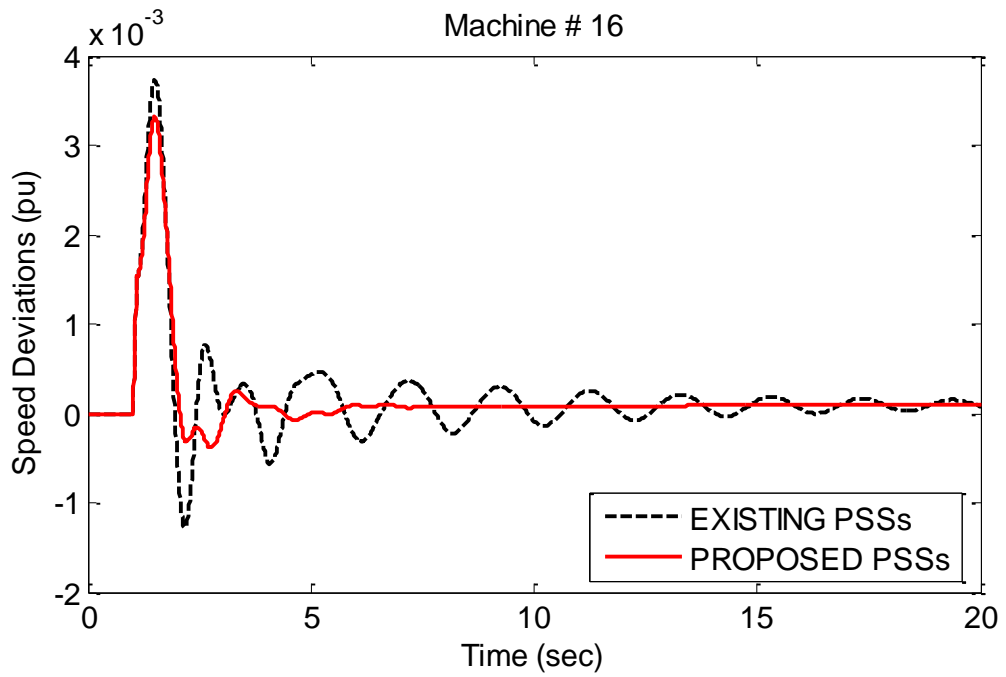


Fig. 6.11 Speed Deviations, Unit 16-Area 1, 3-Ph. Fault for 0.1s, Cord. PSSs

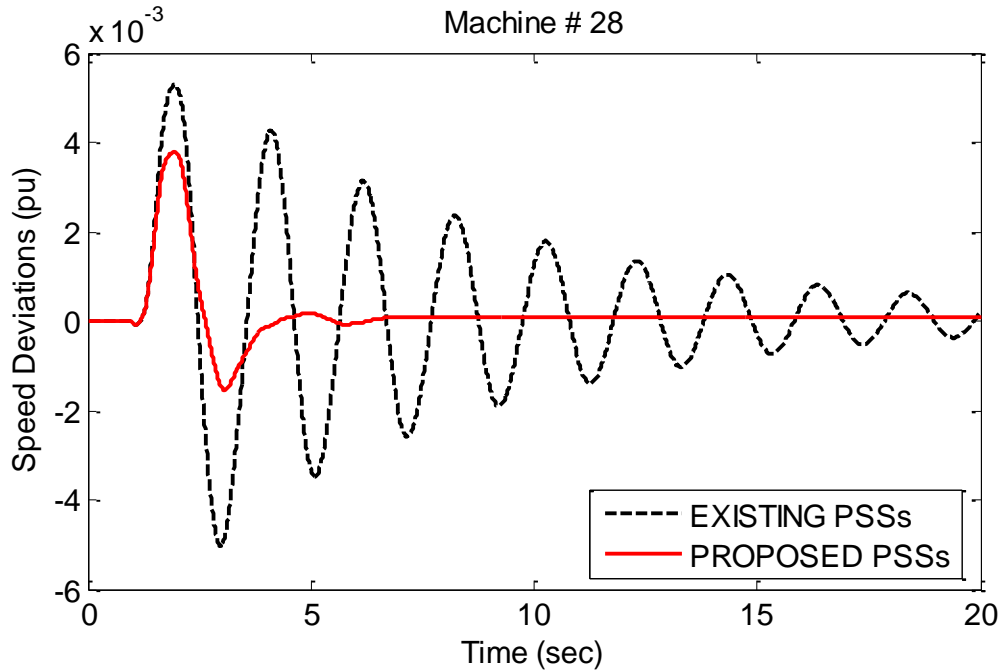


Fig. 6.12 Speed Deviations, Unit 28-Area 2, 3-Ph. Fault for 0.1s, Cord. PSSs

6.6.4 Voltages' Responses

By analyzing Fig. 6.13 to Fig. 6.15, it is quite evident that even the voltage profile is markedly improved after deploying the proposed controller. For example, the existing voltage oscillations at buses 44 and 63 rapidly damp with the new controller. Moreover, most of the voltages in all areas settle down to their steady state values after around 6 to 7 seconds with the coordinated design compared to 15 to 20 seconds without it.

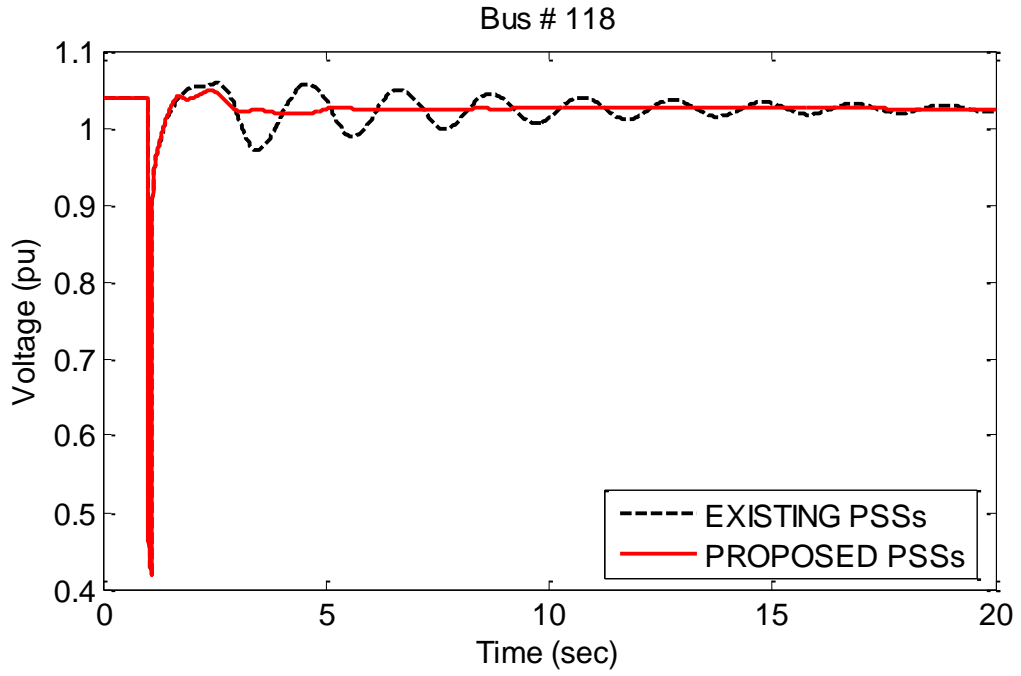


Fig. 6.13 Voltage, Bus 118-Area 3, 3-Ph. Fault for 0.1s, Cord. PSSs

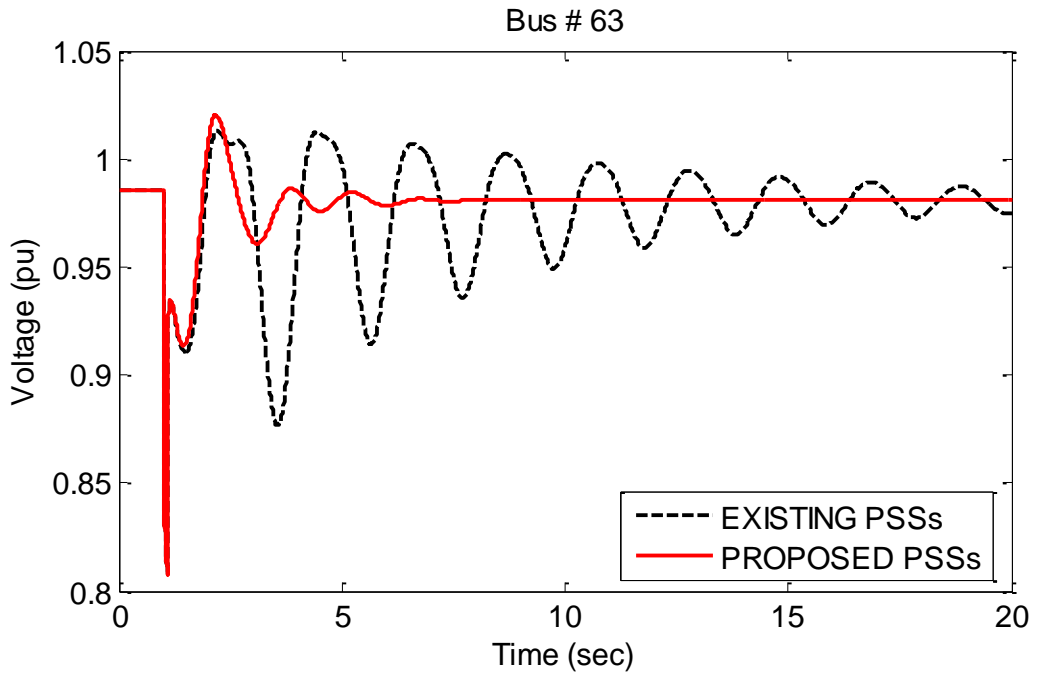


Fig. 6.14 Voltage, Bus 63-Area 2, 3-Ph. Fault for 0.1s, Cord. PSSs

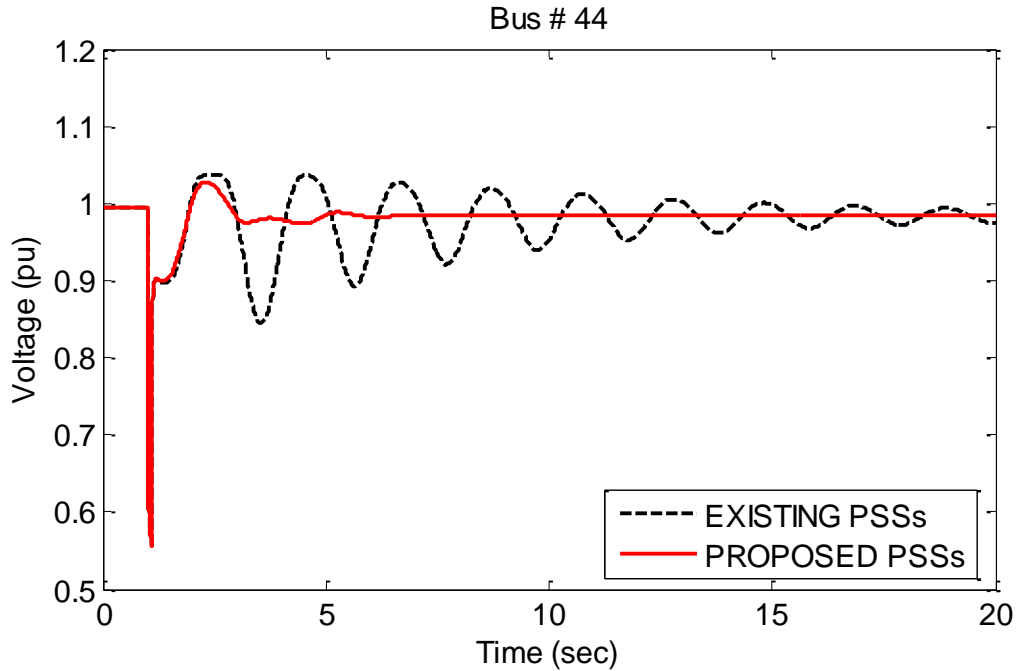


Fig. 6.15 Voltage, Bus 44-Area 1, 3-Ph. Fault for 0.1s, Cord. PSSs

6.6.5 Active Power Flow Responses

Last but not least, the below Fig. 6.16 to Fig. 6.18 depict the active power flow of the 380 kV intertie lines. The first two figures demonstrate the substantial increase in the active power flow of the intertie lines between area 3 and 1 due to the tripping of one double circuit line connecting these areas. By analyzing the below figures, it can be realized that the overall dynamic stability of the considered power system is greatly enhanced after deploying the coordinated design of the PSSs. Thus, the transfer limit capability among these areas can be significantly increased.

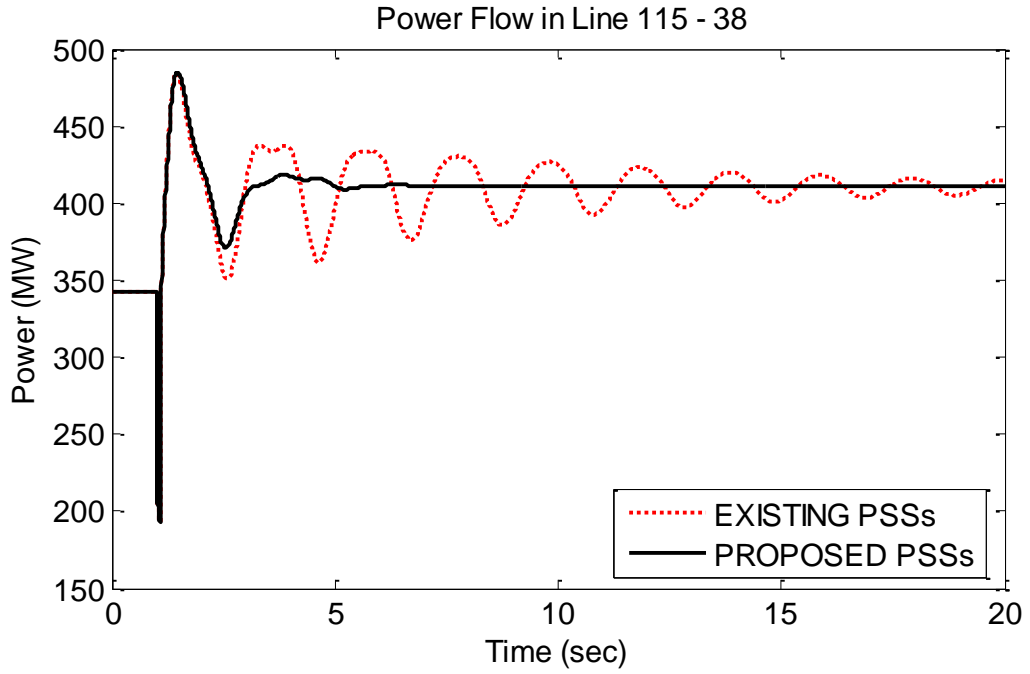


Fig. 6.16 Active Power, Line 115 to 38, 3-Ph. Fault for 0.1s, Cord. PSSs

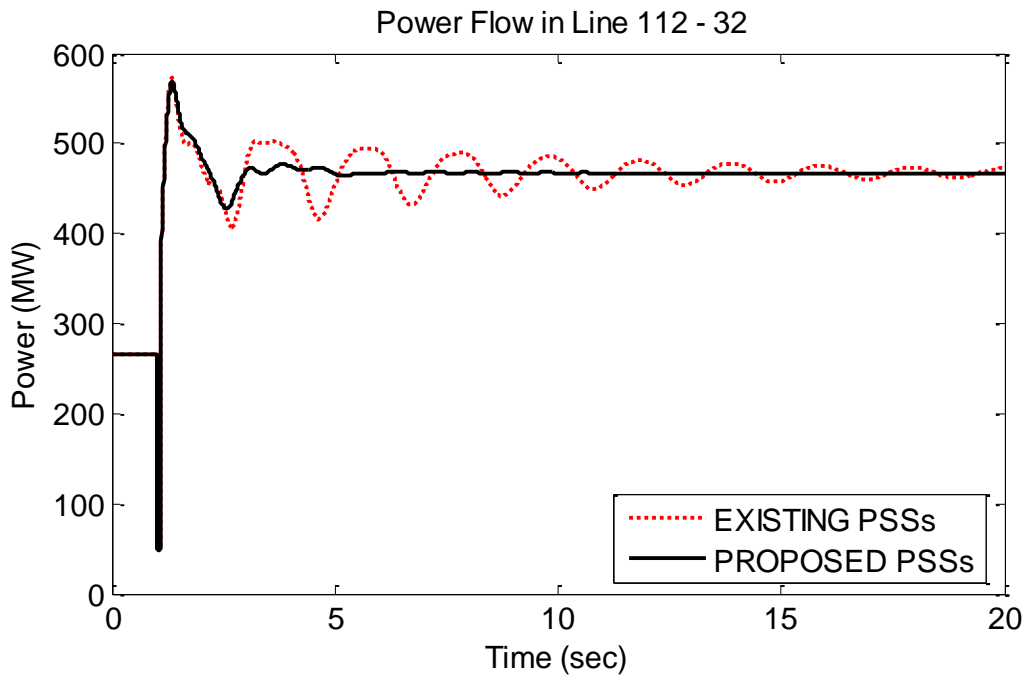


Fig. 6.17 Active Power, Line 112 to 32, 3-Ph. Fault for 0.1s, Cord. PSSs

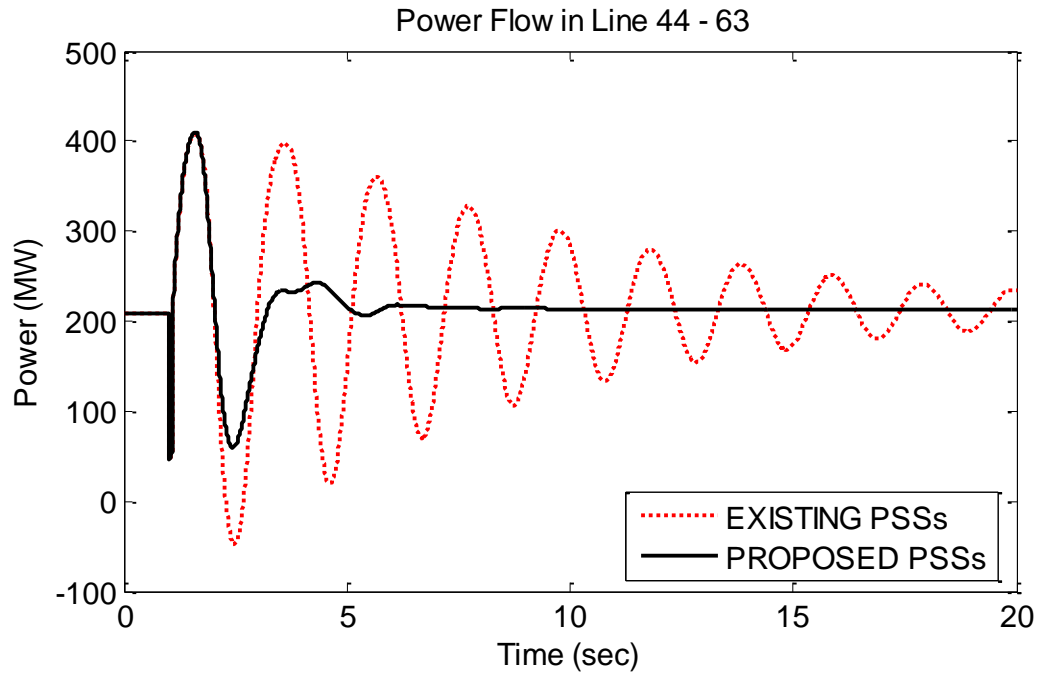


Fig. 6.18 Active Power, Line 44 to 63, 3-Ph. Fault for 0.1s, Cord. PSSs

6.7 Robustness of the Proposed Coordination of the PSSs

To validate the robustness of the proposed controller, the following analyses are investigated:

- 1) Comparison of the existing maximum power transfer with and without the proposed PSSs.
- 2) Identification of the new maximum power transfer limit after deploying the proposed controller.
- 3) Execution of several faults at different locations considering the new maximum power transfer.

In order to calculate the maximum power transfer between areas 1 and 2 for the existing base case without any additional controllers, contingency analyses are carried out to detect the worst contingencies that produce high mismatch or do not converge. Then, nonlinear time-domain simulations are executed to monitor the active power flow of the weak line connecting area 1 and 2 for the worst contingencies.

From the contingency analyses, three incidents are identified as severe cases as described below:

Incident 1 : A three phase fault at bus 110 for 0.1 second and cleared by tripping the double circuit line connecting bus 110 and 30.

Incident 2 : A three phase fault at bus 115 for 0.1 second and cleared by tripping the double circuit line connecting bus 115 and 38.

Incident 3 : A three phase fault at bus 38 for 0.1 seconds and cleared by tripping the double circuit line connecting bus 38 and 37.

The below Fig. 6.19 shows the nonlinear time-domain simulations of the active power flow of line 44 – 63 for these cases considering the existing power transfer of 420 MW between these areas. It is quite obvious that the worst incident is incident 2. Since it produces the highest magnitude of oscillations. Therefore, it is used to identify the maximum power transfer that can be attained for the existing power system.

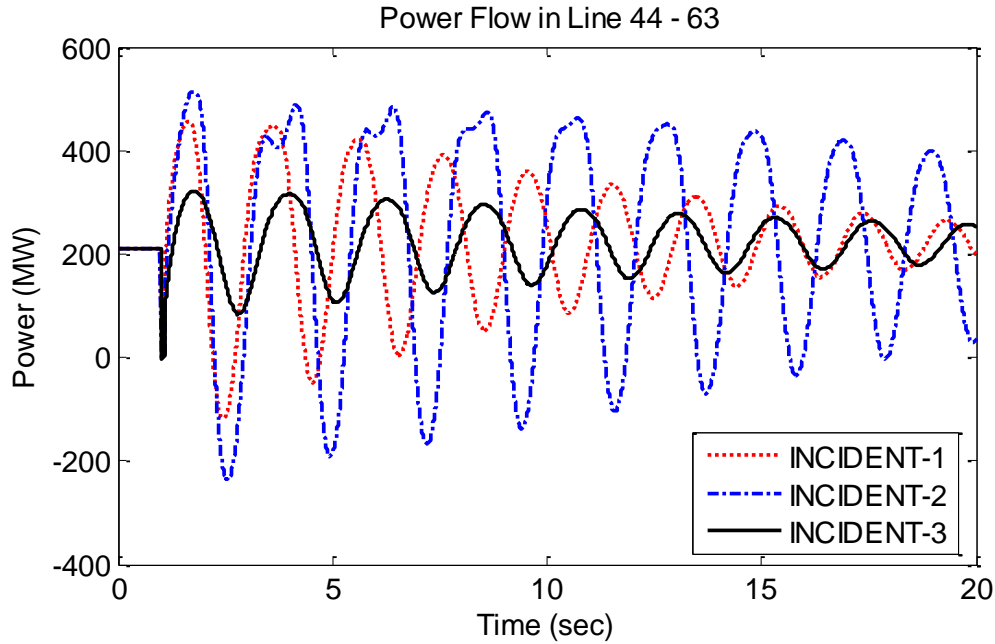


Fig. 6.19 Identification of the Critical Incident, 420 MW Power Transfer

6.7.1 Existing Maximum Power Transfer Limit

To compare the power system performance considering the existing maximum power transfer with and without the proposed coordinated design of the PSSs, incident 2 is applied. Fig. 6.20 shows the maximum power transfer between area 1 and 2 for the existing system compared with the same level of power transfer but after implementing the proposed coordinated PSSs. It is quite clear that the dynamic stability of the system is considerably enhanced after employing the coordinated design of the PSSs.

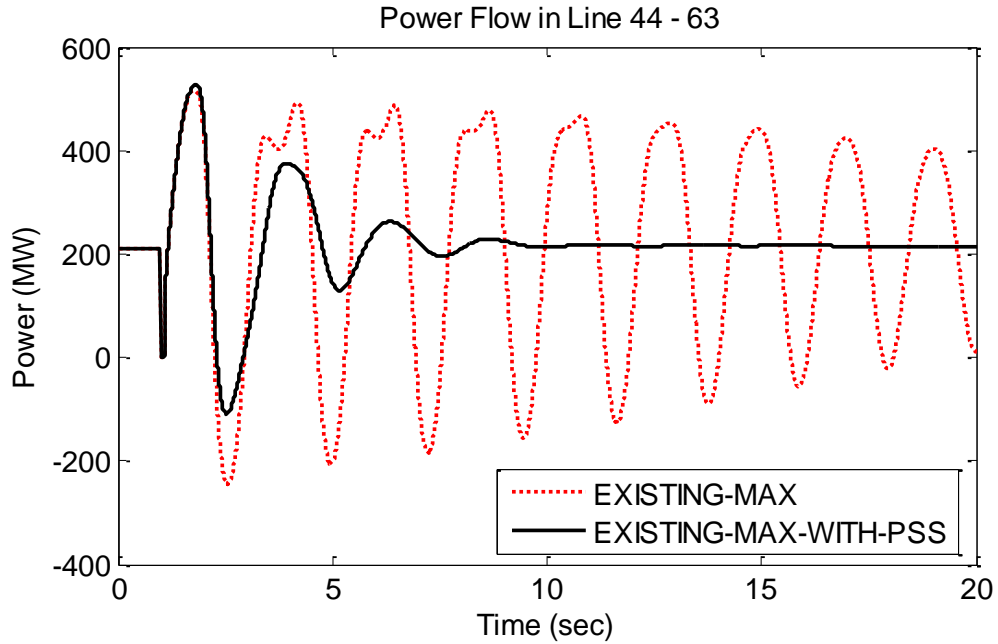


Fig. 6.20 Ex. Max. Power Transfer, Line 44 to 63, 3-Ph. Fault for 0.1s, Cord. PSSs

6.7.2 Maximum Power Transfer Limit with the Proposed PSSs

The same Incident 2 is repeated after employing the proposed coordinated PSSs to calculate the new maximum power transfer. Fig. 6.21 shows that the new maximum power could reach up to 700 MW with the coordinated design of the PSSs.

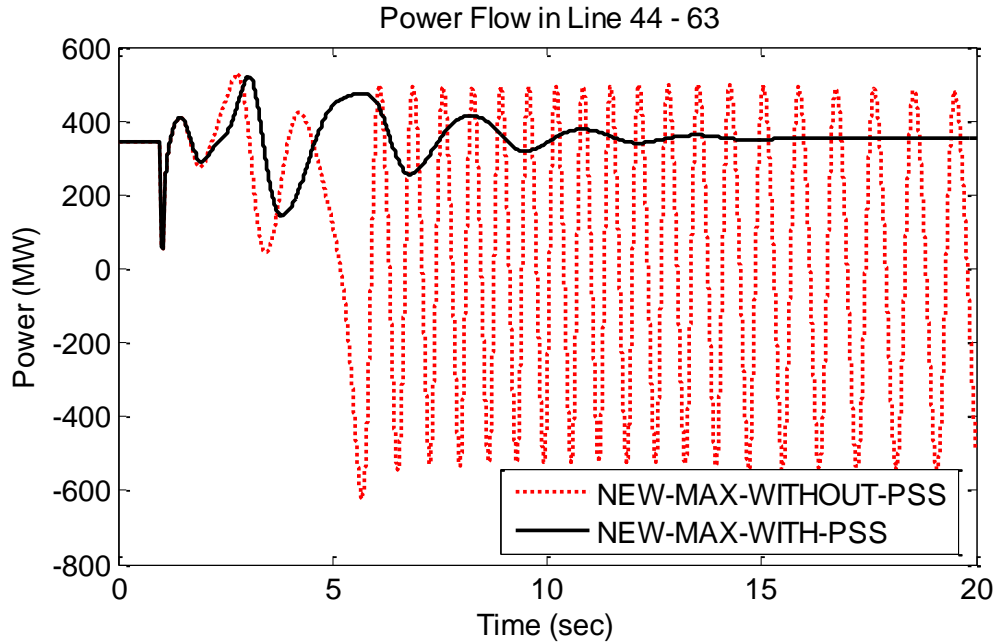


Fig. 6.21 New Max. Power Transfer, Line 44 to 63, 3-Ph. Fault for 0.1s, Cord. PSSs

6.7.3 Sensitivity Analyses

To assess the robustness of the proposed design, two additional incidents are executed considering the new maximum power transfer in these analyses.

Sensitivity Incident 1 : A three phase fault at bus 41 for 0.1 second and cleared by tripping the double circuit line connecting bus 41 and 40. This fault is located in area 1.

Sensitivity Incident 2: A three phase fault at bus 56 for 0.1 second and cleared by tripping double circuit line connecting bus 56 and 50. This fault is located in area 2.

Fig. 6.22 and Fig. 6.23 confirm the robustness of the designed controller. The power oscillations rapidly attenuate after deploying the proposed coordination of the PSSs compared to the existing situation.

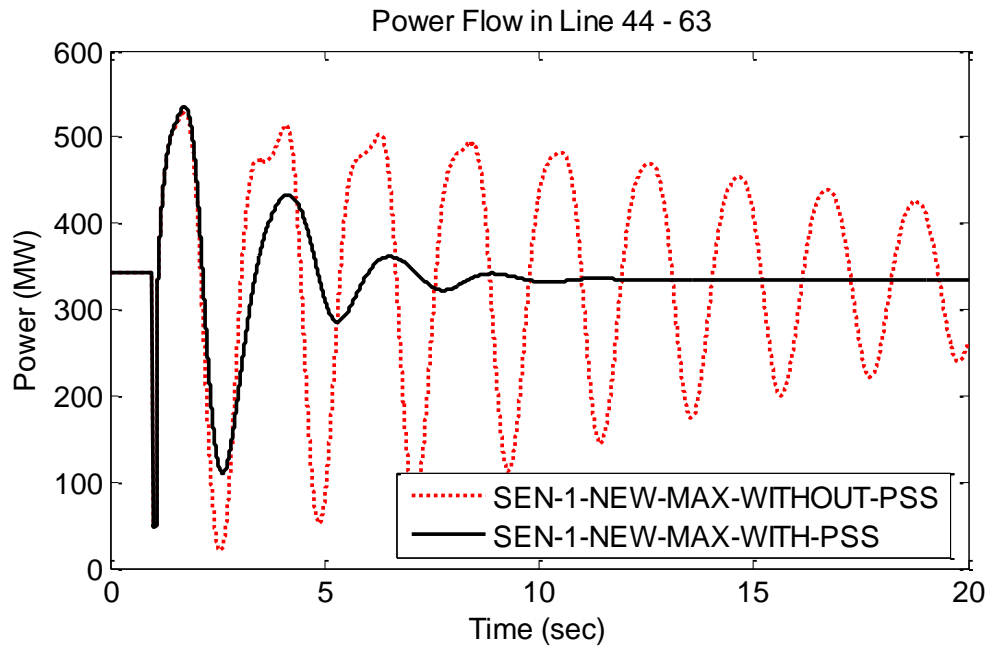


Fig. 6.22 New Max. Power Transfer, Line 44 to 63, Sensitivity 1, Cord. PSSs

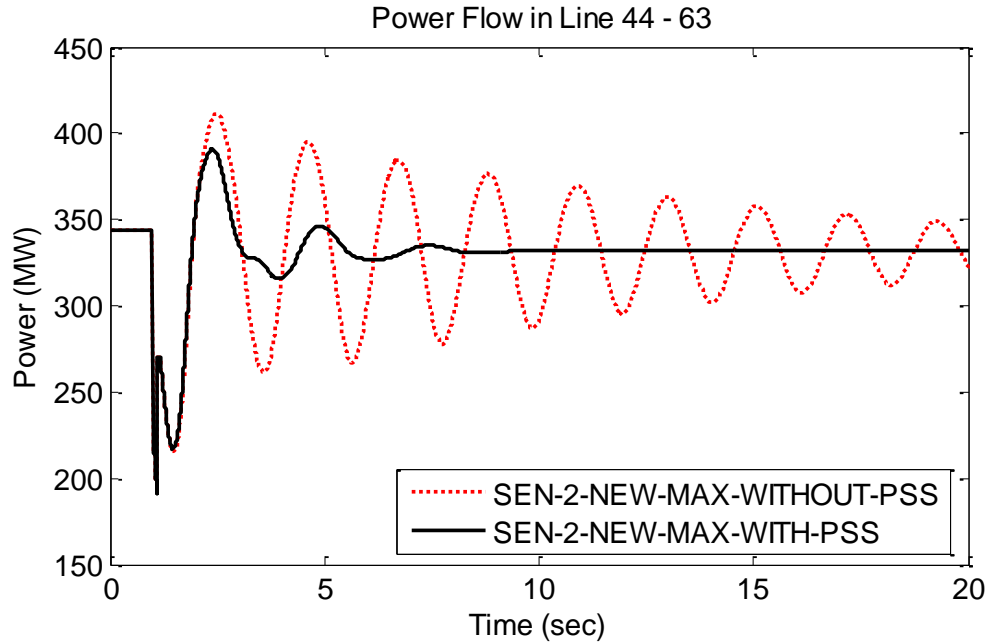


Fig. 6.23 New Max. Power Transfer, Line 44 to 63, Sensitivity 2, Cord. PSSs

6.8 Summary of the Coordinated Design of PSSs

This chapter shows the impact of the simultaneous design of the PSSs on improving the overall dynamic stability of the considered power system. It has been proven that by installing the new PSS and designing its parameters in coordination with the existing PSSs, the existing power oscillations rapidly attenuate. Moreover, the maximum power transfer between areas 1 and 2 is considerably increased from 420 MW to 700 MW. Also, it has been confirmed from the additional sensitivity analyses that the proposed simultaneous design of the PSSs is a robust design.

CHAPTER 7

INDIVIDUAL DESIGN OF TCSC

7.1 Overview

In this chapter, the TCSC is deployed to investigate its impact on attenuating the existing low frequency oscillations. The second section of this chapter discusses the most feasible location for installing the TCSC. Also in the same section, MPSO is employed to individually design the TCSC's parameters. Then, several input signals are fed to the TCSC-POD to find the most observable one. In the third and fourth sections, modal analysis and nonlinear time-domain simulations are conducted, respectively. This is to validate the effectiveness of the proposed design in enhancing the overall dynamic stability of the considered power system. In the last section, the optimized parameters of the proposed TCSC are modeled in the full version of the considered power system to examine its impact on improving the overall dynamic stability and to determine the new maximum power transfer between areas 1 and 2. In the same section, two sensitivity analyses are executed to test the robustness of the proposed TCSC.

7.2 Placement and Design of TCSC Controller

7.2.1 Site Selection

The location of the TCSC can be selected by deploying one of controllability techniques. Controllability means that the device must be able to impact critical lightly damped oscillations. It can be used to determine the most suitable line for installing the TCSC. This can be done by applying a small and temporary change to the reactance of candidate circuits and assessing the magnitude of the resulting network oscillations. Modal analysis can be used to perform the aforementioned assessments by monitoring any strongly participating rotor angle amplitude [106].

However in this work, the TCSC is installed in series with the weak transmission line connecting areas 1 and 2 as can be seen in Fig. 7.1 below. This is due to several reasons as listed below:

- Currently, a Fixed Series Capacitors (FSC) is installed in series with this line. Fortunately, a space for upgrading the FSC to TCSC is dedicated.
- The line is considered as a strategic connection. Since, it interconnect two huge power systems.
- High probability of having small signal oscillations between these two systems due to the weak interconnection.

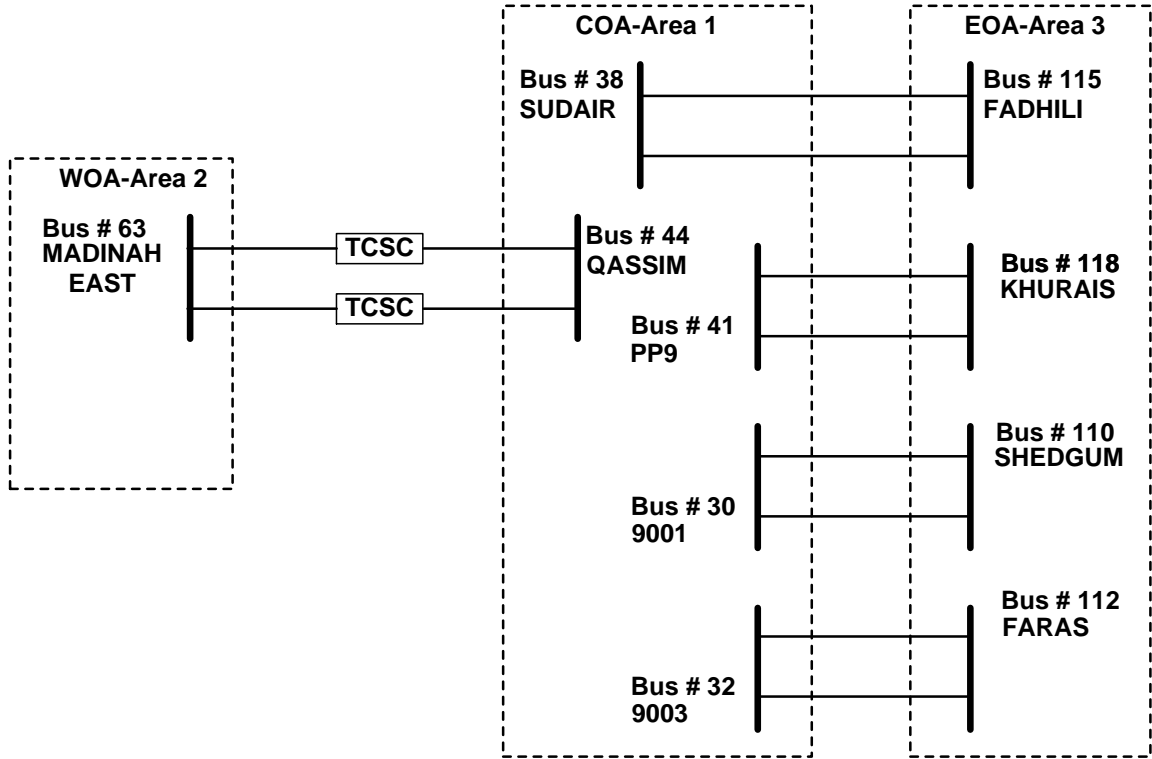


Fig. 7.1 Interconnected Areas with TCSC Installed Between Area 1 and 2

7.2.2 Design of TCSC Controller

In order to design the TCSC, an input signal has to be selected. Therefore, the voltage of bus 44 is fed to the TCSC-POD as a first trial. Then, MPSO is implemented to optimize the TCSC parameters according to the objective function described in chapter 4. The convergence curve of the fitness function is shown in Fig. 7.2 and the optimal parameters (T_{1TCSC} , T_{2TCSC} and K_{TCSC}) are listed in Table 7-1 below. It is worth noting that only the existing PSSs are modeled in this case and their parameters are kept unchanged as per the existing settings.

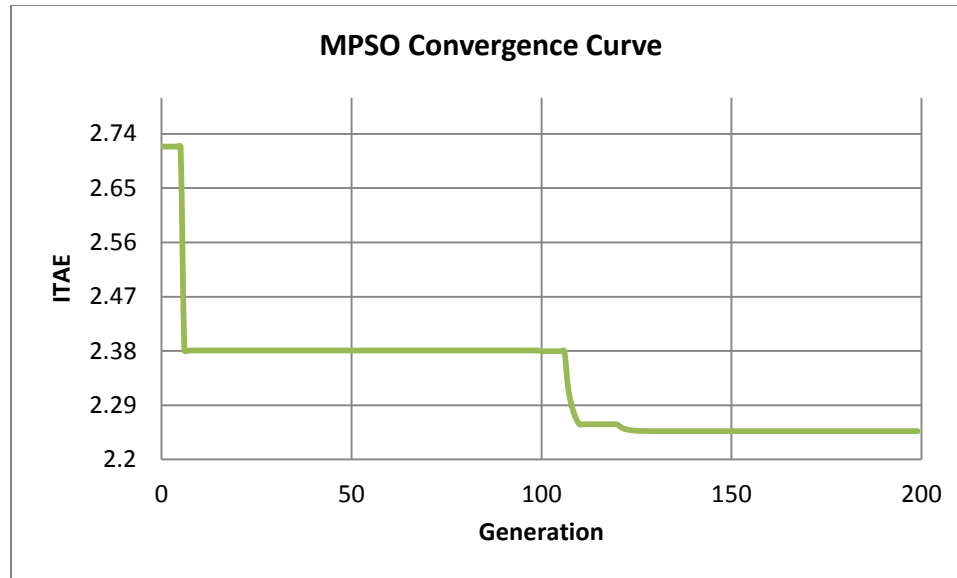


Fig. 7.2 MPSO Convergence Curve for Individual Design of TCSC

Table 7-1 Optimized TCSC Parameters, Individual Design of TCSC

TCSC	T_{1TCSC}	T_{2TCSC}	T_{3TCSC}	T_w	K_{TCSC}	X_{max}	X_{min}
	0.4	0.5	0.025	0.21	1	0.135	0.02

7.2.3 Comparison of Alternative Input Signals

After determining the optimal TCSC's parameters, five input signals are assessed as alternative input signals to the TCSC-POD. Then, in order to rank them according to the most observable one, several nonlinear time-domain simulations are executed. The applied incident is a three phase fault on bus 110 cleared after 0.1 second by tripping line 110 - 30. The input signal which produces the best dynamic performance in terms of minimum overshoot and settling time is selected as the most observable one.

7.2.3.1 Impact of Voltage Input Signals

Fig. 7.3 shows the responses of the active power flow of line 44 – 63 with and without the TCSC for different voltage input signals. It is quite clear that the best input signal is the voltage of bus 44. Since, it produces better damping and settling time than the other input signal.

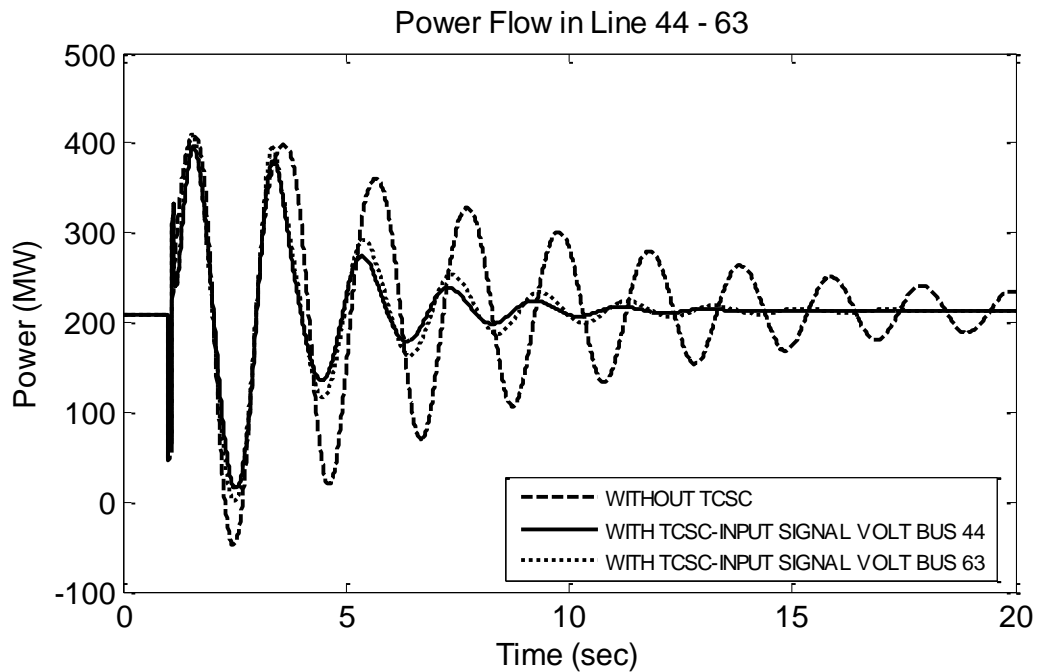


Fig. 7.3 Active Power, Line 44 to 63, Prop. TCSC-Volt. Input Signal

7.2.3.2 Impact of Frequency Input Signals

Similarly, Fig. 7.4 depicts the active power responses of the same aforementioned line with and without the TCSC. The dynamic responses show that the damping effect of the frequency input signal of bus 63 is much better than that of bus 44. The settling time is

reduced from more than 20 seconds to about 13 seconds while the overshoot is reduced from more than 400 MW to less than 390 MW.

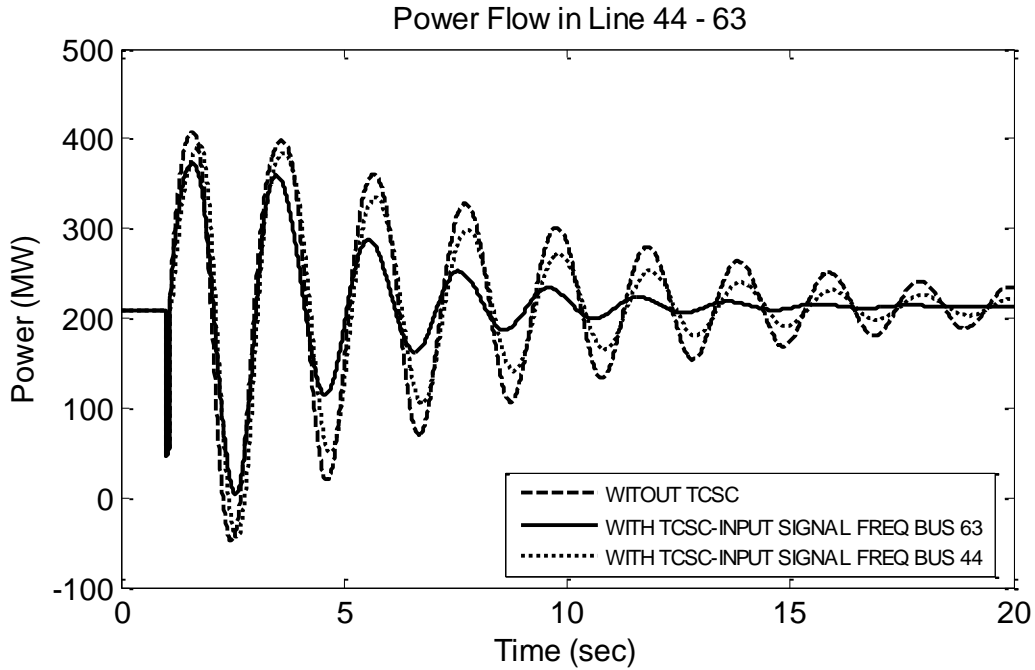


Fig. 7.4 Active Power, Line 44 to 63, Prop. TCSC-Freq. Input Signal

7.2.3.3 Impact of Active Power Flow Input Signal

Last but not least, in this case, the active power flow of line 44 - 63 is utilized as the input signal to the TCSC-POD. By analyzing Fig. 7.5, it can be seen that the power oscillations of this line are substantially decreased with the optimized TCSC. However, the transient overshoot of the power flow is higher than the case without the TCSC.

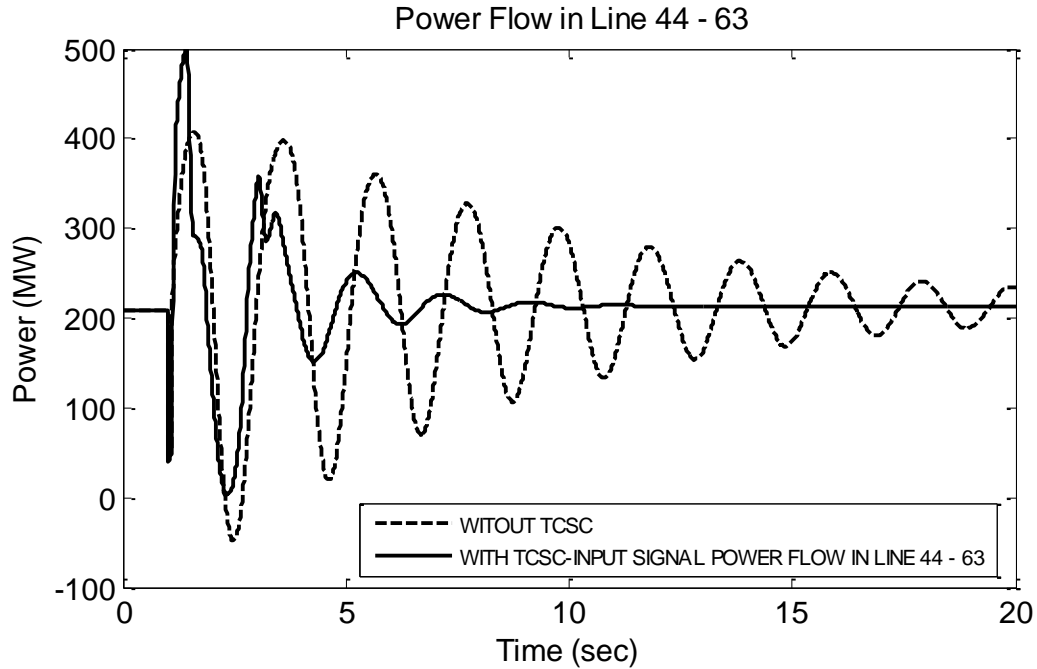


Fig. 7.5 Active Power, Line 44 to 63, Prop. TCSC-Active Power Input Signal

7.2.3.4 Comparison of Best Alternative Input Signals

Fig. 7.6 reflects the impact of the TCSC on the dynamic behavior of the power flow of line 44 - 63 utilizing the most observable TCSC-POD's input signals. It can be observed that the best input signal to the TCSC in terms of settling time is the active power flow of line 44 - 63. Then, the second best is the voltage input of bus 44. The last best input signal is the frequency of bus 63. However, in terms of the overshoot the best input signal is the voltage of bus 44. Therefore, in this work the latter is used as the input signal of the TCSC-POD for the whole proceeding analyses.

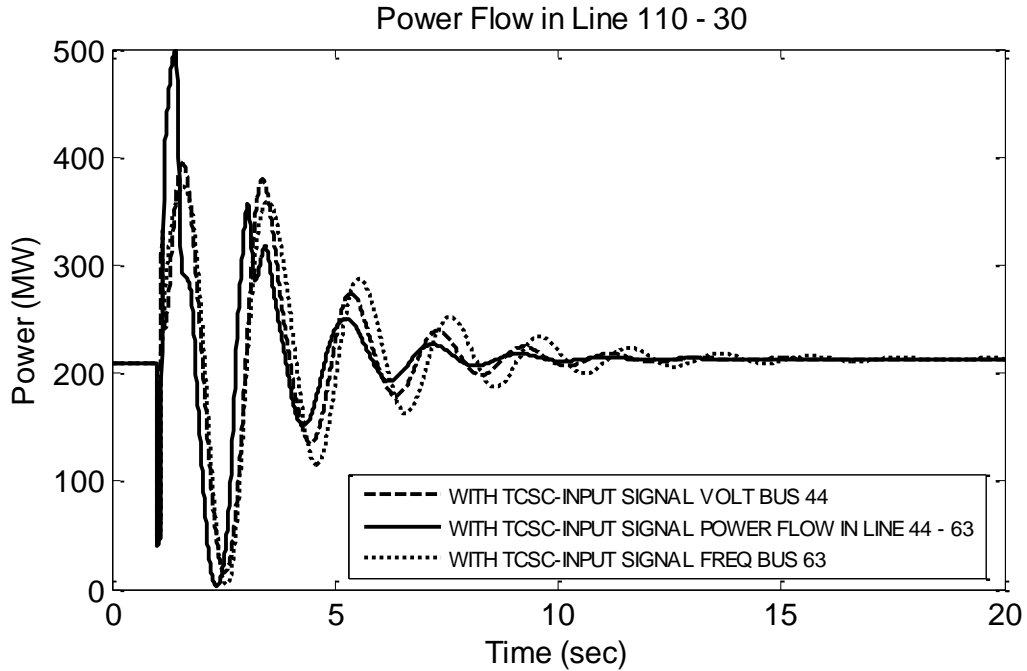


Fig. 7.6 Active Power, Line 44 to 63, Prop. TCSC-Best Input Signals

7.3 Modal Analysis Results with the Proposed TCSC

Modal analyses are carried out for both rotor speed deviations of all units as well as active power flow of the intertie lines. The considered incident is a three phase fault at bus 110 for 0.1 second and then it is cleared by tripping line 110-30. The following two sections discuss the comparison between the power system performance with and without the optimized TCSC.

7.3.1 Eigenvalue Results Concomitant with Rotor Speed Deviations

Reference is made to Table 6-2 in the previous chapter and Table 7-2 below. By comparing the two results, it can be seen that before the installation of the TCSC, the highest damping ratio of the rotor speed deviations for the EM mode of oscillations is 0.08. Whereas, after deploying the optimized TCSC, the highest damping ratio is 0.224. On the other hand, the smallest damping ratio for the existing power system without TCSC is 0.071. While after incorporating the new optimized TCSC, the lowest damping ratio is 0.167. In general, by comparing Table 6-2 with Table 7-2, it can be observed that by deploying the optimized TCSC most of the rotor speed deviations' damping factors are shifted to more stable regions. Also, their magnitudes are substantially reduced and their damping ratios are greatly improved. Thus, it is quite clear that the overall dynamic performance is significantly enhanced after the deployment of the TCSC.

7.3.2 Eigenvalue Results Concomitant with Active Power Flow

Table 7-3 below shows the comparison between the existing modal analysis results and the proposed one. It is quite clear that the line active power eigenvalue and damping ratio are noticeably enhanced after the installation of the optimized TCSC. The new damping factor of -0.58 is much better than the existing one which is -0.24. Moreover, the damping ratio is significantly improved from 0.077 to 0.176. Also, the magnitude of oscillations is markedly reduced from 17.011 MW to 0.23 MW.

Table 7-2 Modal Analysis for the Inter Area 0.5 Hz – Mode, Prop. TCSC

M/C	Eigenvalue		Eigen Vector		Freq. (Hz)	ζ
	Real (σ)	Imaginary (ω)	Magnitude (pu)	Angle (deg.)		
1	-0.599082	3.214530	0.000001	-115	0.512	0.183
2	-0.606516	3.24951	0.000001	-120	0.517	0.183
3	-0.580556	3.22700	0.000001	-120	0.514	0.177
4	-0.502915	2.96850	0.000001	-67	0.472	0.167
5	-0.629616	3.22378	0.000001	-111	0.513	0.192
6	-0.603538	3.24105	0.000001	-116	0.516	0.183
7	-0.605659	3.23024	0.000001	-122	0.514	0.184
8	-0.612177	3.21119	0.000001	-124	0.511	0.187
9	-0.680534	3.17652	0.000001	-131	0.506	0.209
10	-0.589614	3.16032	0.000001	-118	0.503	0.183
11	-0.634160	3.24469	0.000001	-134	0.516	0.192
12	-0.598307	3.24989	0.000001	-134	0.517	0.181
13	-0.585392	3.17755	0.000001	-122	0.506	0.181
14	-0.601513	3.24707	0.000001	-133	0.517	0.182
15	-0.615993	3.26089	0.000001	-124	0.519	0.186
16	-0.671055	3.22903	0.000001	-129	0.514	0.203
17	-0.724330	3.15635	0.000001	-114	0.502	0.224
18	-0.705227	3.29234	0.000001	-134	0.524	0.209
19	-0.575339	3.24841	0.000004	73	0.517	0.174
20	-0.574748	3.24849	0.000004	73	0.517	0.174
21	-0.577445	3.25732	0.000004	71	0.518	0.175
22	-0.573889	3.24673	0.000004	73	0.517	0.174
23	-0.571280	3.24580	0.000003	72	0.517	0.173
24	-0.582332	3.24907	0.000003	71	0.517	0.176
25	-0.570756	3.24332	0.000004	73	0.516	0.173
26	-0.573714	3.24770	0.000004	73	0.517	0.174
27	-0.578222	3.24238	0.000004	74	0.516	0.176
28	-0.587739	3.24478	0.000004	66	0.516	0.178
29	-0.576011	3.24807	0.000004	73	0.517	0.175

Table 7-3 Active Power Modal Analysis, 0.5 Hz – Mode, Prop. TCSC

Case	Eigenvalue		Eigen Vector		Freq. (Hz)	ζ
	σ	ω	Mag. (MW)	Ang. (deg.)		
Without TCSC	-0.24338	3.14977	17.011	73.05	0.501	0.077
With TCSC	-0.57826	3.24332	0.22682	163.6	0.516	0.176

7.4 Nonlinear Time-domain Simulation Results

7.4.1 Rotor Angles' Responses

Fig. 7.7 to Fig. 7.9 show the rotor angles for three machines in different areas. These figures compare the dynamic stability of the power system before and after deploying the proposed TCSC. By analyzing the figures, it is quite evident that the dynamic behavior of the power system with the optimized TCSC is significantly enhanced. For instance, the overshoot and settling time of machine 28 are considerably reduced. The overshoot is decreased to about two third of its previous value. Also, the settling time is reduced from 20 to 6 seconds. The other figures show that even the machines, which are sited far away from the TCSC, are noticeably enhanced.

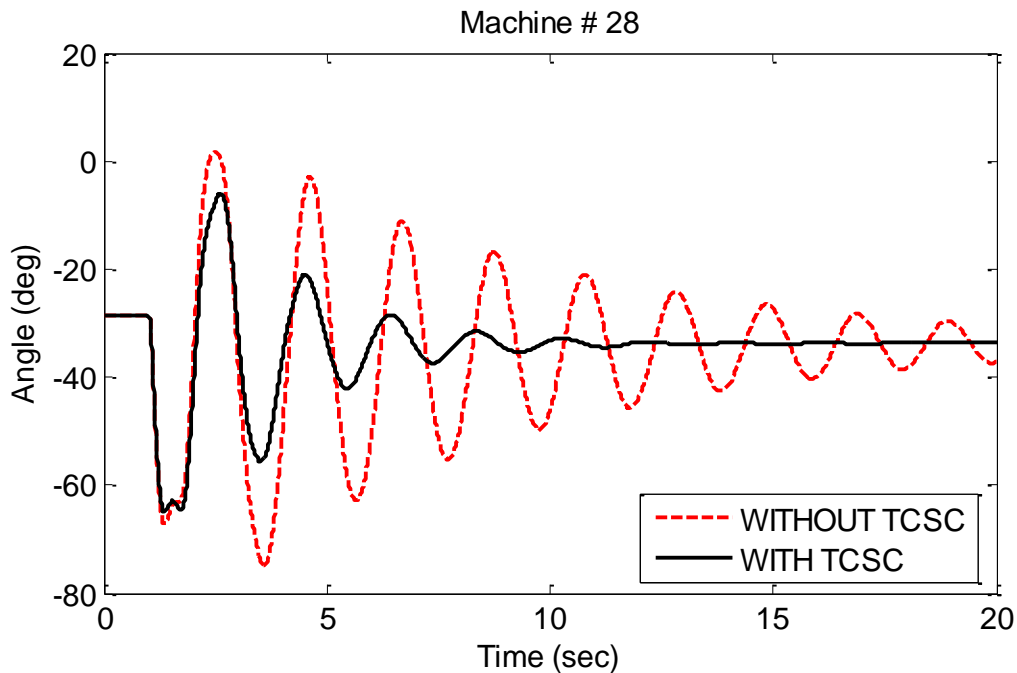


Fig. 7.7 Rotor Angle, Unit 28-Area 2, 3-Ph. Fault for 0.1s, Prop. TCSC

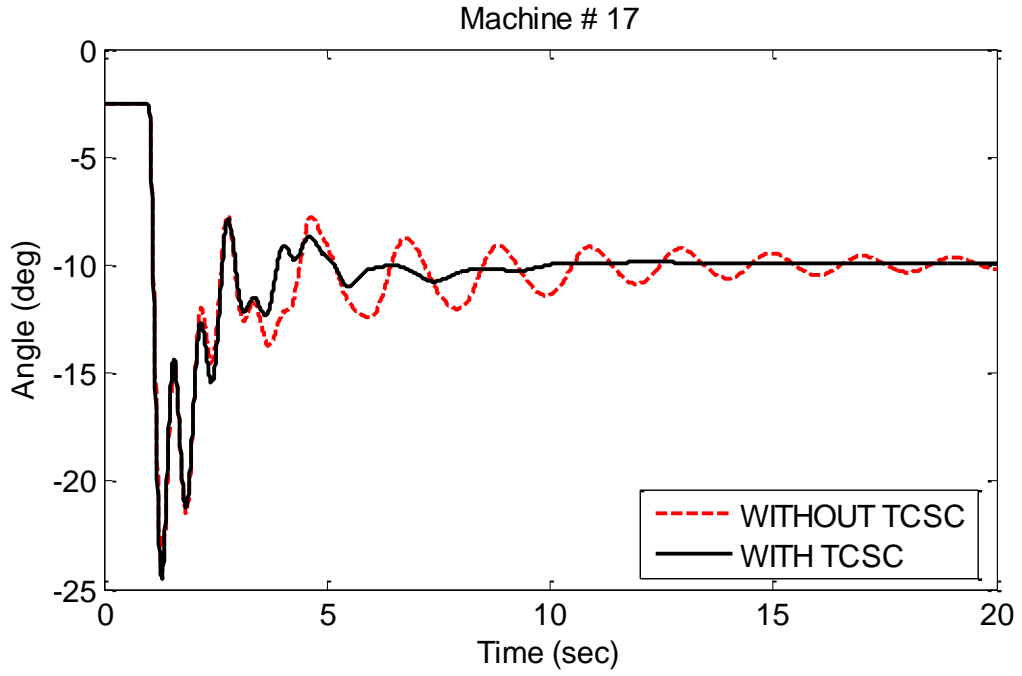


Fig. 7.8 Rotor Angle, Unit 17-Area 1, 3-Ph. Fault for 0.1s, Prop. TCSC

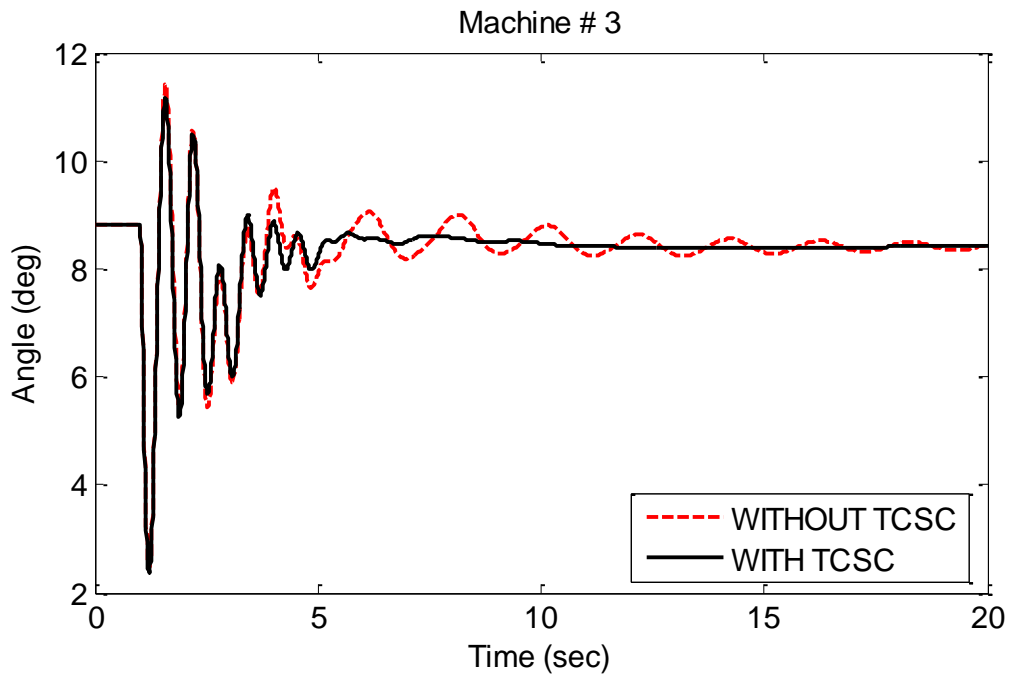


Fig. 7.9 Rotor Angle, Unit 3-Area 3, 3-Ph. Fault for 0.1s, Prop. TCSC

7.4.2 Machines' Electrical Power Responses

Fig. 7.10 to Fig. 7.12 show the electrical power for several machines in different areas. As can be observed, the dynamic performance of the system with the optimized TCSC is significantly improved. For instance, it can be seen that the electrical power of machine 28 has overshoot and settling time much less than without TCSC. Moreover, the settling time of machines 18 in area 1 and machine 11 in area 3 is satisfactorily reduced after the deployment of the TCSC.

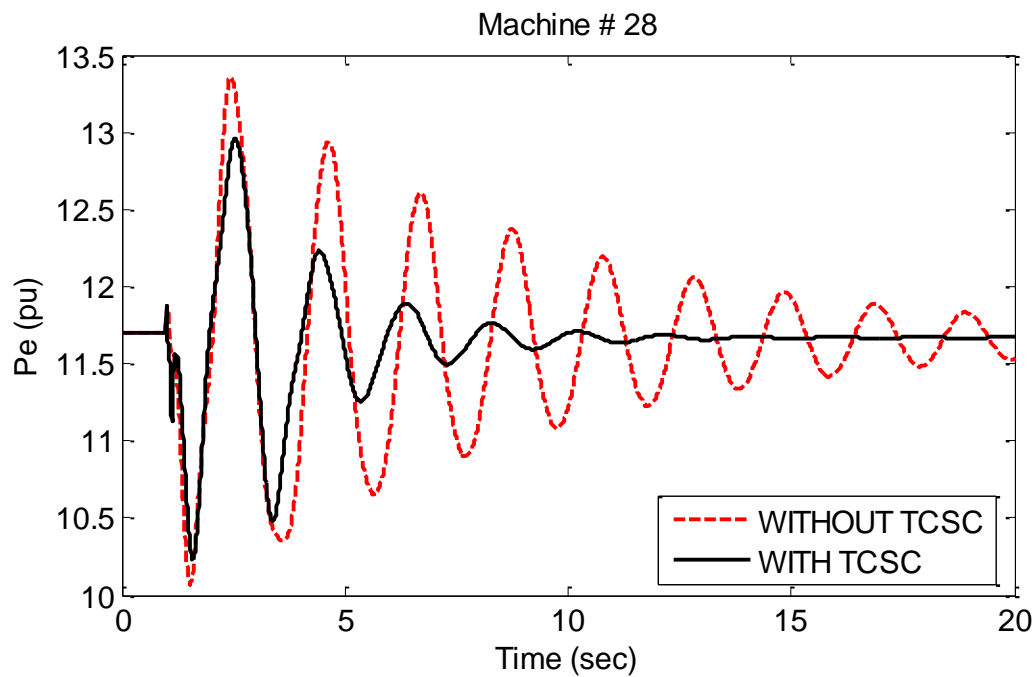


Fig. 7.10 Electrical Power, Unit 28-Area 2, 3-Ph. Fault for 0.1s, Prop. TCSC

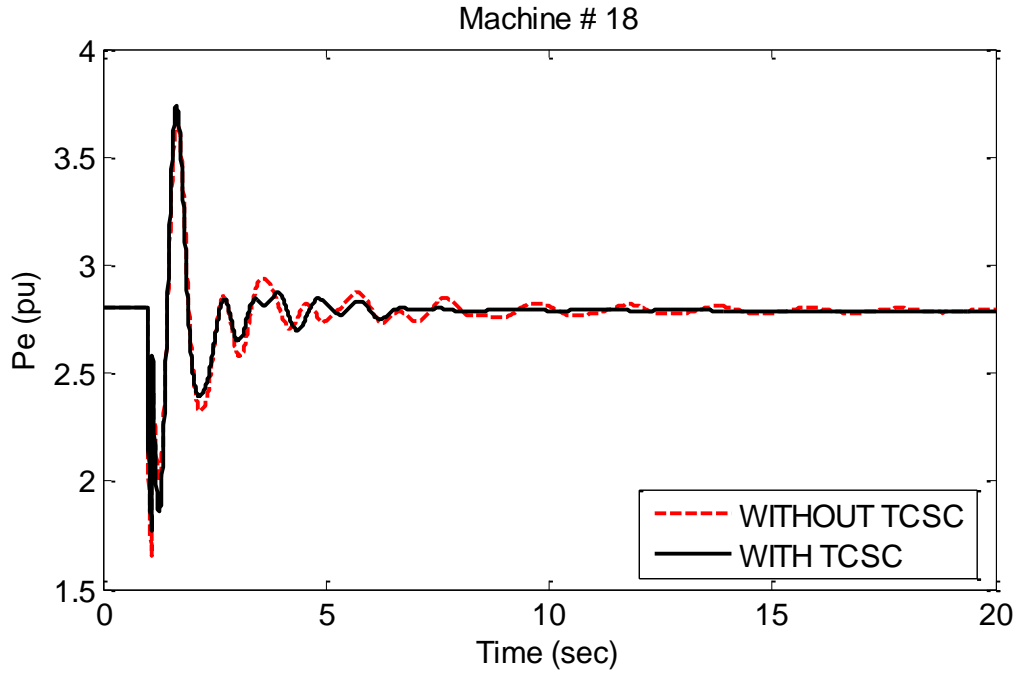


Fig. 7.11 Electrical Power, Unit 18-Area 1, 3-Ph. Fault for 0.1s, Prop. TCSC

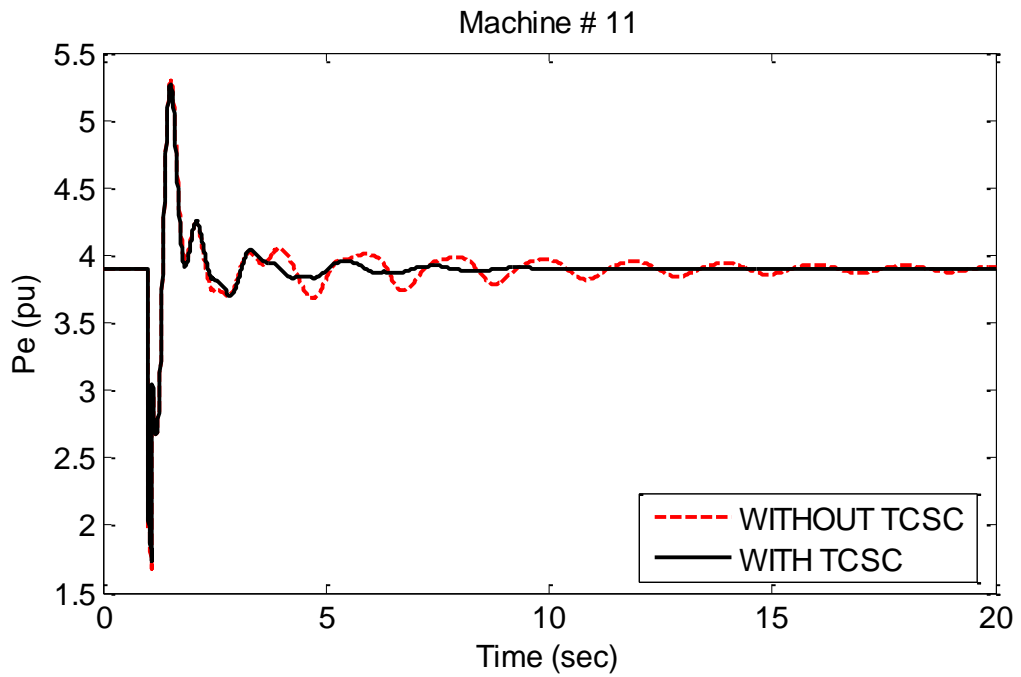


Fig. 7.12 Electrical Power, Unit 11-Area 3, 3-Ph. Fault for 0.1s, Prop. TCSC

7.4.3 Rotor Speed Deviations' Responses

Similarly, Fig. 7.13 to Fig. 7.18 show the rotor speed deviations for different machines located in different areas. It can be easily figured out that the speed deviations' performances of all machines after the employment of the TCSC are noticeably improved. For illustration, it can be seen that machine 28 and 24 in area 2 have overshoot and settling time much less than the existing case. Also, the responses of other machines, such as machines 18 and 16 from area 1 and machines 7 and 3 from area 3, indicate that the overall dynamic stability is markedly enhanced.

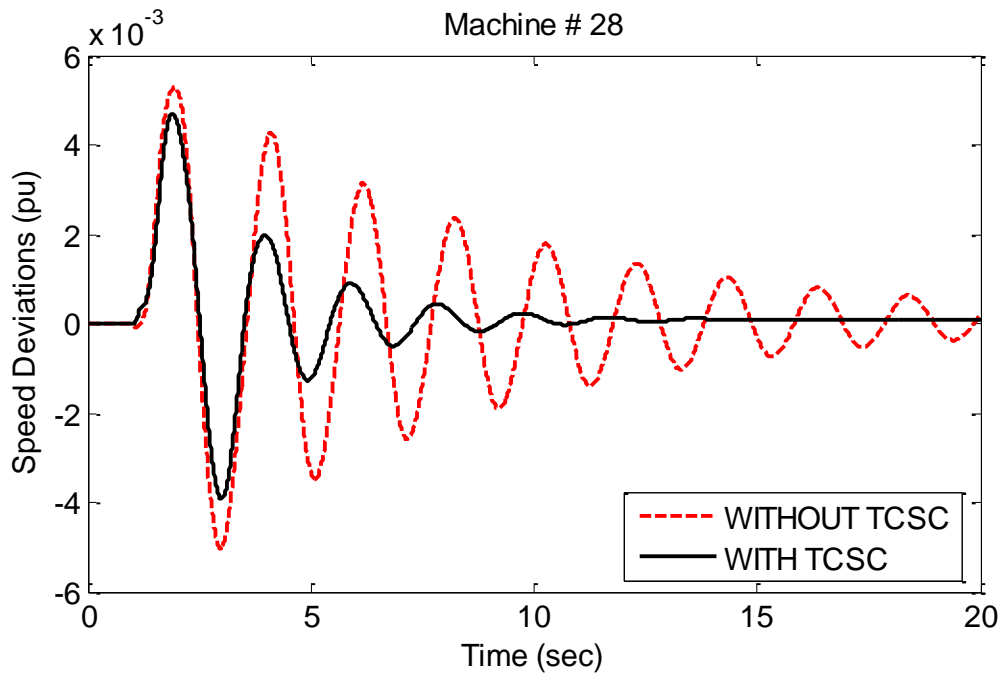


Fig. 7.13 Speed Deviations, Unit 28-Area 2, 3-Ph. Fault for 0.1s, Prop. TCSC

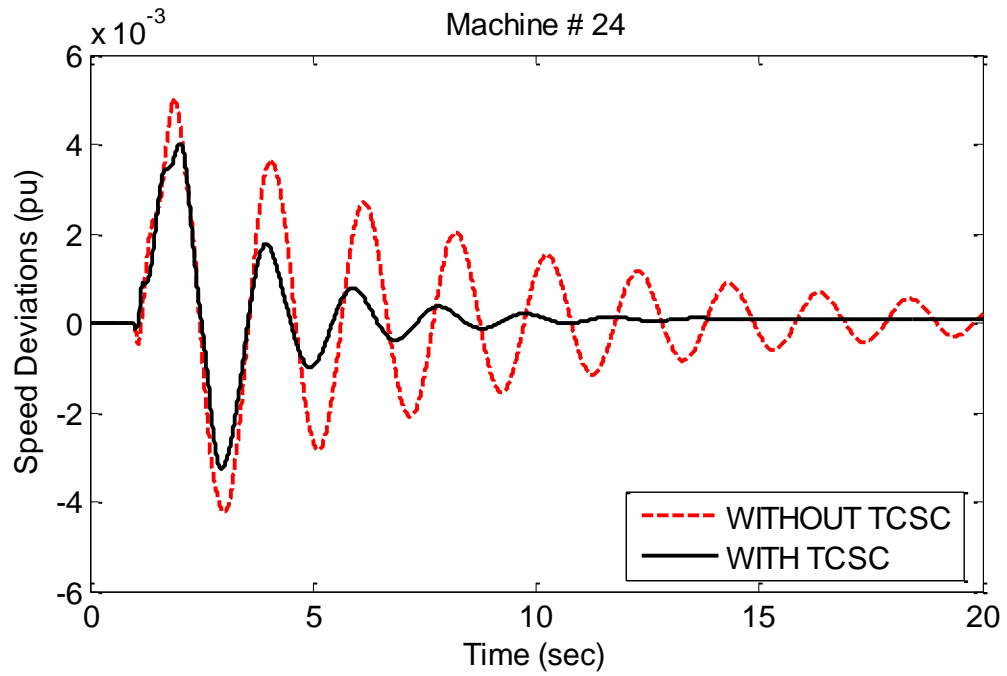


Fig. 7.14 Speed Deviations, Unit 24-Area 2, 3-Ph. Fault for 0.1s, Prop. TCSC

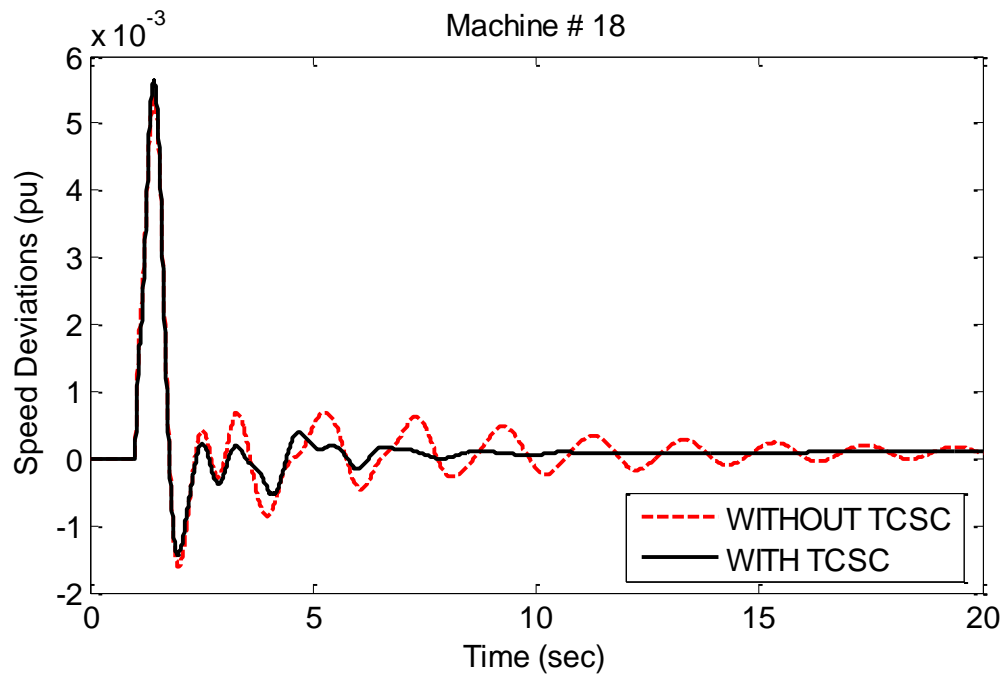


Fig. 7.15 Speed Deviations, Unit 18-Area 1, 3-Ph. Fault for 0.1s, Prop. TCSC

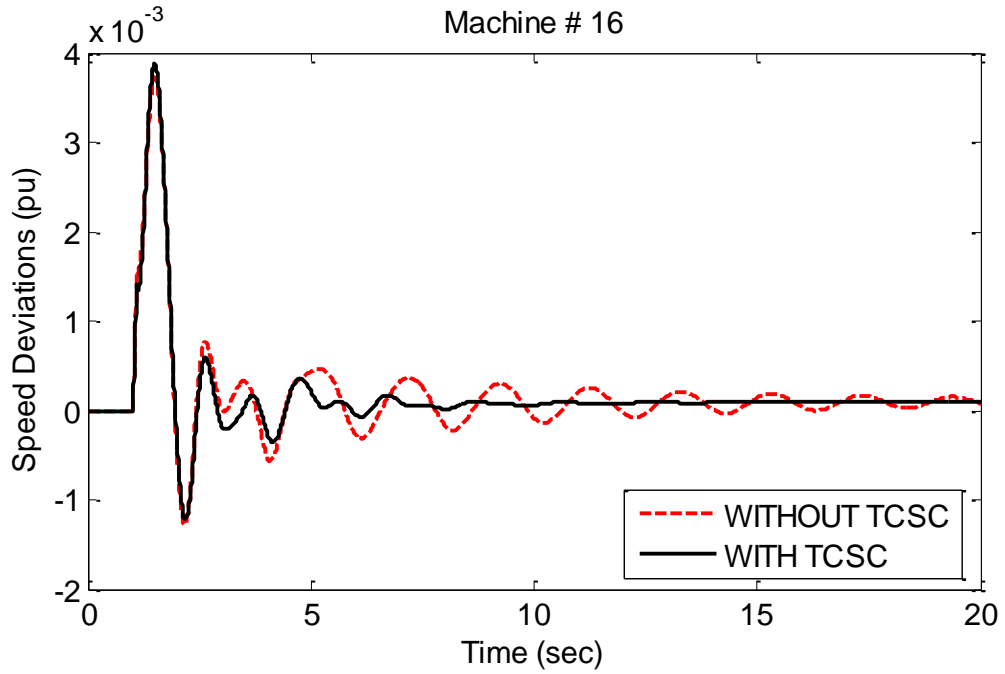


Fig. 7.16 Speed Deviations, Unit 16-Area 1, 3-Ph. Fault for 0.1s, Prop. TCSC

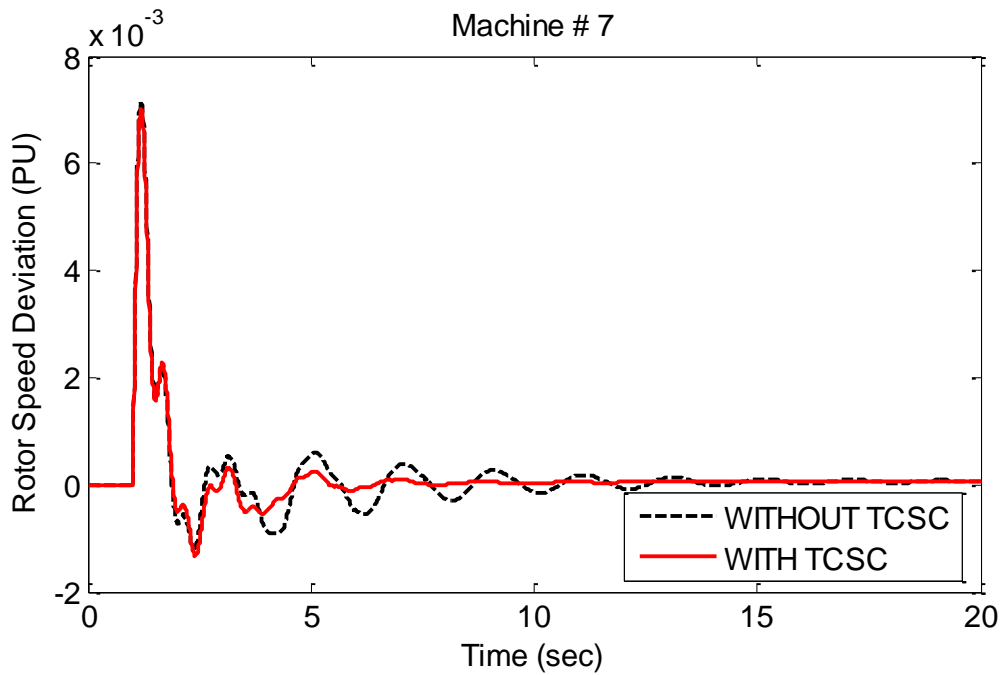


Fig. 7.17 Speed Deviations, Unit 7-Area 3, 3-Ph. Fault for 0.1s, Prop. TCSC

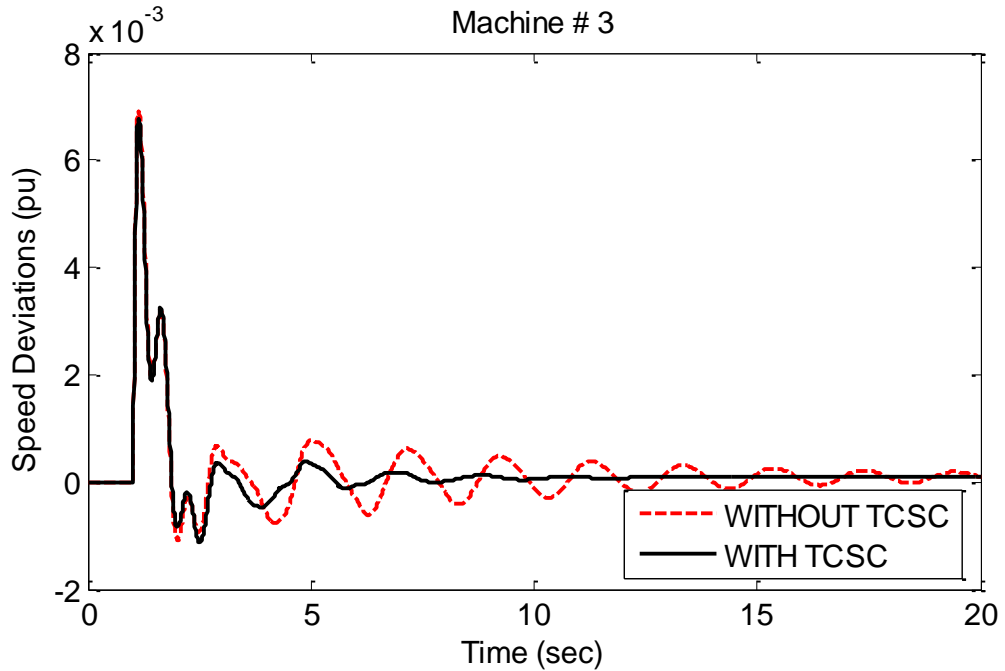


Fig. 7.18 Speed Deviations, Unit 3-Area 3, 3-Ph. Fault for 0.1s, Prop. TCSC

7.4.4 Voltages' Responses

Fig. 7.19 to Fig. 7.22 show the voltages' responses for the boundary buses. By analyzing these figures, it is quite evident that even the voltage profiles of the considered power system is improved after deploying the TCSC. For example, the existing voltage oscillations of buses 44 and 63 are rapidly damped after the installation of the TCSC. Also, most of the voltages in all areas return to their steady state values after around 6 to 7 seconds with the TCSC compared to 15 to 20 seconds without it.

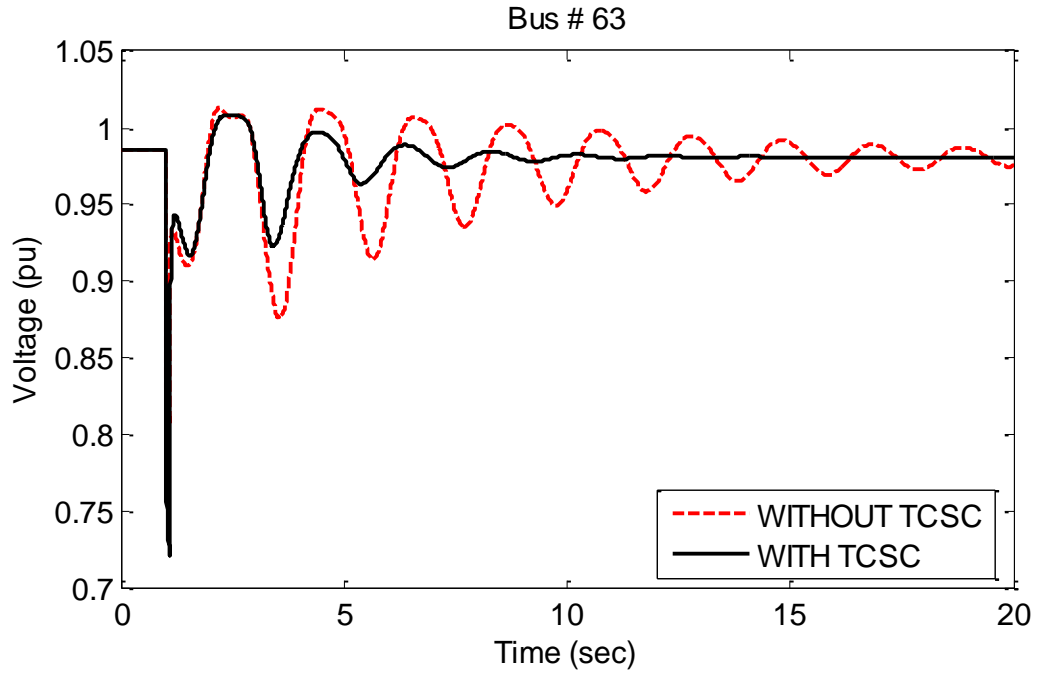


Fig. 7.19 Voltage, Bus 63-Area 2, 3-Ph. Fault for 0.1s, Prop. TCSC

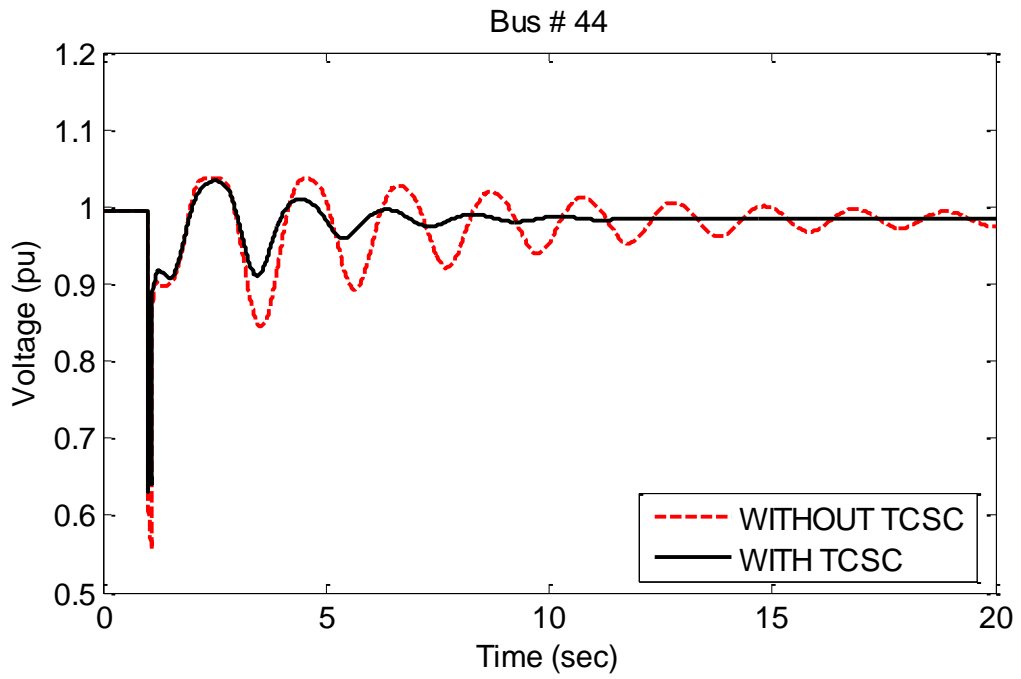


Fig. 7.20 Voltage, Bus 44-Area 1, 3-Ph. Fault for 0.1s, Prop. TCSC

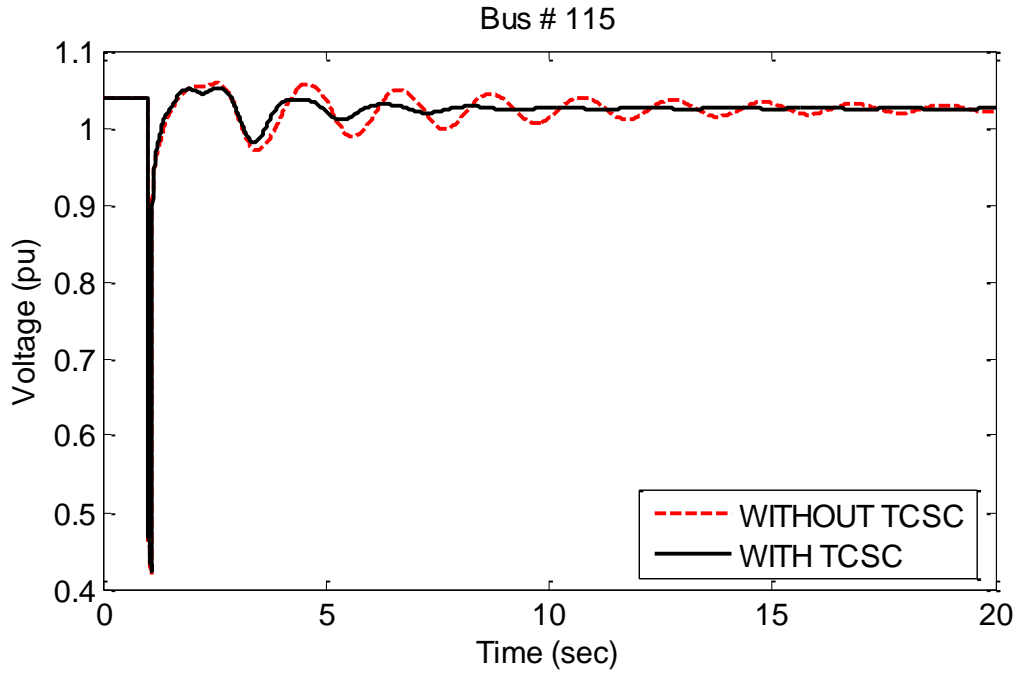


Fig. 7.21 Voltage, Bus 115-Area 3, 3-Ph. Fault for 0.1s, Prop. TCSC

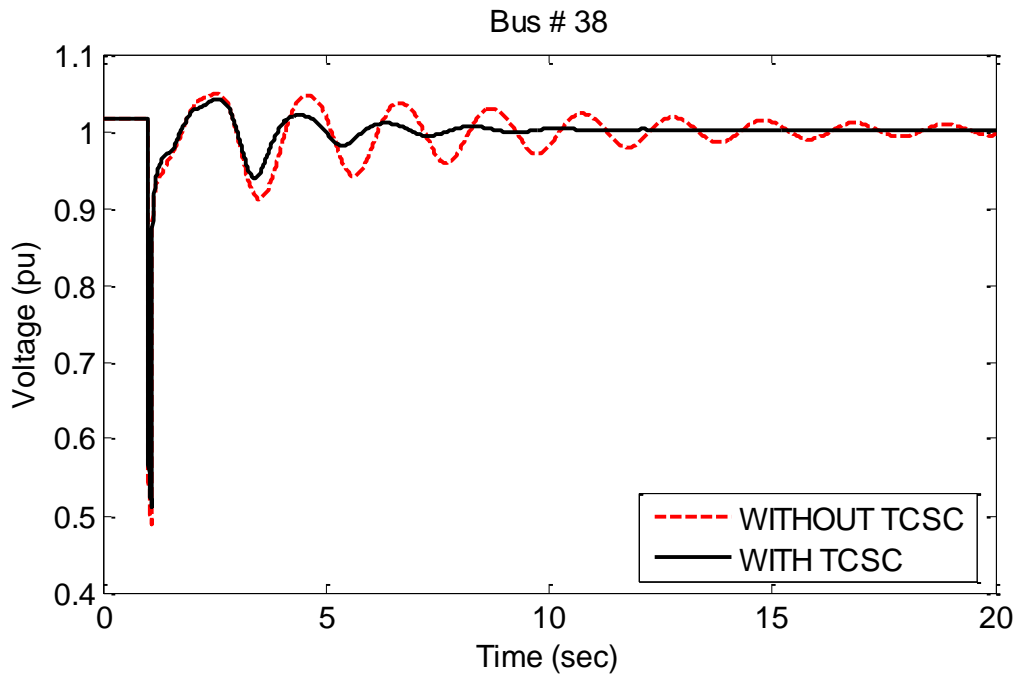


Fig. 7.22 Voltage, Bus 38-Area 1, 3-Ph. Fault for 0.1s, Prop. TCSC

7.4.5 Active Power Flow Responses

Beside the above quantities, the below Fig. 7.23 to Fig. 7.26 show the active power flow of the 380 kV inter-tie lines. The first three figures depict the substantial increase in the active power flow of the inter-ties between area 3 and 1 due to the tripping of one double circuit line connecting these areas. The fourth figure shows the active power response of line 44 – 63. By analyzing these figures, it is quite clear that the overall dynamic stability of the power system with the TCSC is greatly enhanced. Consequently, the power transfer capabilities among the interconnected areas can be significantly increased.

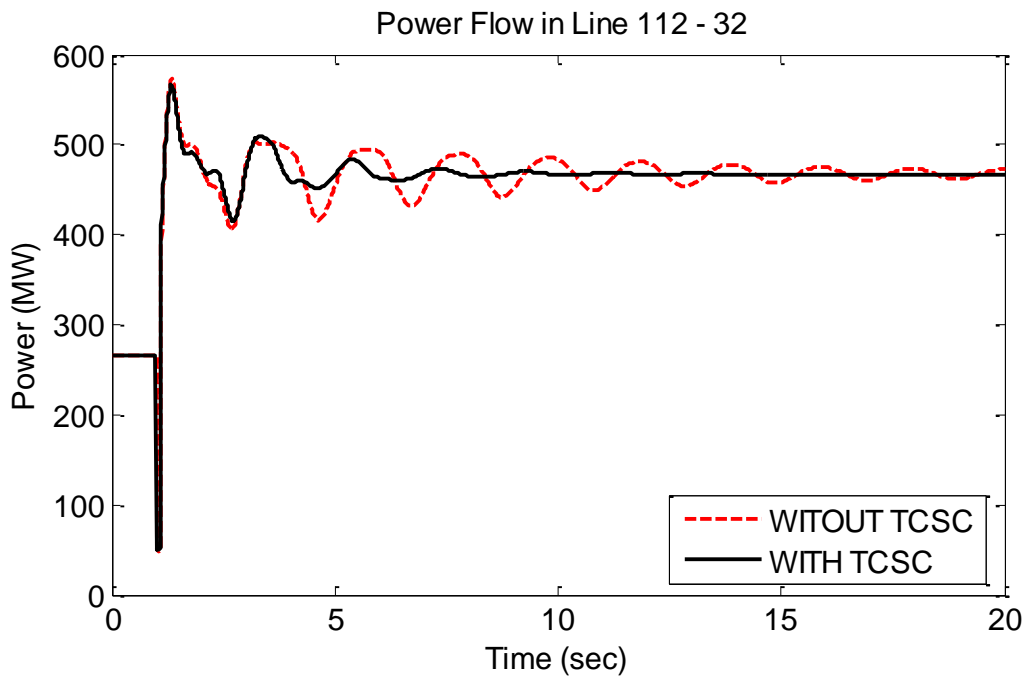


Fig. 7.23 Active Power, Line 112 to 32, 3-Ph. Fault for 0.1s, Prop. TCSC

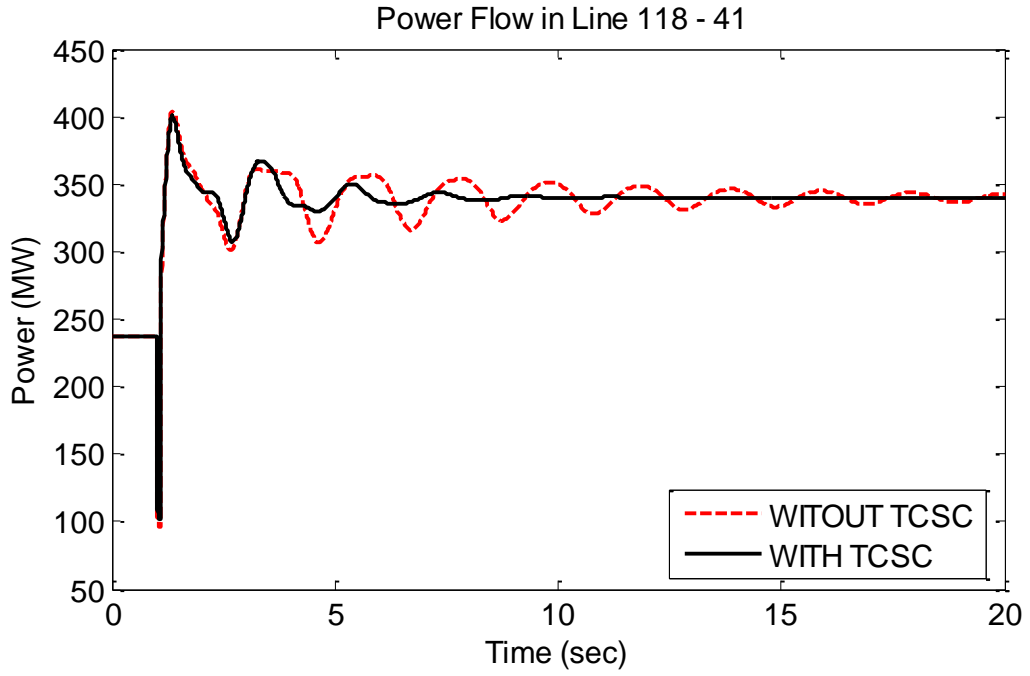


Fig. 7.24 Active Power, Line 118 to 41, 3-Ph. Fault for 0.1s, Prop. TCSC

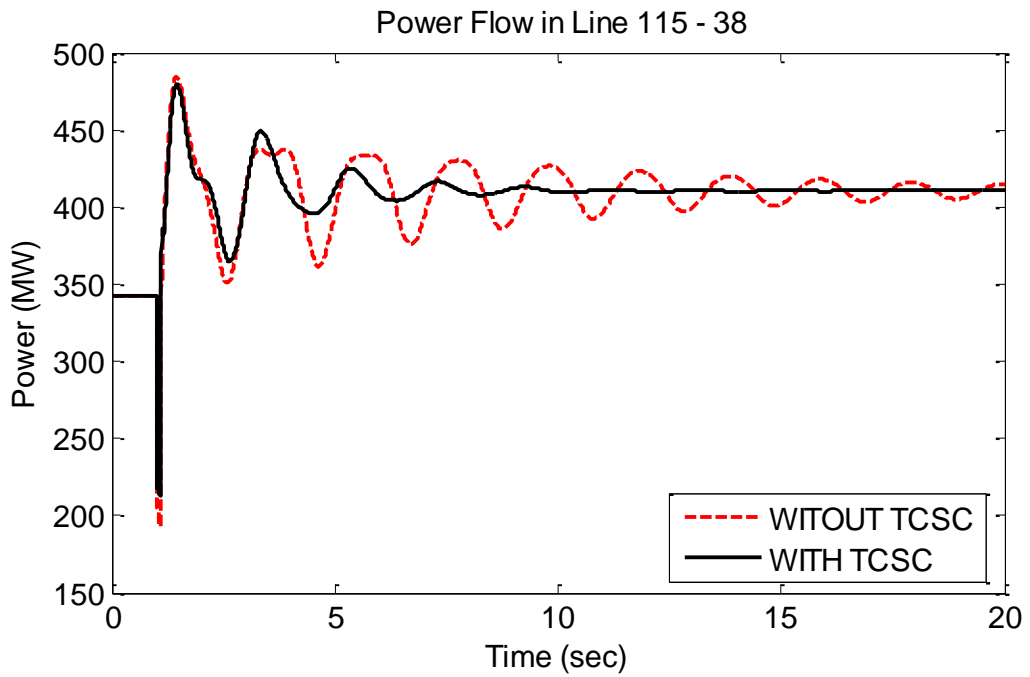


Fig. 7.25 Active Power, Line 115 to 38, 3-Ph. Fault for 0.1s, Prop. TCSC

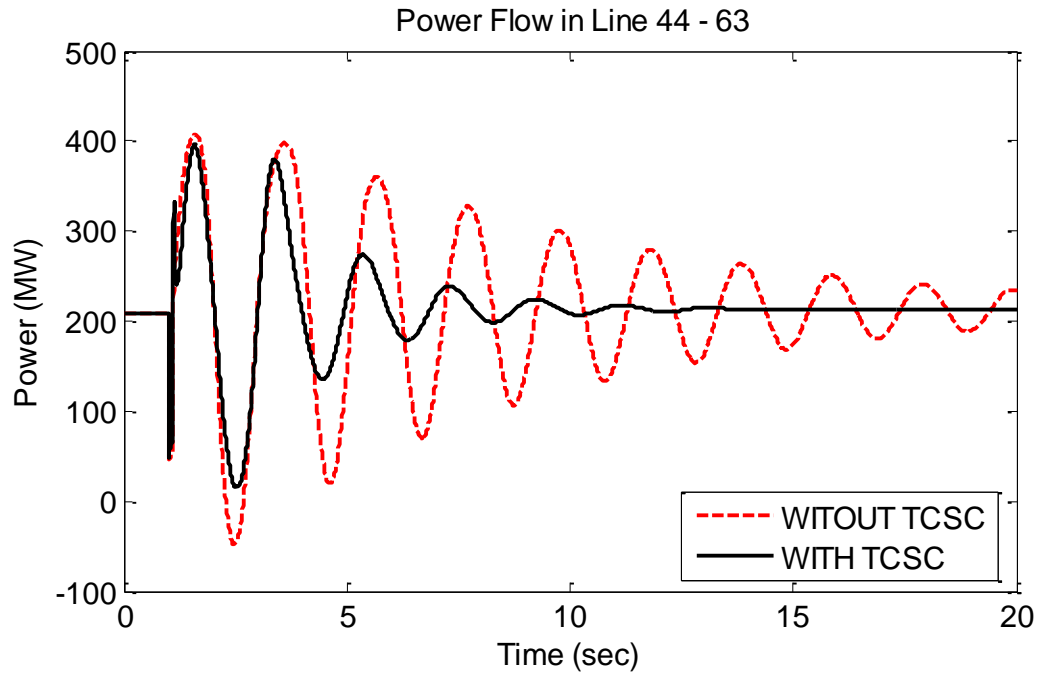


Fig. 7.26 Active Power, Line 44 to 63, 3-Ph. Fault for 0.1s, Prop. TCSC

7.5 Robustness of the Proposed TCSC

To validate the robustness of the proposed TCSC, the following analyses are performed:

- 1) Comparison of the maximum power transfer of the existing system with and without the proposed TCSC.
- 2) Identification of the new maximum power transfer limit with the proposed TCSC.
- 3) Execution of several faults at different locations for the case of the new maximum power transfer with and without the proposed TCSC.

7.5.1 Existing Maximum Power Transfer Limit

To compare the power system performance considering the existing maximum power transfer with and without the proposed TCSC, the same incident 2 defined in the previous chapter 6 section 6.7, is repeated in this chapter. Fig. 7.27 depicts the existing maximum power transfer between area 1 and 2. It can be seen that the maximum power is about 420 MW after which the system goes out of synchronism and continuously oscillates. However, it can be observed that after deploying the optimized TCSC, the dynamic stability of the system is considerably improved. Thus, the power transfer between the two areas can be increased much more beyond the existing transfer level.

7.5.2 Maximum Power Transfer with the Proposed TCSC

To determine the maximum power transfer with the proposed TCSC, the same incident 2, defined in the previous chapter, is repeated in this chapter. Fig. 7.28 shows that the maximum power is substantially increased from 420 to 800 MW.

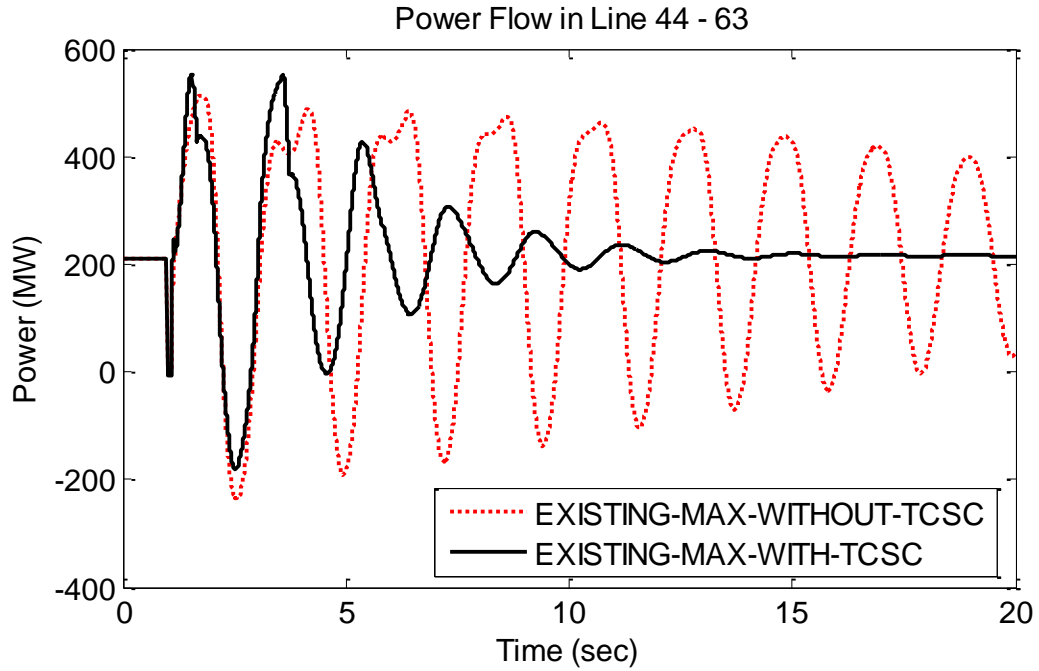


Fig. 7.27 Ex. Max. Power Transfer, Line 44 to 63, 3-Ph. Fault for 0.1s, Prop. TCSC

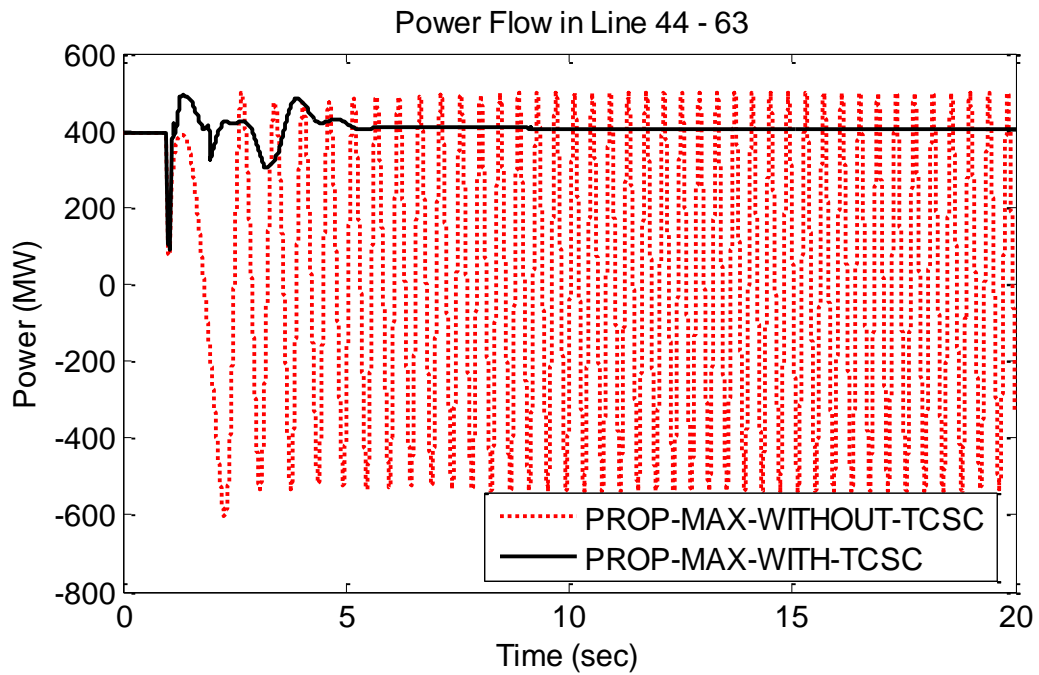


Fig. 7.28 New Max. Power Transfer, Line 44 to 63, 3-Ph. Fault for 0.1s, Prop. TCSC

7.5.3 Sensitivity Analyses

To assess the effectiveness and robustness of the proposed individual design of the TCSC, the same sensitivity cases executed in chapter 6 sections 6.7.2 are repeated in this section. Fig. 7.29 and Fig. 7.30 confirm the robustness of the proposed TCSC. It is quite clear that the power oscillations rapidly disappear with the TCSC while they continuously oscillate or slowly damp without it.

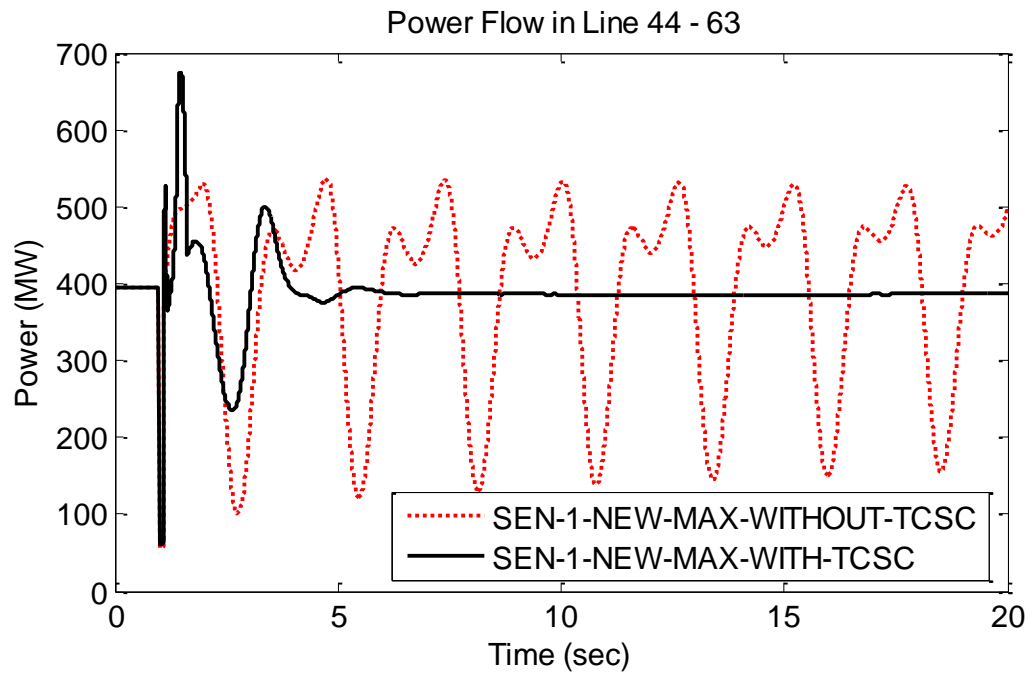


Fig. 7.29 New Max. Power Transfer, Line 44 to 63, Sensitivity 1, Prop. TCSC

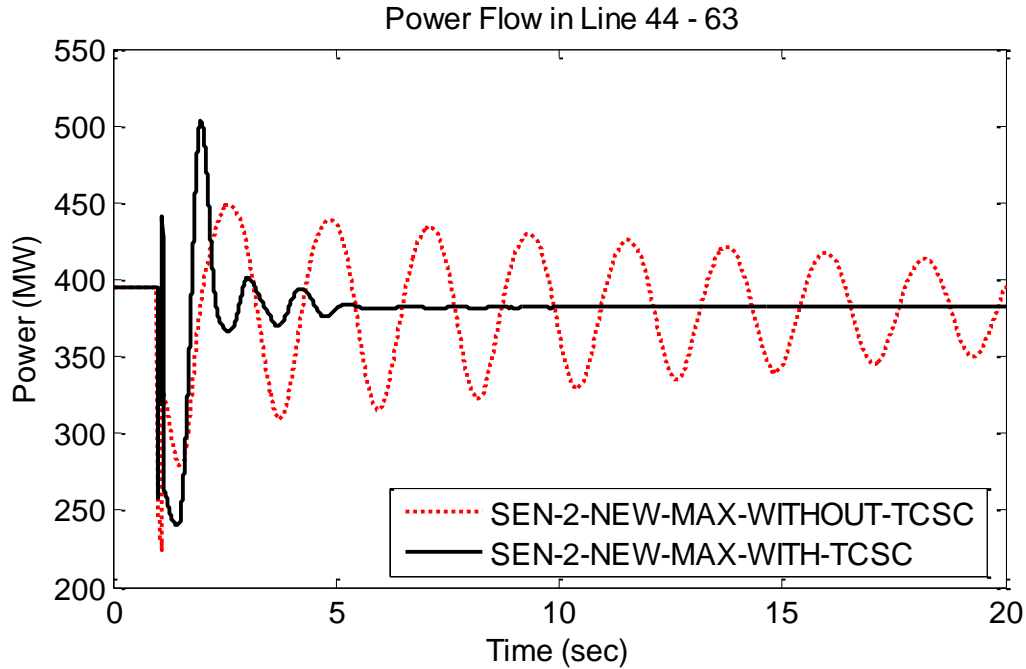


Fig. 7.30 New Max. Power Transfer, Line 44 to 63, Sensitivity 2, Prop. TCSC

7.6 Summary of the Individual Design of TCSC

This chapter demonstrates the impact of the TCSC on improving the overall dynamic stability of the considered power system. It has been confirmed that by installing the TCSC in series with the inter-tie line connecting area 1 and 2 and by optimizing its parameters using MPSO, the existing power oscillations considerably decrease. Moreover, it has been shown that the maximum power transfer between area 1 and 2 is significantly increased from 420 MW to 800 MW with the proposed TCSC. Finally, it has been proven from the additional sensitivity analyses that the proposed design is a robust design.

CHAPTER 8

COORDINATION OF PSSs AND TCSC

8.1 Overview

This chapter investigate the impact of simultaneous design of PSSs and TCSC on improving the overall dynamic stability of the considered interconnected power systems. In the first section of this chapter, MPSO is executed to optimize the TCSC and PSSs parameters. After determining the best parameters, modal analysis and nonlinear time-domain simulation are performed to test the effectiveness of the proposed design utilizing the reduced power system. Then, the optimized parameters of the proposed TCSC and PSSs are modeled in the full version of the considered power system to examine its impact on enhancing the overall dynamic stability and to determine the new maximum power transfer between areas 1 and 2. Finally, several sensitivity analyses are carried out to confirm the robustness of the proposed coordinated design of the TCSC and PSSs.

8.2 Coordinated Design of PSSs and TCSC

MPSO is applied to coordinate the design of the TCSC and the PSSs. The optimization problem is based on nonlinear objective function targeting to minimize the ITAE described in chapter 4 equation (4.7). The convergence curve of the objective function is shown in Fig. 8.1 while the optimized parameters of the PSSs and TCSC are presented in

Table 8-1 and Table 8-2, respectively. It has been found that the optimized parameters of both the PSSs and TCSC are very close to the previously found in chapter 6 and 7. Thus, the same parameters are implemented in this case.

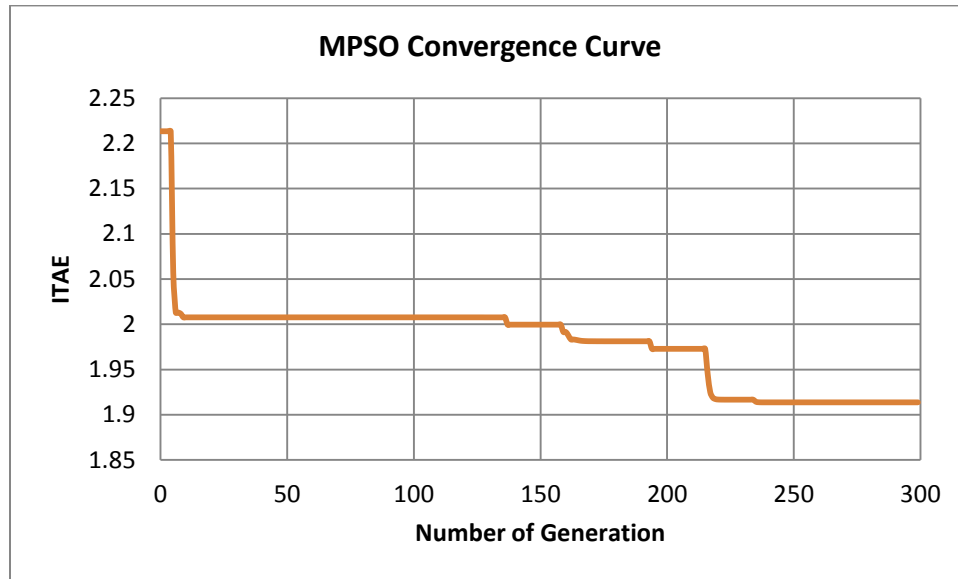


Fig. 8.1 MPSO Convergence Curve for the Coordinated Design of PSSs&TCSC

Table 8-1 Optimized PSSs Parameters, Cord. PSSs&TCSC

Machine	K_{s1}^*	T_1^*	T_2^*	T_3^*	T_4^*
1	-1.2769	0.2	0.0099	0.2	0.0099
2	-1.2769	0.2	0.0099	0.2	0.0099
3	-0.5	0.5	0.05	0.5	0.05
9	50	2.5	1.57	0.2	0.05
10	5	0.4	0.02	0.4	0.02
11	15	0.3	0.04	0.3	0.04
12	15	0.3	0.04	0.3	0.04
13	10	0.3	0.02	0.3	0.02
14	15	0.3	0.04	0.3	0.04
16	10	0.75	0.202	0.75	0.202
17	18	0.15	0.02	0.15	0.02
28	15	0.15	0.02	0.15	0.02

* The optimized time constants for PSS type IEE2ST are T_5, T_6, T_7, T_8 instead of $T_1 - T_4$ and K_1 instead of K_{s1}

Table 8-2 Optimized TCSC Parameters, Cord. PSSs&TCSC

TCSC	T_{1TCSC}	T_{2TCSC}	T_{3TCSC}	T_w	K_{TCSC}	X_{max}	X_{min}
		0.4	0.5	0.025	0.21	1.2	0.135

8.3 Modal Analysis Results

Modal analysis are carried out for both rotor speed deviations of all units as well as active power flow of line 44 - 63. The considered incident is a three phase fault at bus 110 for 0.1 second. The fault is cleared by tripping line 110 - 30. The following two sections discuss the comparison between the power system performance with and without the optimized PSSs and TCSC.

8.3.1 Eigenvalue Results Concomitant with Rotor Speed Deviations

By analyzing the results in Table 8-3, it can be observed that most of the EM inter-Area oscillations for area 1 and 3 are completely eliminated except those associated with machine 9 and 11 which have very low frequency of 0.2 and 0.15 Hz, respectively. Moreover, there is a substantial improvement in both damping ratios and damping factors for all machines having frequency in the range of 0.1 up to 0.73 Hz. In addition to that, the magnitude of oscillations for most of the machines are markedly reduced compared to the previous design approaches.

Table 8-3 Modal Analysis for the Inter Area 0.1-0.7 Hz – Modes, Cord. PSSs&TCSC

M/C	Eigenvalue		Eigen Vector		Freq. (Hz)	ζ
	Real (σ)	Imaginary (ω)	Magnitude (pu)	Angle (deg.)		
9	-0.394962	0.93141	0.00000386	-54.4	0.148	0.390397
11	-1.104530	1.32164	0.00000273	76.6	0.210	0.641268
19	-0.711286	4.36373	0.00000080	-73.2	0.695	0.160876
20	-0.625304	4.25129	0.00000118	-79.1	0.677	0.145520
21	-0.945580	3.67435	0.00000186	-52.9	0.585	0.249226
22	-0.832353	3.71102	0.00000170	-44.3	0.591	0.218855
23	-0.611435	4.53468	0.00000129	-105.3	0.722	0.133626
24	-0.813451	4.13834	0.00000135	-84.5	0.659	0.192874
25	-0.655305	4.11387	0.00000120	-70.6	0.655	0.157308
26	-0.925468	3.57148	0.00000260	-44.8	0.568	0.250842
27	-0.980794	3.87956	0.00000181	-66.9	0.617	0.245099
28	-0.573275	3.75385	0.00000035	-64.4	0.597	0.150966
29	-0.527051	3.82311	0.00000088	-44.3	0.608	0.136568

Table 8-4 below shows a comparison of rotor speed deviation's eigenvalue and eigenvectors of machine 28 for all cases. From the results, it can be noticed that the worst damping ratio and damping factor are those associated with the existing system. While,

the rest of the cases have very close values. Regarding the magnitude of oscillations, the highest one is that associated with the existing case while the lowest one is the one resulted from the coordinated design of the PSSs and TCSC.

Table 8-4 Machine 28 Rotor Speed Deviation Modal Analysis, Cord. PSSs&TCSC

Case	M/C	Eigenvalue		Magnitude (pu)	Freq. (Hz)	ζ	
		Real (σ)	Imaginary (ω)				
1	Existing	28	-0.253335	3.15040	0.0002600	0.501	0.08
2	PSSs		-0.623019	3.57495	0.0000004	0.569	0.17
3	TCSC		-0.587739	3.24478	0.0000040	0.516	0.18
4	PSSs & TCSC		-0.573275	3.75385	0.0000003	0.597	0.15

Similarly, Table 8-5 below demonstrates the comparison of rotor speed deviation's eigenvalues and eigenvector for machine 24. It can be observed that the worst damping ratio and damping factor are those associated with the existing system, whereas, the best are those concomitant with the simultaneous design of TCSC and PSSs. Regarding the magnitude of oscillations, the highest one is that resulted from the existing case while the lowest one is the one associated with the simultaneous design of PSSs (case 2) as well as the one concomitant with the coordinated design of the PSSs and TCSC (case 4).

Table 8-5 Machine 24 Rotor Speed Deviation Modal Analysis, Cord. PSSs&TCSC

Case	M/C	Eigenvalue		Magnitude (pu)	Freq. (Hz)	ζ	
		Real (σ)	Imaginary (ω)				
1	Existing	24	-0.242818	3.15403	0.000216	0.502	0.077
2	PSSs		-0.700889	4.20346	0.000001	0.669	0.164
3	TCSC		-0.582332	3.24907	0.000003	0.517	0.176
4	PSSs & TCSC		-0.813451	4.13834	0.000001	0.659	0.193

The eigenvalues and eigenvectors of machine 9, shown in Table 8-6, have two different modes of oscillations. The first mode has frequency of about 0.5 Hz. This mode appears in the existing case and in the case of the individual design of the TCSC. While, the other mode is about 0.15 Hz which occurs after installing the new PSS at machine 28 in both case 2 and case 4. In such situation, it could be difficult to identify the best power system performance among these cases using modal analysis. However, case 2 and case 4 can be compared easily since they have the same mode. Thus, by comparing these two cases, it can be observed that the best performance among them is due to the simultaneous design of the TCSC and PSSs. Since, it has better damping factor and damping ratio.

Table 8-6 Machine 9 Rotor Speed Deviation Modal Analysis, Cord. PSSs&TCSC

Case	M/C	Eigenvalue		Magnitude (pu)	Freq. (Hz)	ζ
		Real (σ)	Imaginary (ω)			
Existing	9	-0.226894	3.16663	0.000024	0.504	0.071
PSSs		-0.319430	0.93601	0.000003	0.149	0.323
TCSC		-0.680534	3.17652	0.000001	0.506	0.209
PSSs & TCSC		-0.394962	0.93141	0.000003	0.148	0.390

8.3.2 Eigenvalue Results Concomitant with Active Power Flow

Table 8-7 presents the modal analysis results of the active power flow of line 44 – 63 for the four studied cases. It is quite clear that the first three cases have the same mode of oscillations which is about 0.5 Hz, while, the forth case has new mode of about 0.15 Hz. The best power system performance among the first three cases is associated with the simultaneous design of PSSs. Since it has the best damping factor and the lowest magnitude of oscillations. However, when two different EM modes of oscillations

appear, nonlinear time-domain simulation analyses can be executed to identify the best controller design approach among the proposed three approaches as performed in the following section.

Table 8-7 Active Power Modal Analysis for Inter Area Modes, Cord. PSSs&TCSC

Case	Eigenvalue		Eigen Vector		Freq. (Hz)	ζ
	σ	ω	Mag. (MW)	Ang. (deg.)		
Existing	-0.24332	3.14816	17.426	71.87	0.501	0.077
PSSs	-0.59105	4.23575	0.063	111.27	0.674	0.138
TCSC	-0.57826	3.24332	0.227	163.6	0.516	0.176
PSSs & TCSC	-0.42259	0.92002	0.057	153.32	0.146	0.420

8.4 Nonlinear Time-domain Simulation Results

8.4.1 Rotor Angles' Responses

Fig. 8.2 to Fig. 8.8 show the rotor angles for several machines in different areas. These figures compare the rotor angles' dynamic performance for all cases. By analyzing the figures, it is quite clear that the best dynamic performance is the one resulted from case four where the design of the TCSC and PSSs are coordinated. For example, in this case the overshoot and settling time of machine 27 are much better than the rest of the cases. Similarly, the dynamic enhancement can be observed in other machines which are located in areas 1 and 3, such as machine 17 and 3, respectively.

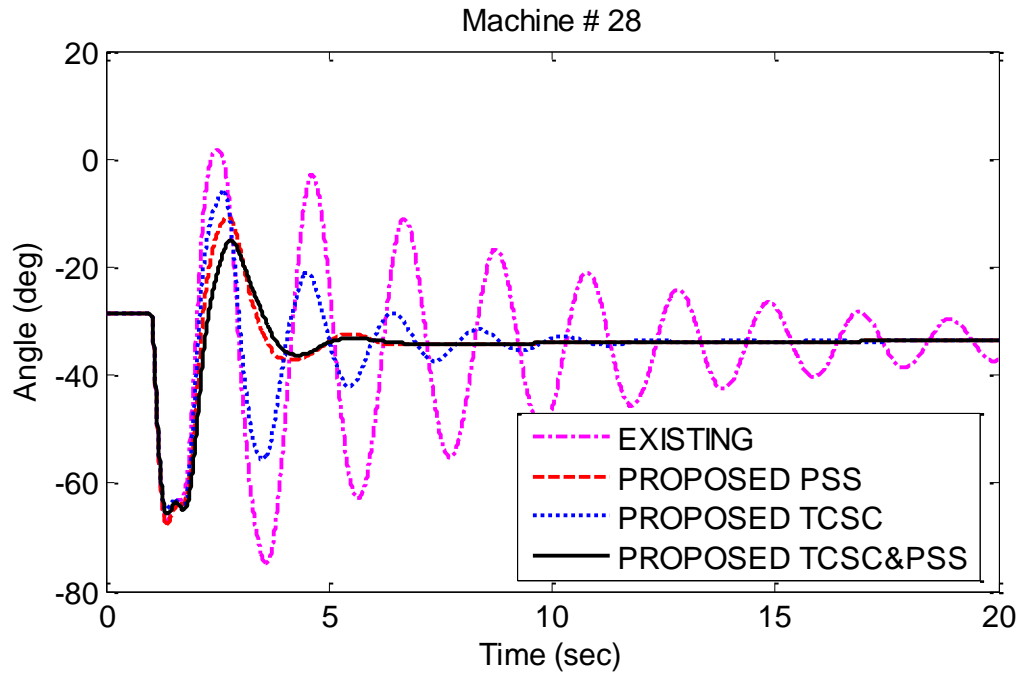


Fig. 8.2 Rotor Angle, Unit 28-Area 2, 3-Ph. Fault for 0.1s, Cord. PSSs&TCSC

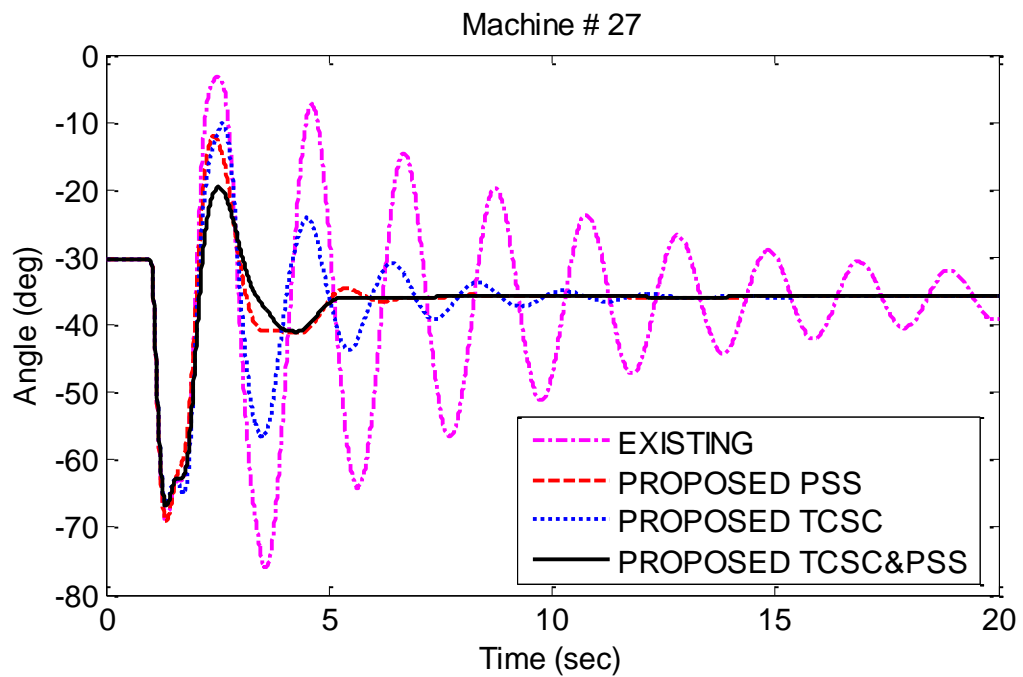


Fig. 8.3 Rotor Angle, Unit 27-Area 2, 3-Ph. Fault for 0.1s, Cord. PSSs&TCSC

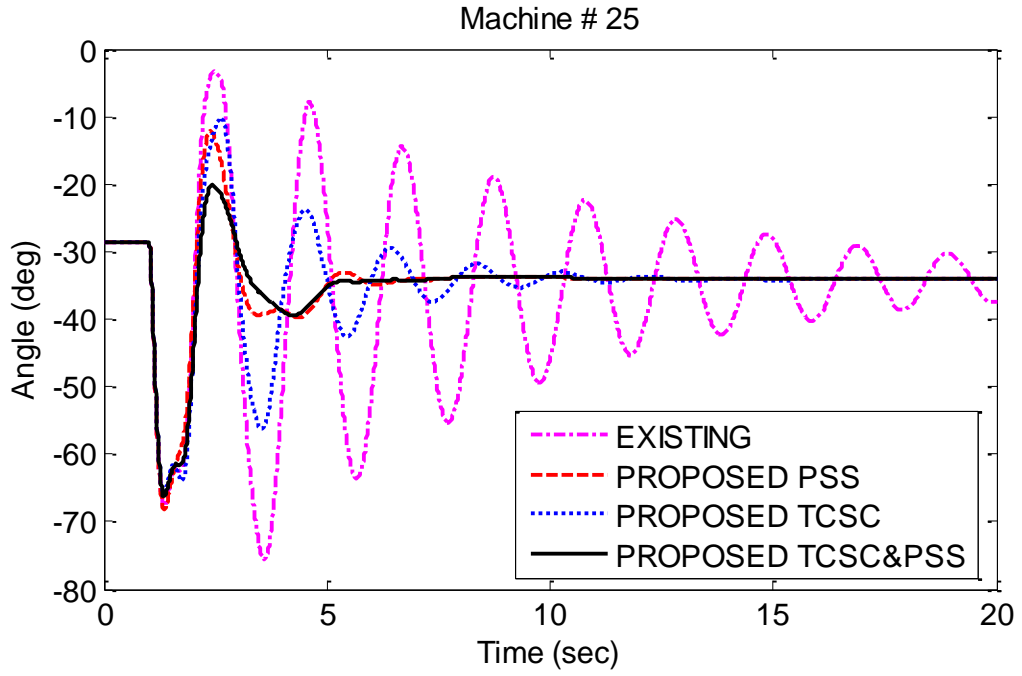


Fig. 8.4 Rotor Angle, Unit 25-Area 2, 3-Ph. Fault for 0.1s, Cord. PSSs&TCSC

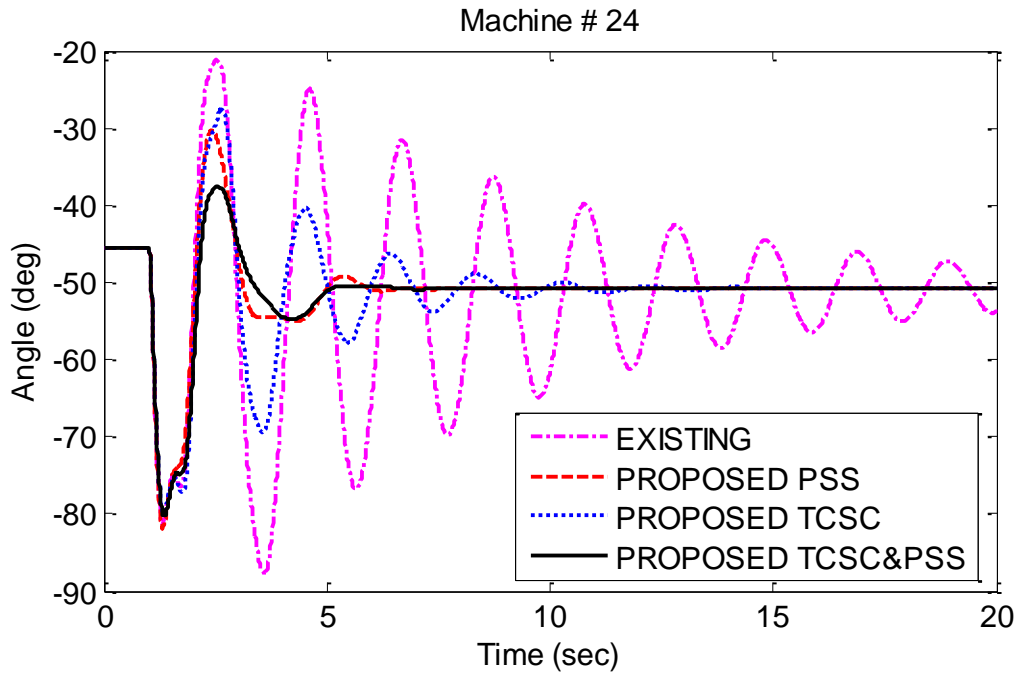


Fig. 8.5 Rotor Angle, Unit 24-Area 2, 3-Ph. Fault for 0.1s, Cord. PSSs&TCSC

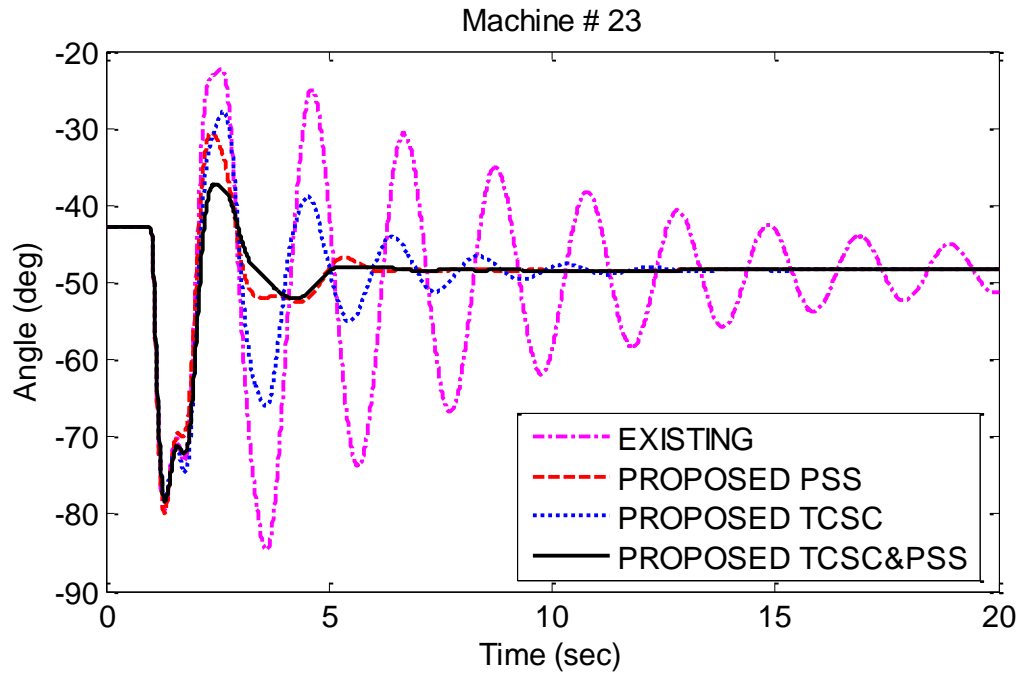


Fig. 8.6 Rotor Angle, Unit 23-Area 2, 3-Ph. Fault for 0.1s, Cord. PSSs&TCSC

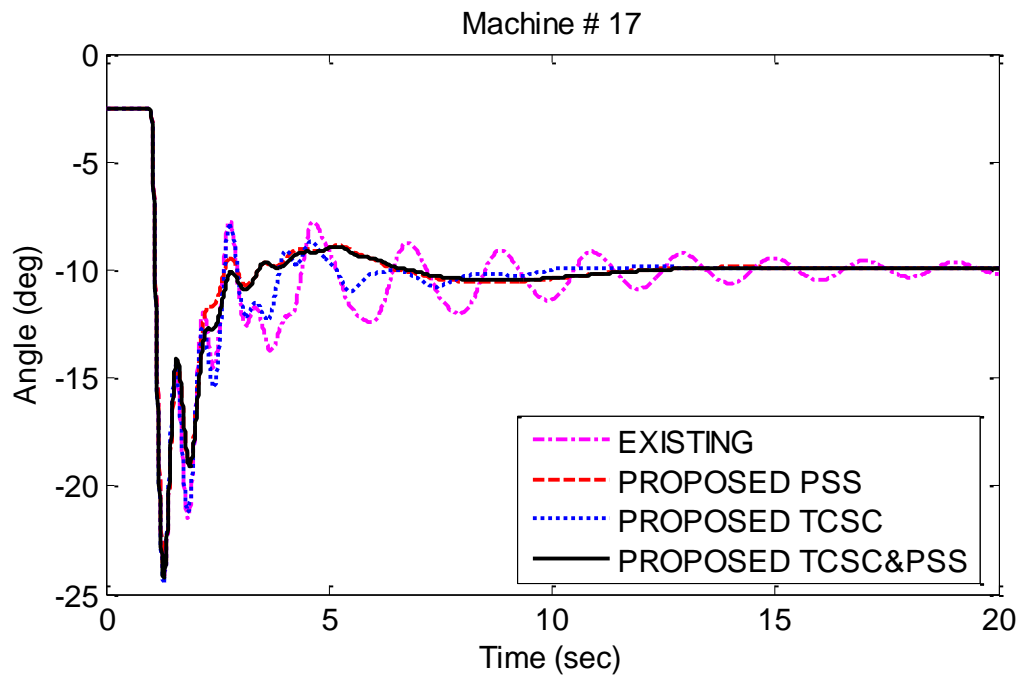


Fig. 8.7 Rotor Angle, Unit 17-Area 1, 3-Ph. Fault for 0.1s, Cord. PSSs&TCSC

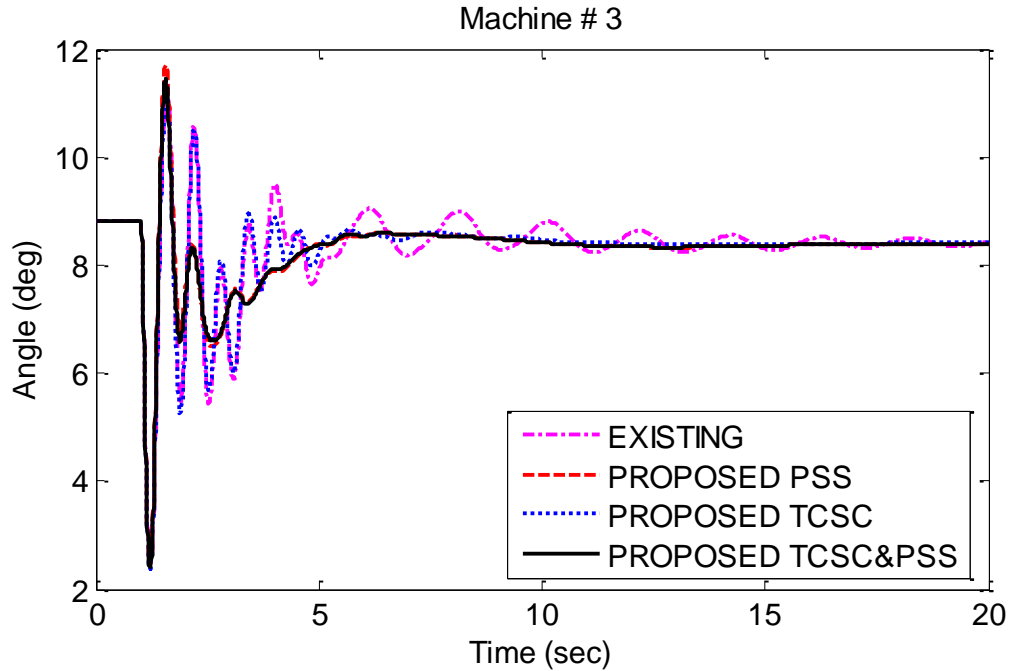


Fig. 8.8 Rotor Angle, Unit 3-Area 3, 3-Ph. Fault for 0.1s, Cord. PSSs&TCSC

8.4.2 Machines' Electrical Power Responses

Fig. 8.9 to Fig. 8.13 depict the electrical power for six machines in different areas. Similar to the previous figures, these figures show the dynamic performances of the existing power system without any additional controller and with the proposed controllers. As can be observed, the best dynamic performance in terms of minimum overshoot and fast settling time is the one concomitant with the simultaneous design of the TCSC and PSSs.

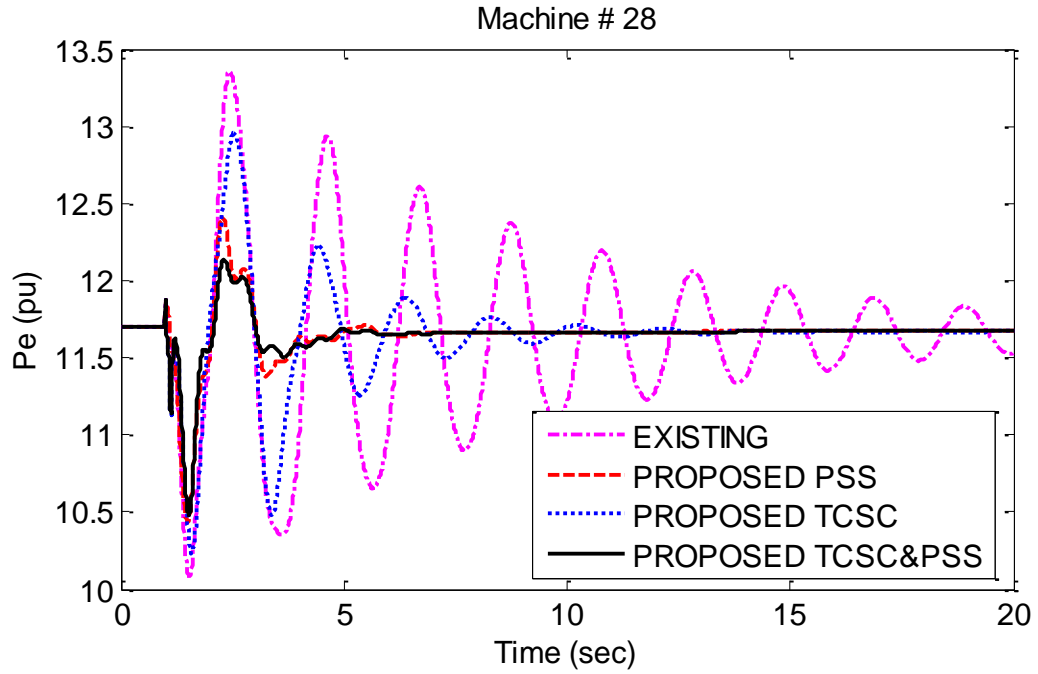


Fig. 8.9 Electrical Power, Unit 28-Area 2, 3-Ph. Fault for 0.1s, Cord. PSSs&TCSC

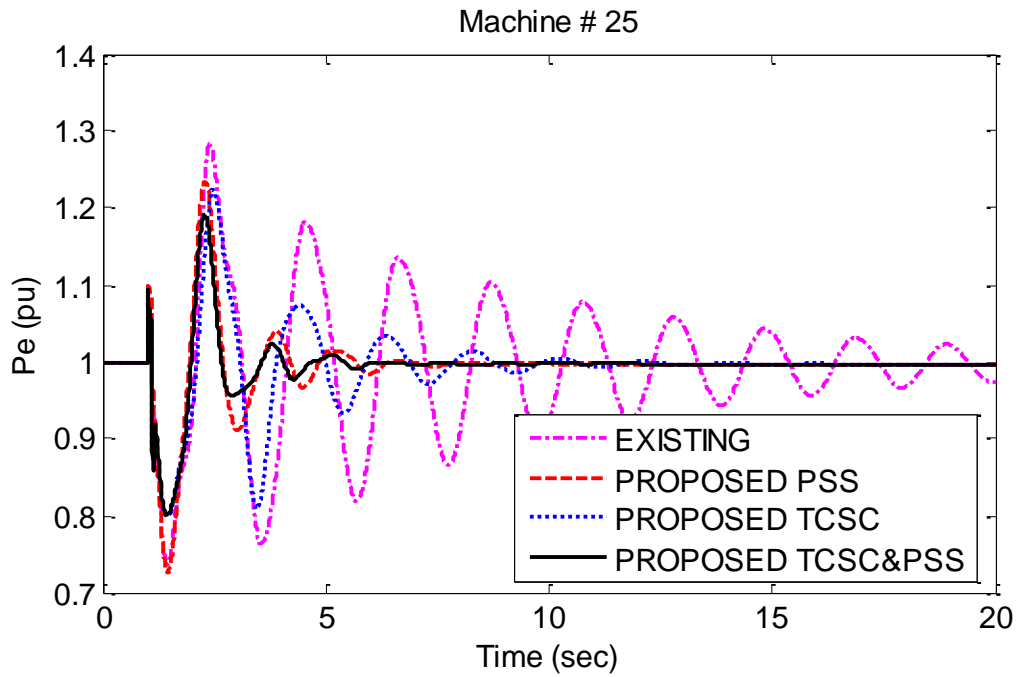


Fig. 8.10 Electrical Power, Unit 25-Area 2, 3-Ph. Fault for 0.1s, Cord. PSSs&TCSC

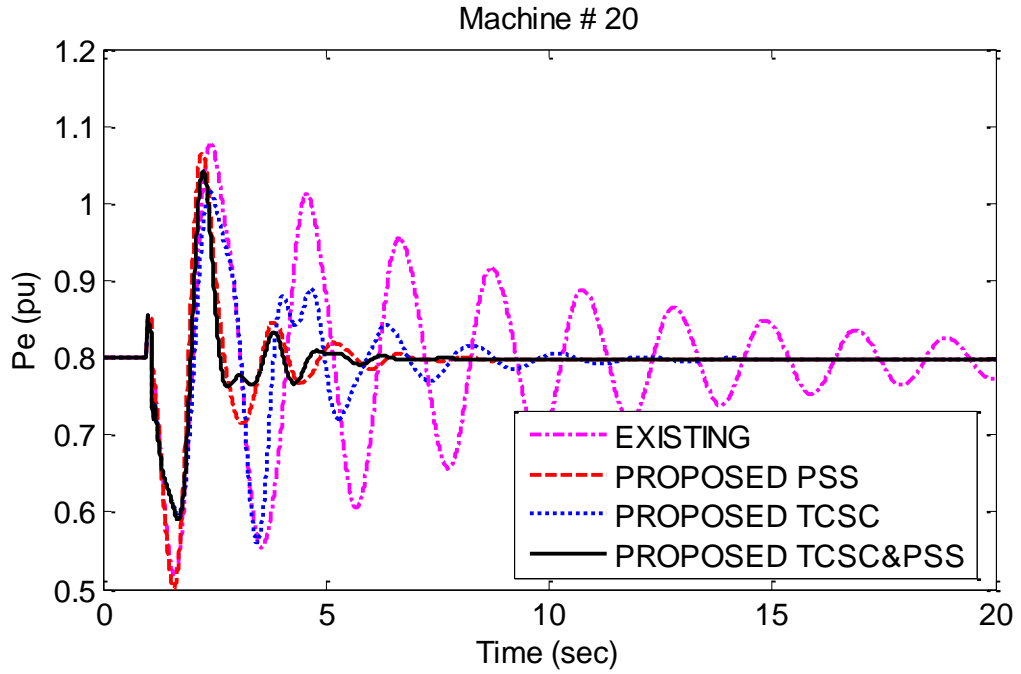


Fig. 8.11 Electrical Power, Unit 20-Area 2, 3-Ph. Fault for 0.1s, Cord. PSSs&TCSC

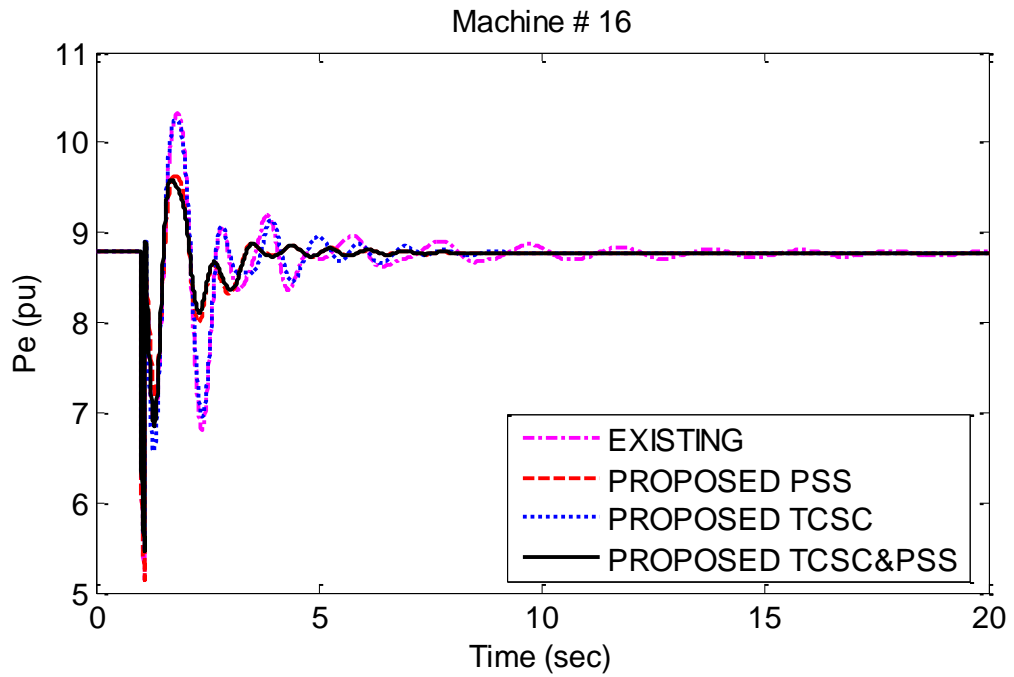


Fig. 8.12 Electrical Power, Unit 16-Area 1, 3-Ph. Fault for 0.1s, Cord. PSSs&TCSC

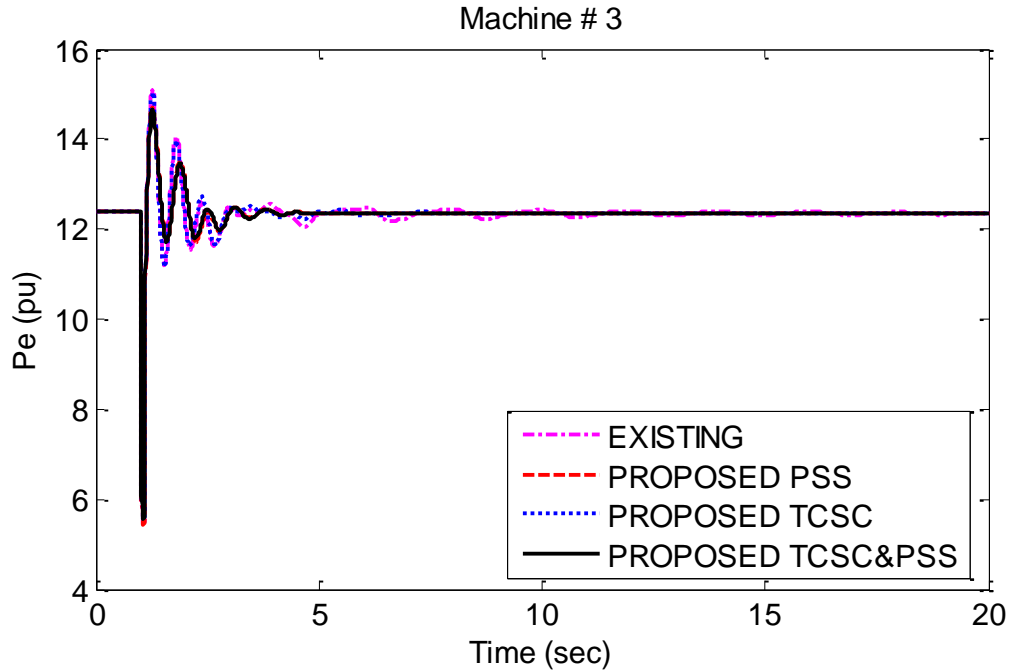


Fig. 8.13 Electrical Power, Unit 3-Area 3, 3-Ph. Fault for 0.1s, Cord. PSSs&TCSC

8.4.3 Rotor Speed Deviations' Responses

Fig. 8.14 to Fig. 8.17 below show the rotor speed deviations' responses for the four cases. As can be seen, the coordinated design of PSSs and TCSC has the best dynamic behavior compared to the others. It considerably improves the overall dynamic stability of the tested power system. More specifically, it has a great impact on most of the machines sited in area 2 which are rapidly stabilized due to the implementation of the optimized TCSC and PSSs.

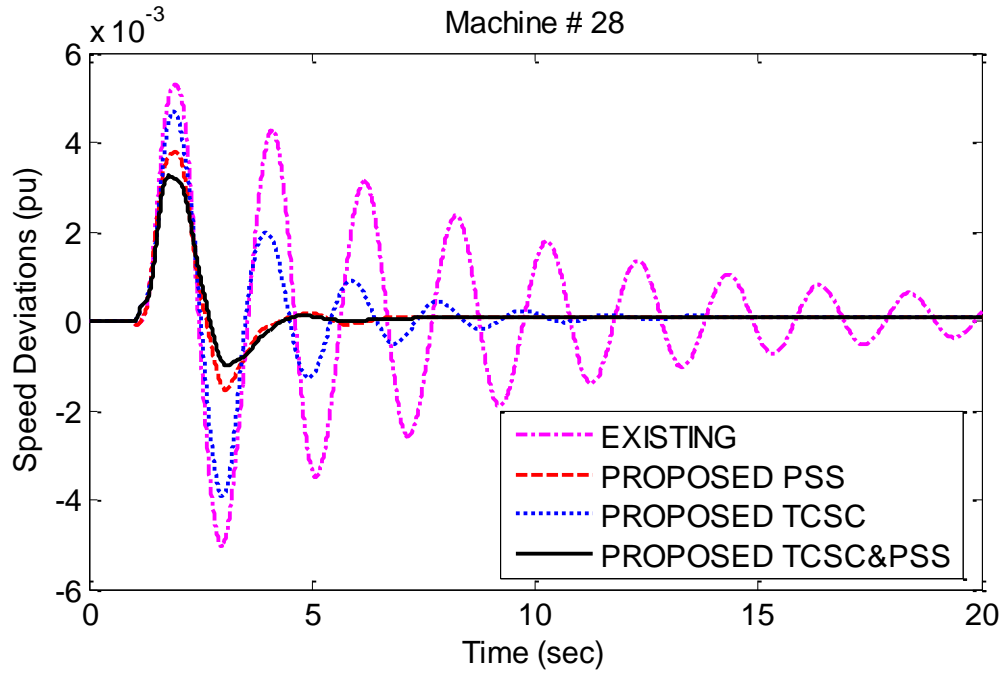


Fig. 8.14 Speed Deviations, Unit 28-Area 2, 3-Ph. Fault for 0.1s, Cord. PSSs&TCSC

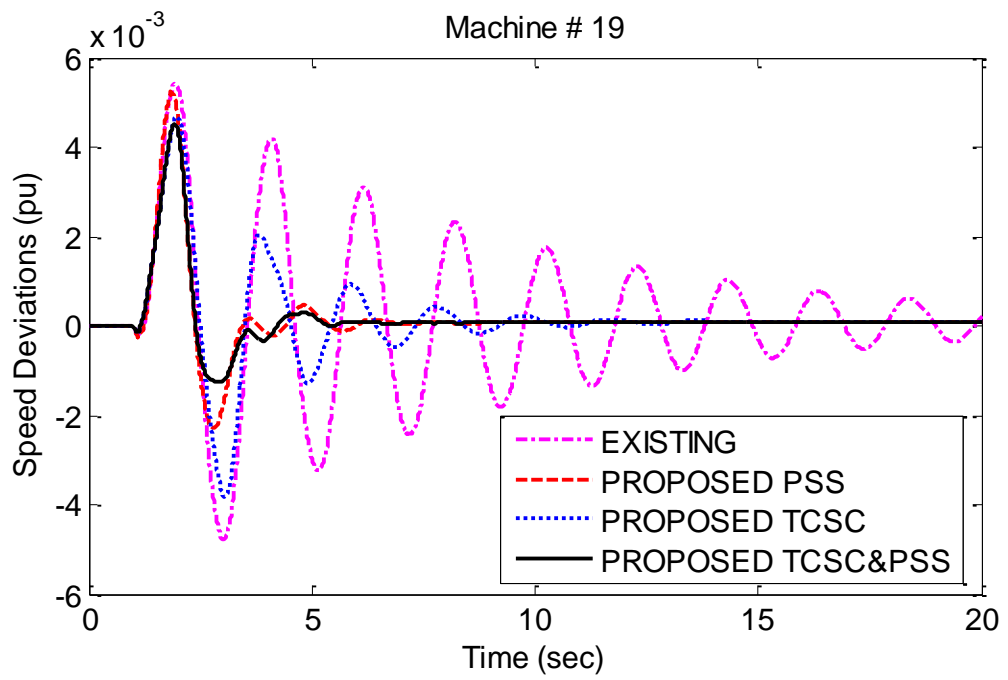


Fig. 8.15 Speed Deviations, Unit 19-Area 2, 3-Ph. Fault for 0.1s, Cord. PSSs&TCSC

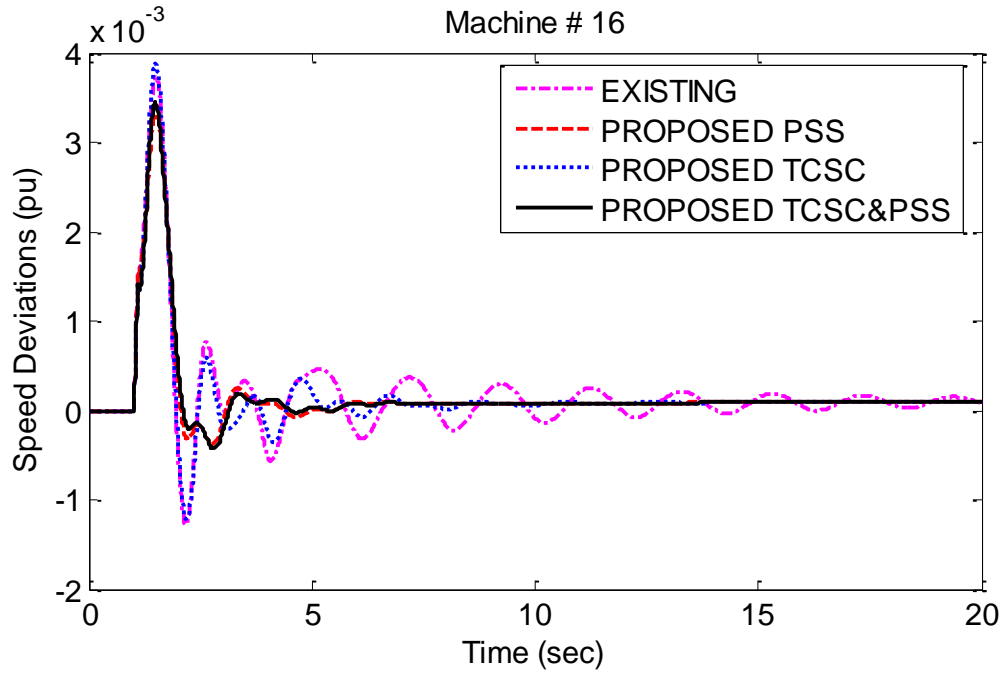


Fig. 8.16 Speed Deviations, Unit 16-Area 1, 3-Ph. Fault for 0.1s, Cord. PSSs&TCSC

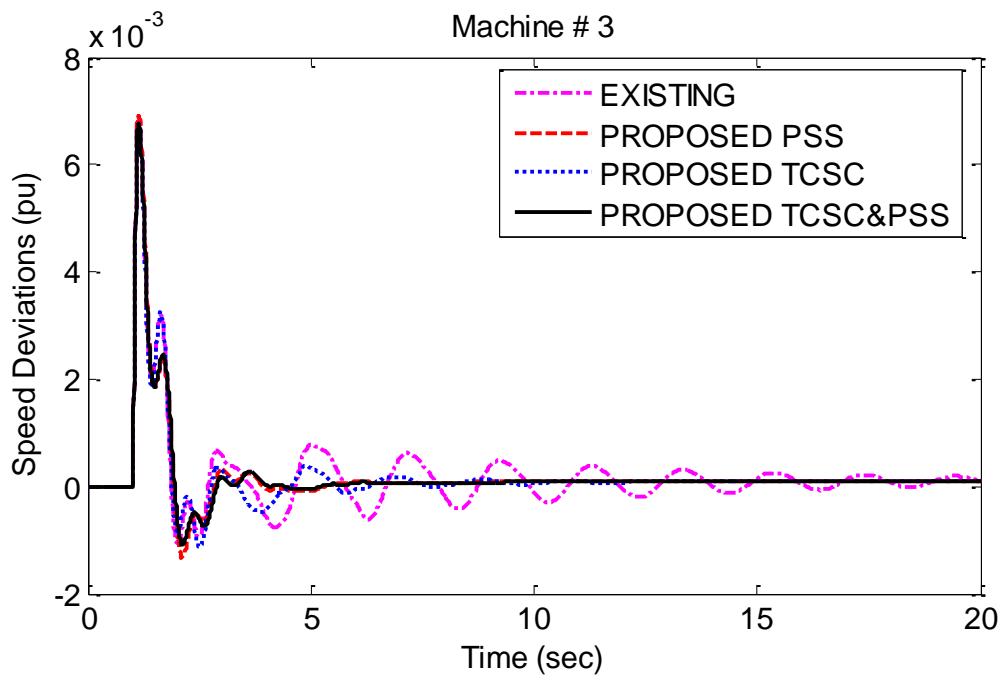


Fig. 8.17 Speed Deviations, Unit 3-Area 3, 3-Ph. Fault for 0.1s, Cord. PSSs&TCSC

8.4.4 Voltages' Responses

The voltages' responses of the boundary buses are shown in Fig. 8.18 to Fig. 8.20. By looking at these figures, it is quite evident that even the voltage dynamics are greatly enhanced after deploying the coordinated design of the TCSC and PSSs. For example, the existing voltage oscillations at buses 44 and 63 are substantially decreased after employing the proposed controllers. As shown in these figures the best dynamic behavior among the four cases is the one concomitant with the third design approach.

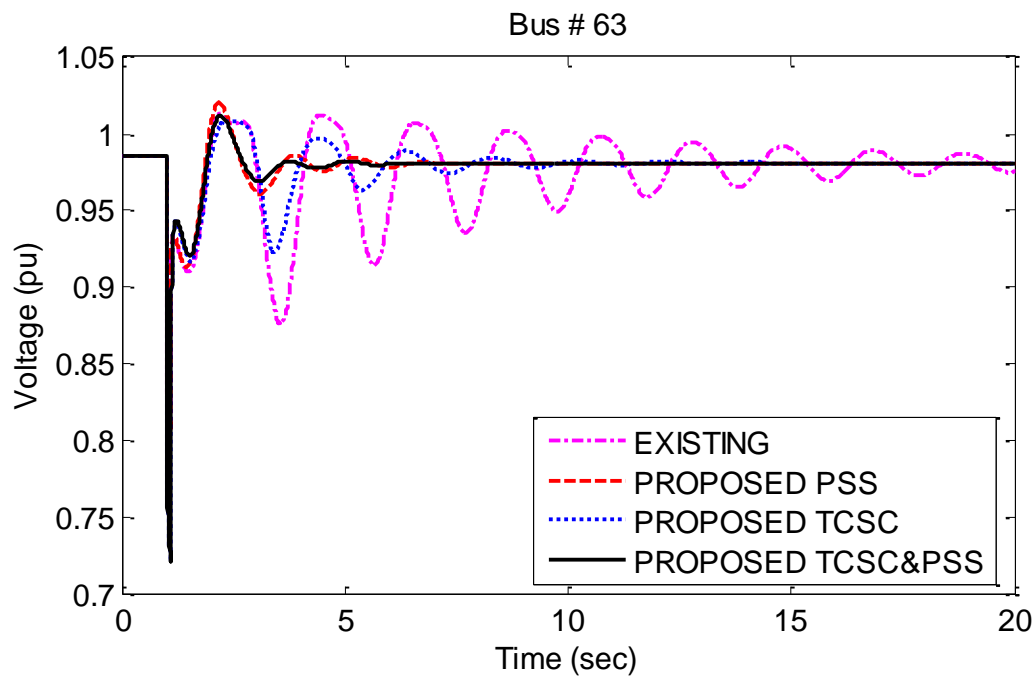


Fig. 8.18 Voltage, Bus 63-Area 2, 3-Ph. Fault for 0.1s, Cord. PSSs&TCSC

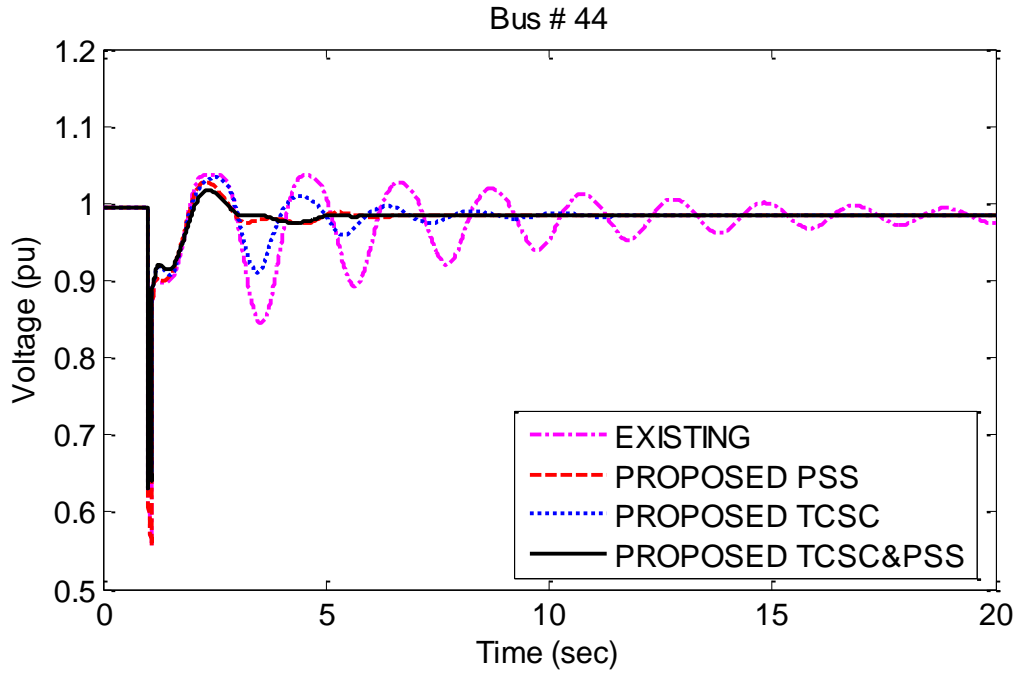


Fig. 8.19 Voltage, Bus 44-Area 1, 3-Ph. Fault for 0.1s, Cord. PSSs&TCSC

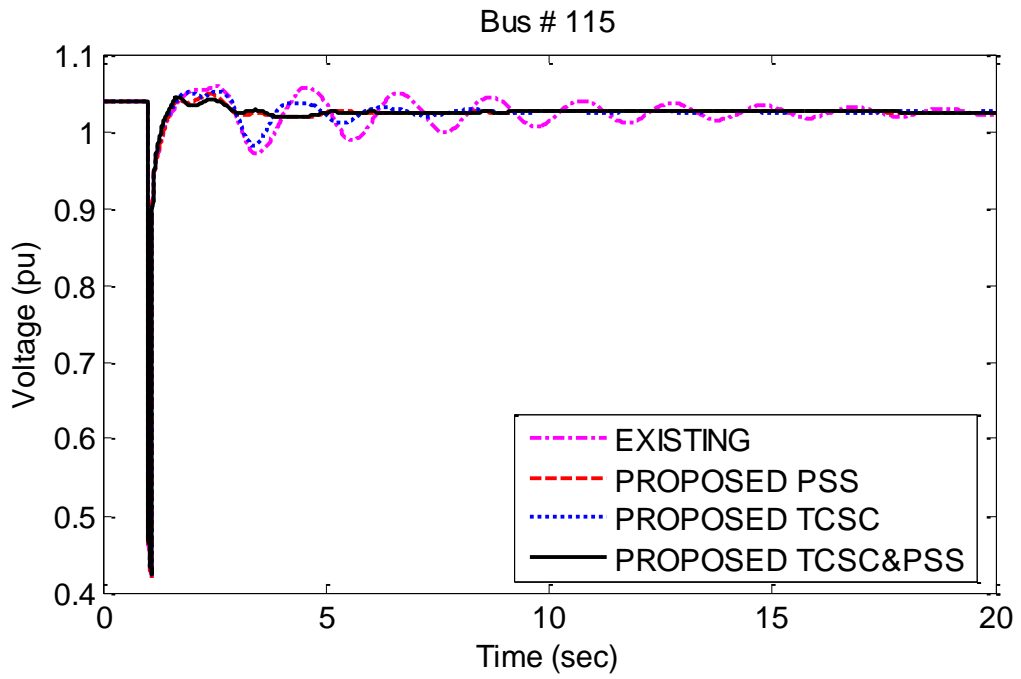


Fig. 8.20 Voltage, Bus 115-Area 3, 3-Ph. Fault for 0.1s, Cord. PSSs&TCSC

8.4.5 Active Power Flow Responses

Fig. 8.21 to Fig. 8.22 plots the active power flow of the 380 kV inter-ties. The first figure shows the active power flow of line 44 - 63. It is quite clear that the power oscillations are rapidly damped after employing the three proposed controllers. However, it can be seen that the best performance is that associated with the simultaneous design of both TCSC and the PSSs.

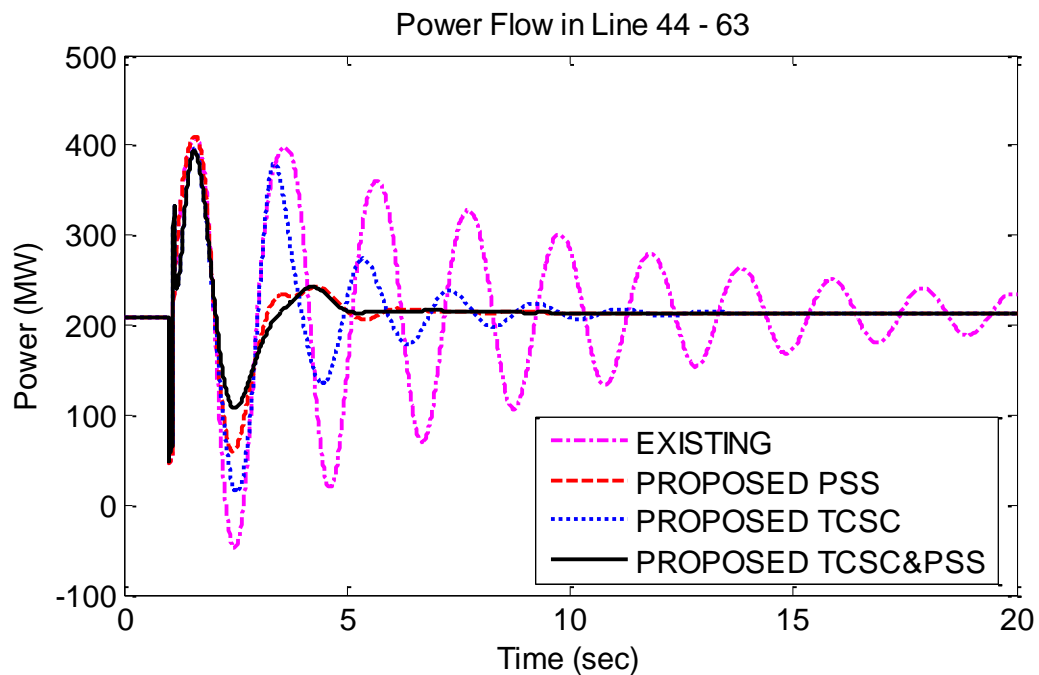


Fig. 8.21 Active Power, Line 63 to 44, 3-Ph. Fault for 0.1s, Cord. PSSs&TCSC

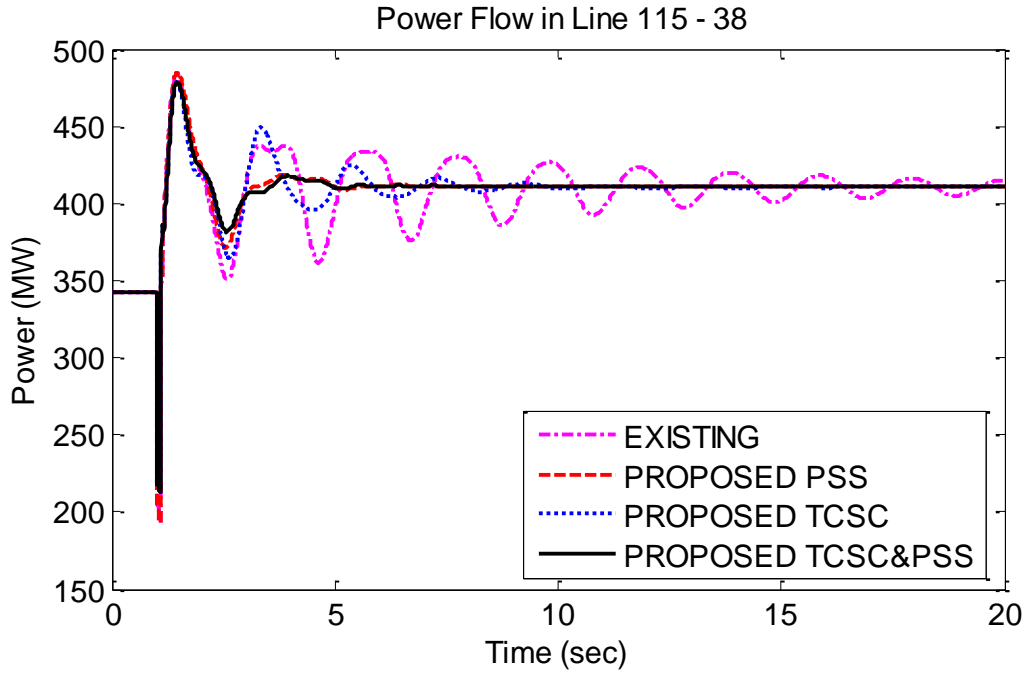


Fig. 8.22 Active Power, Line 115 to 38, 3-Ph. Fault for 0.1s, Cord. PSSs&TCSC

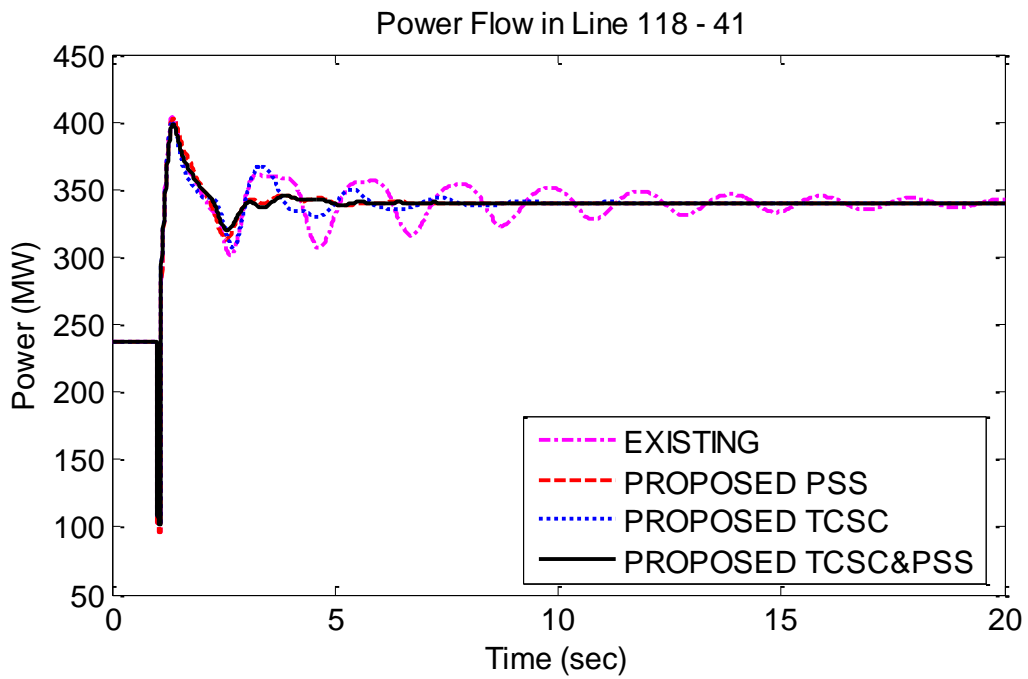


Fig. 8.23 Active Power, Line 118 to 41, 3-Ph. Fault for 0.1s, Cord. PSSs&TCSC

8.5 Robustness of the Proposed Coordinated Design of the TCSC and PSSs

Similar to the previous design approaches, to validate the robustness of the proposed controller, the following analyses are carried out:

- 1) Comparison of the maximum power transfer of the existing system with and without the proposed coordinated design of the PSSs and TCSC.
- 2) Identification of the new maximum power transfer limit after deploying the proposed controller.
- 3) Execution of several faults at different locations for the case of the maximum power transfer after deploying the proposed controller.

8.5.1 Existing Maximum Power Transfer Limit

To compare the power system performance considering the existing maximum power transfer with and without the proposed TCSC and PSSs, the same incident 2 defined in chapter 6 section 6.7, is repeated in this chapter. Fig. 8.24 shows the maximum power transfer between area 1 and 2 for the existing system compared with the same level of power transfer after the employment of the proposed TCSC and PSSs. It is quite clear that the dynamic stability is considerably enhanced. So, the transfer limit capability between area 1 and 2 can be significantly increased.

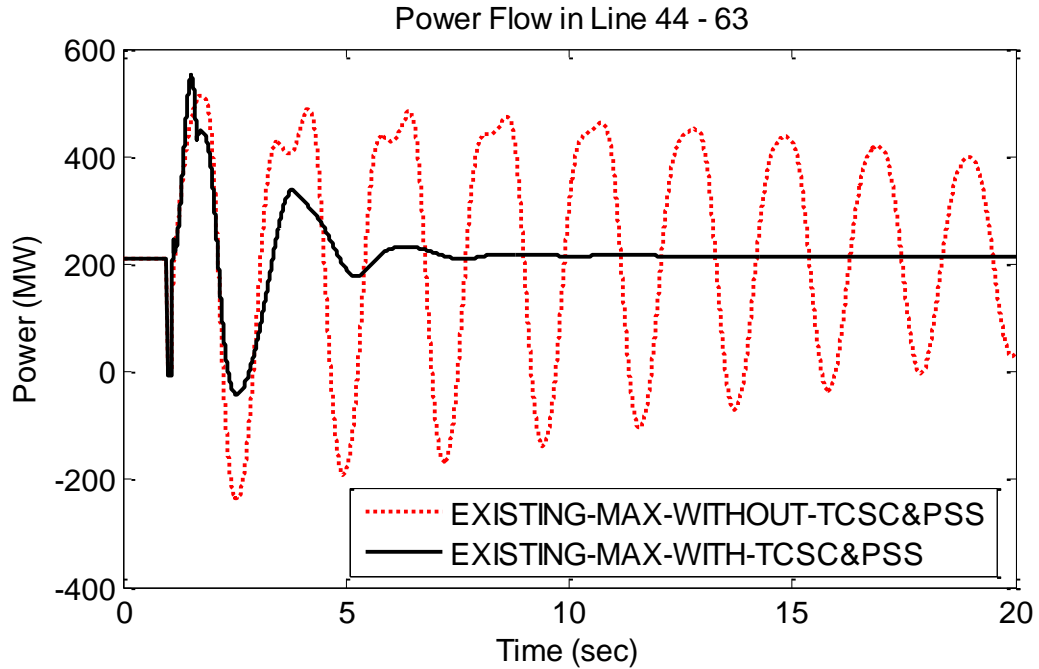


Fig. 8.24 Ex. Max. Power Transfer, 3-Ph. Fault for 0.1s, Cord. PSSs&TCSC

8.5.2 Maximum Power Transfer Limit with the Proposed PSSs and TCSC

Similarly, to calculate the new maximum power transfer, the same incident 2 described in chapter 6 is repeated here. Fig. 8.25 shows that the maximum power is significantly increased from 420 MW to 800 MW after implementing the coordinated design of the TCSC and PSSs.

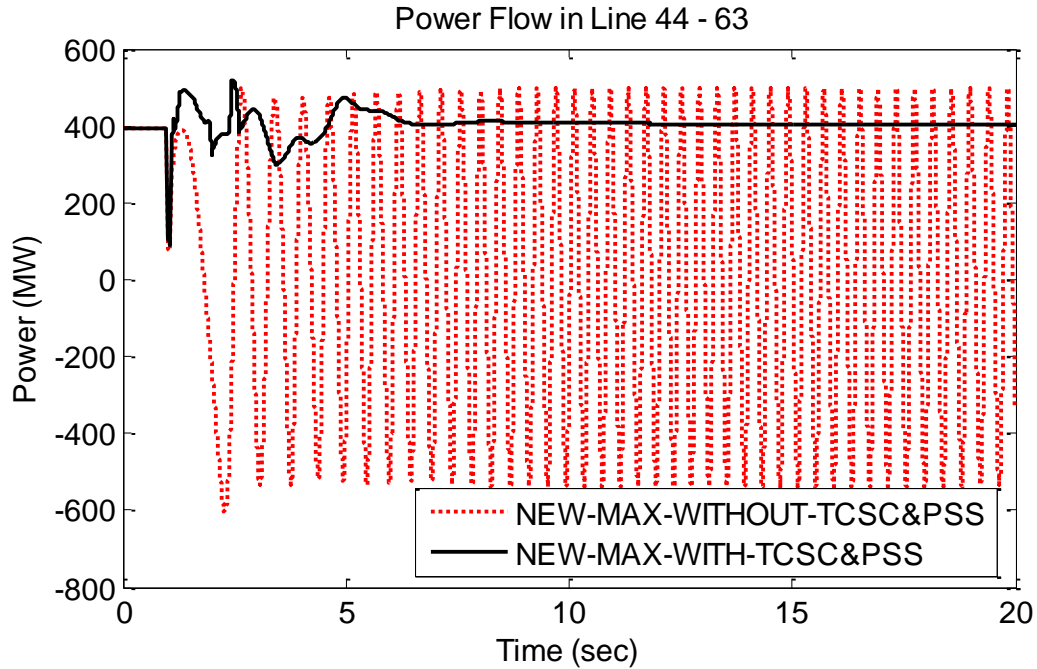


Fig. 8.25 New Max. Power Transfer, 3-Ph. Fault for 0.1s, Cord. PSSs&TCSC

8.5.3 Sensitivity Analyses

To assess the effectiveness and robustness of the proposed TCSC and PSSs, the same sensitivity cases executed in the previous chapters are repeated in this section. Fig. 8.26 and Fig. 8.27 confirm the robustness of the designed controller. The power oscillations are markedly reduced after the employment of the proposed TCSC and PSSs compared to the existing situation.

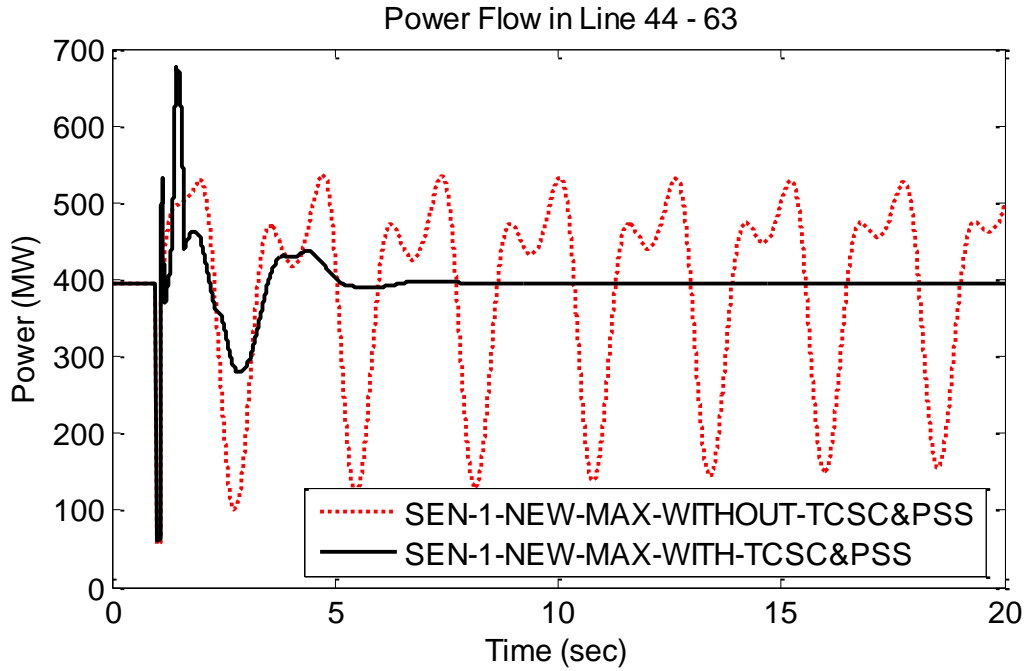


Fig. 8.26 New Max. Power Transfer, Line 44 to 63, Sensitivity 1, Cord. PSSs&TCSC

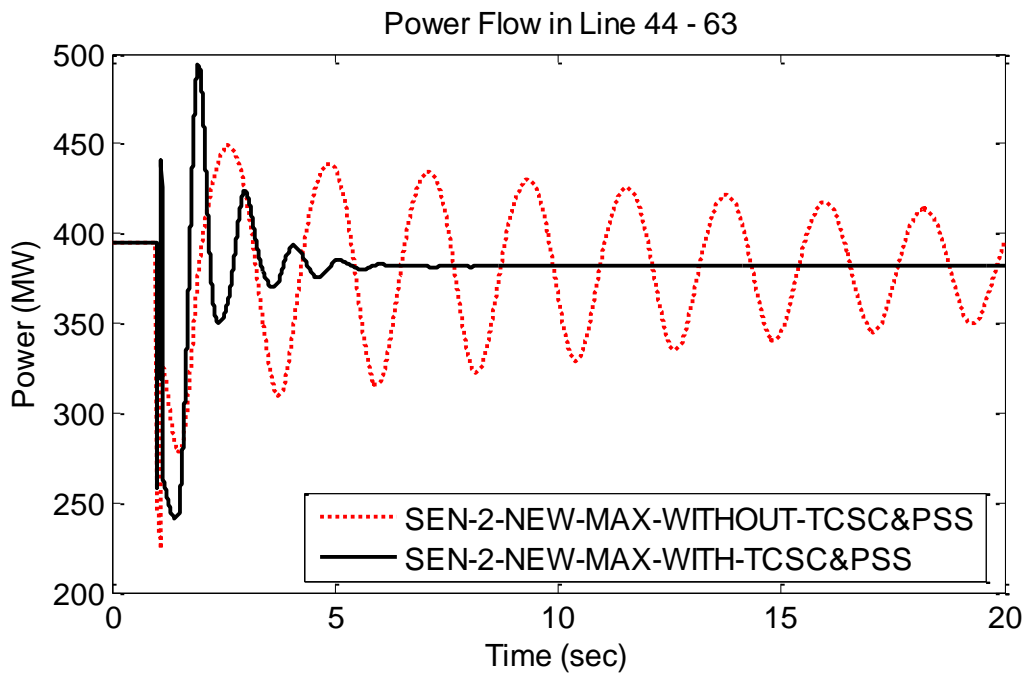


Fig. 8.27 New Max. Power Transfer, Line 44 to 63, Sensitivity 2, Cord. PSSs&TCSC

8.6 Summary of the Coordinated Design of the TCSC and PSSs

This chapter illustrates the influence of the simultaneous design of the PSSs and TCSC on improving the overall dynamic stability of the considered power system. It has been proven that the best dynamic behavior is concomitant with the coordinated design of the TCSC and PSSs. Since most of the dynamic performance of the electric and electromechanical quantities are markedly enhanced. Moreover, the maximum power transfer between area 1 and 2 is significantly increased from 420 MW without any controller to 800 MW with the proposed coordinated design of the PSSs and TCSC. In addition to that, it is quite obvious from the additional sensitivity analyses that the proposed controller design approach is a robust design.

CHAPTER 9

CONCLUSION AND RECOMMENDATIONS

9.1 Conclusion

In this thesis, the power system dynamic stability enhancement via three control design approaches have been investigated. The three approaches are stated hereafter:

- 1) Coordinated design of multiple Power System Stabilizers (PSSs).
- 2) Individual design of Thyristor Controlled Series Capacitors (TCSC) based stabilizers.
- 3) Coordinated design of multiple PSSs and TCSC.

A real power system has been considered and it has been statically and dynamically reduced before starting any analyses. A comparison of both the full version of the considered power system and the reduced one has been done. The comparison was done for both the steady state and dynamic simulation results. It has been found that the adopted reduction method is quite accurate for constructing the dynamic equivalent of a large scale power system. Since, the steady state and the dynamic simulation results for the full and the reduced power systems are closely matching.

The dynamic stability of the reduced power system has been investigated via modal analysis as well as nonlinear time-domain simulation. It has been found that low frequency oscillations phenomenon exist once a severe three phase fault occurs. Therefore, a novel technique has been developed to improve the dynamic stability of the tested power system and to increase the efficiency of its existing transmission line facilities via maximizing the power transfer capability among its weakly interconnected areas. This has been done via the employment of one of the aforementioned controller design approaches as described below.

Firstly, the impact of the coordination of multiple PSSs on improving the overall dynamic stability has been examined. At the beginning of the analysis, residue method and PSS installation criteria have been used to identify the best location for installing a new PSS. Accordingly, a new PSS was proposed to be installed at power plant 28 which is located in area 2. Then, the Modified Particle Swarm Optimization Technique (MPSO) was deployed to tune the proposed PSS in coordination with the existing PSSs. The MPSO is based on a nonlinear objective function for minimizing the Integral weighted Absolute Error (ITAE). The rotor speed deviations of all machines were considered as the error signals of the ITAE. Modal analysis as well as nonlinear time-domain simulation results have proved the importance of designing the PSSs simultaneously for improving the overall dynamic stability of the considered power system. Moreover, the power transfer capability between areas 1 and 2 has increased from 420 MW to 700 MW after implementing the proposed PSSs.

Secondly, the impact of the individual design of the TCSC on improving the dynamic stability of the considered power system has been tested. The TCSC-POD's input signal has been selected via the assessment of several nonlinear time-domain simulation runs for different candidate input signals. It has been shown that the best TCSC performance occurs when the voltage of bus 44 is fed to TCSC-POD. After selecting the input signal and similar to the multiple PSSs design approach, the MPSO has been used to determine the optimal parameters of the TCSC. Then, modal analysis and nonlinear time-domain simulation results have been carried out and proved the great impact of the TCSC on improving the overall dynamic stability performance. However, by comparing the results of the first and the second design approaches, it has been shown that the coordinated design of the PSSs has better dynamic performance in case of 420 MW power transfer between area 1 and 2, while, the TCSC has better dynamic performance in case of 700 MW. In addition to that, the power transfer capability between these areas has increased to 800 MW after utilizing the proposed TCSC compared to 700 MW in case of the simultaneous design of the PSSs.

Finally, both TCSC based stabilizer and the PSSs have been coordinately designed, tuned and tested. Similar to the previous design approaches, MPSO has been used to determine the optimal parameters of the PSSs in coordination with the TCSC. It has been proven that the coordinated design of the TCSC and PSSs has the best effect in enhancing the overall dynamic stability of the considered power system in case of 420 MW power transfer. In addition to that, the maximum power transfer between area 1 and 2 has increased to 800 MW which is similar to second design approach.

9.2 Recommendations

All of the above analyses have been repeated for different operating conditions to validate the effectiveness of the proposed controllers. The simulation results have demonstrated the robustness of the proposed design for all cases. Therefore, it is highly recommended to implement the following proposed projects as applicable:

- 1- New PSSs should be installed at power plant number 28. The design of these PSSs should be done in coordination of the rest of the existing PSSs.
- 2- If the above point is not feasible, a new TCSC based stabilizer should be installed in series with the line connecting area 1 and 2. The input signal of the TCSC-POD should be carefully selected via utilizing one of observability methods.
- 3- If both of the above projects are feasible, simultaneous design of the PSSs and TCSC based stabilizer should be considered while designing these controllers.

9.3 Future Work

The following subjects are some of possible future works in the same research direction:

- Multi-objective functions might be considered in the design stage in order to improve the proposed stabilizer performance.
- Incorporation of other kinds of FACTS controllers, such as, STATCOM, UPFC, IPFC to the study system can be investigated.

- The optimal number of FACTS devices to be installed in a multi-machine system can also be considered as an extension to this work.
- Optimal selection of the percentage of both fixed and thyristor controlled series compensation can be further investigated.
- The input signal of the TCSC to be further assessed via utilizing one of observability methods such as merit factor method.
- Impact of air-conditioning dynamic load model on exciting small signal oscillations need to be considered in future work.
- Impact of High Voltage Direct Current (HVDC) transmission lines on damping power oscillations, might be investigated.
- Renewable energy sources could be deployed and their effects on improving the overall dynamic stability could be studied.

REFERENCES

- [1]. R. Mohan and R. K. Varma, **Thyristor Based FACTS Controllers for Electrical Transmission Systems**, New York: John Wiley & Sons Inc, 2002.
- [2]. P. Kundur, **Power System Stability and Control**, New York: McGraw, Inc, 1994.
- [3]. Kundur, P.; Paserba, J.; Ajarapu, V.; Andersson, G.; Bose, A; Canizares, C.; Hatziargyriou, N.; Hill, D.; Stankovic, A; Taylor, C.; Van Cutsem, T.; Vittal, V., "Definition and classification of power system stability IEEE/CIGRE joint task force on stability terms and definitions," *Power Systems, IEEE Transactions on* , vol.19, no.3, Page(s): 1387-1401, Aug. 2004
- [4]. R. Patel, T. S. Bhatti and D. P. Kothari, "MATLAB/Simulink Based Transient Stability Analysis of a Multi-machine Power System," *International Journal of Electrical Engineering Education*, vol. 39, no. 4, Page(s): 320-336, 2002.
- [5]. Prabhashankar, K.; Janischewsyj, W., "Digital Simulation of Multimachine Power Systems for Stability Studies," *Power Apparatus and Systems, IEEE Transactions on* , vol.PAS-87, no.1, Page(s): 73-80, Jan. 1968
- [6]. Padiyar, K.R.; Ramshaw, R.S., "Dynamic Analysis of Multi -Machine Power Systems," *Power Apparatus and Systems, IEEE Transactions on* , vol.PAS-91, no.2, Page(s): 526-535, March 1972
- [7]. P. W. Sauer and M. A. Pai, **Power System Dynamics and Stability**, Prentice Hall, Upper Saddle River, New Jersey, 1998.
- [8]. Gallai, A; Thomas, R.J., "Coherency identification for large electric power systems," *Circuits and Systems, IEEE Transactions on* , vol.29, no.11, Page(s): 777-782, Nov 1982
- [9]. Newell, R. J.; Risan, M. D.; Allen, L.; Rao, IS.; Stuehm, D.L., "Utility Experience With Coherency-Based Dynamic Equivalents Of Very Large Systems," *Power Apparatus and Systems, IEEE Transactions on* , vol.PAS-104, no.11, Page(s): 3056-3063, Nov. 1985
- [10]. Lo, C. M.; Tse, C. T., "Application of coherency-based dynamic equivalents in small perturbation stability studies," *Advances in Power System Control, Operation and Management*, 1993. APSCOM-93., 2nd International Conference on , Page(s): 916-921 vol.2, 7-10 Dec 1993

- [11]. Hussain, M. Y.; Rau, V. G., "An efficient and simple method of dynamic equivalent construction for large multi-machine power system," *Advances in Power System Control, Operation and Management*, 1991. APSCOM-91., 1991 International Conference on , Page(s): 90-94 vol.1, 5-8 Nov 1991
- [12]. Sung-Kwan Joo; Chen-Ching Liu; Jong-Woong Choe, "Enhancement of coherency identification techniques for power system dynamic equivalents," *Power Engineering Society Summer Meeting*, 2001 , vol.3, no., Page(s): 1811-1816 vol.3, 2001
- [13]. Lei, X.; Povh, D.; Ruhle, O., "Industrial approaches for dynamic equivalents of large power systems," *Power Engineering Society Winter Meeting*, 2002. IEEE , vol.2, no., Page(s): 1036-1042 vol.2, 2002
- [14]. Eduardo J. S., Pires de Souza, Maria B. D., Araujo Pedro and Fabio L. Souza, "Selection Equivalent Models in the Excitation Systems Dynamic Aggregation Problems ", *IEEE 4th PSCC*, 2002.
- [15]. Sung-Kwan Joo; Chen-Ching Liu; Jones, L.E.; Jong-Woong Choe, "Coherency and aggregation techniques incorporating rotor and voltage dynamics," *Power Systems*, *IEEE Transactions on* , vol.19, no.2, Page(s): 1068-1075, May 2004
- [16]. Gil, M.A; Rios, M.A; Gomez, O., "Coherency identification based on maximum spanning tree partitioning," *PowerTech (POWERTECH)*, 2013 IEEE Grenoble , vol., no., Page(s): 1-6, 16-20 June 2013
- [17]. Artenstein, M.; Giusto, A, "Equivalent model of the Argentinian electrical power system for stability analysis of the Uruguayan network," *Transmission and Distribution Conference and Exposition: Latin America*, 2008 IEEE/PES , Page(s): 1-5, 13-15 Aug. 2008
- [18]. Abdul-Majeed, Mohammed Arif (1985) Coherency based equivalents for long-term dynamic studies. Master's thesis, King Fahd University of Petroleum and Minerals. Ann Arbor : UMI, (Publication No. MI 48106-1346)
- [19]. De Oliveira, S.E.M.; Massaud, AG., "Modal dynamic equivalent for electric power systems. II. Stability simulation tests," *Power Systems*, *IEEE Transactions on* , vol.3, no.4, Page(s): 1731-1737, Nov 1988
- [20]. Lo, K.L.; Qi, Z. Z.; Urqhart, B., "Dynamic equivalents of power stations for optimal control of power system security," *Systems, Man and Cybernetics*, 1993. 'Systems Engineering in the Service of Humans', *Conference Proceedings.*, International Conference on , Page(s): 456-461 vol.2, 17-20 Oct 1993

- [21]. Nath, R.; Lamba, S.S., "Development of coherency-based time-domain equivalent model using structure constraints," *Generation, Transmission and Distribution, IEE Proceedings C* , vol.133, no.4, Page(s): 165-175, May 1986
- [22]. Zin, AAM.; Kok, B. C.; Mustafa, M.W.; Lo, K.L.; Ariffin, AE., "Time-domain dynamic aggregation of generating unit based on structure preserving approach," *Power Engineering Conference, 2003. PECon 2003. Proceedings. National* , Page(s): 154-160, 15-16 Dec. 2003
- [23]. Ourari, M.L.; Dessaint, L-A; Do, V.Q., "Generating units aggregation for dynamic equivalent of large power systems," *Power Engineering Society General Meeting, 2004. IEEE* , Page(s): 1535-1541 Vol.2, 10-10 June 2004
- [24]. Ning Mi; Boyuan Yan; Tan, S.X.; Fan, J.; Hao Yu, "General Block Structure-Preserving Reduced Order Modeling of Linear Dynamic Circuits," *Quality Electronic Design, 2007. ISQED '07. 8th International Symposium on* , Page(s): 633-638, 26-28 March 2007
- [25]. Yongbo Yang; Xiaoming Zha, "Time-domain Aggregation of Generating Units for Shipboard Power Systems," *Power and Energy Engineering Conference, 2009. APPEEC 2009. Asia-Pacific* , Page(s): 1-4, 27-31 March 2009
- [26]. Singhavilai, T.; Anaya-Lara, O.; Lo, K.L., "Identification of the dynamic equivalent of a power system," *Universities Power Engineering Conference (UPEC), 2009 Proceedings of the 44th International* , Page(s): 1-5, 1-4 Sept. 2009
- [27]. Byung Ha Lee, "A study on stability enhancement of large scale systems using H_{∞} control based on dynamic reduction," *Transmission & Distribution Conference & Exposition: Asia and Pacific, 2009* , Page(s): 1-4, 26-30 Oct. 2009
- [28]. Wang, L.; Klein, M.; Yirga, S.; Kundur, P., "Dynamic reduction of large power systems for stability studies," *Power Systems, IEEE Transactions on* , vol.12, no.2, Page(s): 889-895, May 1997
- [29]. Price, W.W.; Hargrave, AW.; Hurysz, B.J.; Chow, J.H.; Hirsch, P.M., "Large-scale system testing of a power system dynamic equivalencing program," *Power Systems, IEEE Transactions on* , vol.13, no.3, Page(s): 768-774, Aug 1998
- [30]. Galarza, R.J.; Chow, J.H.; Price, W.W.; Hargrave, AW.; Hirsch, P.M., "Aggregation of exciter models for constructing power system dynamic equivalents," *Power Systems, IEEE Transactions on* , vol.13, no.3, Page(s): 782-788, Aug 1998

- [31]. Yang, J.P.; Cheng, G.H.; Xu, Z., "Dynamic Reduction of Large Power System in PSS/E," Transmission and Distribution Conference and Exhibition: Asia and Pacific, 2005 IEEE/PES , Page(s): 1-4, 2005
- [32]. G. Pyo, J. Park and S. Moon, "A New Method for Dynamic Reduction of Power System Using PAM Algorithm," Power and Energy Society General Meeting, 2010 IEEE , Page(s): 1 - 7, 2010.
- [33]. Rahim and A. J. Ramadhan, "Dynamic Equivalent of External Power System and its Parameter Estimation Through Artificial Neural Networks," International Journal of Electrical Power & Energy Systems, vol. 24, no. 2, Page(s): 113–120, 2002.
- [34]. Enrico De Tuglie, Lorenzo Guida, Francesco Torelli, Dario Lucarella, Massimo Pozzi and Giuliano Vimercati, "Identification of Dynamic Voltage Current Power System Equivalents through Artificial Neural Networks", IEEE Bulk Power System Dynamics and Control, 2004.
- [35]. Feng Ma; Vittal, V., "A Hybrid Dynamic Equivalent Using ANN-Based Boundary Matching Technique," Power Systems, IEEE Transactions on , vol.27, no.3, Page(s): 1494-1502, Aug. 2012
- [36]. Soobae Kim; Overbye, T.J., "Enhanced measurement-based dynamic equivalence using coherency identification," Power and Energy Conference at Illinois (PECI), 2013 IEEE , Page(s): 200-205, 22-23 Feb. 2013
- [37]. Matar, M.; Fernandopulle, N., "Dynamic model reduction using integrated PSS/E and Matlab," Electrical & Computer Engineering (CCECE), 2012 25th IEEE Canadian Conference on , Page(s): 1-5, April 29 2012-May 2 2012
- [38]. F. Milano and K. Srivastava, "Dynamic REI Equivalents for Short Circuit and Transient Stability Analyses," Electric Power Systems Research, vol. 79, no. 6, Page(s): 878–887, 2009.
- [39]. Maria, A; Ghasemi, Hassan, "Development of a dynamic equivalent model for Ontario's external system," Power & Energy Society General Meeting, 2009. PES '09. IEEE , Page(s): 1-5, 26-30 July 2009
- [40]. Almeida, AB.; Reginatto, R.; da Silva, R.J.G.C., "A software tool for the determination of dynamic equivalents of power systems," Bulk Power System Dynamics and Control (iREP) - VIII (iREP), 2010 iREP Symposium , Page(s): 1-10, 1-6 Aug. 2010

- [41]. Annakkage, U.D.; Nair, N. -K C; Liang, Y.; Gole, AM.; Dinavahi, V.; Gustavsen, B.; Noda, T.; Ghasemi, Hassan; Monti, A; Matar, M.; Iravani, R.; Martinez, J.A, "Dynamic System Equivalents: A Survey of Available Techniques," Power Delivery, IEEE Transactions on , vol.27, no.1, Page(s): 411-420, Jan. 2012
- [42]. DeMello, F.P.; Concordia, Charles, "Concepts of Synchronous Machine Stability as Affected by Excitation Control," Power Apparatus and Systems, IEEE Transactions on , vol.PAS-88, no.4, Page(s): 316-329, April 1969
- [43]. Larsen, E.V.; Swann, D. A, "Applying Power System Stabilizers Part I: General Concepts," Power Apparatus and Systems, IEEE Transactions on , vol.PAS-100, no.6, Page(s): 3017-3024, June 1981
- [44]. Larsen, E.V.; Swann, D. A, "Applying Power System Stabilizers Part II: Performance Objectives and Tuning Concepts," Power Apparatus and Systems, IEEE Transactions on , vol.PAS-100, no.6, Page(s): 3025-3033, June 1981
- [45]. Larsen, E.V.; Swann, D. A, "Applying Power System Stabilizers Part III: Practical Considerations," Power Apparatus and Systems, IEEE Transactions on , vol.PAS-100, no.6, Page(s): 3034-3046, June 1981
- [46]. Kamwa, I; Grondin, R.; Trudel, G., "IEEE PSS2B versus PSS4B: the limits of performance of modern power system stabilizers," Power Systems, IEEE Transactions on , vol.20, no.2, Page(s): 903-915, May 2005
- [47]. Jan Machowski, Janusz W. Bialek and James R., A 2008, "**Power System Dynamics Stability & Control**", John Wiley & Sons, Inc, New York.
- [48]. Xi-Fan Wang, Yonghua Song and Malcolm Irving, A 2008, "**Modern Power System Analysis**", Springer Science and Business Media, LLC ,New York.
- [49]. Zhuang, Y.; Feliachi, A, "Identification of optimal location for power system stabilizers," System Theory, 1988., Proceedings of the Twentieth Southeastern Symposium on , Page(s): 236-238, 1988
- [50]. Koessler, R.J.; Prabhakara, F.S.; Al-Mubarak, AH., "Analysis of Oscillations with Eigenanalysis and Prony Techniques," Power Engineering Society General Meeting, 2007. IEEE , Page(s): 1-8, 24-28 June 2007
- [51]. Hsu, Yuan-Yih; Chen, Chern-Lin, "Identification of optimum location for stabilizer applications using participation factors," Generation, Transmission and Distribution, IEE Proceedings C , vol.134, no.3, Page(s): 238-244, May 1987

- [52]. Trudnowski, D.J.; Pierre, D.A; Smith, J.R.; Adapa, R., "Coordination of multiple adaptive PSS units using a decentralized control scheme," Power Systems, IEEE Transactions on , vol.7, no.1, Page(s): 294-300, Feb 1992
- [53]. Gu, Wenyan; Bollinger, K.E., "A Self-Tuning Power System Stabilizer for Wide-Range Synchronous Generator Operation," Power Engineering Review, IEEE , vol.9, no.8, Page(s): 63-64, Aug. 1989
- [54]. Hiyama, T., "Application of neural network to real time tuning of fuzzy logic PSS," Neural Networks to Power Systems, 1993. ANNPS '93., Proceedings of the Second International Forum on Applications of , Page(s): 421-426, 1993
- [55]. Yang, T.-C., "Weighting function selection for H_{∞} based power system stabilizer design," Control Applications, 1995., Proceedings of the 4th IEEE Conference on , Page(s): 1033-1034, 28-29 Sep 1995
- [56]. Andreis P. Engelbrecht, "**Computation Intelligence**", Second Edition, 2007.
- [57]. He, P.; Wei, Y.B.; Yang, C.X.; Wang, K.W., "Adaptive power system stabilizer design for multi-machine power systems," Advances in Power System Control, Operation and Management (APSCOM 2009), 8th International Conference on , Page(s): 1-6, 8-11 Nov. 2009
- [58]. Folly, K.A; Venayagamoorthy, G.K., "Optimal tuning of Power System Stabilizer parameters using PBIL with adaptive learning rate," Power and Energy Society General Meeting, 2010 IEEE , Page(s): 1-6, 25-29 July 2010
- [59]. Sil, Amitava; Gangopadhyay, T. K.; Paul, S.; Maitra, AK., "Design of robust Power System Stabilizer using H_{∞} mixed sensitivity technique," Power Systems, 2009. ICPS '09. International Conference on , Page(s): 1-4, 27-29 Dec. 2009
- [60]. Abido, M.A., "Optimal design of power-system stabilizers using particle swarm optimization," Energy Conversion, IEEE Transactions on , vol.17, no.3, pp.406,413, Sep 2002
- [61]. Abido, M.A; Abdel-Magid, Y.L., "Optimal design of power system stabilizers using evolutionary programming," Energy Conversion, IEEE Transactions on , vol.17, no.4, Page(s): 429-436, Dec 2002
- [62]. Vani, M.U.; Raju, G.S.; Prasad, K. R L, "Robust Supplementary Controllers for AVR and PSS," India Conference (INDICON), 2009 Annual IEEE , Page(s): 1-4, 18-20 Dec. 2009
- [63]. Seung-Mook Baek; Jung-Wook Park; Hiskens, IA, "Optimal Tuning for Linear and Nonlinear Parameters of Power System Stabilizers in Hybrid System

- Modeling," Industry Applications Conference, 2007. 42nd IAS Annual Meeting. Conference Record of the 2007 IEEE , Page(s): 1665-1672, 23-27 Sept. 2007
- [64]. Abdel-Magid, Y.L.; Abido, M.A; Al-Baiyat, S.; Mantawy, A H., "Simultaneous stabilization of multimachine power systems via genetic algorithms," Power Systems, IEEE Transactions on , vol.14, no.4, Page(s): 1428-1439, Nov 1999
- [65]. Chansareewittaya, S.; Jirapong, P., "Power transfer capability enhancement with multitype FACTS controllers using particle swarm optimization," TENCON 2010 - 2010 IEEE Region 10 Conference , Page(s): 42-47, 21-24 Nov. 2010
- [66]. Malakar, T.; Sinha, N.; Goswami, S.K.; Saikia, L.C., "Optimal location and size determination of FACTS devices by using multiobjective optimal power flow," TENCON 2010 - 2010 IEEE Region 10 Conference , Page(s): 474-478, 21-24 Nov. 2010
- [67]. Mahdad, B.; Bouktir, T.; Srairi, K., "Strategy of location and control of FACTS devices for enhancing power quality," Electrotechnical Conference, 2006. MELECON 2006. IEEE Mediterranean , Page(s): 1068-1072, 16-19 May 2006
- [68]. Nagalakshmi, S.; Kamaraj, N., "Loadability enhancement for pool model with FACTS devices in transmission system using Differential Evolution and Particle Swarm Optimization," Power Electronics (IICPE), 2010 India International Conference on , Page(s): 1-8, 28-30 Jan. 2011
- [69]. Ongsakul, W.; Jirapong, P., "Optimal allocation of FACTS devices to enhance total transfer capability using evolutionary programming," Circuits and Systems, 2005. ISCAS 2005. IEEE International Symposium on , Page(s): 4175-4178 Vol. 5, 23-26 May 2005
- [70]. Shakib, AD.; Balzer, G., "Optimal location and control of shunt FACTS for transmission of renewable energy in large power systems," MELECON 2010 - 2010 15th IEEE Mediterranean Electrotechnical Conference , Page(s): 890-895, 26-28 April 2010
- [71]. Shaheen, H. I; Rashed, G.I; Cheng, S.J., "Optimal Location and Parameters Setting of Unified Power Flow Controller Based on Evolutionary Optimization Techniques," Power Engineering Society General Meeting, 2007. IEEE , Page(s): 1-8, 24-28 June 2007
- [72]. Phadke, A R.; Fozdar, M.; Niazi, K. R., "Multi-objective fuzzy-GA formulation for optimal placement and sizing of shunt FACTS controller," Power Systems, 2009. ICPS '09. International Conference on , Page(s): 1-6, 27-29 Dec. 2009

- [73]. Kiran, S.H.; Subramani, C.; Dash, S.S.; Arunbhaskar, M.; Jagadeeshkumar, M., "Particle Swarm Optimization Algorithm to Find the Location of Facts Controllers for a Transmission Line," Process Automation, Control and Computing (PACC), 2011 International Conference on , Page(s): 1-5, 20-22 July 2011
- [74]. Gitizadeh, M., "A modified simulated annealing approach to congestion alleviation in a power system using FACTS devices," Universities Power Engineering Conference (UPEC), 2010 45th International , Page(s): 1-6, Aug. 31 2010-Sept. 3 2010
- [75]. Lashkar Ara, A; Kazemi, A; Niaki, S.AN., "Multiobjective Optimal Location of FACTS Shunt-Series Controllers for Power System Operation Planning," Power Delivery, IEEE Transactions on , vol.27, no.2, Page(s): 481-490, April 2012
- [76]. Kumar, B.K.; Singh, S.N.; Srivastava, S.C., "Placement of FACTS controllers using modal controllability indices to damp out power system oscillations," Generation, Transmission & Distribution, IET , vol.1, no.2, Page(s): 209-217, March 2007
- [77]. Mondal, D.; Sengupta, A, "PSO based tuning and optimal allocation of TCSC controllers to mitigate small-signal stability problem," India Conference (INDICON), 2010 Annual IEEE , Page(s): 1-4, 17-19 Dec. 2010
- [78]. Zarghami, M.; Crow, M.L.; Jagannathan, S., "Nonlinear Control of FACTS Controllers for Damping Interarea Oscillations in Power Systems," Power Delivery, IEEE Transactions on , vol.25, no.4, Page(s): 3113-3121, Oct. 2010
- [79]. S. Panda and N. P. Padhy, "A PSO-based SSSC controller for improvement of transient stability performance," International Journal of Intelligent Systems and Technologies, vol. 2, no.1, Page(s): 28-35, winter 2007.
- [80]. Abido, M. A; Al-Awami, AT.; Abdel-Magid, Y.L., "Analysis and Design of UPFC Damping Stabilizers for Power System Stability Enhancement," Industrial Electronics, 2006 IEEE International Symposium on , vol.3, no., Page(s): 2040-2045, 9-13 July 2006
- [81]. Hajizadeh, M.; Sadeh, J., "Simultaneous coordination and tuning of PSS and FACTS for improving damping by genetic algorithm," Electric Utility Deregulation and Restructuring and Power Technologies (DRPT), 2011 4th International Conference on , Page(s): 1311-1315, 6-9 July 2011

- [82]. Bati, AF., "Optimal interaction between PSS and FACTS devices in damping power systems oscillations: part I," Systems Signals and Devices (SSD), 2010 7th International Multi-Conference on , Page(s): 1-6, 27-30 June 2010
- [83]. Bati, AF., "Optimal interaction between PSS and FACTS devices in damping power systems oscillations: Part II," Energy Conference and Exhibition (EnergyCon), 2010 IEEE International , Page(s): 452-457, 18-22 Dec. 2010
- [84]. Najafi, M.; Kazemi, A, "Coordination of PSS and FACTS Damping Controllers in Large Power Systems for Dynamic Stability Improvement," Power System Technology, 2006. PowerCon 2006. International Conference on , Page(s): 1-6, 22-26 Oct. 2006
- [85]. Aghazade, A; Kazemi, A; Alamuti, M.M., "Coordination among facts POD and PSS controllers for damping of power system oscillations in large power systems using genetic algorithm," Universities Power Engineering Conference (UPEC), 2010 45th International , Page(s): 1-6, Aug. 31 2010-Sept. 3 2010
- [86]. Nguyen, T.T.; Gianto, R., "Stability Improvement of Electromechanical Oscillations by Control Co-ordination of PSSs and FACTS Devices in Multi-Machine Systems," Power Engineering Society General Meeting, 2007. IEEE , Page(s): 1-7, 24-28 June 2007
- [87]. Atmakuru, R.; Kumar, R.S., "ANN based adaptive control coordination of PSSs and FACTS devices in multi-machine power systems," Modern Electric Power Systems (MEPS), 2010 Proceedings of the International Symposium , Page(s): 1-7, 20-22 Sept. 2010
- [88]. Nguyen, T.T.; Gianto, R., "Optimization-based control coordination of PSSs and FACTS devices for optimal oscillations damping in multi-machine power system," Generation, Transmission & Distribution, IET , vol.1, no.4, Page(s): 564-573, July 2007
- [89]. Zhijian, L.; Shu Hongchun; Jilai, Y., "Coordination control between PSS and SVC based on improved genatic - tabu hybrid algorithm," Sustainable Power Generation and Supply, 2009. SUPERGEN '09. International Conference on , Page(s): 1-5, 6-7 April 2009
- [90]. Sebaa, K.; Boudour, M., "Power system dynamic stability enhancement via coordinated design of PSSs and SVC-based controllers using hierarchical real coded NSGA-II," Power and Energy Society General Meeting - Conversion and Delivery of Electrical Energy in the 21st Century, 2008 IEEE , Page(s): 1-8, 20-24 July 2008

- [91]. Aghazade, A; Kazemi, A, "Simultaneous coordination of power system stabilizers and STATCOM in a multi-machine power system for enhancing dynamic performance," Power Engineering and Optimization Conference (PEOCO), 2010 4th International , Page(s): 13-18, 23-24 June 2010
- [92]. L. J. Cai and I Erlich, "Fuzzy coordination FACTS controllers for damping power system oscillation", Modern Electric Power Systems Proc. Of the International Symposium Wroclaw, 11-13 Sept., 2002.
- [93]. Lei, X.; Lerch, E.; Povh, D., "Optimization and coordination of damping controls for improving system dynamic performance," Power Engineering Society Summer Meeting, 2001 , vol.2, no., Page(s): 473-480 vol.2., 2001
- [94]. Sanchez-Gasca, Juan J.; Chow, J.H., "Power system reduction to simplify the design of damping controllers for interarea oscillations," Power Systems, IEEE Transactions on , vol.11, no.3, Page(s): 1342-1349, Aug 1996
- [95]. Pourbeik, P.; Gibbard, M.J., "Simultaneous coordination of power system stabilizers and FACTS device stabilizers in a multimachine power system for enhancing dynamic performance," Power Systems, IEEE Transactions on , vol.13, no.2, Page(s): 473-479, May 1998
- [96]. Arnautovic, D.; Medanic, J., "Design of Decentralized Multivariable Excitation Controllers in Multimachine Power Systems by Projective Controls," Power Engineering Review, IEEE , vol.PER-7, no.12, Page(s): 35, Dec. 1987
- [97]. Narne, R.; Panda, P.C.; Therattil, J.P., "Damping of inter-Area oscillations in power system using genetic optimization based coordinated PSS with FACTS stabilizers," India Conference (INDICON), 2012 Annual IEEE , Page(s): 853-858, 7-9 Dec. 2012
- [98]. Morsali, J.; Kazemzadeh, R.; Azizian, M.R.; Morsali, H., "Novel coordination of dual-channel PSS, AVR and TCSC damping controller to enhance power system overall stability," Electrical Engineering (ICEE), 2012 20th Iranian Conference on , Page(s): 552-557, 15-17 May 2012
- [99]. Simfukwe, D.D.; Pal, B.C.; Jabr, R.A; Martins, N., "Robust and low-order design of flexible ac transmission systems and power system stabilizers for oscillation damping," Generation, Transmission & Distribution, IET , vol.6, no.5, Page(s): 445-452, May 2012
- [100]. Suman, R. K.; Lal, C.; Kumar, M.; Alam, I; Goswami, AK., "Cost-benefit analysis of TCSC installation to power system operation," Energy, Automation,

and Signal (ICEAS), 2011 International Conference on , Page(s): 1-6, 28-30 Dec. 2011

- [101]. Tiwari, P.K.; Sood, Y.R., "An Efficient Approach for Optimal Allocation and Parameters Determination of TCSC With Investment Cost Recovery Under Competitive Power Market," *Power Systems, IEEE Transactions on* , vol.28, no.3, Page(s): 2475-2484, Aug. 2013
- [102]. Tlijani, K.; Guesmi, T.; Hadj Abdallah, H.; Ouali, A, "Optimal location and parameter setting of TCSC based on Sensitivity analysis," *Renewable Energies and Vehicular Technology (REJET)*, 2012 First International Conference on , Page(s): 420-424, 26-28 March 2012
- [103]. Kamel, T.; Tawfik, G.; Hsan, H.A, "Optimal number, location and parameter setting of multiple TCSCs for security and system loadability enhancement," *Systems, Signals & Devices (SSD)*, 2013 10th International Multi-Conference on , Page(s): 1-6, 18-21 March 2013
- [104]. Wartana, IM.; Singh, J.G.; Ongsakul, W.; Agustini, N.P., "Optimal Placement of a Series FACTS Controller in Java-Bali 24-bus Indonesian System for Maximizing System Loadability by Evolutionary Optimization Technique," *Intelligent Systems, Modelling and Simulation (ISMS)*, 2012 Third International Conference on , Page(s): 516-521, 8-10 Feb. 2012
- [105]. Rashed, G.I; Yuanzhang Sun; Shaheen, H. I, "Optimal location of thyristor controlled series compensation in a power system based on differential evolution algorithm considering transmission loss reduction," *Intelligent Control and Automation (WCICA)*, 2011 9th World Congress on , Page(s): 610-616, 21-25 June 2011
- [106]. NYPA, PTI, GE, OH, "FACTS: Application of TCSC in New York State", EPRI report, 1993.
- [107]. Mondal, D.; Sengupta, A, "PSO based tuning and optimal allocation of TCSC controllers to mitigate small-signal stability problem," *India Conference (INDICON)*, 2010 Annual IEEE , Page(s): 1-4, 17-19 Dec. 2010
- [108]. Hassan, M.O.; Zakaria, Z.A; Cheng, S.J., "Impact of TCSC on Enhancing Power System Stability," *Power and Energy Engineering Conference, 2009. APPEEC 2009. Asia-Pacific* , Page(s): 1-6, 27-31 March 2009
- [109]. Vikal, R.; Goyal, G., "TCSC Controller Design Using Global Optimization for Stability Analysis of Single Machine Infinite-Bus Power System," *Intelligent*

System Applications to Power Systems, 2009. ISAP '09. 15th International Conference on , Page(s): 1-7, 8-12 Nov. 2009

- [110]. Bamasak, S.M.; Abido, M.A, "Improving power oscillation damping via TCSC in interconnected power networks," Innovative Smart Grid Technologies - Middle East (ISGT Middle East), 2011 IEEE PES Conference on , Page(s): 1-6, 17-20 Dec. 2011
- [111]. Mahapatra, S.; Jha, AN., "PSS & TCSC coordinated design using particle swarm optimization for power system stability analysis," Power, Control and Embedded Systems (ICPCES), 2012 2nd International Conference on , Page(s): 1-5, 17-19 Dec. 2012
- [112]. Eslami, M.; Shareef, H.; Mohamed, A, "Coordinated design of PSS and TCSC controller for power system stability improvement," IPEC, 2010 Conference Proceedings , Page(s): 433-438, 27-29 Oct. 2010
- [113]. Nguyen, T.T.; Gianto, R., "Stability Improvement of Electromechanical Oscillations by Control Co-ordination of PSSs and FACTS Devices in Multi-Machine Systems," Power Engineering Society General Meeting, 2007. IEEE , Page(s): 1-7, 24-28 June 2007
- [114]. Song Yu, Zhijian Wu, Hui Wang, Zhangxin Chen, and He Zhong,” A Hybrid Particle Swarm Optimization Algorithm Based on Space Transformation Search and a Modified Velocity Model”, International Journal Of Numerical Analysis And Modeling, Vol. 9, no. 2, Page(s): 371–377, 2012
- [115]. Siemens Power Technologies Institute (2010), PSS/E32. PSSPLT Program Manual. Section 4.13.3, Modal Analysis Plotting. Siemens Energy INC, USA.
- [116]. Siemens Power Technologies Institute (2010), PSS/E32: Program Application Guide, Siemens Energy INC, USA.
- [117]. Siemens Power Technologies Institute (2010), PSS/E32: Program Operation Manual, Siemens Energy INC, USA.

APPENDICES

APPENDIX A Generator Model

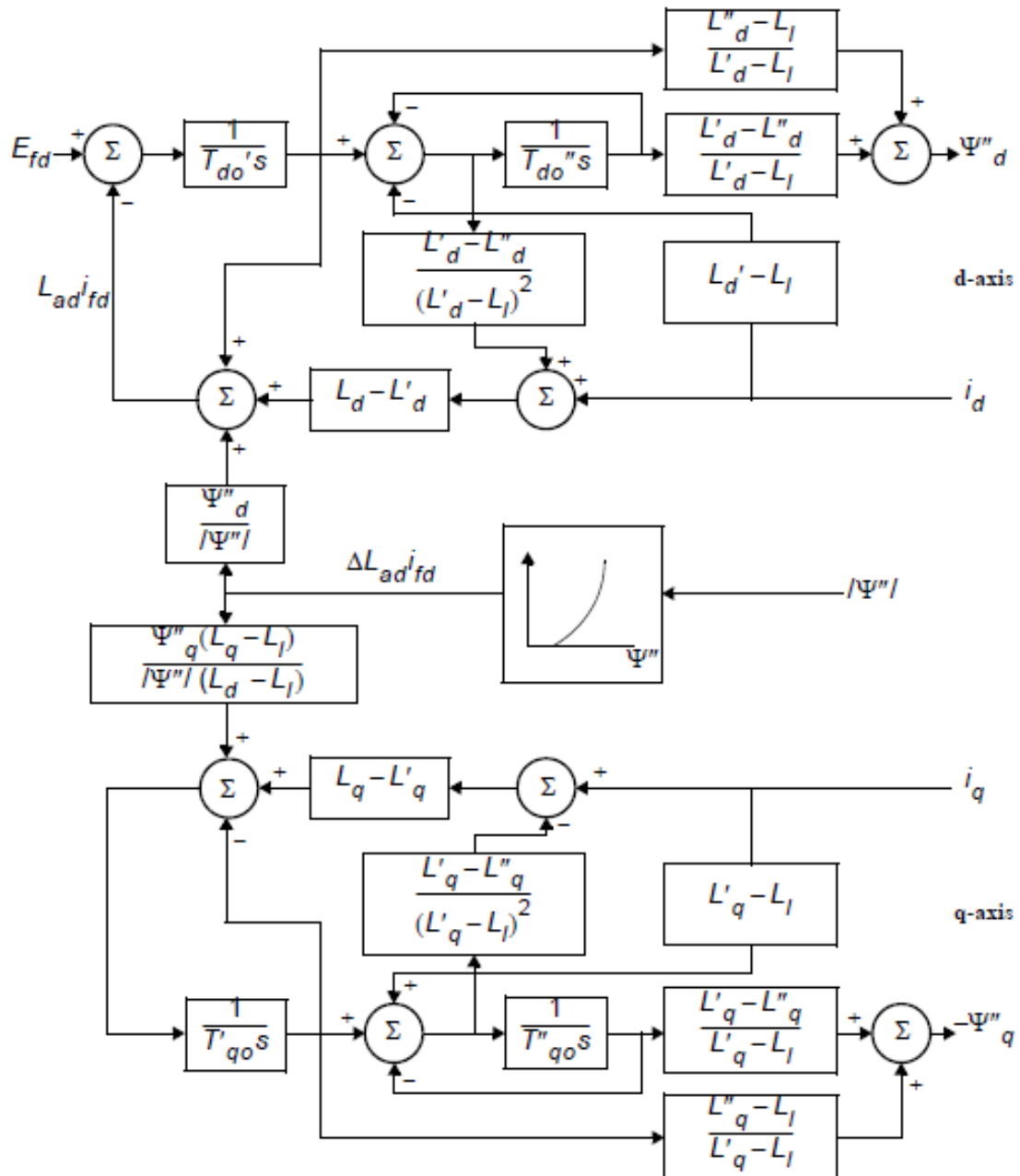


Figure A.1 Electromagnetic Model of Round Rotor Generator

APPENDIX B Turbine Governor Models

B.1. Modified IEEE Type 1 Speed-Governing Model With Fast Valving (TGOV3)

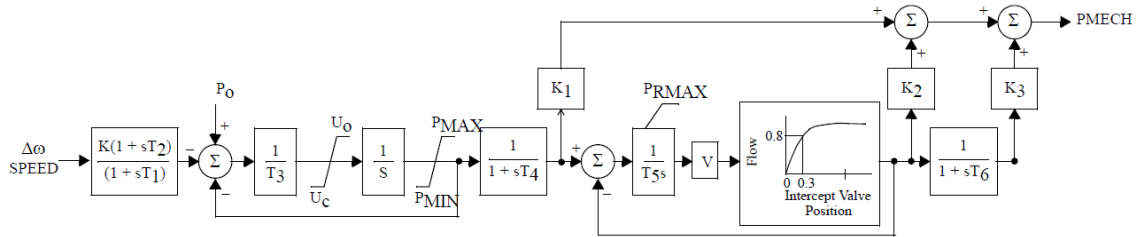


Figure B.1 Modified IEEE Type 1 Speed-Governing Model With Fast Valving

B.2. IEEE Type 1 Speed-Governing Model (IEEEG1)

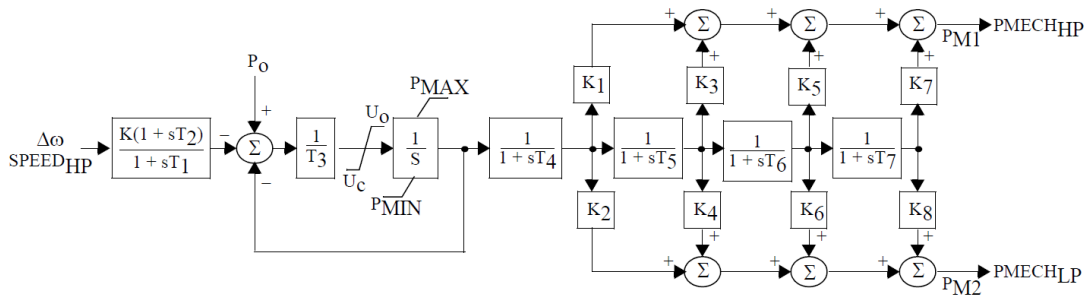


Figure B.2 IEEE Type 1 Speed-Governing Model

B.3. Gas Turbine-Governor (GAST)

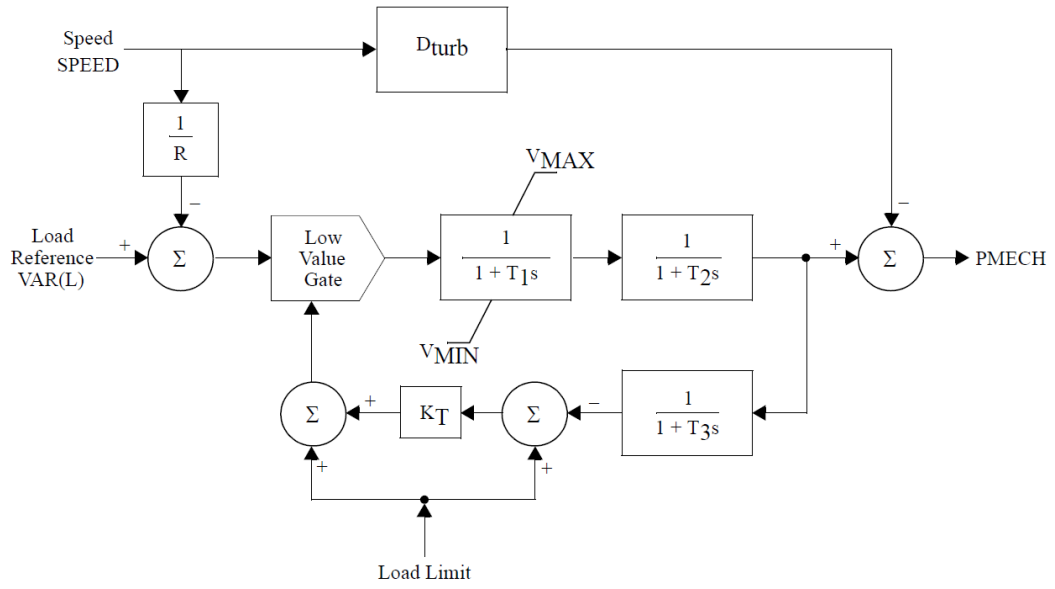


Figure B.3 Gas Turbine-Governor

B.4. Steam Turbine-Governor (TGOV1)

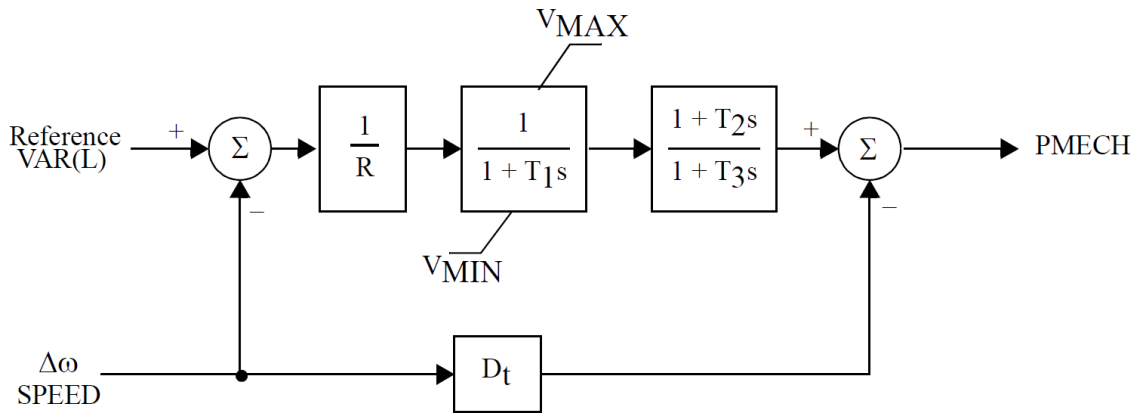


Figure B.4 Steam Turbine-Governor

APPENDIX C Excitation Systems Models

C.1. IEEE ST4B Potential or Compounded Source-Controlled Rectifier Exciter

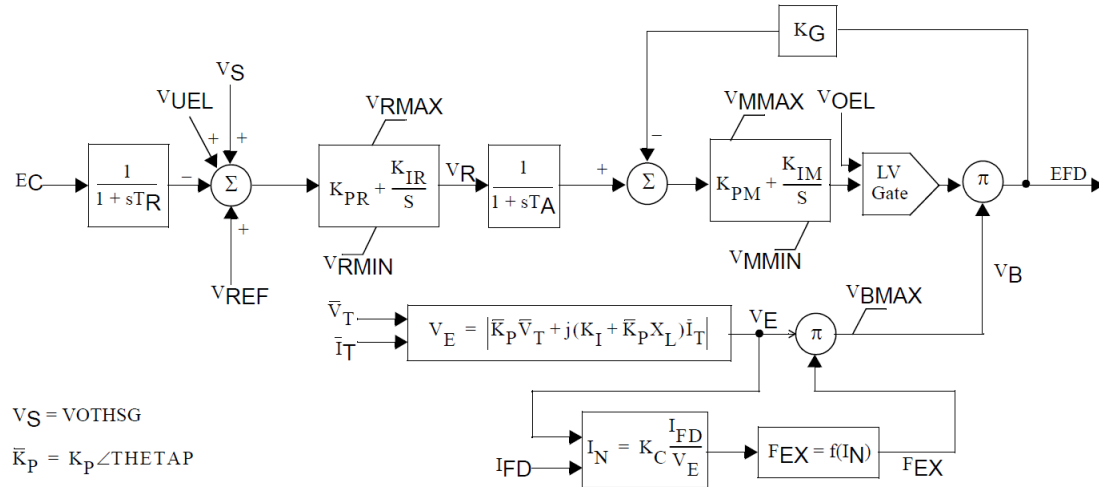


Figure C.1 IEEE Type ST4B Potential or Compounded Source-Controlled Rectifier Exciter

C.2. Proportional/Integral Excitation System (EXPIC1)

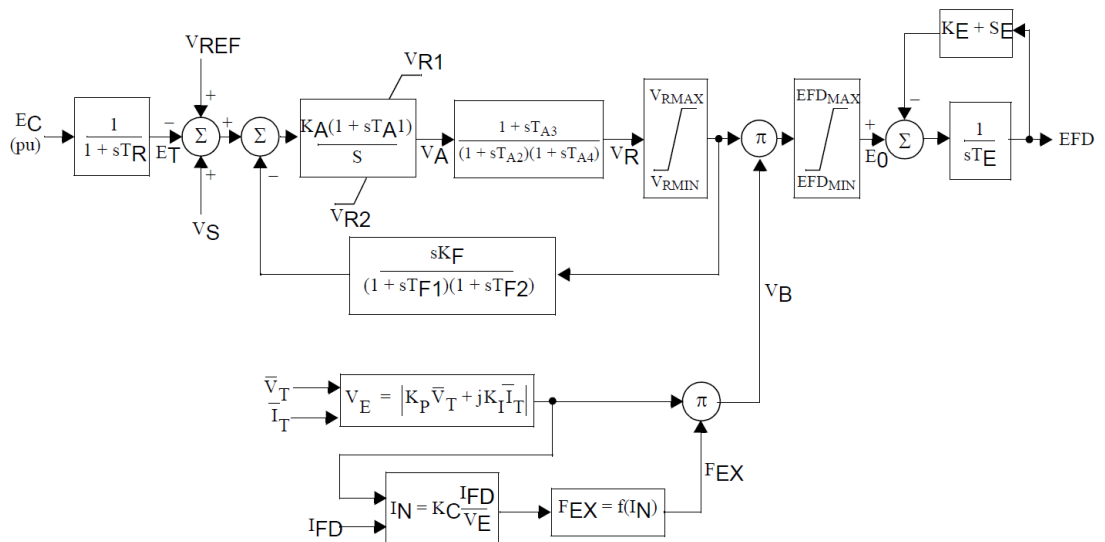


Figure C.2 Proportional/Integral Excitation System (EXPIC1)

C.3. IEEE Type ST2 Excitation System (EXST2)

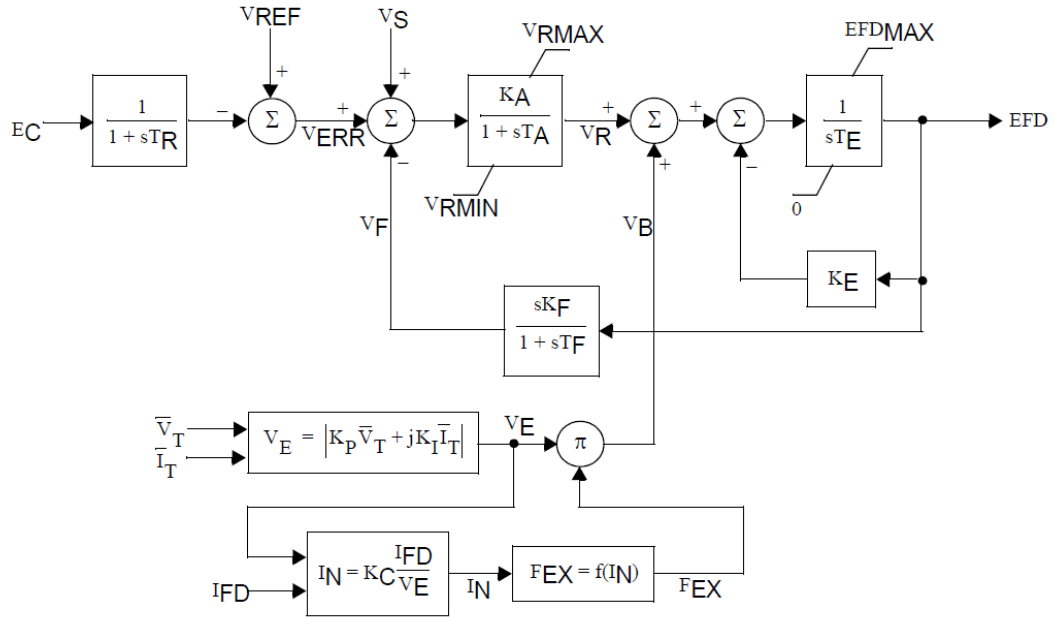


Figure C.3 IEEE Type ST2 Excitation System

C.4. IEEE Type ST1 Excitation System (EXST1)

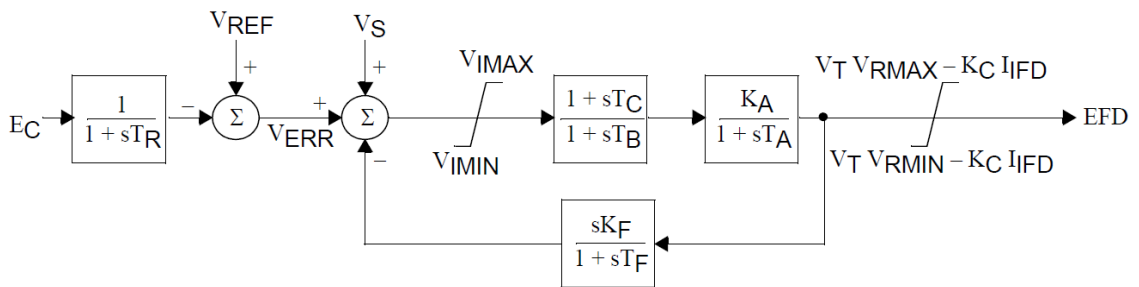


Figure C.4 IEEE Type ST1 Excitation System

C.5. IEEE Type AC2 Excitation System (EXAC2)

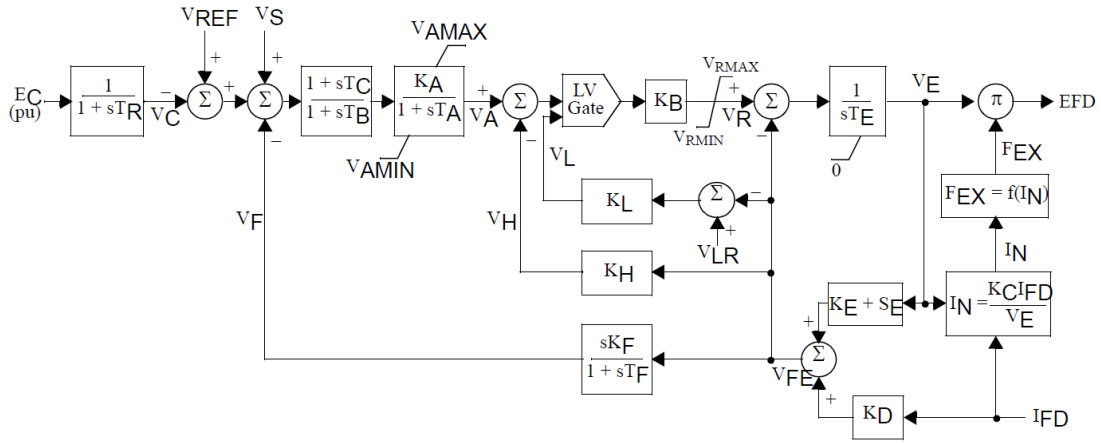


Figure C.5 IEEE Type AC2 Excitation System

C.6. IEEE Type AC1 Excitation System (EXAC1)

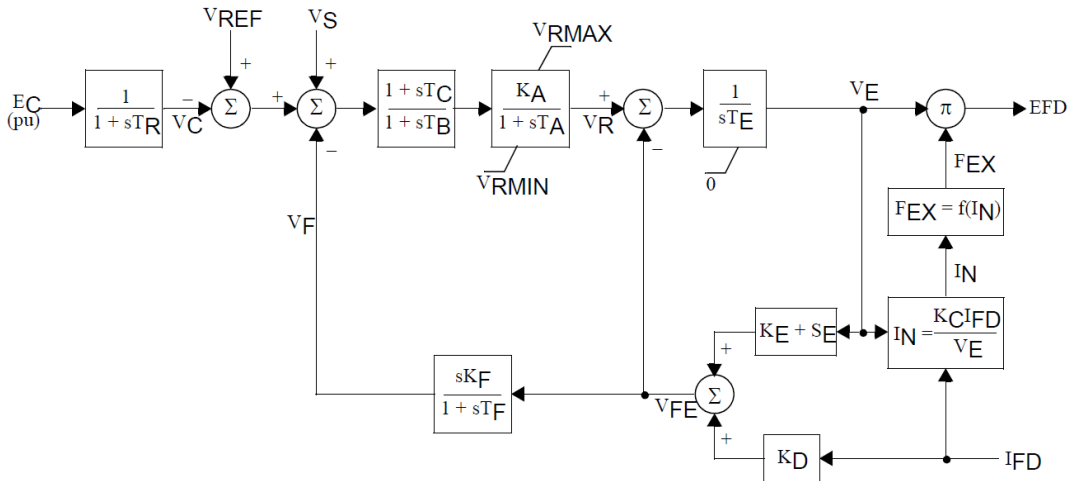


Figure C.6 IEEE Type AC1 Excitation System

C.7. Bus Fed or Solid Fed Static Exciter (SCRX)

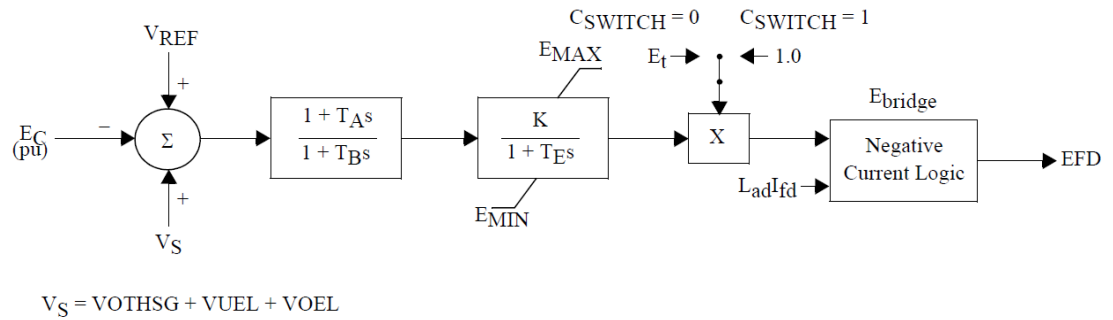


Figure C.7 Bus Fed or Solid Fed Static Exciter

C.8. IEEE Type 1 Excitation System (IEEET1)

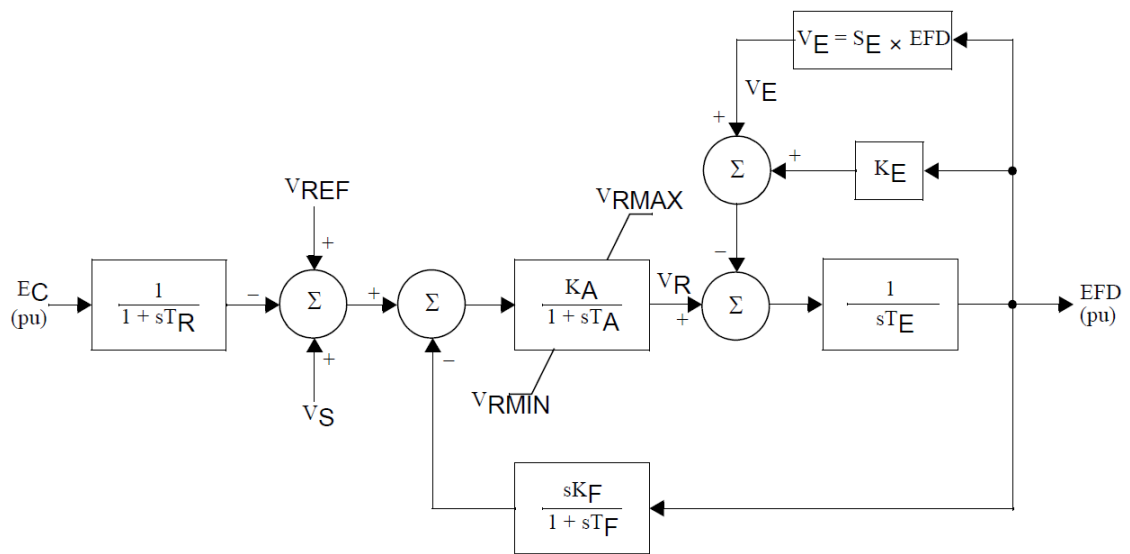


Figure C.8 IEEE Type 1 Excitation System

APPENDIX D Power System Stabilizer Models

D.1. IEEE Stabilizing Model (IEEEEST)

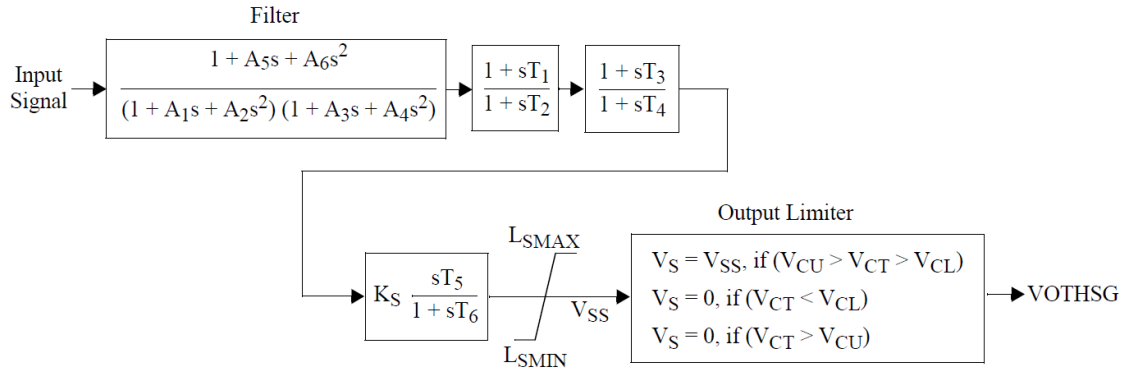


Figure D.1 IEEE Stabilizing Model

D.2. IEEE Stabilizing Model With Dual-Input Signals (IEE2ST)

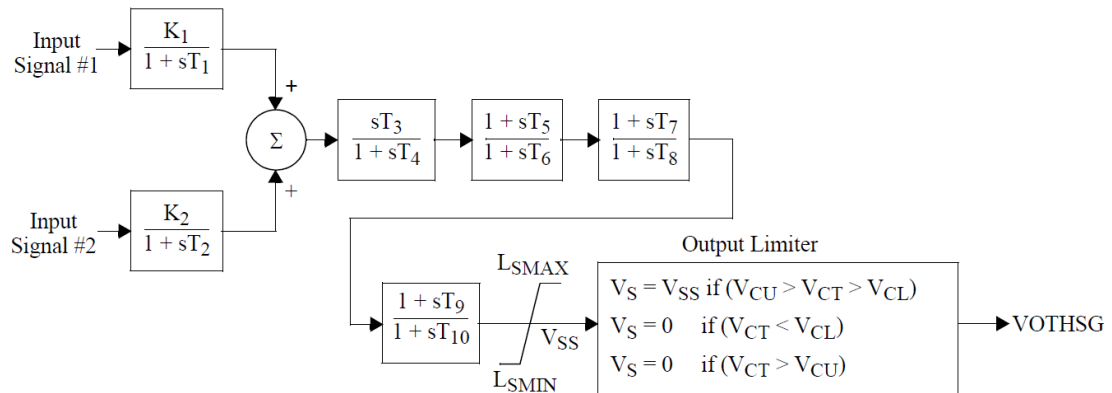


Figure D.2 IEEE Stabilizing Model With Dual-Input Signals

D.3. IEEE Dual-Input Stabilizer Model (PSS2A)

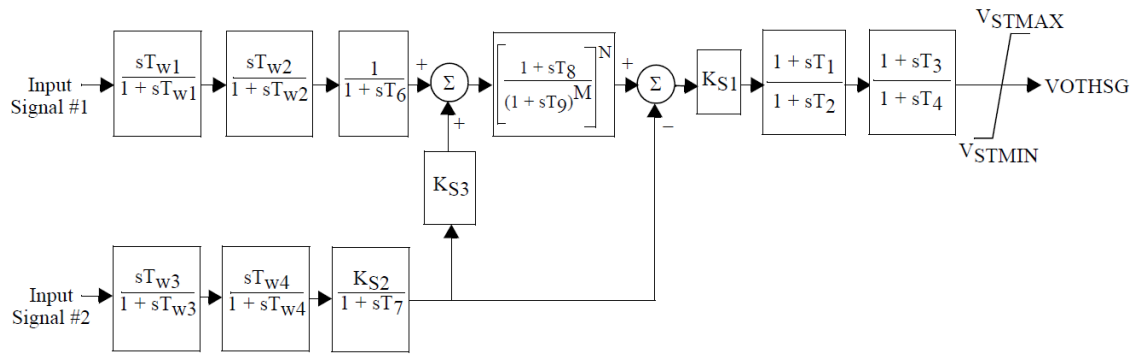


Figure D.3 IEEE Dual-Input Stabilizer Model

For more details about the above models refer to [116,117].

VITA

Name : Malik Mohammed Ashtar Al Hajji

Nationality : Saudi

Date of Birth : 1/31/1982

Email : alashtar240@hotmail.com

Address : Saudi Arabia - Dammam

Academic Background :

B.Sc. in Electrical Engineering from King Fahd University of Petroleum & Minerals (KFUPM)

M.Sc. in Electrical Engineering from King Fahd University of Petroleum & Minerals (KFUPM)

Work Experience:

From **2005 to 2008** worked with JAL International Company as Electric Design Engineer For Commercial and Residential Areas.

From **2008 to Present** working with Saudi Electricity Company in Extra High Voltage Network Planning Department as a Senior Power Transmission Engineer.

Publications:

Published paper:

Attended as a speaker in the 10th International GCC CIGRE Conference in Bahrain on 10-12 of November, 2014. The below paper has been presented and will be published very soon.

Al-Hajji, M.; Abido, M., "Systematic Approach for Dynamic Equivalents Development of Large-Scale Power System Using PSS/E ," *GCC CIGRE, 10th International Conference, Bahrain*, November 10-12, 2014.

Published Papers:

In addition to the above presented paper the following are proposed paper to be presented and published:

- [1]. Al-Hajji, M.; Abido, M., "A Novel Integrated Technique for Simultaneous Design of Power System Stabilizers in Multi-Machine Power Systems ,".
- [2]. Al-Hajji, M.; Abido, M., "A Novel Integrated Technique for Indivisible Design of Thyristor Controlled Series Capacitor in Multi-Machine Power Systems ,"
- [3]. Al-Hajji, M.; Abido, M., "Different Controller Design Approaches for Enhancing the Dynamic Stability of Weakly Interconnected Power Systems ,"